

**MOLECULAR EVENTS OCCURRING DURING THE INDUCTION
AND EXECUTION OF APOPTOSIS**

Thesis submitted for the degree of

Doctor of Philosophy

at the University of Leicester

by

Elizabeth Audrey Slee B.Sc. (Liverpool)

Centre for Mechanisms of Human Toxicity/

MRC Toxicology Unit

University of Leicester

March 1997

UMI Number: U529903

All rights reserved

INFORMATION TO ALL USERS

The quality of this reproduction is dependent upon the quality of the copy submitted.

In the unlikely event that the author did not send a complete manuscript and there are missing pages, these will be noted. Also, if material had to be removed, a note will indicate the deletion.



UMI U529903

Published by ProQuest LLC 2013. Copyright in the Dissertation held by the Author.
Microform Edition © ProQuest LLC.

All rights reserved. This work is protected against
unauthorized copying under Title 17, United States Code.



ProQuest LLC
789 East Eisenhower Parkway
P.O. Box 1346
Ann Arbor, MI 48106-1346

MOLECULAR EVENTS OCCURRING DURING THE INDUCTION AND EXECUTION OF APOPTOSIS

Elizabeth A. Slee, MRC Toxicology Unit, Centre for Mechanisms of Human Toxicity, University of Leicester, Leicester, U.K.

ABSTRACT

Apoptosis is a particular mode of cell death, identified by chromatin condensation, cell shrinkage and fragmentation into bodies that are subsequently phagocytosed by a neighbouring cell without inflammation. Apoptosis is vital in maintaining homeostasis, and its deregulation can have dire pathological consequences. Recent years have seen a dramatic increase in interest in the biochemical mechanisms of this phenomenon.

During the later stages of apoptosis there is extensive internucleosomal cleavage of DNA. In the first part of the work, eighteen dinucleosomal fragments from apoptotic mouse thymocytes were sequenced to ascertain whether there were any trends in the sequence of the DNA which could influence its likelihood to be cleaved. No such patterns could be identified.

The second part of this thesis deals with the participation of Ca^{2+} in the signalling mechanisms that induce apoptosis in rat thymocytes. A comparison of apoptosis induced by thapsigargin, cyclopiazonic acid and 2,5-di-(*t*-butyl)-1,4-benzohydroquinone, three inhibitors of the microsomal Ca^{2+} -ATPase, with that caused by the steroid dexamethasone, the chemotherapeutic drug etoposide and the protein kinase inhibitor staurosporine established that the three Ca^{2+} -ATPase inhibitors use the pathway of an early elevation in intracellular free Ca^{2+} concentration to trigger apoptosis.

The discovery of the homology between the nematode death gene *ced-3* and the human interleukin-1 β converting enzyme (ICE) has established that enzymes such as these are ubiquitous effectors of apoptosis. The final section of work involves the compound benzyloxycarbonyl-Val-Ala-Asp-fluoromethylketone (Z-VAD.FMK), which inhibits apoptosis in many cell models. Using an *in vitro* system incorporating the radiolabelled protein substrates [^{35}S]PARP and [^{35}S]proIL-1 β , it was found that Z-VAD.FMK inhibits the proteolytic activation of the ICE/Ced-3 homologue CPP32 induced by both Fas-mediated apoptosis and apoptosis induced by chemical stimuli. Furthermore, it was deduced that ICE is not involved in Fas-mediated apoptosis in Jurkat T cells.

ACKNOWLEDGEMENTS

Firstly, I would like to thank my supervisors, Professor Gerry Cohen and Professor David Critchley, for all their advice, encouragement (and criticism) during the undertaking of this thesis.

Next, I would like to single out the following people for their help. I am indebted to Dr. Gary Willars from the Department of Cell Physiology and Pharmacology for his assistance and advice with respect to the work in Chapter 4. Also, I would like to thank Dr. Sek Chow from the Centre for Mechanisms of Human Toxicity for his general advice and encouragement, particularly in relation to the work in Chapter 5, and also for supplying Fas/Jurkat lysates. I am also very grateful to Dr. Marion MacFarlane and Huijun Zhu for allowing me to use some of their work in Chapter 5.

As well as those people mentioned above, I would also like to acknowledge my colleagues from Lab 416 over the past three years for their help and companionship, namely (in no particular order) Dave Brown, Salmaan Hussein, Howard Fearnhead, Xiaoming Sun, Gareth Bicknell, Roger Snowdon, Katharine Ayres, James Wolfe, Joan Riley, Fang Zhang, Carole Couet, Julia Chandler, Siobhan Harkin and Kelvin Cain.

Finally, I would like to dedicate this thesis to my mother for her unfailing support, and to the memory of my father, despite his advice that I should become a mechanical engineer.

CONTENTS

Abstract	ii
Acknowledgements	iii
Contents	iv
List of figures	vii
List of tables	x
Abbreviations	xi

CHAPTER 1. INTRODUCTION

1.1. Classifications of cell death	2
1.2. Developmental programmed cell death	4
1.2.1. <i>Caenorhabditis elegans</i>	4
1.2.2. <i>Drosophila melanogaster</i>	7
1.3. Signalling events associated with apoptosis	8
1.3.1. The Bcl-2 family	8
1.3.2. p53	10
1.3.3. Calcium	11
1.3.4. The ICE/ Ced-3 family of proteases	12
1.3.4.1. Interleukin-1 β converting enzyme	15
1.3.4.2. CPP32/ Yama/ apopain	19
1.3.4.3. Substrates of the ICE family of proteases	21
1.3.5. The Fas receptor and its signalling mechanism	24
1.4. The pathological implications of apoptosis	26
1.5. Background to the cell models used in this thesis	29
1.5.1. The thymus	29
1.5.2. THP.1 cells	31
1.5.3. Jurkat T lymphocytes	31

CHAPTER 2. MATERIALS AND METHODS

2.1. Induction and assessment of apoptosis	34
2.1.1. Isolation of thymocytes	34
2.1.2. Induction of apoptosis	34
2.1.3. Quantification of apoptosis by flow cytometry	35
2.1.4. Conventional agarose gel electrophoresis	37
2.1.5. Field inversion gel electrophoresis	38
2.2. Preparation, cloning and sequencing of dinucleosomes	39
2.2.1. Treatment of thymocytes	39
2.2.2. Preparation of laddering gel	39
2.2.3. Preparation of dinucleosomes	40
2.2.4. Cloning of the dinucleosomal fragments	40
2.2.5. Plasmid isolation from <i>E. Coli</i>	41
2.2.6. Verification of insert	42
2.2.7. Sequencing of the dinucleosomes	43
2.3. Measurement of intracellular free calcium	44
2.3.1. The mechanism of action of fura-2	44
2.3.2. The measurement of intracellular free Ca ²⁺	45

2.4. Assessment of the cleavage of radiolabelled substrates <i>in vitro</i>	46
2.4.1. The use of <i>in vitro</i> systems to study events in the execution of apoptosis	46
2.4.2. Cell culture and preparation of lysates	46
2.4.3. Detection of PARP and CPP32 cleavage in intact cells	47
2.4.4. [³⁵ S] PARP/[³⁵ S] pro IL-1 β cleavage assay	48

CHAPTER 3. DNA SEQUENCE ANALYSIS OF DINUCLEOSOMES GENERATED DURING THYMOCYTE APOPTOSIS

3.1. Introduction	50
3.1.1. Chromatin structure	50
3.1.2. The degradation of DNA during apoptosis	51
3.2. Results	56
3.3. Discussion	63

CHAPTER 4. DIFFERING REQUIREMENTS FOR EXTRACELLULAR CALCIUM IN THE INDUCTION OF APOPTOSIS IN THYMOCYTES

4.1. Introduction.	67
4.2. Results.	71
4.2.1. The induction of apoptosis and [Ca ²⁺] _i elevation by microsomal Ca ²⁺ ATPase inhibitors	71
4.2.2. The relationship between [Ca ²⁺] _i increase and the initiation of apoptosis by thapsigargin.	73
4.2.3. EGTA inhibits apoptosis induced by microsomal Ca ²⁺ -ATPase inhibitors to a greater degree than that induced by other stimuli.	74
4.2.4. Econazole inhibits apoptosis induced by microsomal Ca ²⁺ -ATPase inhibitors but not by other apoptotic stimuli.	77
4.2.5. TLCK inhibits apoptosis by acting downstream of Ca ²⁺ release	79
4.3. Discussion.	82

CHAPTER 5. THE PARTICIPATION AND INHIBITION OF ICE/CED-3 PROTEASES IN THE EXECUTION PHASE OF APOPTOSIS

5.1. Introduction	88
5.2. Results	92
5.2.1. Analysis of the cleavage <i>in vitro</i> of [³⁵ S]PARP and [³⁵ S]proIL-1 β by lysates derived from THP.1 cells.	92
5.2.2. Z-VAD.FMK inhibits PARP breakdown <i>in vivo</i> but not <i>in vitro</i>	94
5.2.3. Z-VAD.FMK inhibits the activation of CPP32 in THP.1 cell apoptosis.	101
5.2.4. Z-VAD.FMK prevents the activation of CPP32 in Fas-induced apoptosis.	103
5.2.5. Ac-DEVD-CHO, Ac-YVAD-CHO and Z-VAD.FMK all inhibit the cleavage of [³⁵ S]proIL-1 β by purified recombinant ICE	107
5.2.6. Fas-induced apoptosis in Jurkat T lymphocytes occurs without the participation of ICE	107
5.3. Discussion	110

CHAPTER 6. GENERAL DISCUSSION

REFERENCES

LIST OF FIGURES

CHAPTER 1.

1a.	Schematic of the morphological changes occurring during both apoptosis and necrosis.	3
1b.	A diagram illustrating the relationships between the genes identified as being involved in programmed cell death in the nematode <i>C. elegans</i> .	5
1c.	The phylogenetic relationship between the ICE/ Ced-3 family of proteases.	13
1d.	An illustration of the Schechter and Berger system for the interaction between protease and substrate.	15
1e.	An illustration of the proform of ICE	18
1f.	Diagram of CPP32 showing the points at which it is cleaved to yield the active mature enzyme	20
1g.	Poly(ADP-ribose) polymerase (PARP) and the sequence at which cleavage occurs during apoptosis.	22
1h.	The development of thymocytes from immature progenitor CD4 ⁺ CD8 ⁻ double negative cells into mature T lymphocytes	30

CHAPTER 2.

2a.	Method for the separation of normal and apoptotic thymocytes by flow cytometry.	36
2b.	Agarose gel used for the separation of internucleosomal DNA fragments.	37
2c.	The structure of the free acid form of fura-2.	44

CHAPTER 3.

3a.	Levels of higher order chromatin structure.	51
3b.	The DNA sequences of dinucleosomes from apoptotic mouse thymocytes	59
3c.	The similarity of 105 bp (bases 199-304) of dinucleosome D213 with the B2 repeat consensus sequence and B2 repeats from an arbitrary selection of other genes.	62

CHAPTER 4.

4a.	An illustration of capacitative Ca ²⁺ influx showing the point and mechanism of action of thapsigargin, CPA and tBHQ.	68
4b.	The chemical structures of the three Ca ²⁺ -ATPase inhibitors used in this study.	69
4c.	The concentration-response curves of thapsigargin, CPA and tBHQ with respect to apoptosis.	71
4d.	The elevation in [Ca ²⁺] _i in response to the three Ca ²⁺ -ATPase inhibitors in comparison with the elevation in [Ca ²⁺] _i caused by dexamethasone.	72

4e.	A comparison of the concentration-response curves for thapsigargin-induced apoptosis and elevation of $[Ca^{2+}]_i$.	73
4f.	The effect of removal of extracellular Ca^{2+} on apoptosis by buffering with EGTA.	74
4g.	The effect of depleting extracellular Ca^{2+} on internucleosomal DNA degradation	75
4h.	The effect upon the formation of high molecular weight DNA fragments of depleting extracellular Ca^{2+}	76
4i.	The effect of econazole upon apoptosis induced by a variety of different stimuli.	78
4j.	The effect upon internucleosomal cleavage of inhibiting the uptake of extracellular Ca^{2+}	79
4k.	The inhibition by TLCK of apoptosis induced by the Ca^{2+} -ATPase inhibitors.	80
4l.	TLCK does not inhibit the elevation of $[Ca^{2+}]_i$ in response to Ca^{2+} -ATPase inhibitors.	81

CHAPTER 5.

5a.	The reversible ICE inhibitor, Acetyl-Tyr-Val-Ala-Asp-CHO (Ac-YVAD-CHO).	88
5b.	The reversible inhibitor of CPP32, Acetyl-Asp-Glu-Val-Asp-aldehyde (Ac-DEVD-CHO).	89
5c.	Benzyloxycarbonyl-Val-Ala-Asp-(OMe)-fluoromethylketone (Z-VAD.FMK), an irreversible inhibitor of ICE-like proteases.	90
5d.	Time course for the cleavage of $[^{35}S]$ PARP and $[^{35}S]$ proIL-1 β by lysate prepared from THP.1 cells exposed to cycloheximide and TLCK	92
5e.	Lysates from THP.1 cells exposed to a variety of stimuli cleave $[^{35}S]$ PARP but not $[^{35}S]$ proIL-1 β	93
5f.	Ac-DEVD-CHO and Ac-YVAD-CHO partially inhibit and Z-VAD.FMK	95
5g.	Ac-DEVD-CHO, but not Ac-YVAD-CHO or Z-VAD.FMK, inhibits the cleavage of $[^{35}S]$ PARP by lysate from THP.1 cells incubated with cycloheximide and TLCK	97
5h.	Z-VAD.FMK inhibits the activation of PARP protease activity in control cell lysates.	99
5i.	Z-VAD.FMK inhibits the proteolytic activation of CPP32 in whole THP.1 cells.	100
5j.	Ac-DEVD-CHO, but not Ac-YVAD-CHO or Z-VAD.FMK, inhibits the proteolysis of $[^{35}S]$ PARP by lysates prepared from Jurkat cells exposed to anti-Fas antibody	102
5k.	Z-VAD.FMK inhibits the proteolytic activation of CPP32 during Fas-mediated apoptosis in Jurkat T lymphocytes.	102

5l.	Ac-YVAD-CHO, Z-VAD.FMK and Ac-DEVD-CHO all inhibit the cleavage of [³⁵ S]proIL-1 β by purified recombinant ICE	104
5m.	Lysates from Jurkat cells exposed to anti-Fas antibody for 1 hour do not possess ICE activity	105
5n.	Lysates from Jurkat T cells undergoing Fas-mediated apoptosis do not cleave [³⁵ S]proIL-1 β	105
5o.	An inhibitor of ICE activity is not present in lysates prepared from unstimulated Jurkat cells.	106
5p.	A speculative scheme illustrating the potential mechanism(s) by which the ICE/Ced-3 family cause apoptosis.	114

CHAPTER 6.

6a.	The relationships between the inducers and inhibitors of apoptosis used in this thesis.	122
-----	-----------------------------------------------------------------------------------------	-----

LIST OF TABLES

CHAPTER 1.

Table 1.	Properties of the mammalian ICE family of proteases, including the Caspase nomenclature.	14
----------	------------------------------------------------------------------------------------------	----

CHAPTER 3.

Table 2.	The base composition of the sequenced dinucleosomes and comparison with the base composition of the mouse genome as a whole.	57
Table 3.	Comparison of microsatellites and homopurine/ pyrimidine tracts with the number expected in the genome as a whole.	57

ABBREVIATIONS

Ac-DEVD-CHO :	acetyl-Asp-Glu-Val-Asp-aldehyde
Ac-YVAD-CHO :	acetyl-Tyr-Val-Ala-Asp-aldehyde
AM :	acetoxymethylester
bp :	base pairs
BSA :	bovine serum albumin
[Ca ²⁺] _i :	intracellular free calcium concentration
CHAPS :	3-[(3-cholamidopropyl)-dimethylammonio]-1-propanesulphonate
CPA :	cyclopiazonic acid
CPP32 :	cysteine protease p32
DEX :	dexamethasone
DNA-PK _{cs} :	DNA-dependent protein kinase catalytic subunit
DMSO :	dimethyl sulphoxide
DTT :	dithiothreitol
EDTA :	ethylenediaminetetraacetic acid
EGTA :	ethylene glycol-bis (β-aminoethyl ether) <i>N,N,N',N'</i> -tetraacetic acid
ER :	endoplasmic reticulum
FCS :	foetal calf serum
FIGE :	field inversion gel electrophoresis
GraB :	granzyme B
HEPES :	<i>N</i> -2-hydroxyethylpiperazine- <i>N'</i> -2-ethanesulphonic acid
kbp :	kilobasepairs
kDa :	kilodaltons
ICE :	interleukin-1β converting enzyme
Ich1 :	ICE/ Ced-3 homologue 1
IL-1β :	interleukin-1β
IPTG :	isopropylthio-β-D-galactoside
Mch2,3 etc. :	mammalian CPP32 homologue 2, 3 etc.
μM :	micromolar
mM :	millimolar
nm :	nanometre
nM :	nanomolar
PAGE :	polyacrylamide gel electrophoresis
PARP :	poly(ADP-ribose) polymerase
PBS :	phosphate buffered saline
PIPES :	1,4-piperazinediethanesulphonic acid
PMSF :	phenylmethylsulphonyl fluoride
SDS :	sodium dodecyl sulphate
tBHQ :	2,5-di-(<i>t</i> -butyl)-1,4-benzohydroquinone
TLCK :	<i>N</i> α-tosyl-L-lysiny chloromethylketone
TNF :	tumour necrosis factor
X-Gal :	5-bromo-4-chloro-3-indolyl-β-D-galactoside
Z-VAD.FMK :	benzyloxycarbonyl-Val-Ala-Asp fluoromethylketone

CHAPTER 1

INTRODUCTION

1.1. CLASSIFICATIONS OF CELL DEATH

Apoptosis is a means by which a cell participates in its own demise. It happens continually in all multicellular organisms, and is essential for the maintenance of the health of the organism. However, the importance of such an apparently fundamental biological process has only been recognised comparatively recently. The phenomenon was first described in detail by John Kerr, Andrew Wyllie and Alastair Currie in 1972 (Kerr et al., 1972), although cell loss as a means of counterbalancing mitosis had been recognised for some time and referred to loosely as 'necrobiosis', a term that was never strictly defined. The term 'apoptosis' was coined by James Cormack, Professor of Greek at the University of Aberdeen, from the Greek for the falling of leaves from a tree or petals from a flower.

An apoptotic cell has a distinct morphology. Firstly, the cell loses its junctions with neighbouring cells and rounds up. The chromatin condenses, and the nucleus fragments. Vesicles formed by the dilation of the endoplasmic reticulum fuse with the plasma membrane, and the cell decreases in volume (Schwartzman and Cidlowski, 1993). Intracellular organelles such as the mitochondria appear histologically normal, although the plasma membrane gains a ruffled or blebbed appearance. The cell then disintegrates into membrane bound apoptotic bodies, containing organelles and nuclear fragments. These apoptotic bodies are then phagocytosed and rapidly degraded by either professional phagocytes or neighbouring cells. Apoptosis occurs in dispersed, isolated cells, and as membrane integrity is preserved throughout, it does not provoke an immune response (Kerr et al., 1972).

Prior to the paper of Kerr et al. (1972), what was in fact apoptosis was sometimes referred to as 'shrinkage necrosis'. Necrosis had been recognised as a means of cell death prior to apoptosis, possibly because it exhibits itself in a far more dramatic fashion than apoptosis. In contrast to apoptosis, the cell plays a passive role in necrosis. It has no control over its fate and the results can be highly damaging to the organism as a whole. Both by the nature of its induction and its execution, necrosis tends to affect tracts of cells rather than the isolated cells that undergo apoptosis.

The morphology of necrosis is distinct from that of apoptosis. Necrosis occurs in response to gross damage to the cell, such as would occur during hyperthermia, hypoxia,

ischaemia, infection or from poisons. The cytoplasm and subcellular organelles, in particular the mitochondria, swell due to a loss of selective permeability of the membrane to ions, either due to direct damage or via the depletion of ATP which prevents the action of membrane-bound ATPases. Lysosomes are also lysed, releasing degradative enzymes. Eventually the cell bursts, releasing its contents into the exterior. All these cellular components are highly immunogenic, so as a consequence necrosis frequently causes inflammation (Buja et al., 1993).

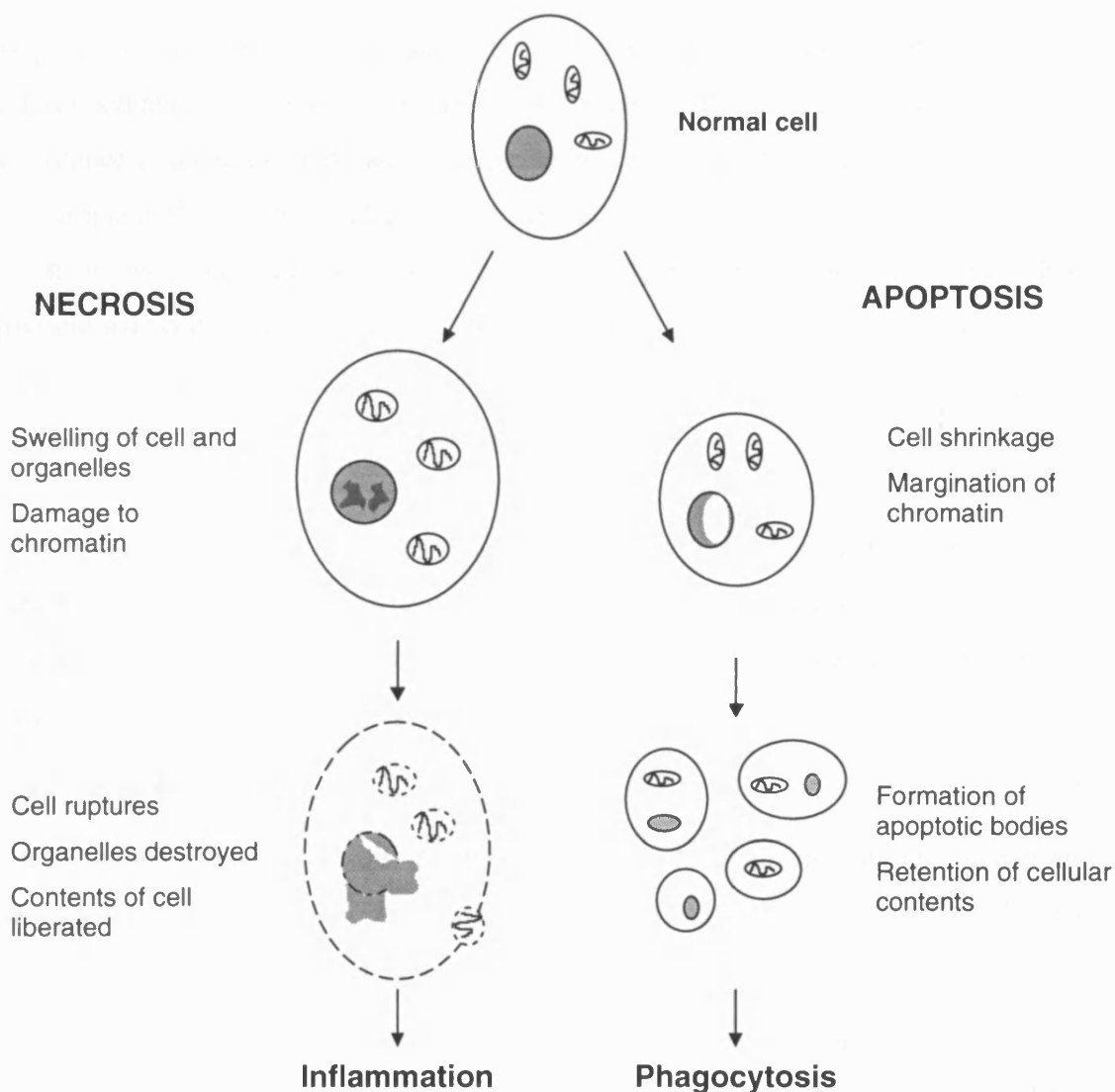


Figure 1a. Comparison of the morphological changes occurring during both apoptosis and necrosis. (Adapted from Williams et al., 1992).

A theory proposed by Martin Raff is that all cells, with the possible exception of blastomeres, are capable of killing themselves. Just as signals are required from other

cells for proliferation, so signals are required from other cells to prevent a cell from dying, i.e. the default state of the cell is to die, and signals from other cells are required to enable it to survive (Raff, 1992). Experimental evidence exists to support this hypothesis, as cells in culture tend to undergo apoptosis in the absence of serum, and in a developing organism a surplus of cells is produced, that are deleted by a limiting supply of survival signals.

1.2. DEVELOPMENTAL PROGRAMMED CELL DEATH

Apoptosis, strictly speaking, is the name given to a particular morphology of a dying cell, as described above (section 1.1.1). Programmed cell death, on the other hand, refers to the instance of a cell dying because it is predestined to die as it has outlived its purpose, for example during foetal development. Whatever the stimulus is that triggers the cell to die, it is an event that occurs with strict temporal and spatial reproducibility. Programmed cell death frequently possesses the morphological and biochemical characteristics of apoptosis, but not all apoptosis is programmed cell death. Apoptosis can be caused, for example, by ionising radiation, or by the presence of a suitable chemical stimulus. In these instances, the cell would continue in its usual manner were it not for the presence of the stimulus causing it to initiate apoptosis, and thus it does not enter the category of programmed cell death. Despite these differences, genetic studies of programmed cell death in two organisms in particular have been invaluable in the study of apoptosis in mammalian systems.

1.2.1. *Caenorhabditis elegans*

Studies into programmed cell death during the development of the nematode *Caenorhabditis elegans* by Robert Horvitz and his colleagues have provided vital clues about the biochemistry of mammalian apoptosis.

During the development of *C. elegans*, 131 out of the 1090 cells that are formed undergo programmed cell death. The mutation of fourteen genes has been found to affect the death process in one way or another (Figure 1b). Of these fourteen genes, three (*ces-2*, *ces-1* and *egl-1*) are required for making the decision that the cell will die, but these only seem to operate in small subsets of cells. *Ces-2*, (*ces* standing for cell death specification) has recently been shown to encode a transcription factor containing a basic leucine zipper (bZIP) domain, with homology to the proline- and acid-rich (PAR) family

of bZIP proteins (Metzstein et al., 1996). One member of this family of transcription factors is the hepatic leukaemia factor (HLF), the expression of which is affected by a chromosomal translocation involved in leukaemia, and the resulting fusion protein has been shown to suppress apoptosis in pro-B lymphocytes (Inaba et al., 1996).

The genes *ced-1*, *ced-2*, *ced-5*, *ced-6*, *ced-7*, *ced-8* and *ced-10* (*ced* standing for cell death defective) are required for engulfment of the dead cell (Figure 1b). These genes fall into two subsets; firstly *ced-2*, *ced-5* and *ced-10*, and secondly *ced-1*, *ced-6*, *ced-7* and *ced-8*. Loss of the function of one gene from each group results in the accumulation of undegraded cell corpses, which suggests two parallel and (partially) redundant pathways exist for phagocytosis, although cell death still goes ahead (Ellis et al., 1991). A further gene, *nuc-1*, encodes an endonuclease, but unlike the DNA degradation that occurs in mammalian cells, the nematode endonuclease is only active following phagocytosis of the dead cell (Hedgecock et al., 1983).

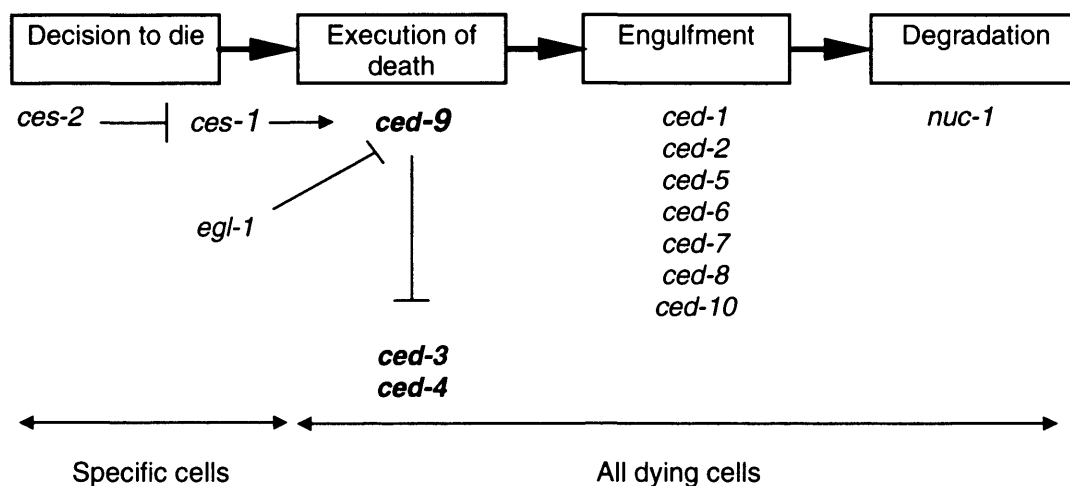


Figure 1b. A diagram illustrating the relationships between the genes identified as being involved in programmed cell death in the nematode *C. elegans*.

The *ced-9* gene acts to protect the cell from death. Gain of function mutations in this gene result in the suppression of all cell death in the developing nematode, whereas a loss of function mutation of this gene has the opposing (and fatal) effect of increasing the number of cells that die (Hengartner et al., 1992). The *ced-9* gene product has 23% amino acid sequence homology to the mammalian protein Bcl-2, which has a similar inhibitory role to *ced-9*, and can in fact substitute for *ced-9* in *C. elegans* (Hengartner

and Horvitz, 1994).

Two further genes, *ced-3* and *ced-4*, are required for the execution of cell death (Ellis and Horvitz, 1986) (Figure 1b). Loss of function mutations in either of these two genes enables cells which would normally be deleted in the wild type to survive. The genes are expressed principally during embryogenesis, when 113 of the 131 cell deaths occur. A mutation in one of the genes but not the other still prevents cell death, so both of these genes must be functional for the cell to die. The mutation of one of the two genes does not affect the expression of the other, so although it is possible that they may be interacting with each other at some later stage, they are transcribed independently (Ellis and Horvitz, 1986). Loss of function mutations in either *ced-3* or *ced-4* can completely prevent the excess cell death caused by a loss of function mutation in *ced-9* (Hengartner et al., 1992). This indicates that the *ced-9* gene acts prior to the *ced-3* and *ced-4* genes, as both these two genes need to operate correctly for a loss of function mutation in *ced-9* to have its effect.

To date, no mammalian homologue of *ced-4* has been found, and no function has been ascribed to it, although in a recent review it was suggested that *ced-4* may be acting upstream of *ced-3* as a positive regulator (Yuan 1996). The apoptotic activity of the *ced-4* gene product is controlled post-transcriptionally, as the gene appears to be expressed in cells whether they are destined to die or not. The Ced-4 protein is thought to have a molecular mass of approximately 63 kDa, and to be highly hydrophilic with no apparent transmembrane domains. A search for protein sequence motifs that could indicate a possible function for this protein found two possible calcium-binding EF-hand domains (Yuan and Horvitz 1992). However, Ced-4 seems to be unable to bind calcium *in vitro*, suggesting that if the protein exhibits any calcium binding activity *in vivo* it will be of low affinity (Yuan 1996).

The product of the *ced-3* gene, on the other hand, has 29% amino acid identity to the human protein interleukin-1 β -converting enzyme (ICE) and 27% amino acid identity to the product of *nedd-2*, a gene that is highly expressed in the developing murine brain (Yuan et al., 1993). Both the mammalian proteins are cysteine proteases, and, like *ced-3*, contain the amino acid sequence motif QACRG at the active site, the central cysteine being the residue that is absolutely required for the activity of these enzymes (see section

1.3.4.) Overexpression of either Ced-3 or ICE in Rat-1 fibroblasts causes the cells to undergo apoptosis (Miura et al., 1993), which demonstrates both the potential for cysteine proteases such as these to cause apoptosis in mammalian cells, and the conservation of the cell death process through evolution. Since the initial finding of the homology between *ced-3* and ICE, a new family of Ced-3 related proteases has emerged, all of which are cysteine proteases with a structure related to that of Ced-3 (see section 1.3.4.). The Ced-3 protein itself has been demonstrated to have proteolytic properties similar to those of this family of proteases (Xue and Horvitz, 1995; Hugunin et al., 1996; Xue et al., 1996). However, whilst the simultaneous existence of a number of ICE family members within one mammalian cell points to the possibility of these enzymes acting in series, parallel or both, *ced-3* is the only such protease in the more simple nematode.

1.2.2. *Drosophila melanogaster*

Studies in the fruit fly *Drosophila melanogaster* are not as advanced as those in the nematode. However, the vast majority of programmed cell deaths in *Drosophila* are mediated by a mechanism involving the product of the *reaper* gene, which activates cell death (White et al., 1994). Loss of function mutations in *reaper* prevent cell death, and in the developing embryo the gene is only expressed in those cells which are destined to die. The only means of circumventing the *reaper*-based mechanism is by extremely high doses of radiation. Relatively little is known about how *reaper* actually works. It is thought that it may act as some sort of positive regulator of cell death rather than an effector molecule, as the deaths that occur in cells exposed to high levels of x-rays exhibit the same morphology as those deaths that require *reaper*. However, *reaper* bears amino acid homology with the death domains of the mammalian tumour necrosis factor receptor TNFR-1 and the Fas/APO-1/CD95 receptor (Golstein et al., 1995) (section 1.3.5.), both of which are able to transmit death signals. This again indicates the conservation of elements of the death programme through evolution.

Another gene, *head involution defective* (*hid*), has been found which modulates cell death in *Drosophila* (Grether et al., 1995). Like *reaper*, *hid* is a positive regulator of cell death, and mutants without a functioning *hid* gene exhibit decreased programmed cell death, particularly in the head. The *hid* gene is expressed in the embryo in regions undergoing cell death, and the ectopic expression of *hid* results in cell death. The

function of the protein is unknown, although it shares a certain amount of homology with *reaper* in the amino terminal region. *Hid* functions independently of *reaper*, as loss of function *hid* mutants still demonstrate a certain amount of cell death, and *hid* can cause cell death in the absence of *reaper*.

Recently another *Drosophila* death gene, *grim*, has been identified which lies on the chromosome between *reaper* and *hid*, and like these two genes it is a positive regulator of cell death (Chen et al., 1996). It displays a greater degree of similarity to *reaper* in the amino terminal region than *hid*, but unlike *reaper* does not include a death domain. *Grim* can cause death independently of *reaper* and *hid*, and *grim*-induced death is blocked by p35, a baculovirus inhibitor of ICE/Ced-3 like proteases (Bump et al., 1995) (section 1.3.4). This would indicate that *grim* lies upstream of an ICE/Ced-3 like protease in the death pathway. An ICE/Ced-3 homologue has yet to be identified in *Drosophila*, although the inhibition of *Drosophila* cell death by p35 (White et al., 1996) and the broad spectrum inhibitor of ICE/Ced-3 proteases Z-VAD.FMK (section 5.1) (Pronk et al., 1996) is evidence for the participation of enzyme(s) of this type.

1.3. SIGNALLING EVENTS ASSOCIATED WITH APOPTOSIS

For many years, the actual molecular events involved in the disintegration of a cell were unknown, and most intracellular signalling mechanisms have been implicated in the execution of apoptosis in one way or another. Here, some of the more important and widely researched aspects of the biochemistry of apoptosis are described.

1.3.1. The Bcl-2 family

The Bcl-2 gene was initially found as a result of its location at the junction of the t(14;18) chromosomal translocation found in 85% of follicular lymphomas and 20% of diffuse B cell lymphomas. This chromosomal translocation brings together the immunoglobulin heavy chain promoter with the coding region of Bcl-2, resulting in an up-regulation in the expression of the latter and an increase in the lifespan of the host cell. Bcl-2 has subsequently been found to protect cells against apoptosis in a whole range of circumstances, e.g. it protects T cells against apoptotic stimuli such as γ -irradiation and anti-CD3 antibodies, and can also render cells resistant to chemotherapeutic agents such as cisplatin, etoposide and vincristine (Miyashita and Reed, 1992). However, it is known not to be a universal inhibitor of apoptosis, as cell

killing by cytotoxic T lymphocytes and also Fas-induced apoptosis occur independently of Bcl-2 (reviewed by Wang and Korsmeyer, 1996).

Bcl-2 is a 26 kDa membrane-bound protein, principally located in the outer mitochondrial membrane and on the cytoplasmic surfaces of the nuclear envelope and the endoplasmic reticulum (Krajewski et al., 1993). Its presence within a membrane seems to be required for it to function fully, although it can still function partially in the absence of a membrane binding domain (Hockenbery et al., 1993). The correct functioning of Bcl-2 is essential for the proper development and well-being of the animal as a whole: Bcl-2 knockout mice are normal until birth, when they develop retarded growth, kidney failure due to polycystic kidney disease, impaired melanin production and a severely crippled immune system (Veis et al., 1993).

The mechanism of action is unknown, and Bcl-2 bears no homology to any other proteins of known function, although there is now a family of at least ten proteins with related structure and function to Bcl-2, e.g. Ced-9, from the nematode *C. elegans*, has a similar role to Bcl-2 in preventing programmed cell death (see section 1.2.1.). The mammalian protein Bcl-x exists as two splice variants, the long Bcl-x_L and the shorter Bcl-x_S. Bcl-x_L has an analogous function to Bcl-2 in preventing apoptosis, whereas Bcl-x_S antagonises Bcl-x_L and thus promotes apoptosis (Boise et al., 1993). Bcl-x_L appears to function in tissues which have little or no Bcl-2 and vice versa (Wang and Korsmeyer, 1996), and moreover Bcl-x_L knockout mice, unlike Bcl-2 knockouts, die *in utero* having suffered extensive cell death in the brain and spinal cord (Motoyama et al., 1995).

Bax (Oltvai et al., 1993) and Bak (Chittenden et al., 1995; Farrow et al., 1995; Kiefer et al., 1995) both act to nullify the actions of Bcl-2 by forming heterodimers with Bcl-2. If they form homodimers, they also render the cell more susceptible to apoptosis. All these proteins contain the Bcl-2 homology domains BH1 and BH2, through which the proteins anchor to the membrane and form homo- or heterodimers. The existence of Bcl-2 homologues that are able to abrogate the activity of anti-apoptotic members of the family by forming complexes with them has implications regarding the regulation of such proteins. The crucial event in regulating the action of the apoptosis suppressors may lie not in the levels of expression of these proteins *per se* but in the levels of expression of proteins like Bax.

The exact manner in which Bcl-2 and its homologues prevent or induce apoptosis remains a mystery, although a number of hypotheses has been proposed. The crystal structure of Bcl-x_L has been determined, and it reveals that the protein has a pore-like structure and the transmembrane domains are similar in form to those in the diphtheria toxin (Muchmore et al., 1996). This could infer that the actions of Bcl-2 and its homologues are in a membrane regulatory role. Bcl-2 has also been shown to interfere with the transport of Ca²⁺ across the endoplasmic reticulum (Lam et al., 1994), which suggests that it may function as some form of ion channel.

The localisation of Bcl-2 to the outer membrane of the mitochondria has also lead to the examination of whether Bcl-2 functions as an anti-oxidant. It is capable of inhibiting apoptosis caused by hydrogen peroxide and other inducers of oxygen radicals (Hockenbery et al., 1993). However, Bcl-2 can still protect from apoptosis in cells maintained at low oxygen levels to reduce the levels of reactive oxygen species (Jacobson and Raff, 1995). This evidence suggests both that apoptosis can still occur in in an environment which reduces the production of reactive oxygen species, and that Bcl-2 can still function in the absence reactive oxygen species.

1.3.2. p53

p53, a tumour suppressor gene, is the most widely mutated gene in human cancers. The p53 protein is able to bind to DNA in a sequence-specific manner, and it is the domain responsible for this function which is mutated most frequently. p53 knockout mice develop normally, but have an increased susceptibility to tumour formation following birth. p53 levels are increased in response to DNA damaging agents, with two possible outcomes: either cell cycle arrest is induced allowing the cell to repair the DNA, or the cell enters apoptosis (reviewed by Hale et al., 1996).

The participation of p53 in the modulation of apoptosis appears to be restricted to instances of DNA damage. Thymocytes isolated from p53 knockout mice are resistant to apoptosis induced by either ionising irradiation or etoposide, an agent which creates double-stranded DNA breaks via the stabilisation of the catalytic intermediate of topoisomerase II, whilst the same cells are still susceptible to other apoptosis-inducing agents such as calcium ionophore or glucocorticoid (Clarke et al., 1993; Lowe et al., 1993). In addition to thymocytes, bone marrow cells and intestinal epithelial cells derived

from p53 knockout mice have been shown to be less sensitive to apoptosis in response to irradiation (reviewed by Götz and Montenarh, 1995).

p53 acts as a transcription factor, and has been demonstrated to regulate the expression of a number of genes including p21/WAF1/CIP1 and GADD45. The products of both these genes are believed to be instrumental in the prevention of progression through the cell cycle, although they have not been linked with apoptosis (Götz and Montenarh, 1995). The exact mechanism by which p53 induces apoptosis is unclear. However, it does appear to have a role in the expression of Bcl-2 and Bax. p53 has been shown to suppress the expression of Bcl-2 and up-regulate the expression of Bax in a number of cell types, and p53 knockout mice have higher levels of Bcl-2 and lower levels of Bax than the wild-type. Furthermore, the Bax promoter contains a number of p53 binding motifs (reviewed by Reed, 1995).

1.3.3. Calcium

Ca^{2+} has been implicated as a potential central mediator of mammalian apoptosis since it was found that the endonuclease responsible for the internucleosomal cleavage of DNA in isolated mouse thymocyte nuclei is dependent upon Ca^{2+} and magnesium (Cohen and Duke 1984).

Thapsigargin, an inhibitor of the Ca^{2+} -ATPase in the endoplasmic reticulum (Thastrup et al., 1990), is able to induce apoptosis in thymocytes (Jiang et al., 1994), which suggests a possible involvement of Ca^{2+} in the apoptotic signalling pathway. When rat thymocytes are treated with thapsigargin, the chelation of both intra- and extracellular Ca^{2+} can prevent chromatin degradation and the formation of nuclei with an apoptotic morphology (Zhivotovsky et al., 1994; Jiang et al., 1994), indicating that the rise in intracellular free calcium ($[\text{Ca}^{2+}]_i$) must be sustained for apoptosis to be induced. An elevation in $[\text{Ca}^{2+}]_i$ has been implicated in the induction of apoptosis in thymocytes by a number of other mechanisms. The chelation of intra- or extracellular Ca^{2+} has been demonstrated to significantly reduce apoptosis when thymocytes are exposed to γ -irradiation (Story et al., 1992), and tributyl-*n*-tin, an environmental pollutant, induces apoptosis in thymocytes via an elevation of $[\text{Ca}^{2+}]_i$ (Chow et al., 1992). The binding of anti-CD3 antibodies to the T cell receptor complex causes apoptosis in immature ($\text{CD4}^+ \text{CD8}^+$) thymocytes (Smith et al., 1989), alongside a sustained elevation in $[\text{Ca}^{2+}]_i$ (McConkey et al., 1989a) via the

hydrolysis of phosphatidyl inositol diphosphate (PtdInsP₂) (Conroy et al., 1995). In addition, Ca²⁺ ionophores such as ionomycin and A23187, that elevate [Ca²⁺]_i by forming pores in the plasma membrane, are also extremely effective inducers of apoptosis. These examples illustrate the prospect of Ca²⁺ having a widespread role in the induction of apoptosis in thymocytes. In systems other than thymocytes, the depletion of the ER of Ca²⁺ has been shown to occur when apoptosis is induced by glucocorticoids in a T cell lymphoma cell line (Lam et al., 1993). Also, there is an elevation of [Ca²⁺]_i in the target cell prior to it being killed by cytotoxic T lymphocytes (Allbritton et al., 1988), although the Ca²⁺ is probably from an extracellular source and enters the cytosol because of the presence of perforin in the plasma membrane.

A number of Ca²⁺-dependent proteins have been implicated in apoptosis. The activation of the Ca²⁺-dependent protease calpain has been described in thymocytes (Squier et al., 1994), and the calmodulin inhibitor calmidazolium can inhibit DNA fragmentation in thymocytes (McConkey et al., 1989b), which suggests that an elevation in [Ca²⁺]_i can cause the activation of calmodulin.

Although an elevation in [Ca²⁺]_i causes apoptosis in thymocytes, it does not necessarily have the same effect in other cell systems. For example, in raising [Ca²⁺]_i, thapsigargin prevents rat sympathetic neurons from undergoing apoptosis in response to nerve growth factor deprivation (Lampe et al., 1995) and in an IL-3 dependent haematopoietic progenitor cell line, calcium ionophore suppresses apoptosis upon the production of IL-4 (Rodriguez-Tarduchy et al., 1992). A transient elevation in [Ca²⁺]_i in neutrophils also protects against apoptosis, an effect which is abolished by the chelation of [Ca²⁺]_i (Whyte et al., 1993). Furthermore, the chelation of extracellular Ca²⁺ by EGTA induces apoptosis in myeloma, lymphoma and leukaemia cell lines (Kluck et al., 1994).

1.3.4. The ICE/Ced-3 family of proteases

The study of apoptosis has been altered dramatically by the discovery that programmed cell death in the nematode has elements in common with mammalian systems of cell death. In particular, the similarity between the gene *ced-3* and the then unique interleukin-1 β converting enzyme (ICE) (Yuan et al., 1993) has led to the discovery both of other proteases related to *ced-3* and their substrates.

To date, there are eleven mammalian members of the ICE/Ced-3 family (Figure 1c; table

1). These enzymes are all cysteine proteases, and contain the motif QACXG at the active site. X is usually an arginine residue, although homologues with the motifs QACQG (Boldin et al., 1996; Muzio et al., 1996; Fernandes-Alnemri et al., 1996) and QACGG (Duan et al., 1996b; Srinivasula et al., 1996) have also been isolated (Table 1). The enzymes are all initially translated as inactive proforms which are proteolytically cleaved to give a heterodimer (see Figures 1e and f). From the evidence provided by the elucidation of the crystal structure of ICE (Section 1.3.4.1.) and CPP32 (section 1.3.4.2.), the active form of these enzymes consists of two heterodimers in association to give a tetramer. They all appear to be expressed constitutively, and there is no evidence that their expression is induced by some form of death signal (Jacobson et al., 1996). Overexpression of these enzymes results in apoptosis, although the validity of such experiments is debatable, for a couple of reasons. Firstly, it has been suggested that because of the excess enzyme in the cell, they are acting non-specifically. The overexpression of many far less specific proteases such as trypsin will also send a cell into apoptosis (Williams and Henkart, 1994). Secondly, it is impossible to tell whether the artificially expressed protein is actually participating in the death pathway, or stressing the cell in such a way that the mere presence of the protein forces the cell to initiate its endogenous cell death programme.

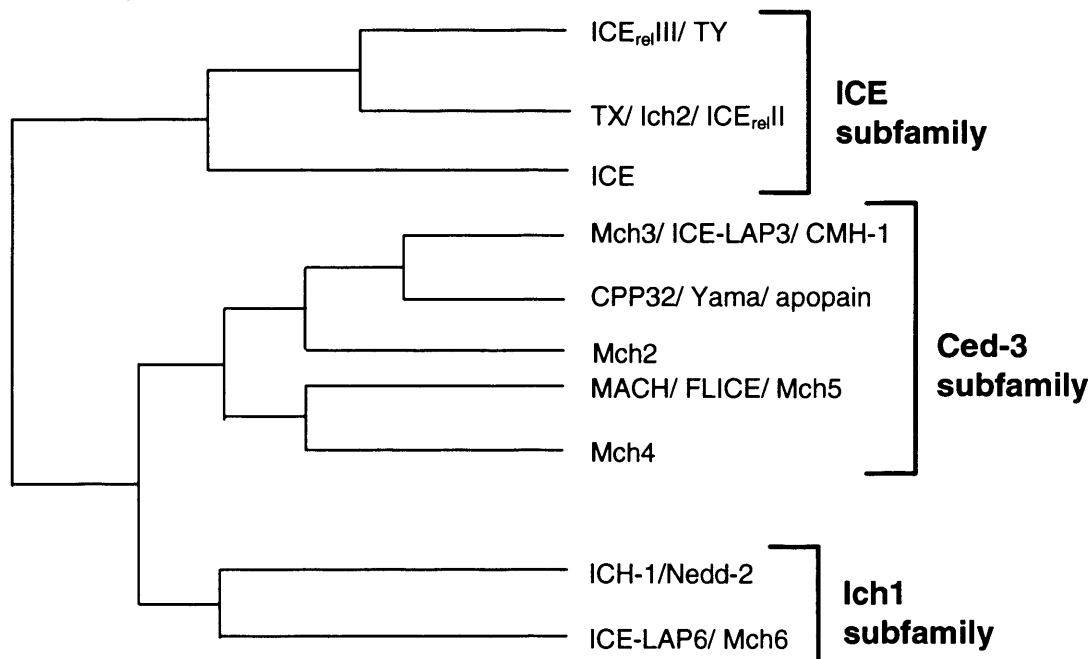


Figure 1c. The phylogenetic relationships between the ICE/Ced-3 family of proteases.

The three subfamilies, i.e. the ICE subfamily, Ced-3 subfamily and Ich-1 subfamily are indicated. For details of the Caspase nomenclature see Table 1 (Figure adapted from Alnemri et al., 1996).

PROTEASE	CASPASE	KNOWN SUBSTRATES	ACTIVE SITE	SIZE (PROFORM)	IDENTITY WITH Ced3	IDENTITY WITH ICE	ACTIVATED BY GraB [†]	REFS
ICE	1	proIL-1 β , proICE, proCPP32	QACRG	45kDa	29%	100%	No	1, 2, 3, 30
CPP32/Yama/apopain	3	PARP, U170kDa snRNP, DNA PK ϵ , Huntingtin, proMch3, proMch2, SREBP 1&2, D4-GDI, pro Mch6.	QACRG	32 kDa	35%	30%	Yes	4, 5, 6, 7, 8, 9, 10, 11, 12, 30
Mch2	6	Nuclear lamins, proCPP32, proMch3	QACRG	34kDa	35%	29%	Yes	13, 14, 15, 16, 30
Mch3/CMH1/ICE-LAP3	7	PARP	QACRG	35kDa	33%	<30%	Yes	17, 18, 19, 30
Ich-1/Nedd-2	2	none known	QACRG	51 kDa	28%	27%	?	20, 30, 31
ICE _{relII} /TX/Ich2	4	proICE	QACRG	43kDa	26%	53%	?	21, 22, 23, 30
ICE _{relIII} /TY	5	proICE _{relIII} /TY	QACRG	42kDa/ 48kDa	24%	51%	?	21, 24, 30
FLICE/MACH/Mch5	8	PARP	QACQG	55kDa	34%*	28%*	Yes	25, 26, 29, 30
Ich3	11	none known	QACRG	42kDa	26%	45%	Yes	27, 30
Mch4	10	proMch3, proCPP32	QACQG	55kDa	32%*	?	Yes	29, 30
ICE-LAP6/Mch6	9	PARP?	QACGG	46kDa	31%*	25-28%*	Yes	10, 28, 30

Table 1. *Properties of the mammalian ICE family of proteases, including the Caspase nomenclature.*

* Indicates homology excluding the prodomain. †GraB; Granzyme B. References: (1.) Thornberry et al., (1992); (2.) Cerretti et al., (1992); (3.) Darmon et al., (1994); (4.) Fernandes-Alnemri et al., (1994); (5.) Nicholson et al., (1995); (6.) Tewari et al., (1995); (7.) Casciola-Rosen et al., (1996); (8.) Goldberg et al., (1996); (9.) Wang et al., (1995); (10.) Srinivasula et al., (1996); (11.) Na et al., (1996); (12.) Darmon et al., (1995); (13.) Fernandes-Alnemri et al., (1995a); (14.) Orth et al., (1996a); (15.) Takahashi et al., (1996); (16.) Orth et al., (1996b); (17.) Fernandes-Alnemri et al., (1995b); (18.) Lippke et al., (1996); (19.) Duan et al., (1996); (20.) Wang et al., (1994); (21.) Munday et al., (1995); (22.) Faucheu et al., (1995); (23.) Kamens et al., (1995); (24.) Faucheu et al., (1996); (25.) Muzio et al., (1996); (26.) Boldin et al., (1996); (27.) Wang et al., (1996); (28.) Duan et al., (1996); (29.) Fernandes-Alnemri et al., (1996); (30.) Alnemri et al., (1996) (31.) Kumar et al., 1994

As a family of proteases, they are extremely specific with regard to their action. They all have a unique requirement for an aspartate residue in the P_1 position of the substrate (Sleath et al., 1990), with a preference for a small amino acid such as alanine in the P_1' position. By the Schechter and Berger nomenclature for protease/ substrate interactions (see Figure 1d), the residues on the substrate to the N-terminal side of the scissile bond are numbered P_1 , P_2 , P_3 etc., counting away from the cleavage site. Those on the carboxyl terminal are numbered P_1' , P_2' , P_3' etc., again counting away from the cleavage site. The corresponding sites on the protease itself are numbered S_1 , S_2 , S_3 etc. As an aspartate residue is present at each of the points at which the proforms are cleaved for conversion into an active enzyme, this requirement for aspartate establishes potential inter-relationships between the proteases so that the enzymes either cleave each other in a hierarchical manner, or they cleave themselves.

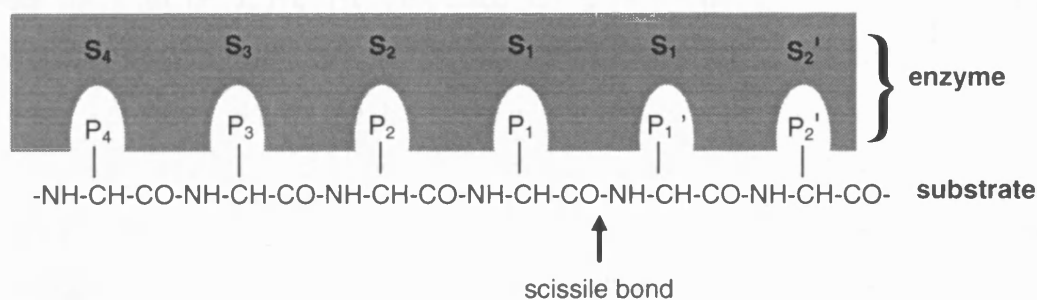


Figure 1d. An illustration of the Schechter and Berger system for the interaction between protease and substrate.

P_4 to P_2' represent amino acid residues in the substrate: in the context of ICE-like proteases this would represent either a peptide inhibitor like Ac-YVAD-CHO, or a protein substrate such as poly(ADP-ribose) polymerase. S_4 to S_2' represent subsites within the protease itself.

Whilst some of the mammalian ICE/Ced-3 proteases have been extensively characterised, very little is understood about other members of the family. Much of what is known about these proteases is summarised in Table 1, but ICE and CPP32 are described in more detail, both because their properties have been investigated more extensively and as much of the work in chapter 5 involves these two enzymes.

1.3.4.1. Interleukin- 1β converting enzyme

Interleukin- 1β converting enzyme (ICE) was the enzyme that was recognised to be homologous to the *ced-3* gene product (Yuan et al., 1993) (section 1.2.1.), although

with only 29% amino acid sequence identity, it is now known to be one of the ICE family members least resembling Ced-3. ICE was originally under investigation because of its action in cleaving the inactive prointerleukin-1 β into the active form. Interleukin-1 exists in two forms, IL-1 α and IL-1 β , with IL-1 β being the predominant form. Interleukin-1 β is a multifunctional cytokine that principally mediates both fever and chronic and acute inflammation. Its actions have also been linked with rheumatoid arthritis, diabetes, depression and anorexia, and in addition, it is also known to act to promote growth in leukaemic progenitor cells. The expression of IL-1 β is stimulated by nearly all microbes and their secretions like lipopolysaccharide, and can also be enhanced by xenobiotics such as the pharmaceutical agents taxol, amphotericin-B and methamphetamine, and the environmental toxins dioxin and asbestos (reviewed by Dinarello, 1996). Following translation, proIL-1 β remains in the cytosol as the inactive 31 kDa precursor which must be cleaved to the 17.5 kDa form at the peptide bond between Asp 116 and Ala 117 in order for it to be active. No processed IL-1 β is found within the cytosol, and its secretion from the cell seems to be related to the cleavage of the proform at the cell surface, a putative relationship that has been reinforced by the localisation of active ICE to the plasma membrane (Singer et al., 1995). The secretion of IL-1 β is tightly regulated, although it is unknown whether this regulation occurs directly at the point of conversion of proIL-1 β to the mature form, or indirectly by affecting the activation of proICE to the active form. In characterising the manner in which ICE cleaves proIL-1 β , it was hoped that it would be possible to design novel pharmaceutical agents to inhibit this process and thus suppress inflammation.

ICE is originally translated as an inactive proenzyme of 404 amino acids (45 kDa), which is the form in which it is predominantly found in monocytes (Ayala et al., 1994). This proform requires cleavage at residues Asp 119-Asn 120, Asp 297-Ser 298 and Asp 316-Ala 317 to form a p20/p10 heterodimer (see Figure 1e), which then complexes with another p20/p10 pairing to give the active, tetrameric enzyme. Structural studies (Walker et al., 1994a; Wilson et al., 1994) have shown that the two p10 subunits lie adjacent to each other at the centre of the holoenzyme, with the two p20 subunits on the exterior. The active site of the enzyme lies between the p10 subunit from one p10/p20 pair and the p20 subunit of the other. The QACRG motif, which encompasses the crucial cysteine (Cys 285), lies within the p20 subunit. His 237 (also in the p20 subunit) sits with its side

chain close to Cys 285 and is also required to form the catalytic site. The S_1 subsite, which confers the specificity for aspartate, is composed principally of the side chains of Arg 179 from the p20 subunit and Arg 341 from the p10 subunit, with additional interaction with Gln 283 (p20) and Ser 347 (p10). The S_2 to S_4 subsites on the enzyme (see section 1.3.4.) that the tetrapeptide inhibitors Ac-YVAD-H or Ac-YVAD-CMK (Thornberry et al., 1992) bind to are composed of side chains from the p10 subunit. The P_2 and P_3 residues in the inhibitor (alanine and valine respectively), which are accommodated by the S_2 and S_3 subsites, are exposed on the exterior. This accounts for the ability of these residues to be substituted quite liberally without a dramatic decrease in the inhibitory ability of the tetrapeptide. The P_4 residue, in this instance tyrosine, sits in a hydrophobic groove formed by the p10 subunits, explaining why the substitution of this residue in the inhibitor for a non-hydrophobic amino acid results in a decrease in its effectiveness. All of the residues that are required for either catalytic activity or the specificity of the enzyme towards aspartate residues are conserved between ICE and Ced-3, and also appear to be present in the other homologues. The mutation of Cys 285, His 237 or Arg 179 residues abolishes the ability of ICE to cleave either pro IL-1 β or itself (Walker et al., 1994a; Wilson et al., 1994).

ICE is able to autoprocess, i.e. it cleaves itself to form the mature active enzyme (Thornberry et al., 1992; Cerretti et al., 1992), and in order to do this the enzyme is required to form oligomers (Gu et al., 1995). There appears to be a defined sequence of events in the autoactivation of proICE. ProICE (p45), present in the cytoplasm, has no enzymatic activity towards proIL-1 β , but is weakly active towards itself, as evaluated by the ability of a biotinylated, irreversible inhibitor of ICE to bind to a particular form of the enzyme. This activity of the p45 results in the formation of a p33/p12 intermediate (where p12 is the linker region plus the p10 subunit), which has a greater catalytic activity, and is active towards both p45 and itself. The autocatalysis of p33/p12 gives rise to a p20/p10 dimer, which corresponds to the mature enzyme and the only form that can cleave proIL-1 β . Conversely, if cleavage of p45 initially occurs after the prodomain to yield a p32 protein, this is catalytically inactive (Yamin et al., 1996).

To further complicate matters, Alnemri et al. (1995) have identified four alternatively spliced variants of ICE: ICE α , β , γ , δ and ϵ . ICE α is the whole p45 protein. ICE β , which lacks amino acids 92-112 i.e. part of the prodomain, and ICE γ , which is missing amino

acids 20-112, corresponding to most of the prodomain, are both active. In contrast, ICE δ , which lacks amino acids 288-335 encompassing both the linker region and the cleavage sites that separate the p10 and p20 subunits, and ICE ϵ , which lacks amino acids 20-335 corresponding to the prodomain and the majority of the p20 subunit, are catalytically inactive. Although ICE ϵ is in effect the p10 subunit minus the first nineteen amino acids, when complexed with p20 it is unable to form an active enzyme, due to the involvement of these nineteen amino acids in formation of the tetramer. However, the presence of the translated products of these spliced variants has yet to be detected in whole cells (Alnemri et al., 1995). Some other ICE/Ced-3 homologues have also been shown to have splice variants, notably Ich-1 which has both a long (Ich-1_L) and (inhibitory) short form (Ich-1_S) (Wang et al., 1994). This indicates another means by which these enzymes may be regulated.

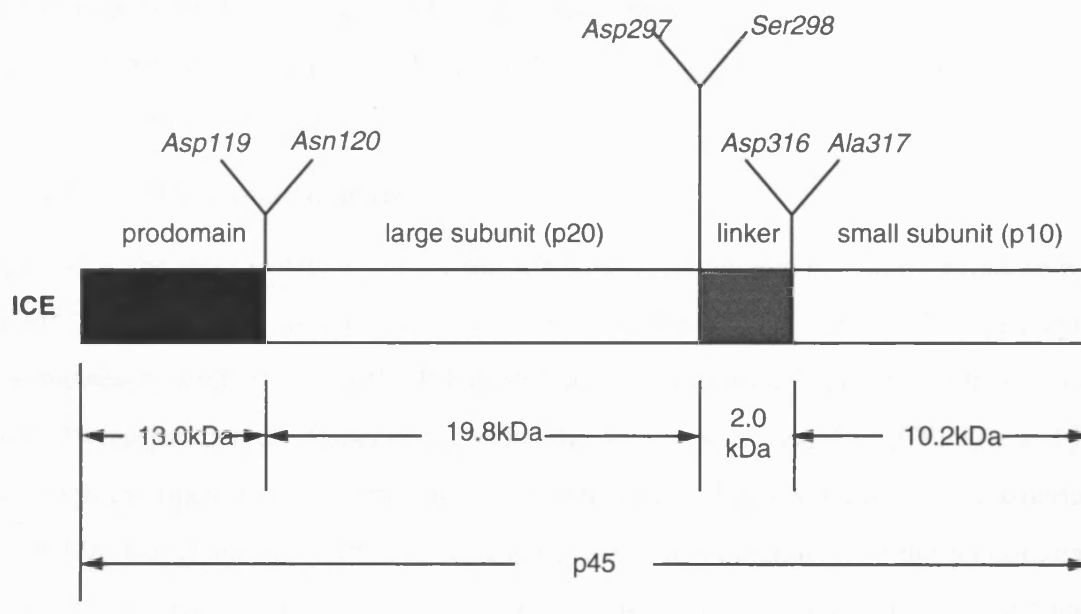


Figure 1e. An illustration of the proform of ICE

The residues indicated are those at which cleavage must occur for conversion of the proenzyme to the mature active form. Note the presence of the 2 kDa linker region between the p10 and p20 subunits, a feature present in only a few ICE-like proteases (Adapted from Thornberry et al., 1992).

Upon finding that *ced-3* showed homology with ICE, it was necessary to demonstrate that ICE was capable of inducing apoptosis. Miura et al. (1993) demonstrated that overexpression of either the *ced-3* or ICE genes in Rat-1 fibroblasts was able to induce apoptosis. In both instances this was dependent upon the cysteine protease activity of the proteins, as mutations in the active site QACRG motif prevented the induction of apoptosis (Miura et al., 1993).

The possibility does exist that ICE may be a family member that is not responsible for causing apoptosis. Evidence to this effect was provided by two studies in which ICE knockout mice were generated (Li et al., 1995; Kuida et al., 1995). In both instances the development of ICE^{-/-} mice was apparently normal by general anatomical and histological examination. The mice reached maturity, were fertile and did not develop spontaneous tumours during the time period during which the studies took place (16-25 weeks). Unsurprisingly, monocytes from the ICE^{-/-} mice failed to produce any mature IL-1 β upon stimulation with lipopolysaccharide, a proinflammatory endotoxin. Thymocytes isolated from the ICE^{-/-} mice also underwent apoptosis in response to dexamethasone and ionising radiation as normal, but were resistant to apoptosis induced by cross linking of the Fas receptor (Kuida et al., 1995). Thus, it seems that the only absolute requirement of ICE is in the production of mature IL-1 β and in Fas-induced apoptosis in thymocytes: it certainly does not seem to be vital for the programmed cell death that must occur during the development of the mouse. Either ICE is not involved in apoptosis at all, or its function can be substituted for by other ICE/Ced-3 family members.

1.3.4.2. CPP32/ Yama/ apopain

After ICE, the most widely characterised ICE/Ced-3 homologue is cysteine protease p32 (CPP32), a 32 kDa protein that was originally cloned from Jurkat T lymphocytes (Fernandes-Alnemri et al., 1994). It has 35% identity with Ced-3, and 30% identity with ICE. Two separate mRNA species encoding the protein were identified (CPP32 α and β), although the open reading frames in both differ only in the substitution of an aspartate (CPP32 α) for glutamate (CPP32 β), and the β isoform is thought to be the predominant form. It appears to be widely expressed: it is present in all haemopoietic cell lines examined, and has also been detected in the brain and embryonic cell lines. CPP32 was found to be the enzyme responsible for the apoptotic breakdown of poly (ADP-ribose) polymerase (PARP) (Lazebnik et al., 1994; Nicholson et al., 1995; Tewari et al., 1995), and using a tetrapeptide inhibitor based upon the amino acid sequence in PARP recognised by CPP32 (Asp-Glu-Val-Asp) (see Figure 1f), the enzyme was purified to homogeneity from THP.1 cells (Nicholson et al., 1995).

The three dimensional structure of CPP32 has been determined (Rotonda et al., 1996), and its structure is broadly similar to that of ICE. Like ICE it combines two heterodimers

to form a tetramer with two-fold rotational symmetry. The catalytic site and S₁ aspartate recognition site of CPP32 are similar to the corresponding sites in ICE. The S₂ and S₃ subsites in CPP32 are orientated so that the side chains of the P₂ and P₃ residues of the substrate point away from the protein and towards the solvent, allowing these residues to be liberally substituted without detriment to the efficiency of cleavage by the enzyme. The most radical difference between ICE and CPP32, however, involves the structure of the S₄ pocket. In ICE this pocket is a large shallow cavity bordered by hydrophobic residues which are able to accommodate the tyrosine that is present in the P₄ position of the inhibitor Ac-YVAD-CHO (see section 5.1). The S₄ subsite in CPP32 is much narrower, and closely surrounds the P₄ aspartate of the CPP32 inhibitor Ac-DEVD-CHO (see section 5.1.). CPP32 also contains an additional loop which is not present in ICE, which also participates in defining the dimensions of the S₄ pocket. The residues that form this loop are conserved amongst the Ced-3 subfamily, but are not present in those proteases that resemble ICE more closely such as TX or ICE_{relIII}. This suggests that those enzymes that bear a close structural relationship to CPP32 may also share substrate specificity.

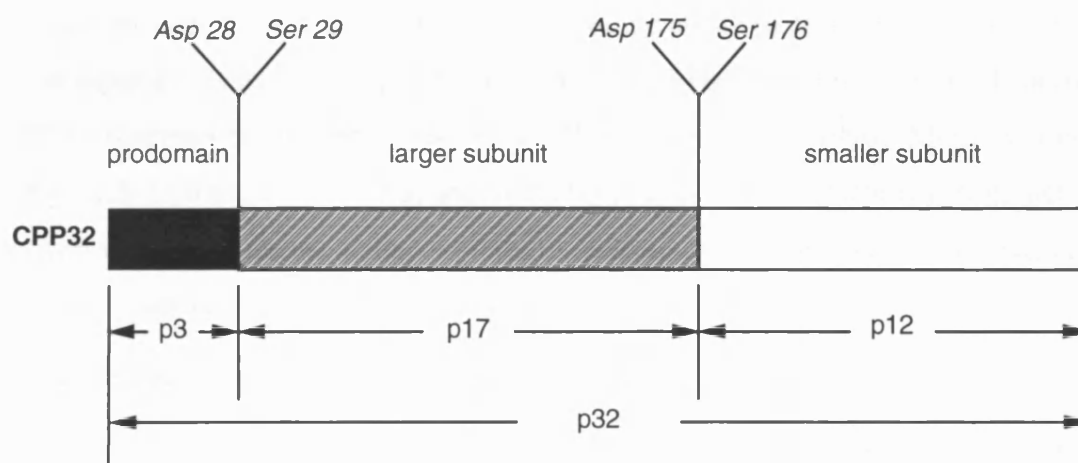


Figure 1f. Diagram of CPP32 indicating the points at which it is cleaved to yield the active mature enzyme

CPP32 is cleaved at the sequence Glu-Ser-Met-Asp²⁸-Ser to release the prodomain and again at the sequence Ile-Glu-Thr-Asp¹⁷⁵-Ser to separate the large and small subunits (adapted from Nicholson et al., 1995).

There is conflicting evidence regarding the activation of CPP32. It has been demonstrated that partially purified CPP32 from HeLa cells is itself capable of cleaving

CPP32 labelled with [³⁵S] methionine (Wang et al., 1996b), although the possibility of another enzyme also being present in the HeLa cell extract which could also be responsible for this activation cannot be ruled out. It has also been demonstrated that ICE can activate CPP32 (Tewari et al., 1995), although the fact that apoptosis on the whole proceeds in a normal manner in ICE knockout mice (Li et al., 1994; Kuida et al., 1994) would indicate that CPP32 can be activated by other mechanism(s).

CPP32 can be activated by granzyme B (Darmon et al., 1995; Quan et al., 1996; Martin et al., 1996). Cytotoxic T lymphocytes and Natural Killer cells kill their target cells by making contact with them and releasing granules into the cytoplasm of the target cell by exocytosis, following which the target cell undergoes apoptosis (reviewed by Greenberg, 1996). Both the protein perforin and a series of serine proteases known as granzymes are required for the death of the cell. Perforin is related to members of the complement protein family, and oligomerises to form pores in the plasma membrane of the target cell. Cytotoxic T cells are unable to kill the target cell without this happening.

Four granzymes from humans have been purified to homogeneity: granzymes A, B, 3 and M. They all have varying substrate specificities and seem to act synergistically to cause the death of the target cell. Granzyme B is the most potent, and is the only known enzyme outside of the ICE/Ced-3 family to have the ability to cleave proteins C-terminal to an aspartate residue. Granzyme B has been shown to be able to proteolytically activate CPP32 (Darmon et al., 1995; Quan et al., 1996; Martin et al., 1996), Mch3 (Gu et al., 1996), Ich-3 (Wang et al., 1996a) and Mch2 (Orth et al., 1996a) (table 1a). Although not universally applicable, the ability of granzyme B to activate these enzymes illustrates how apoptosis may be induced in this particular instance.

1.3.4.3. Substrates of the ICE family of proteases

Substrates of the ICE/Ced-3 family are being discovered at a comparable rate to that at which new proteases are being identified. The first recognised substrate was, of course, interleukin-1 β , which is cleaved by ICE. However, the cleavage of proIL-1 β has never been conclusively connected with apoptosis. The first substrate to be linked with apoptosis was PARP (Kaufmann et al., 1993; Lazebnik et al., 1994). PARP is a DNA repair enzyme, which binds to single stranded breaks and attaches long chains of ADP-ribose to certain nuclear proteins such as nuclear matrix proteins (including itself). The

ADP-ribose is derived from nicotinamide adenine dinucleotide (NAD^+), the precursor of which is ATP which is utilised as a source of energy to enable the cell to die in a controlled manner. Thus, it has been postulated that if PARP remained functional during the later stages of apoptosis when DNA is substantially degraded, it may deplete the energy stores of the cell and, having insufficient energy to complete the cellular fragmentation of apoptosis, the cell could die by necrosis resulting in an inflammatory response (Earnshaw, 1995).

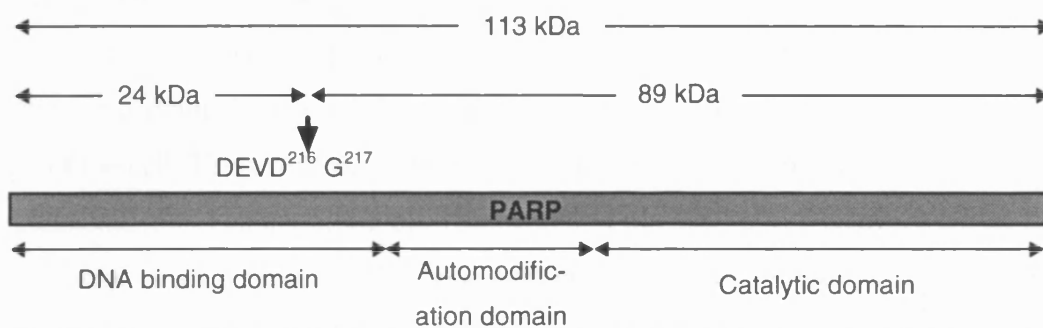


Figure 1g. Poly(ADP-ribose) polymerase (PARP) and the sequence at which cleavage occurs during apoptosis.

The protease which cuts PARP (113 kDa) e.g. CPP32, recognises the amino acid sequence Asp-Glu-Val-Asp (DEVD) within PARP and cuts between Asp 216 and Gly 217 to yield two fragments of 24 and 89 kDa. In doing this, the DNA binding domain is separated from the catalytic and automodification domains and the activity of PARP is prevented.

PARP was first found to be broken down in HL-60 cells stimulated to undergo apoptosis by treatment with chemotherapeutic agents (Kaufmann, 1989; Kaufmann et al., 1993). It is cleaved into two discrete fragments of 24 kDa (containing the zinc-finger domain via which the enzyme detects damaged DNA) and 89 kDa (the catalytic domain and automodification domain) (see Figure 1g). PARP was found to be cleaved by extracts from transformed chicken DU249 hepatoma cells that had been arrested at S-phase with aphidicolin followed by accumulation in M-phase by treatment with nocodazole. As an Asp residue was present at the cleavage site, the degradation of PARP was consistent with it being cut by a protease resembling ICE (prICE), although not by ICE itself (Lazebnik et al., 1994). Subsequently, PARP has been shown to be cleaved by CPP32 (Nicholson et al., 1995; Tewari et al., 1995) and by Mch3 (Fernandes-Alnemri et al., 1995b). DNA-dependent protein kinase, another DNA repair enzyme, which participates in the repair of double-stranded DNA lesions, is also cleaved by CPP32 during apoptosis (Casciola-Rosen et al., 1995; Casciola-Rosen et al., 1996; Song et al., 1996). In addition,

the 70 kDa protein component of the U1 small nuclear ribonucleoprotein (U1-70KDa snRNP), which is essential for the processing of mRNA, is also degraded by this enzyme (Casciola-Rosen et al., 1994; Casciola-Rosen et al., 1996). The cleavage of U1-70KDa snRNP could participate in shutting down transcription and translation, which are required for the function of the DNA repair machinery.

In addition to DNA repair enzymes, another emerging subset of proposed substrates for ICE/Ced-3 homologues during apoptosis consists of structural proteins. Gas2, the product of one of the growth arrest specific genes, has around 40 amino acids removed from its C terminus during apoptosis at a cleavage site adjacent to an aspartate residue, resulting in a dramatic rearrangement of the actin cytoskeleton and an alteration in the shape of the cell. This event may contribute to the formation of the membrane blebs that are characteristic of an apoptotic cell (Brancolini et al., 1995). The cleavage by an ICE-like protease of actin itself has also been demonstrated, albeit only *in vitro* (Mashima et al., 1995; Kayalar et al., 1996). Another component of the cytoskeleton, α -fodrin/ non-erythroid spectrin, is also cleaved during apoptosis (Martin et al., 1995) by an ICE-like protease activity which is distinct from that responsible for cleaving PARP (Cryns et al., 1996). The D4 haemopoietic cell GDP dissociation inhibitor (D4 GDI), a member of the Ras-related rho family of G proteins is degraded by CPP32 during apoptosis, resulting in the activation of G proteins which has also been suggested to have effects upon the actin cytoskeleton (Na et al., 1996). Nuclear lamins (lamins A, B₁ and B₂) are degraded by Mch2 α (Takahashi et al., 1996; Orth et al., 1996a) and the inhibition of this step prevents the condensation of chromatin against the nuclear membrane during apoptosis, although it does not prevent the degradation of DNA (Lazebnik et al., 1995).

Tumour suppressor genes are another potential subset of targets for the ICE/Ced-3 family. The cleavage of the hypophosphorylated form of the retinoblastoma protein (Rb), which has been proposed to have an inhibitory effect against apoptosis, has been shown to be cleaved in HL-60 and U937 cells exposed to chemotherapeutic agents (An and Dou, 1996) and in THP.1 cells exposed to a variety of stimuli (Browne et al., submitted). In addition, the adenomatous polyposis coli (APC) protein, which is constitutively expressed in many tissue types and is thought to regulate cell-cell adhesion via its interaction with β -catenin, is also cleaved in THP.1 cells (Browne et al., submitted). The

implications of this are not yet understood.

Various members of signal transduction families have also been identified as substrates, including protein kinase c δ (Emoto et al., 1995) and sterol regulatory element binding proteins (SREBP) 1 and 2 (Wang et al., 1995; Wang et al., 1996b). The reasons why the cleavage of these proteins during apoptosis would be required are unclear.

1.3.5. The Fas receptor and its signalling mechanism

The Fas receptor or antigen, also referred to as APO-1 and CD95, has attracted particular interest due to its role in inducing apoptosis in cells expressing the receptor on their surface, which are predominantly cells of the immune system. The Fas receptor is a 45 kDa Type I membrane bound receptor, and is part of the tumour necrosis factor (TNF)/ nerve growth factor receptor family (reviewed by Nagata and Golstein, 1995). The cytoplasmic region of the receptor does not contain any consensus sequences that are commonly seen on other receptors. It does however, contain a region of approximately 65 amino acids known as the 'death domain', which is also present in TNF receptor type I (TNFR-1) and in the product of the *Drosophila* gene *reaper* (Golstein et al., 1995), both of which can cause a cell to enter apoptosis. The death domain is also found on many of the proteins which interact with the receptor in the cytoplasm, and it appears to act as a specific protein structure which enables the aggregation of these proteins.

The pathological importance of this mechanism of inducing cell death is illustrated by mice with the *lpr* (lymphoproliferation) mutation, which results in the greatly reduced expression of the Fas receptor (Watanabe-Fukunaga et al., 1992). These mice have fatal phenotypic abnormalities including raised levels of autoantibodies, enlarged lymph nodes and splenomegaly. These symptoms are akin to those of the autoimmune disease systemic lupus erythematosus (SLE), which implies that an abnormality in Fas-induced cell death may also be involved in the aetiology of this condition.

The Fas receptor is bound by the Fas ligand (FasL), which is a type II membrane-bound protein belonging to the tumour necrosis factor family (Suda et al., 1993). It is constitutively expressed in the testis, the kidney, the small intestine and the lung, and it is also expressed on the surface of activated T cells. Binding of FasL to the Fas receptor is frequently via contact between two cells, one bearing the Fas receptor and the other

FasL, although FasL can also be released as a soluble form following cleavage by a cell surface Zn^{2+} dependent metalloproteinase (Mariani et al., 1995; Kayagaki et al. 1995). Mice bearing the *gld* (generalised lymphoproliferative disease) mutation, which is non-allelic to the *lpr* mutation, display a phenotype virtually indistinguishable from that of the *lpr* mice. The *gld* mutation is the result of a Phe → Leu alteration in the C-terminus of the FasL, which prevents it binding to the Fas receptor (Takahashi et al., 1994; Hahne et al., 1995).

Upon ligation, the receptor forms a trimer with neighbouring receptors which allows the assembly of the death-inducing signalling complex (DISC), the constituents of which are gradually being identified (reviewed by Peter et al., 1996). The DISC consists of a number of proteins that interact via the death domain on either the TNF receptor or the Fas receptor. Mice with the *lpr^{cg}* mutation have a point mutation in the death domain of the Fas receptor, and display the same phenotype as *lpr* mice. This mutation prevents the aggregation of these proteins to form the DISC, preventing the initiation of the death signal (Watanabe-Fukunaga et al., 1992).

Despite the identification of a series of other proteins that may or may not be part of the DISC, current evidence suggests that the Fas-associated death domain protein/ mediator of receptor-induced toxicity (FADD/MORT-1) is a crucial component of this complex. FADD/MORT-1 is a 28 kDa protein associating with the death domain of both the Fas receptor (Boldin et al., 1995; Chinnaiyan et al., 1995) and TNFR-1 (Chinnaiyan et al., 1996a), via a homologous death domain on its own C-terminus. The N-terminus of the protein is required for self-association and the induction of apoptosis (Boldin et al., 1995). Overexpression of the protein induces apoptosis independent of ligation of the Fas receptor. All tissues examined that express Fas also express FADD/MORT-1, and FADD/MORT-1 mutants that are able to associate with the Fas receptor are unable to attach other identified members of the DISC (Boldin et al., 1995; Chinnaiyan et al., 1995; Chinnaiyan et al., 1996a).

In addition to FADD/MORT-1, there are four CAP proteins (cytotoxicity-dependent APO-1-associated proteins) which also bind to Fas upon ligation and trimerisation of the receptor. CAP 1 and CAP 2 have subsequently been identified as serine and threonine phosphorylated FADD/MORT-1, whereas CAP 4 has recently been identified as a

member of the ICE-like protease family and re-termed MACH or FLICE, with CAP 3 being the cleaved prodomain of CAP 4 (Boldin et al., 1996; Muzio et al., 1996). This is the first instance of an ICE-like protease family member which has been found to be associated with another protein, in this instance a membrane-bound receptor, and it may give an insight into why Fas-induced cell death occurs so quickly.

Further down the signalling pathway, a number of ICE-like proteases have been shown to be involved. Initial evidence suggested that ICE itself is involved in the pathway (Los et al., 1995; Enari et al., 1995), and this will be further discussed in chapter 5. It has also been found that CPP32 is activated in Fas-mediated apoptosis (Schlegel et al., 1996; Hasegawa et al., 1996). However, it remains to be seen whether the enzyme that is activating CPP32 is MACH/FLICE.

1.4. THE PATHOLOGICAL IMPLICATIONS OF APOPTOSIS

The explosion of research into apoptosis that has occurred in recent years mainly stems from the pathological implications of inappropriate apoptosis. Some of the most widespread and distressing ailments of modern times have been linked to malfunctions in the regulation of this form of cell death. Such diseases fall into two categories: those that are caused by insufficient apoptosis and those that are caused by excess apoptosis. Into the latter category falls the acquired immune deficiency syndrome (AIDS), caused by the human immunodeficiency virus (HIV). One of the symptoms of HIV infection is the depletion of CD4⁺ T lymphocytes, which are important in forming immunity against a variety of viral infections, and the depletion of these cells ultimately results in the weakening of the immune system. This depletion most probably arises through an increased susceptibility of the CD4 cells to apoptosis. This has been proposed to be mediated via an increased expression of the Fas receptor (Debatin, 1996), or as a result of the action of the HIV glycoprotein gp120. Normally, the simultaneous occupation of CD4 and the T cell receptor by antigen/ major histocompatibility class II complexes on the surface of antigen presenting cells results in the activation of the T cell. However, the occupation of CD4 by gp120 prior to the ligation of the T cell receptor may result in a confusion of signals causing the cell to commit suicide once the T cell receptor becomes occupied (Orrenius, 1995; Thompson, 1995). Furthermore, an increase in the production of certain cytokines, e.g. tumour necrosis factor α , has been documented, some of which

are capable of causing apoptosis. Also, an elevation in oxidative stress has been documented in the early stages of HIV infection, a situation which can lead to apoptosis (Orrenius, 1995).

A number of neurodegenerative conditions have also been linked with an increase in apoptosis. In Alzheimer's disease, for instance, it seems that neurons in the hippocampus die prematurely resulting in progressive memory loss. This cell death is thought to be by apoptosis, although the exact mechanisms are unknown. Increased deposits of the β -amyloid peptide have been linked with the progression of Alzheimer's disease, and this protein has been shown to cause apoptosis in neuronal cells, possibly by preventing neuronal growth factors necessary for the survival of these cells from reaching their targets (Thompson, 1995).

Huntington's disease, a genetic disorder resulting in neurodegeneration which again is thought to be caused by apoptosis has been associated with a lesion in the *HD* gene. The function of huntingtin, the product of the *HD* gene, is unknown, but an indication of the importance of its function can be seen in *HD* null mice which die early on in embryonic development. The nature of the genetic fault in this disease is the expansion of a CAG repeat which results in the presence of a polyglutamine tract, and the length of this repeat results in the increased sensitivity of huntingtin to cleavage by CPP32 (Goldberg et al., 1996) (section 1.3.4.2.). However, the implications of this discovery are uncertain (reviewed by Rosen, 1996).

The product of the NAIP (neuronal apoptosis inhibitory protein) gene has been linked to the hereditary spinal muscular atrophy neurodegenerative disorders that result in the progressive loss of motor neurons in the spinal column. The product of this gene has homology to the inhibitor of apoptosis (IAP) protein from the baculovirus, which prevents apoptosis in insect cells. This would suggest that the loss of this protein results in the increased sensitivity of motor neurons such cells to apoptosis (Roy et al., 1995).

Into the category of diseases where insufficient apoptosis occurs falls diseases such as psoriasis, insulin-dependent diabetes mellitus, rheumatoid arthritis and systemic lupus erythematosus (SLE). A murine model of autoimmunity has been established in *lpr* and *gld* mice which have mutations in the Fas receptor and Fas ligand respectively resulting in the failure of target cells to undergo apoptosis via the Fas receptor (see section 1.3.5.).

A rare mutation of the Fas receptor similar to that of *lpr* mice has been identified in humans, and patients with this mutation display a similar phenotype to the *lpr* mice (Debatin, 1996).

Insufficient apoptosis can also be a contributory factor in both the initiation and progression of cancer. It was initially assumed that a tumour arose as a consequence of an increase in the rate of division in the cells therein. The supposition that tumour cells divided more frequently than normal cells was the basis for the design of many chemotherapeutic agents, for example inhibitors of topoisomerase II. However, it is becoming increasingly apparent that the deregulation of apoptosis plays an equally important role in cancer development. Apoptosis does occur within tumours, although probably to a lesser extent than in normal tissues. As in normal cells this acts to balance out mitosis, and the relative rates of cell division and cell death determine the speed at which the cancer grows.

Much of the disruption of apoptosis in the advance towards malignancy arises as a result of the expression of Bcl-2 and/or its homologues (see section 1.3.1). Bcl-2 was first isolated from a B cell lymphoma, and an elevation in its expression has been detected in a number of cancers such as non-Hodgkin's lymphomas and cancers of the lung, prostate and colon. An elevation of Bcl-2 and Bcl-x and a decrease in the expression of Bax has been observed in breast carcinomas and has been associated with a poor response to chemotherapy and a low survival rate. The expression of both Bcl-2 and Bax has been linked to the actions of the tumour suppressor gene p53 (section 1.3.2.), which responds to DNA damage by causing either cell cycle arrest or apoptosis. Radiotherapy and many chemotherapeutic agents cause DNA damage, and in response to such stimuli a down regulation in Bcl-2 expression has been observed, potentially due to the action of p53 as a transcriptional repressor. If p53 function is lost, then an elevation in Bcl-2 levels would prevent the cell from dying, but would not stop the genomic damage occurring as a result of the therapy. This enhances the potential for mutation and the acquisition of an increasingly transformed phenotype, and increases the likelihood of relapse (reviewed by Reed, 1995). Bcl-2 has also been shown to act co-operatively with the oncogene *c-myc*. The deregulation of *c-myc* has been demonstrated to cause apoptosis in fibroblasts deprived of serum, whereas the expression of Bcl-2 rescues these cells in the same circumstances (Fanidi et al., 1992).

In contrast to HIV, which exerts its effects by killing those cells whose purpose it is to combat viral infection, a number of viral gene products have been found to act to prevent the host cell from undergoing apoptosis on infection. This is necessary for the cell to survive: if the cell was to die upon infection the virus would be unable to use the replicative machinery of the host and proliferation of the virus would be impossible.

When infected by a virus, it is the response of the host cell to go into apoptosis in order to prevent the virus from reproducing. Therefore, the acquisition of a means of preventing the death of the host cell represents a significant survival advantage for the virus. For example, the adenovirus encoded protein E1B19K, which is homologous in both structure and behaviour to the Bcl-2 family of proteins, is functionally interchangeable with Bcl-2, and can form a heterodimer with Bax via the BH1 and BH2 domains present within all members of the Bcl-2 family. Bcl-2 homologues have also been found in the Epstein-Barr virus and the African swine fever virus (reviewed by White, 1996).

The cowpox virus encodes the serpin cytokine response modifier A (CrmA), which is an extremely effective inhibitor of ICE (Ray et al., 1992; Komiyama et al., 1994), although it is less effective at inhibiting other ICE/Ced-3 proteases (Nicholson et al., 1995). However, it is uncertain whether the function of CrmA is merely to prevent a pro-apoptotic action of ICE, or if its principal purpose is to suppress the inflammatory response which exists as the primary line of defence against viral infection.

The examples provided here illustrate the breadth of conditions which are influenced by apoptosis, but they remain the most intensively investigated cases. It remains to be seen whether deregulated apoptosis is also implicated in other conditions such as osteoporosis or stroke.

1.5 BACKGROUND TO THE CELL MODELS USED IN THIS THESIS

1.5.1. The thymus

Thymocytes have been used extensively in the study of apoptosis, as these cells are undergoing negative selection which results in them dying by apoptosis, and the fact that so many thymocytes die very readily has made this an extremely popular and well-used system with which to study the apoptotic process. In this thesis, they have been used

both for the study of DNA fragmentation (Chapter 3) and Ca^{2+} flux (Chapter 4) in the context of apoptosis.

The thymus gland is a primary lymphoid organ in which progenitor cells from the bone marrow mature and differentiate into T lymphocytes. It is at its largest just after birth, after which it atrophies with ageing. The thymic cortex mainly contains immature thymocytes which undergo maturation and migrate to the medulla, which they leave to enter the blood circulation.

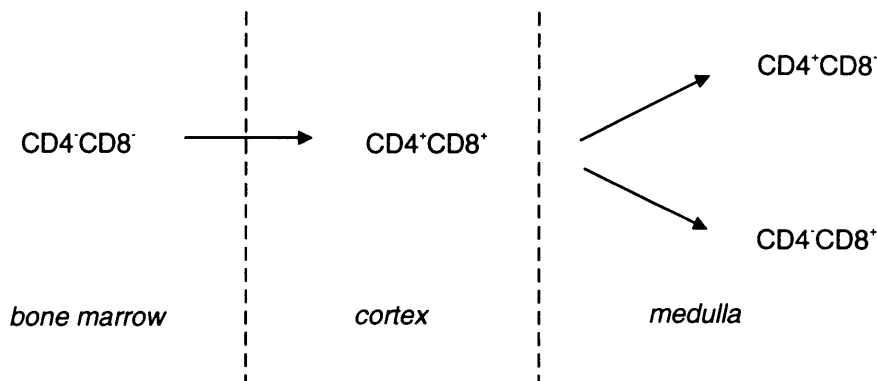


Figure 1h. The development of thymocytes from immature progenitor $\text{CD4}^-\text{CD8}^-$ double negative cells into mature T lymphocytes. Genetic rearrangement of the Ti portion of the T cell receptor occurs within the thymic cortex, followed by negative selection into single positive cells which pass through the medulla to enter the blood stream.

A number of cell-surface markers appear during the development of a T lymphocyte. The T cell receptor (TcR) consists of an antigen-recognising receptor (Ti), in close contact with CD3. CD3 is invariant and thought to act in signal transduction, whereas Ti is variable as a result of genetic recombination, and enables the generation of a cell population that has the potential to recognise a wide variety of antigens. Shortly after the appearance of the T cell receptor, CD8 then CD4 (both invariant) appear on the cell surface. Thus, immature thymocytes consist principally of $\text{Ti}^+\text{CD}^{3+}\text{CD}^{4+}\text{CD}^{8+}$ cells, or double positive cells. Following maturation thymocytes lose either CD4 or CD8, so that the mature cells in the thymic medulla consist of both $\text{Ti}^+\text{CD}^{3+}\text{CD}^{4+}\text{CD}^{8-}$ and $\text{Ti}^+\text{CD}^{3+}\text{CD}^{4-}\text{CD}^{8+}$ cells, known as single positive cells.

However, only around 5-10% reach the single positive stage, with the majority of thymocytes undergoing deletion in the cortex. The 90% or so that do not reach maturity undergo negative selection, as they express T cell receptors that recognise self rather

than foreign antigens, and they die by apoptosis. The appropriate eradication of these cells is essential to prevent autoimmunity.

1.5.2. THP.1 cells

Monocytes are part of the monocyte-macrophage component of the immune response. They originate from myeloid precursor cells in the bone marrow, and do not have any antigenic specificity. Following entry into the blood stream as monocytes, they migrate to other tissues where they differentiate into components of the reticuloendothelial system such as Kupffer cells in the liver or alveolar, splenic and peritoneal macrophages. Human monocytes are difficult to obtain in large quantities so to enable the study of monocyte function in a cell culture environment the THP.1 cell line was established. THP.1 cells are derived from the blood of a boy with acute monocytic leukaemia (Tsuchiya et al., 1980), and they have been used as an *in vitro* model for the role of monocytes in the immune response as they retain many of the features of non-leukaemic monocytes over several months in culture. THP.1 cells have been demonstrated to release mature IL-1 β in response to stimulation by lipopolysaccharide, urea or silica (Matsushima et al., 1986), and thus were used for the purification of ICE (Kronheim et al., 1992; Thornberry et al., 1992; Miller et al., 1993). For this reason they were chosen as an appropriate cell line to use for the study of proteolysis in apoptosis.

1.5.3. Jurkat T lymphocytes

Jurkat cells are derived from a patient with lymphoblastic leukaemia, and have been used as a cell culture model for differentiated T cell function. They retain many of the features of non-leukaemic T cells, despite having a deletion in the short arm of chromosome 2 characteristic of patients with acute lymphoblastic leukaemia (LaGree et al., 1988).

The behaviour of Jurkat cells in response to a monoclonal antibody against the Fas receptor has been characterised (Weis et al., 1995). They take on an apoptotic morphology including plasma membrane blebs and chromatin condensation whilst maintaining membrane integrity at around 45 minutes, coincident with the onset of DNA degradation. This occurred in virtually the whole population, which makes it a useful model for the preparation of lysates with which to study the induction of apoptosis *in vitro*. Fas-induced apoptosis in these cells was unaffected by the presence or absence of the divalent cations Ca²⁺, Mg²⁺ and Zn²⁺, and again was insensitive to chemical inhibitors

of protein kinases, protein phosphatases, calmodulin or free radicals. It was, however, modulated by the protease inhibitors N α -tosyl-L-phenylalaninyl chloromethylketone (TPCK) and 3,4-dichloroisocoumarin.

The experimental work in this thesis has been divided into three chapters. The first deals with an examination of the sequences of the DNA fragments produced during thymocyte apoptosis. The second chapter, also using thymocytes, examines the induction of apoptosis by a series of chemical agents, and the effects of inhibitors of both intracellular Ca²⁺ elevation and proteolysis on this process. The final results chapter describes the manner in which inhibitors of the ICE/Ced-3 family of proteases prevent the execution of apoptosis in both THP.1 cells and Jurkat T cells, and the participation of members of this protease family in Fas-mediated apoptosis is also examined.

CHAPTER 2

MATERIALS AND METHODS

2.1 THE INDUCTION AND ASSESSMENT OF APOPTOSIS

All reagents used in this chapter were purchased from Sigma Chemical Co., Poole, U.K. unless otherwise stated.

2.1.1. Isolation of thymocytes

For the work described in Chapter 4, thymocytes were isolated from 4-5 week old male Fischer 344 rats, bred at the University of Leicester and allowed food and drink *ad libitum*. and sacrificed by overdose with Sagatal (sodium pentobarbitone) (Rhône Mérieux, Harlow, U.K.) (600 mg/kg, intraperitoneal). For the work described in Section 2.2 and Chapter 3, six week old male 129 mice (Harlan and Olac, Bicester, U.K.) were sacrificed by cervical dislocation and the thymus removed as for the rat.

Following sacrifice of the animal, the thymus was rapidly removed, stripped of any connective tissue or lymph nodes that were attached to it and placed in Krebs-Henseleit buffer (pH 7.4, 4°C). Following calculation of the ratio of the thymus to body weight, any animal with a ratio of less than 300 mg/ 100g was discarded. The thymus was then minced by chopping in two directions using a McIlwain tissue chopper (Mickle Laboratory Engineering, Gomshall, U.K.), passed through a nylon sieve into Krebs-Henseleit and then filtered through nylon bolting cloth.

The cells were then diluted 1 in 5 in trypan blue and counted using an Improved Neubauer haemocytometer and the viability, which was normally >97%, was calculated. The cells were then diluted to 20×10^6 cells/ml in RPMI 1640 (Gibco BRL, Paisley, U.K.) containing 10% foetal calf serum (Gibco). Incubations were carried out at 37°C under an atmosphere of 95% air, 5% CO₂.

2.1.2. Induction of apoptosis

The standard concentrations for the agents used were: dexamethasone, 0.1 µM; etoposide, 10 µM; staurosporine, 1 µM. Dexamethasone was made up as a 10 mM stock in 100% ethanol, and etoposide and staurosporine were kept as 10 mM stocks in DMSO. Thapsigargin, 2,5-di-(*t*-butyl)-1,4-benzohydroquinone (tBHQ) (Fluka, Gillingham, U.K.) and cyclopiazonic acid (CPA) (Calbiochem-Novabiochem, Nottingham, U.K.) were kept as stocks in DMSO at 1.5 mM, 100 mM and 10 mM respectively. TLCK (Boehringer Mannheim, Lewes, U.K.) was made up in PBS at 50

mM immediately prior to use. Vehicle was never at a concentration of more than 0.1%. When treating thymocytes, TLCK and econazole were added 1 hour prior to the addition of the agent being used to induce apoptosis, to enable the compounds to bind to their targets. The cells were then incubated for a further 4 hours, following which the level of apoptosis was assessed.

2.1.3. Quantification of apoptosis by flow cytometry

Many studies have quantified apoptosis by counting cells stained under the microscope. This approach has a number of drawbacks: the population of cells is greatly reduced, and it is susceptible to human error. If morphology is the criterion by for distinguishing between a normal and an apoptotic cell, then to an extent the counting relies upon the discretion of the counter. If the assessment of apoptosis within a population is by trypan blue exclusion, it is impossible to tell whether the non-viable cells that take up the dye have undergone apoptotic or necrotic cell death. Whilst it is possible to determine the presence of apoptotic cell within a population by analysing the extent and the manner of DNA degradation for example by agarose gel electrophoresis, this does not allow the quantification of apoptosis.

The flow cytometric method that is used in our laboratory relies on the alteration in dye uptake depending on the state of the cell. The cells are stained with both the bisbenzimidazole dye Hoechst 33342 and with propidium iodide (Sun et al., 1992). Only dead cells are able to include propidium iodide, whilst cells that are either normal or apoptotic (i.e. cells that are still viable) take up the Hoechst 33342. Thus on this basis alone, dead cells can be separated from the rest by plotting red fluorescence against blue fluorescence. In addition, the cells that include Hoechst 33342 can be subdivided by virtue of the apoptotic cells being (a) smaller, and thus having a lower forward light scatter, and (b) having a higher fluorescent intensity in comparison with normal cells, due to their increased membrane permeability enabling the cell to take up a greater quantity of dye (Ormerod et al., 1993). Hence, plotting forward light scatter versus fluorescence intensity allows the separation and quantification of both apoptotic and dead cells within a cell population. If the population of high blue-fluorescing cells is isolated and analysed, they have an apoptotic morphology, and their DNA exhibits a laddering pattern upon

electrophoresis. In contrast, the low blue fluorescing cells have a normal morphology and intact DNA.

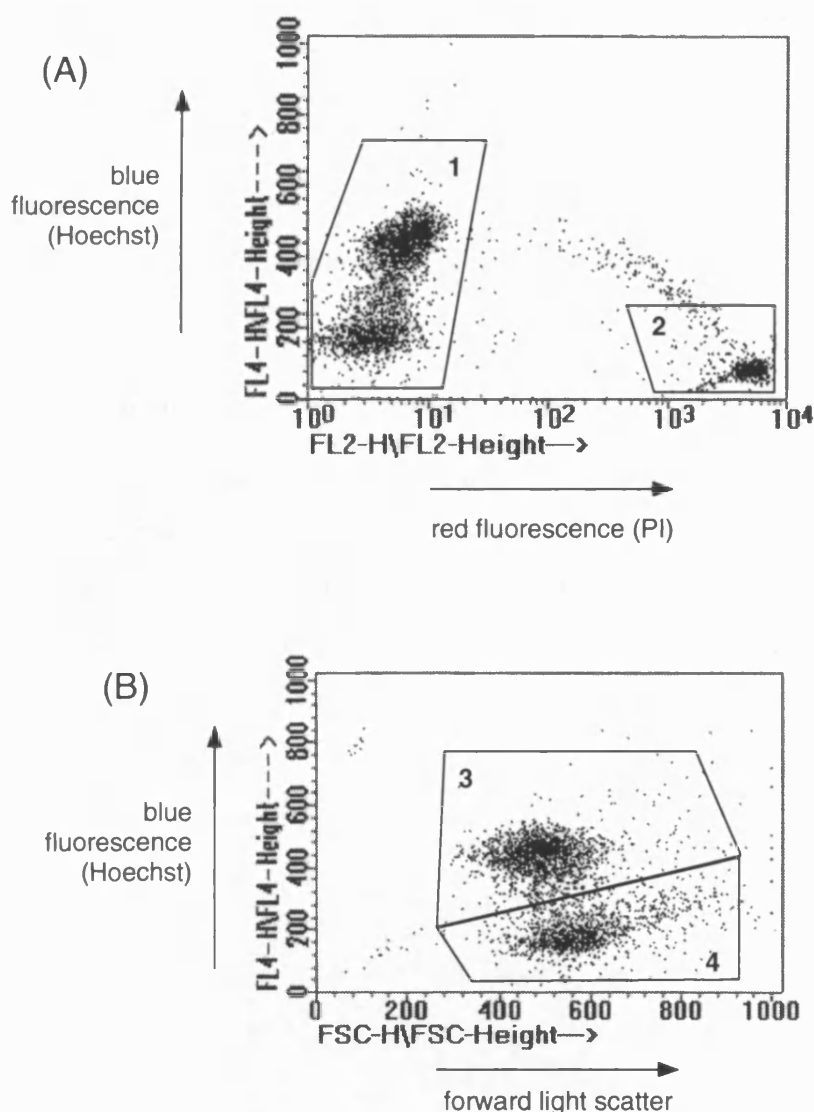


Figure 2a. Method for the separation of normal and apoptotic thymocytes by flow cytometry.

These plots were generated from thymocytes treated for 4 hours with 25 μ M tBHQ. (a) Dot plot of red fluorescence (FL2) against blue fluorescence (FL4). The population (1) represents cells that include Hoechst 33342 and thus fluoresce blue: these cells are still viable, i.e. they exclude propidium iodide. The population (2) represents those cells which take up propidium iodide and fluoresce red, i.e. these are dead cells. (b) Dot plot of forward light scatter (FSC) against blue fluorescence (FL4) using the cells in population (1), i.e. viable cells that include Hoechst 33342. Population (3) represents those cells with a lower forward light scatter and higher blue fluorescence, i.e. the apoptotic cells. Population (4) corresponds to those cells with a higher forward light scatter and a lower blue fluorescence, i.e. the non-apoptotic cells. By gating, the percentage of normal, apoptotic and dead cells can be obtained. In the plot shown above, region (2) contains 24% of the total cell population, and region (3) 57% of the total cell population.

Following culture, 1×10^6 cells suspended in 1 ml RPMI 1640 with 10% FCS were incubated with Hoechst 33342 (1 μ g/ml, w/v) at 37°C for 10 minutes. The cells were

then transferred to ice to prevent further uptake of the dye, and following a 4 minute incubation were pelleted by centrifugation at 400g for 5 minutes at 4°C. The cells were then resuspended in 500 µl PBS containing propidium iodide at 5 µg/ml (w/v).

Flow cytometric analysis was carried out using a FACS Vantage flow cytometer (Becton Dickinson). The cells were excited by a krypton laser at 352 nm (ultra violet), and the resulting red (>630 nm) and blue (400-500 nm) fluorescence recorded by linear amplification. The resulting data was analysed using PC-Lysis software (Becton Dickinson).

2.1.4. Conventional agarose gel electrophoresis

The internucleosomal cleavage that Andrew Wyllie described in 1980 has stood until recently as the most recognisable biochemical characteristic of a population of cells undergoing apoptosis. The method described here allows the loading of whole cells onto the gel and reduces the potential for the introduction of artifactual strand breaks caused by shearing the DNA. The method was first described by Sorenson et al. (1990).

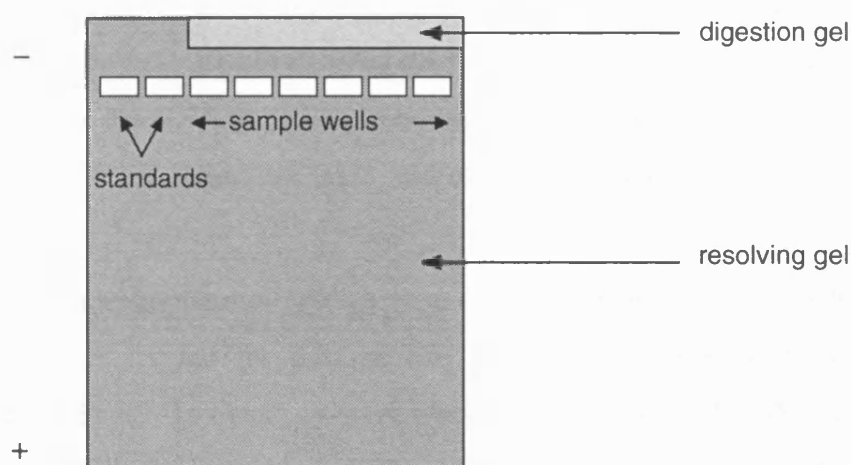


Figure 2b. Agarose gel used for the separation of internucleosomal DNA fragments.

The main gel consisted of 1.8% agarose made up in 1 × TBE buffer (89 mM Tris, 50 mM boric acid and 2 mM EDTA (pH 8.2)). Once the gel had solidified, a slice of agarose behind the wells was cut away so that the digesting gel could be poured into the space left behind (Figure 2a). The digesting gel contained 0.8% agarose, 2% SDS and 1.25 mg/ml proteinase K.

Following incubation, 2×10^6 cells were pelleted at 200g for 5 minutes and resuspended in 15 μ l ultra pure water. To this was added DNase-free RNase A to 10 mg/ml and the cells incubated at room temperature for 15-20 minutes. Loading buffer containing 1 \times TBE, 10% glycerol and 0.2% bromophenol blue was added to the cell suspension and the samples were loaded. After loading, the gel was run at 20 V for 1 hour to enable the SDS and proteinase K to move towards the wells and into contact with the cells, allowing the liberation of the DNA. Subsequently, the gel was run for 3-4 hours at 100 V. The gel was then removed from the tank and incubated overnight in TE (10 mM Tris, 1 mM EDTA, pH 8.0) containing RNase A at 20 μ g/ml. The gel was then stained in ethidium bromide (0.5 μ g/ml) and visualised under ultra violet light.

2.1.5. Field inversion gel electrophoresis

Conventional agarose gel electrophoresis is limited to the separation of DNA of less than 30 kilobasepairs in size. The separation of larger fragments of DNA requires the different technique of pulsed field gel electrophoresis (PFGE). PFGE uses two electric fields of differing strengths which lie at right angles to each other, and these are switched between in turn. The technique works on the assumption that the DNA is orientated parallel to the direction of the electric field. However, when the field is switched to be perpendicular to the original direction, the DNA must also re-orientate itself through ninety degrees, and the larger the molecule the longer this takes, and the greater is its retardation within the gel.

Field inversion gel electrophoresis (FIGE) is a variation on this method, where the electric field switches to and fro through one dimension as opposed to the two dimensions used by PFGE. To obtain an overall forward movement of the DNA, a longer period of time is spent in the forward phase than in the reverse. The cycle length, i.e. the time taken for one forward and one reverse phase, is increased as electrophoresis progresses, a technique known as ramping. This prevents the anomaly of the larger fragments moving further than the small fragments. Using this method described here, it is possible to resolve fragments of up to 600 kilobasepairs.

This method is basically that of Anand and Southern (Anand and Southern, 1990) and Brown et al. (Brown et al., 1993). DNA is loaded onto the gel in the form of an agarose plug. For the preparation of these plugs, 5×10^6 cells were pelleted as described in

section 2.1.4. and resuspended in 100 µl PBS. The cell suspensions were then warmed for 5 minutes in a water bath at 50°C, after which an equal volume of 1% low melting point agarose (Pharmacia, Uppsala, Sweden) in PBS was mixed with the suspension. The agarose/ cell solution was dispensed into plug moulds (containing around 100 µl each) and allowed to set.

Once the plugs had solidified, they were transferred to NDS solution (10 mM Tris pH 9.5, 0.5 M EDTA, 1% lauryl sarcosine) and incubated with Pronase (1 mg/ml) (Boehringer Mannheim) at 50°C for 48 hours. The plugs were washed in TE prior to loading onto the gel.

The separation gel consisted of 1% agarose in 0.5% TBE, and was poured between vertical glass plates that had been pre-warmed to 50°C. Once the agarose had set, and the gel comb removed, an equal portion of each agarose plug was inserted into the wells and the wells were then sealed with 1% agarose, as used for the separation gel.

The gel was run in 0.5% TBE using a 200 V power supply and a Hoefer PC500 Switchback pulse controller. Each run started with a 15 minute continuous forward pulse, followed by a forward pulse of 2.4 seconds to 0.8 second reverse pulse (3:1 ratio) for 1 hour. A ramp factor of 1.5 was then applied to give a forward pulse of 24 seconds to reverse pulse of 8 seconds. The total run time was 7 hours. DNA size markers of 0.1 to 200 kilobasepairs, and *Saccharomyces Cerevisiae* chromosomes (243 - 2200 kilobasepairs) (Clontech, Cambridge, U.K.) were run alongside. The gel was then stained in ethidium bromide and visualised under UV light.

2.2 PREPARATION, CLONING AND SEQUENCING OF DINUCLEOSOMES

2.2.1. Treatment of thymocytes.

Mouse thymocytes were prepared as described in section 2.1. The cells were incubated for four hours at 37°C either alone (control) or in the presence of dexamethasone (0.1 µM).

2.2.2. Preparation of laddering gel.

In this instance, where the laddering gel was for preparative rather than analytical purposes, and also because of the high number of cells that were used, the DNA was purified and precipitated prior to separation on an agarose gel. In section 2.1.4, where

laddering gels were used as a marker for apoptosis, the usual protocol was used.

10×10^7 cells were harvested by centrifugation for 5 minutes at 200g and then lysed by resuspension in 0.5% (v/v) Triton X-100, 20 mM EDTA and 10 mM Tris at 4°C. The cell lysate was then spun at 27 000g for 30 minutes at 4°C in a Beckman SW40 rotor. The resulting supernatant was removed and repeatedly extracted with phenol/chloroform/ isoamyl alcohol (25:24:1) and then finally with chloroform alone to remove any traces of phenol. Following this, the DNA in the aqueous layer was precipitated by combining it with $2 \times$ volume of 100% ethanol and $0.1 \times$ volume of 3M sodium acetate (pH 5.3), followed by incubation for 30 minutes at -20°C and finally centrifugation at 12 000g for 20 minutes at 4°C.

The pellet was resuspended in 30 μ l TE buffer (10 mM Tris, 1 mM EDTA pH 7.5) and the DNA was separated on a 1.8% agarose gel, pre-stained with ethidium bromide at 0.5 μ g/ml. A 123 base pair ladder, λ Hind III and pGEM markers (Promega, Portsmouth, U.K.) were run alongside as size markers. Once the gel had run, it was incubated overnight in TE containing RNase A (20 μ g/ml), and visualised under ultra violet light.

2.2.3. Preparation of dinucleosomes

The bands of interest were excised from the gel and the DNA fragments recovered by electroelution at 150 V for 45 minutes. The recovered fragments were precipitated with 100% ethanol and sodium acetate (pH 5.3) as described previously.

2.2.4. Cloning of the dinucleosomal fragments

The manner in which the apoptotic endonuclease cleaves DNA to produce nucleosomal fragments is unknown. Thus, the only way that these fragments could be inserted into a plasmid vector was by blunt-ended ligation. Assuming the possibility that the fragments produced had overhangs of some form, the ends of the fragments were filled in with the Klenow fragment of *E. Coli* DNA polymerase I to make them blunt-ended.

The plasmid also had to be blunt-ended, and thus the restriction endonuclease *Sma* I was chosen to cut the plasmid. The enzyme leaves the DNA with two 5' phosphate groups which, in the presence of DNA ligase, would allow the plasmid to re-circularise. To prevent this, the cut plasmid was treated with calf intestinal alkaline phosphatase to leave the plasmid with four 3' hydroxyl groups.

The recovered dinucleosomes were incubated at room temperature for 30 minutes with 2 units of the Klenow fragment of *E. Coli* DNA polymerase I (Boehringer Mannheim, Lewes, U.K.). pBluescript (Stratagene, Cambridge, U.K.) was cut with the restriction enzyme *Sma* I (Gibco BRL), then treated with calf intestinal alkaline phosphatase (Gibco BRL). The cut vector was then purified by extraction with phenol/ chloroform extraction and ethanol precipitation.

The plasmid pBluescript contains as part of its structure a portion of the β -galactosidase gene (*lacZ*) and its regulatory elements. This encodes the N terminus of the protein, whilst the C terminus is coded for in the host cell genome. The multiple cloning site lies within the β -galactosidase gene in the plasmid, and normally this does not affect expression of the gene. However, when a fragment of foreign DNA, in this instance a dinucleosome, is inserted into the multiple cloning site, the gene is interrupted and produces a non-functional protein. This forms the basis of blue-white selection for inserts following ligation and transformation when IPTG and X-Gal are incorporated into the agar. Isopropylthio- β -D-galactoside (IPTG) induces the expression of β -galactosidase via the *lacZ* promoter, and if no insert is present (for example if the plasmid has re-circularised on its own) the β -galactosidase is functional and able to metabolise 5-bromo-4-chloro-3-indolyl- β -D-galactoside (X-Gal) to produce a blue dye. However, if an insert is present then the enzyme cannot operate and the X-Gal remains unmetabolised. Thus, only the white colonies on an agar plate contained dinucleosomes.

The dinucleosomes were ligated into pBluescript by incubation with 6 units of T4 DNA ligase (New England Biolabs, Stevenage, U.K.) for 48 hours at 16°C. The resulting constructs were transformed using 50 mM CaCl₂ into the *E. Coli* strain JM101 by heat shock (incubation at 42°C for 2 minutes) as described by Sambrook et al. (Sambrook et al., 1989). The cells were plated out on LB agar containing ampicillin (100 μ g/ml), and incubated at 37°C overnight. Blue/ white screening was used to check for the incorporation of the insert.

2.2.5. Plasmid Isolation from *E. Coli*

The plasmids were prepared by one of two methods: either by precipitation with polyethylene glycol (PEG) or by purification using a Qiagen column (tip 100) (Qiagen, Hilden, Germany). If the plasmid was to be purified by passing through a Qiagen column,

the cultures were grown overnight at 37°C in 10 ml LB broth with continuous shaking, and if PEG precipitation was to be used the colonies were inoculated into 5 ml Terrific Broth and again incubated overnight at 37°C with continuous shaking.

a. PEG precipitation

1.5 ml aliquots of culture were spun down in a microcentrifuge and the supernatants removed by aspiration, with a total of 4.5 ml culture being pelleted in one eppendorf tube by means of repeated centrifugation. The pellet was resuspended in 200 µl GET buffer (50 mM glucose, 25 mM Tris (pH 8.0), 10 mM EDTA) and added to this was 300 µl of freshly mixed 0.2M NaOH/ 1% SDS. The contents were mixed by inversion and the tube incubated on ice for 5 minutes. The solution was neutralised by the addition of 300 µl 3.0M potassium acetate (pH 4.8) followed by incubation on ice for 5 minutes. The tube was then spun for 10 minutes at room temperature in a microcentrifuge at 13 000 r.p.m. to pellet cellular debris, with the supernatant being transferred to a clean tube. DNase-free RNase A was then added to a final concentration of 20 µg/ml and the tube incubated at 37°C for 30 minutes. The solution was then extracted twice with 400 µl chloroform and the DNA precipitated by adding an equal volume of isopropanol at room temperature followed by a 10 minute centrifugation at top speed in a MSE benchtop microcentrifuge. The pellet was resuspended in 32 µl sterile water then 8 µl NaCl and 40 µl sterile 13% sterile PEG 8000 added to the tube. Following incubation on ice for 20 minutes the plasmid was centrifuged at 4°C and 12000g for 15 minutes. The supernatant was removed and the pellet rinsed in 70% ethanol and resuspended in 20 µl sterile water.

b. Preparation using a Qiagen column

Plasmid was extracted using a Qiagen column according to manufacturers instructions.

2.2.6. Verification of insert

As the cloning was blunt-ended, it was possible that more than one fragment had been incorporated into the vector in a concatemeric fashion. Thus, it was necessary to verify (a) whether the blue/ white selection had given false positives, and (b) if an insert was present the number that had been incorporated. This was done by means of a PCR reaction following purification of the DNA by a mini prep. The primers used were the M13 and reverse primers which have complementary sites within the vector. A

dinucleosome is approximately 360 bp in length, and the primer binding sites lie approximately 90 bp from the multiple cloning site. Hence, amplification of a single dinucleosomal fragment would be expected to produce a PCR product of 500-600 bp. Colonies that produced a PCR product in this size range were selected for sequencing.

The primers used were:

M13 primer: 5'-GTA AAA CGA CGG CCA GT-3'

Reverse primer: 5'-AAC AGC TAT GAC CAT G-3'

The cycle program used on the Perkin Elmer 480 PCR machine was:

- (i) 1 minute at 94°C; 30 seconds at 50°C; 30 seconds at 72°C for 1 cycle
- (ii) 30 seconds at 94°C; 30 seconds at 50°C 30 seconds at 72°C for 30 cycles
- (iii) 4°C soak

The products of this were run on a 1% agarose gel against pGEM DNA standards.

2.2.7. Sequencing of the dinucleosomes

Sequencing was initially carried out by the Sanger dideoxy chain termination method using Sequenase (modified T7 polymerase) (United States Biochemical, Cleveland, Ohio, U.S.A.), labelling with [α -³⁵S] dATP, and subsequently using dye labelled terminators and the Applied Biosystems 373 Automatic DNA Sequencer (Applied Biosystems, Warrington, U.K.).

For the automatic sequencing, 1 µg of purified plasmid at approximately 200 ng/µl was mixed with 3.2 pmol of one of the above primers. To this was added 9.5 µl of terminator premix (1.58 µM ddATP, 94.74 µM ddTTP, 0.42 µM ddGTP, 47.37 µM ddCTP (all fluorescently labelled), 78.95 µM dITP, 15.79 µM dATP, 15.79 µM dCTP, 15.79 µM dTTP, 168.42 mM Tris.HCl, 4.21 mM (NH₄)SO₄, 42.10 mM MgCl₂, 0.42U/µl AmpliTaq DNA polymerase (Applied Biosystems)) and sufficient water to make the volume up to 20 µl. After overlaying the reaction with a drop of mineral oil the PCR reaction of 96°C for 30 seconds, 50°C for 15 minutes and 60°C for 4 minutes for 25 cycles then to a 4°C hold was carried out in the Perkin Elmer 480 model.

The reaction products were purified by extraction with phenol: water: chloroform

(68:1:14) (Applied Biosystems) and ethanol precipitation.

Sequence analysis was carried out using the MacVector and AssemblyLign software packages (International Biotechnologies Inc., New Haven, Connecticut, U.S.A.), and the searches of the sequences carried out against Entrez release 7.0 15 October 1993, provided by the National Center for Biotechnology Information on CD ROM.

2.3 MEASUREMENT OF INTRACELLULAR FREE CALCIUM

2.3.1. The mechanism of action of fura-2

There is a wide range of intracellular fluorescent Ca^{2+} indicators available. Their Ca^{2+} binding site is based upon the tetracarboxylic acid Ca^{2+} binding site of the Ca^{2+} chelator EGTA, whilst the body of the molecule is aromatic to increase fluorescence. To enable these dyes to enter the cell, the hydrophilic carboxyl groups are esterified to give the hydrophobic acetoxymethyl ester. Once the dye has crossed the plasma membrane, it is converted to its functional free acid form by endogenous esterases. As the dye is now hydrophilic, it should, in theory, remain in the cell.

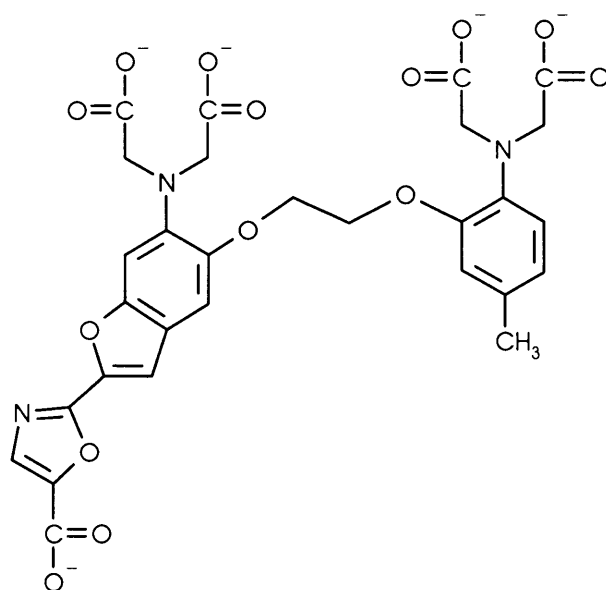


Figure 2c. *The structure of the free acid form of fura-2.*

Fura-2 (Grynkiewicz et al., 1985) is probably the most widely used fluorescent Ca^{2+} indicator, mainly because it has the advantage of being ratiometric, i.e. the compound fluoresces whether it is bound to Ca^{2+} or not, and the association or dissociation of Ca^{2+} is registered by a shift in the fluorescence excitation maximum. The advantage of this is that the sole important factor in quantifying the intracellular free $[\text{Ca}^{2+}]$ ($[\text{Ca}^{2+}]_i$) becomes

the ratio of the fluorescence of the free fura-2 to that of fura-2 complexed with Ca^{2+} . Thus, instrument sensitivity and any inconsistencies in intracellular dye concentration from one assay to the next become insignificant. In contrast another fluorescent Ca^{2+} indicator, fluo-3, only fluoresces when it is bound to Ca^{2+} , so any measurement carried out using this compound requires careful calibration. The two principal drawbacks to using fura-2 are the tendency of the dye to compartmentalise within intracellular organelles such as the mitochondria, and also the incomplete de-esterification of fura-2 AM. Partially de-esterified forms of fura-2 are highly fluorescent but insensitive to Ca^{2+} .

The fluorescence excitation maximum of free, uncomplexed, fura-2 is 380 nm. Upon binding Ca^{2+} , the excitation maximum switches to 340 nm. Thus, the ratio of the fluorescence at 340 nm to that at 380 nm can be used to calculate the concentration of free Ca^{2+} within the cell, using the equation:

$$[\text{Ca}^{2+}]_i = K_d \left\{ \frac{R - R_{\min}}{R_{\max} - R} \right\} \cdot \left(\frac{S_{f2}}{S_{b2}} \right)$$

where R is the ratio of fluorescence at 340 nm to that at 380 nm, and K_d is the dissociation constant for fura-2/ Ca^{2+} . S_{f2} and S_{b2} are proportionality coefficients representing the fluorescence at 380 nm of free and bound fura-2 respectively, and can be measured from the fluorescence intensities of calibration solutions containing known concentrations of free and Ca^{2+} -bound dye (Grynkiewicz et al. 1985).

2.3.2. The measurement of intracellular free Ca^{2+}

2×10^7 thymocytes were spun down and resuspended in 2 ml Krebs HEPES buffer (20 mM HEPES free acid, 4.2 mM NaHCO_3 , 5.5 mM glucose, 1.18 mM $\text{MgSO}_4 \cdot 7\text{H}_2\text{O}$, 1.18 mM KH_2PO_4 , 4.69 mM KCl, 118 mM NaCl, 1.29 mM $\text{CaCl}_2 \cdot 2\text{H}_2\text{O}$, pH 7.4) supplemented with 2% BSA and 5 μM fura-2 AM. The cell suspension was incubated at room temperature for 30 minutes with continuous stirring. The cells were washed once, resuspended in Krebs-HEPES buffer with 2% BSA and allowed to stand at room temperature for 15 minutes to allow de-esterification of the fura-2 AM, with the resultant liberation of the Ca^{2+} -sensitive fura-2 free acid. The cells were then pelleted again and resuspended in a cuvette at 1×10^7 cells/ml in Krebs/HEPES buffer, supplemented with 0.2% BSA. Cells used to study the effects of TLCK upon Ca^{2+} release were incubated

for 1 hour with TLCK as described in section 2.1.2., then kept on ice in the same medium in which they had been incubated until they were required, when a 1 ml aliquot was spun down and resuspended in Krebs/ HEPES ready for loading with fura-2 AM.

All readings of fluorescence intensity were taken approximately every four seconds using a Perkin Elmer LS-5B luminescence spectrometer fitted with a water jacket to maintain the buffer temperature at 30°C, with the cells being stirred continuously. Following the subtraction of autofluorescence (i.e. the background fluorescence of the cells in the absence of fura-2), $[Ca^{2+}]_i$ was calculated using the formula mentioned previously. R_{max} was determined by adding 1% Triton X-100 to the cells at the end of each assay, so that the fura-2 was saturated by being exposed to the Ca^{2+} in the buffer and the 340 nm signal was maximal. R_{min} was determined by the addition of 6 mM EGTA, so that the fura-2 was in the unbound state and the fluorescence at 380 nm was maximal.

2.4. ASSESSMENT OF THE CLEAVAGE OF RADIOLABELLED SUBSTRATES IN VITRO

2.4.1. The use of in vitro systems to study events in the execution of apoptosis

The use of cell lysates to study the intracellular events of apoptosis is proving to be an increasingly popular and useful technique (reviewed by Earnshaw, 1995). Many systems are based upon that of Lazebnik et al. (Lazebnik et al., 1993), consisting of lysates prepared from cells exposed to an apoptotic stimulus and utilising isolated nuclei as a means of evaluating apoptotic changes. In this manner important information regarding the apoptotic process has been revealed, for example the degradation of poly(ADP-ribose) polymerase (PARP) by an ICE-like protease (Lazebnik et al., 1994).

Lysate systems can reduce the time taken to obtain experimental data, and have the advantage of allowing the access of hydrophilic peptide inhibitors, which have difficulty crossing the plasma membrane, to their targets. However, they do have their shortcomings. The reduction of the cell to a lysate results in the loss of sub-cellular compartmentalisation, which may result in inter-molecular encounters that would never occur in an intact cell. Furthermore, the manner in which the lysates are prepared also means that, for example, mitochondria may be removed, which could result in the depletion or loss of molecules such as Bcl-2 that are important participants in the regulation and implementation of cell death.

2.4.2. Cell culture and preparation of lysates

THP.1 cells, a human monocytic tumour cell line, and Jurkat T lymphocytes, another human cell line (both cell lines were obtained from ATCC, Maryland, U.S.A.), were grown in RPMI 1640 with 10% FCS, 100 U/ml penicillin and 100 µg/ml streptomycin. The THP.1 cells were grown to approximately 1×10^6 /ml and incubated at 37°C as previously described (section 2.1.1.; Zhu et al., 1995), either alone or in the presence of an agent to induce apoptosis. To induce apoptosis in Jurkat cells, cells (30×10^6 cells/ml) were stimulated with 100 ng/ml anti-human Fas monoclonal antibody (clone CH-11) (Kamiya Biomedical Company, Thousand Oaks, U.S.A.).

For the preparation of THP-1 cell lysates, cells were incubated as required and then placed on ice, washed twice with ice cold RPMI 1640 without serum and resuspended in PIPES buffer (50 mM PIPES/KOH (pH 6.5), 2 mM EDTA, 0.1% (w/v) CHAPS, 5 mM DTT, 20 µg/ml leupeptin, 10 µg/ml pepstatin A, 10 µg/ml aprotinin and 2 mM PMSF) at a concentration of 6×10^6 cells/10µl. The cells were frozen and thawed three times in liquid nitrogen and then centrifuged for 30 minutes at 20 000g. The supernatant fraction was then centrifuged for a further 30 min at 100 000g. The protein concentration in the supernatant fractions (the lysate) was determined by the Bradford assay (Bio Rad, Hemel Hempstead, U.K.). Lysates from Jurkat cells were prepared essentially as for the THP.1 cells, with the exception that the buffer used for the resuspension of the cells contained 40 mM β-glycerophosphate, 50 mM NaCl, 2 mM MgCl₂, 5 mM EGTA, and 10 mM HEPES (pH 7.0) (Chow et al., 1995).

In order to assess the possible effects of various ICE-like protease inhibitors, cells were pre-treated for 1 hour with Z-VAD.FMK (10µM) (Enzyme Systems, Dublin, U.S.A.), Ac-DEVD-CHO (10µM) (a gift from Merck Frosst, Quebec, Canada) or Ac-YVAD-CHO (10µM) (Bachem, Bubendorf, Switzerland) prior to exposure to the apoptotic stimulus.

2.4.3. Detection of PARP and CPP32 cleavage in intact cells

Cells were prepared for SDS-PAGE as described (Harlow and Lane, 1988). For the analysis of PARP breakdown, cellular proteins were resolved on a 7% polyacrylamide gel, whereas for CPP32 a 12% gel was used. The proteins were then blotted onto

nitrocellulose. Proteolysis of PARP was detected by western blotting using rabbit antiserum (318) to PARP (a gift of Dr. G. Poirier, Quebec, Canada). CPP32 was detected by using an antibody directed to the p17 subunit of CPP32 followed by chemiluminescence (carried out by H. Zhu and Dr. M. MacFarlane).

2.4.4. [³⁵S]PARP/[³⁵S]proIL-1 β cleavage assay

[³⁵S]PARP and [³⁵S]proIL-1 β were synthesised by Merck Frosst, Quebec, Canada. In brief, the cDNAs of human PARP or proIL-1 β were cloned into an appropriate vector under the control of the T7 promoter and translated in vitro using TNT/T7 rabbit reticulocyte lysate (Promega, Madison, U.S.A.) in the presence of [³⁵S] methionine (~1000 Ci/ mmol). The reaction products were purified using a Superdex-75 FPLC column (Pharmacia, Uppsala, Sweden) (Nicholson et al., 1995).

Proteolysis of PARP in cell lysates was measured by the ability of the lysate to cleave [³⁵S]PARP to a 24 kDa fragment (Nicholson et al., 1995). Lysate (10 μ g) in 20 μ l of PIPES buffer was incubated for 30 min at 37°C with 5 μ l of [³⁵S]PARP (128 Bq/ μ l) in the presence or absence of inhibitors as indicated. The reactions were stopped by the addition of Laemmli buffer containing β -mercaptoethanol and SDS. After boiling for 5 minutes, samples were separated on a 10% polyacrylamide gel. Once the gel had run, the gel was fixed by shaking for 10 minutes in a mixture of 10% glacial acetic acid, 20% methanol and 70% water, soaked for 20 minutes in Enlightning Fluorographic enhancer (NEN Dupont, Brussels, Belgium), then dried down and exposed to autoradiography film. For analysis of [³⁵S]proIL-1 β cleavage, the procedure was essentially as described for [³⁵S]PARP, except that 2 μ l of [³⁵S]proIL-1 β (840 Bq/ μ l) was added to the lysate in HEPES buffer (as PIPES buffer but containing 10 mM HEPES/KOH pH 7.5), and the reaction products were resolved on a 12% polyacrylamide gel.

Quantification of PARP and proIL-1 β cleavage was by scanning densitometry using Molecular Dynamics software.

CHAPTER 3

DNA SEQUENCE ANALYSIS OF DINUCLEOSOMES GENERATED DURING THYMOCYTE APOPTOSIS

3.1. INTRODUCTION

3.1.1. Chromatin structure

If the DNA within the average mammalian somatic cell nucleus was present in a linear relaxed form, it would stretch for two metres. Thus, the DNA must be highly compacted to allow it to fit within the cell.

DNA is associated with histone proteins, which bind to DNA because they are rich in basic amino acids and thus have an overall positive charge. There are five histones; H1, H2A, H2B, H3 and H4. Two each of H2A, H2B, H3 and H4 complex to form the histone octamer or core (see Figure 3a). A strand of DNA wraps itself around this almost twice, so that approximately 146 base pairs of DNA are in direct contact with the histone core. Between one of these complexes is a linker region which can range in length from 15 bp to over 100 bp, but is usually somewhere between 30 and 60. This unit comprising the core histones associated with around 200 base pairs of DNA is known as the nucleosome, and forms the basic unit of higher order chromatin structure. When visualised by electron microscopy, chromatin in this state possesses a 'bead on a string' appearance (Latchman, 1990).

Beyond this basic nucleosomal structure the nucleosomes fold around on themselves with the aid of histone H1 to give a coil or solenoid structure of six nucleosomes per turn which is 30 nm in diameter (Figure 3a). Chromatin in this form is then organised into a series of loops of approximately 50 kilobase pairs each, which are anchored at their bases to the nuclear matrix via sequences known as matrix attachment regions. During metaphase, these loops form rosettes or radial coils which lie on top of each other to form a chromosome (reviewed by Getzenberg et al., 1991).

Within a particular cell type, the expression of much of the genome is not required, and during interphase such genes lie within the densely packed loops consisting of the 30 nm solenoid, these regions being known as heterochromatin. This is in contrast to euchromatin, which is more loosely packed during interphase. DNA in this region is often being actively transcribed, as the more diffuse structure of the chromatin enables the access of proteins required for gene expression such as polymerases or transcription factors to the DNA. Euchromatin is thought to be largely nucleosomal in structure. The

DNA in the linker region is more exposed than the DNA which is associated with the nucleosomes, so if euchromatin is subjected to mild digestion by micrococcal nuclease, the DNA can be visualised by gel electrophoresis as a 'ladder' increasing in multiples of around 200 base pairs (Hewish and Burgoyne, 1973).

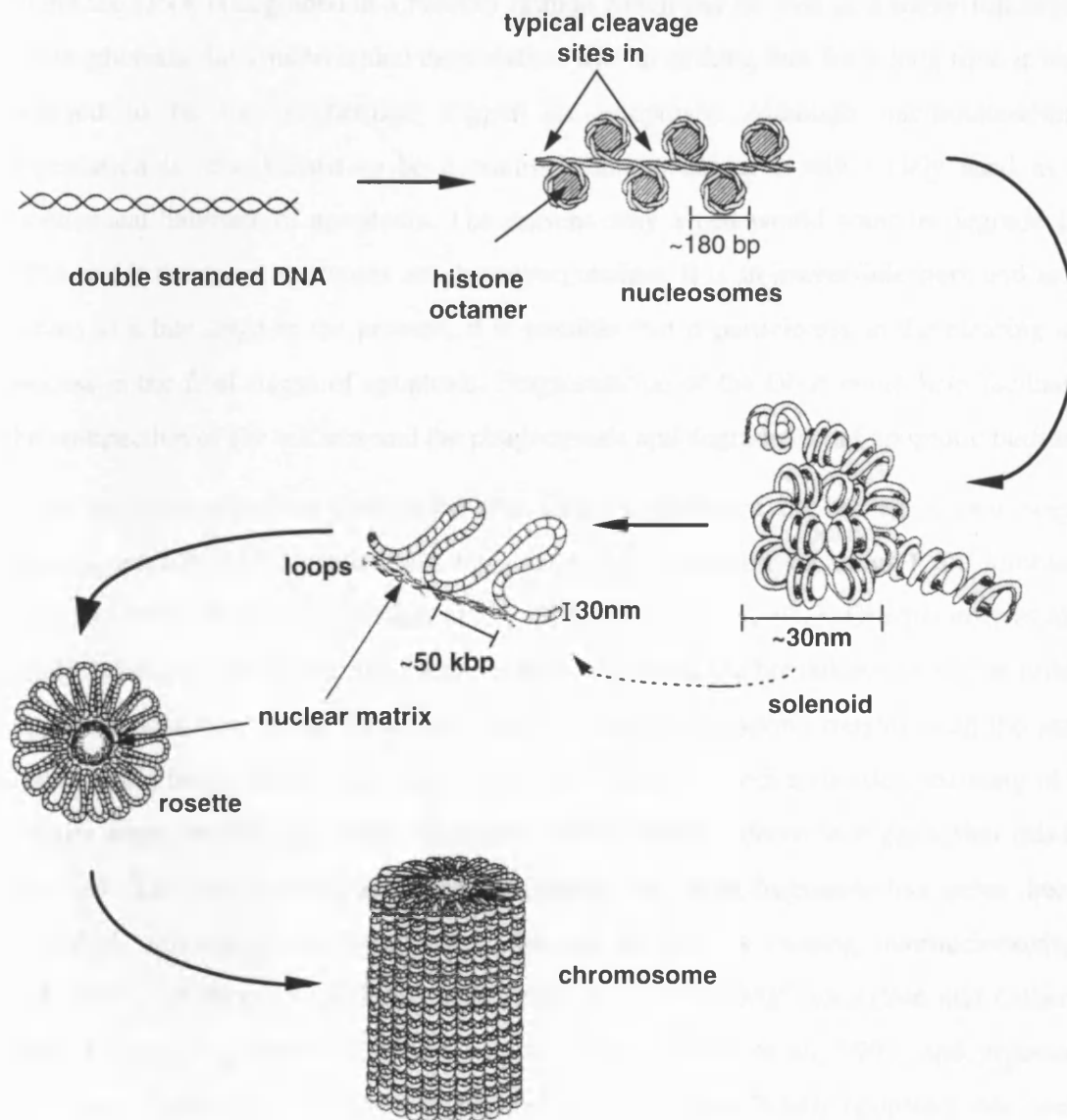


Figure 3a. Levels of higher order chromatin structure.

Double stranded (relaxed) DNA is initially folded around the histone core into nucleosomes. Nucleosomes are able to coil round on themselves to form a solenoid, which becomes attached to the nuclear matrix at specific points to form loops of around 50 kbp in size. At mitosis the loops form rosettes which stack on top of one another to form chromosomes. Adapted from Getzenberg et al. (Getzenberg et al., 1991).

3.1.2. The degradation of DNA during apoptosis

One of the most characteristic morphological changes that is seen in apoptosis is the collapse of the chromatin against the nuclear envelope. Andrew Wyllie found that

separation by conventional agarose gel electrophoresis of the DNA from thymocytes induced to undergo apoptosis in response to the synthetic glucocorticoid methylprednisolone results in a distinctive 'laddering' pattern, caused by the internucleosomal cleavage of DNA (Wyllie 1980). This is in marked contrast to necrosis, where the DNA is degraded in a random fashion which can be seen as a smear following electrophoresis. Internucleosomal degradation was so striking that for a long time it was believed to be the biochemical trigger for apoptosis. Although internucleosomal degradation is now known to be a relatively late event, it is still widely used as a biochemical hallmark of apoptosis. The reasons why a cell would want to degrade its DNA under these circumstances are, however, unclear. It is an irreversible step, and as it occurs at a late stage in the process, it is possible that it participates in the clearing up process in the final stages of apoptosis. Fragmentation of the DNA could help facilitate the compaction of the nucleus and the phagocytosis and degradation of apoptotic bodies.

It has subsequently been discovered that DNA degradation occurs via a two stage process. Initially it is degraded into high molecular weight fragments of >300 kilobase pairs and 50 kilobase pairs (Walker et al., 1991; Brown et al., 1993; Oberhammer et al., 1993). It has been proposed that such cleavage represents the breakdown of higher order chromatin structure, as the 50 kilobase pair fragments correspond roughly with the size of chromatin loops (Figure 3a), and the 300 kbp fragments with a rosette consisting of a circular arrangement of six loops. However, there is little evidence to suggest that this is the case. The enzymatic activity that is causing the large fragments has never been identified, although it is distinct from the activity that is causing internucleosomal degradation, as they have differing sensitivities to Ca^{2+} and Mg^{2+} ions (Sun and Cohen, 1994; Cain et al., 1994), Zn^{2+} (Cohen et al., 1992; Brown et al., 1993) and protease inhibitors (Walker et al., 1994b; Fearnhead et al., 1995a). Whilst apoptosis has been shown to occur in the absence of internucleosomal cleavage (Cohen et al., 1992; Ucker et al., 1992), apoptosis has never been demonstrated in whole cells in the absence of any DNA degradation whatsoever.

Although it was initially thought that DNA degradation and chromatin condensation went hand in hand, experimental evidence seems to suggest that they are in fact separate events. Instances have been observed whereby DNA is fragmented, e.g. by micrococcal nuclease, without the condensation of chromatin (Sun et al., 1994), and conversely the

condensation of chromatin has been observed in the absence of internucleosomal degradation (Cohen et al., 1992; Sun et al., 1994), although large fragments of DNA have been observed in such instances (Brown et al., 1993). It is now widely acknowledged that the nuclear lamina is broken down in apoptosis in the absence of cdc2 kinase activity (Oberhammer et al., 1994; Neamati et al., 1995; Weaver et al., 1996), and whilst this breakdown can be inhibited alongside chromatin condensation, internucleosomal DNA cleavage still occurs (Lazebnik et al., 1995) although it is not known in this instance whether large fragments of DNA are also inhibited. The inhibitor of chymotrypsin-like proteases tosyl-L-phenylalaninyl chloromethyl ketone (TPCK) is able to inhibit both lamin degradation and internucleosomal cleavage in thymocyte nuclei (Neamati et al., 1995; McConkey 1996), although in whole thymocytes incubated with the same compound alone it causes the formation of high molecular weight fragments (Fearnhead et al., 1995a), which could imply that the formation of high molecular weight fragments is also distinct from lamin breakdown.

Although no enzymatic activity has been linked with the formation of the large fragments, a number of candidates has been put forward as putative apoptotic internucleosomal endonucleases. Because internucleosomal DNA degradation was presumed to be the causal event in apoptosis, much effort has been directed towards the identification and regulation this event. Results so far have proved inconsistent, as the nature of the endonuclease appears to vary with cell type, and in the case of thymocytes, distinct endonuclease activities have been isolated from within a single cell type (Peitsch et al., 1993a; Gaido and Cidlowski, 1993; Nikonova et al., 1993).

Firstly, DNase I was identified as an endonucleolytic activity present in thymocyte and lymph node cell nuclei (Peitsch et al., 1993a) by immunohistochemistry, immunodepletion and by the ability of the nucleolytic activity to be inhibited by G actin. It was previously known that the endonuclease activity in isolated thymocyte nuclei is dependent on Ca^{2+} and Mg^{2+} and inhibited by Zn^{2+} (Cohen and Duke, 1984). DNase I is known to be inhibited by Zn^{2+} , and functions in the presence of Ca^{2+} and Mg^{2+} (Melgar and Goldthwaite, 1968). The presence of numerous single stranded nicks in DNA from apoptotic mouse thymocytes (Peitsch et al., 1993b) supplied further weight to the argument for DNase I being the endonuclease as in the presence of Ca^{2+} and Mg^{2+} DNase I produces such a pattern (Melgar and Goldthwaite, 1968). The study by Peitsch

and co-workers (Peitsch et al., 1993b) also suggested that dissociation of the DNA into fragments occurred when two single-stranded nicks occurred in close proximity, and whilst these nicks occurred in DNA directly in contact with the nucleosome, there was a greater chance of finding two nicks close together in the more exposed linker regions between nucleosomes, hence the internucleosomal degradation seen upon gel electrophoresis.

Using a different approach, an 18 kDa protein with $\text{Ca}^{2+}/\text{Mg}^{2+}$ -dependent, Zn^{2+} inhibitable endonuclease activity was isolated from rat thymocytes exposed to glucocorticoid (Gaido and Cidlowski, 1991). Named NUC18, peptide sequencing showed this endonuclease to have homology with the cyclophilin family of proteins (Montague et al., 1994). Cyclophilins are proteins with a high affinity for the immunosuppressant drug cyclosporin A. They have a wide tissue distribution and have both nuclear and cytoplasmic forms. They are known to have peptidyl prolyl cis-trans isomerase activity which is inhibited by the binding of cyclosporin A, although the precise role that cyclophilins play in the action of cyclosporin A is unknown. Recombinant cyclophilins A, B and C have all been demonstrated to possess nuclease activity (Montague et al., 1994), which provides a further link between NUC18 and cyclophilins. Whilst both NUC18 and DNase I are both found in thymocytes, it remains to be seen which, if either of them, is directly involved in apoptosis. $\text{Ca}^{2+}/\text{Mg}^{2+}$ dependent, Zn^{2+} inhibitable nucleases that are distinct from DNase I have also been isolated from a T cell hybridoma cell line (Khodarev and Ashwell, 1996), a cytotoxic T cell line CTLL2 induced to undergo apoptosis in response to IL2 deprivation (Deng and Podack, 1995) and Jurkat T lymphocytes exposed to either staurosporine or anti-Fas antibody (Zhang et al., 1995). However, an endonuclease activity has been isolated from the human leukaemic cell lines HL60, U937 and K562 which is independent of Ca^{2+} and Mg^{2+} (Fernandes and Cotter, 1993).

Despite the apparent reliance on Ca^{2+} and Mg^{2+} in the degradation of DNA in thymocytes, in Chinese hamster ovary cells an enzyme was identified as an apoptotic endonuclease, which is independent of Ca^{2+} and Mg^{2+} concentrations but is dependent upon the pH being below 7.0, with optimal activity at around pH 5. The activity of this enzyme is indistinguishable from that of DNase II when compared with bovine DNase II by Western blotting and immunoprecipitation (Barry and Eastman, 1993). An acidic

endonuclease similar to DNase II was one of three distinct and novel nuclease activities isolated from rat thymocytes (Nikonova et al., 1993).

Previous studies have suggested that the fragmentation of DNA in apoptosis is non-random, and begins in portions of the genome that are enriched in DNA which is not in the usual B conformation (Luokkamäki et al., 1993), and that the shorter nucleosomal fragments are derived from transcriptionally active chromatin (Arends et al., 1990). The work in this chapter involves the cloning and sequencing of dinucleosomal fragments derived from apoptotic thymocytes. This was carried out to determine whether any sequence characteristics could be ascribed to the strand breaks occurring during apoptosis in these cells, and if possible to find out the origin of the fragments within the genome.

3.2. RESULTS

Dinucleosomal fragments were isolated from an agarose gel containing the fragmented DNA from isolated mouse thymocytes which had either undergone apoptosis spontaneously (control) or in response to exposure to dexamethasone. It was decided to use a single size of oligonucleosome to eradicate the possibility of there being any sequence repetition following further degradation of a longer oligonucleosome from one cell to the next, i.e. to avoid the isolation of a fragment which was present as, say, a mononucleosome in one cell and again present as a trinucleosome in another cell, thus artificially enriching the population of fragments with a particular sequence. Dinucleosomes were chosen to reduce the complexity of the sequencing operation. Eighteen dinucleosomal fragments were sequenced, giving 6772 base pairs in total. The average length of the dinucleosomes was 377 ± 10.1 base pairs. The longest fragment was 434 base pairs in length, and the shortest fragment was 278 base pairs.

Of the nucleosomes sequenced, thirteen were from cells incubated with dexamethasone, with the remaining five originating from control cells (Figure 3b). The sequences were analysed for distinguishing patterns or trends that could indicate any pattern to the DNA cleavage.

Firstly, the individual sequences were compared against each other to see if there was any similarity between the fragments. No similarity could be found between any of the sequences. In addition both ends of all eighteen fragments were aligned in an attempt to identify any form of recognition sequence that an enzyme could identify as part of its mechanism of action. Because there is little information on the nature of the ends generated during cleavage, the ends of the fragments had to be filled in with the Klenow fragment to enable cloning. As a result the exact identity of the nucleotide(s) where the cleavage took place is lost, but the alignment was undertaken to identify any possible conserved sequence motif(s) present a short distance from the ends. No sequence trends could be identified.

The base composition of the fragments was compared to the percentage base composition of the entire mouse genome. The base composition did not differ markedly from that of the whole mouse genome (Table 3(i)). Also, no real distinction could be made between the base composition of the sequences derived from control cells and

those from cells treated with dexamethasone.

	CONTROL	DEXAMETHASONE TREATED	OVERALL	WHOLE MOUSE GENOME
%A	30.15%	27.85%	28.37%	28.90%
%G	23.75%	21.01%	21.86%	21.10%
%C	20.56%	22.51%	22.21%	20.30%
%T	25.54%	28.63%	27.56%	30.00%
%AG	53.90%	48.86%	50.23%	50.00%
%TC	46.10%	51.14%	49.77%	50.30%
A+G/T+C	1.17	0.96	1.01	1.00
%AT	55.69%	56.48%	55.93%	58.90%
%GC	44.31%	43.52%	44.07%	41.40%
A+T/G+C	1.26	1.30	1.27	1.44

Table 2. The base composition of the sequenced dinucleosomes and comparison with the base composition of the mouse genome as a whole. *From Singer and Berg, (1991)

	OBSERVED	GENOME
NO. MICROSATELLITES WHERE (x) _{≥10}	1	≤0.2*
POLYPURINE/ POLYPYRIMIDINE TRACTS (≥20 bp)	4	≤1.5*

Table 3. Comparison of microsatellites and homopurine/ pyrimidine tracts with the number expected in the genome as a whole. * Luukkamaki et al., 1993.

The sequences were also examined for distinguishing features such as microsatellites and polypurine/ polypyrimidine tracts. If a microsatellite is defined to be a stretch of sequence from one to six base pairs where the monomeric repeating unit is repeated contiguously ten or more times (Hearne et al., 1992), then only one sequence fulfilled this criterion, a repeat (AT)₂₂ in fragment D27 (Figure 3b.). This is greater than the number of microsatellites that might be expected within the total length of DNA sequenced (see

Table 3(ii)). However, the most commonly observed eukaryotic microsatellite, (CA)_n, was only found here as a heptamer (fragment D213 bases 177 - 190).

Five homopurine tracts of twenty or more base pairs were found within the sequences. Again this is in excess of what might be expected from an equivalent length of DNA taken at random from the murine genome.

The sequences were all searched against Entrez database release 7.0. The only sequence which demonstrated any homology with any sequence in the database was a 106 base pair sequence at the 3' end of fragment D213 (Figure 3c). This sequence contained a portion of the B2 short interspersed repeat sequence, a 180 base pair sequence which is repeated throughout rodent genomes (Figure 3c). However, it was not 100% identical to any of the B2 sequences in the data base. The closest sequence match (91%) was with the B2 sequence from the rat lysozyme gene (Figure 3c). The 5' end of sequence D213 did not show any resemblance to any sequence contained within the database (Figure 3c). In the mouse genome there are approximately 0.8×10^5 copies of the B2 repeat (Rogers, 1985), which corresponds to around 0.48% of the genome. This stretch of 106 base pairs accounts for 1.6% of the DNA sequenced in this study, i.e. this sequence is enriched within these apoptotic fragments compared with the mouse genome in its entirety.

C212

```

1  AGTTGAAAAA AAAAGAAATG ATTTTATTTT TTTTATTTGT ATATCCTATA CTATGGAAAG
61  GTGCTTGGTA ATCCCAAGAG AACCGCAATC TTAATCTTTT GTTTACCTCA ACCTGTAGTA
121 AAAACTGGTC AGAGTACTGA GAATAAGTGA TCACAAGTAT TTACTCATCC TGAAGTGGTA
181 TGTCTTATTA ATTCCTGTGC CAAAGTTCAG AGGATCATT AAGGAAGAGAA GATATAAAGT
241 TGTAGGGAGG GAAGACGGCT ATGAGATACC ATTTCTTCAA CAGGATATTG GATTGCTGTA
301 CTCAGGGCAA CTGTGGGTAC CCTGTACAAT GCCAATCCAG CCAATATTCT TACATGGATC
361 CATTTTGGG TAGG

```

C215

```

1  CTTCGGATTT AGTCAAGGGT AGAACACTTG CCTGCCATCT GCAAGGCCCT GCATTCTTTC
61  CTTAGCACCA AATCAATAAT ATTGCATGGT CCTGCTGGCT ATCCATTATG TTATGGTTCT
121 GTGAGTGCAG CTGCCCAGGG CTGGGGGCAG GAAGAAAAGG GAGTTGTGTC GAGGGAGAGT
181 GCCAGGGTCA CAGCTAAAAC TCTAATGATC TTGTACTTGG GCACATGAAC ACAGTTGACA
241 CCTTCACTAT GTACAATTAA AGTGGCTAAG GTTCCAAACT CCTGTTTTTT TAACCATAAC
301 TTAAAACTT AAGGCTTCAA TATCATATTC TTACTTAATT AACAAGCTTA GAGGATTGAG
361 GGTGGGATTC CATCGGAAAA CCATGAATTT TCCAAGG

```

C218

```

1  CATCCATTGG ACGAAGCACA GGGTCCCCCA ATGAAGGAGC TAGAGAAAGT ACCTAAGGAG
61  CTGAAGGGGG TTTGTGCCCC ATAGGAGAAA CAACAATATG AACTAACCAG TACCCCCAGA
121 GCTCCCTGGG ACTAAACCAC CAACCAAAAG AAAACATATG GTGGGACTCA TGGCTCTAGC
181 TACATATGTA GCAGAGGATG GTCTAGTCGG ACATCAATGA GAGGAGTGGC CTTGTTCCT
241 GTGAAGACTC TATCCCCCAG TATAGGGGAA TGCCAGAGCC AGGAAGCAGG AGTGGGTAGG
301 TTGGTGAGCA GTGGGAGTGG GGAGAGGATG GGTTCGGA GGGGAAACCA GGAAAGG

```

C224

```

1  GCTTTGTAA TCTGTGTACA CTTCTCTCTC TGAACAATGC ACCTAGCAAC CTCAGACCCT
61  ACCAGCCCTG GGCTACACAG AACCTCCTCT CTTAATGGTG GGATAACTTT CCCTCCCCTT
121 TGACAATTCT TACATCTACA TTTTGTTCAG TCAGATACTC TTTACATCTA GGAATGAGAC
181 CAGAAAAGTA GATCCAGCTT GACCGGTTTG GGGTGTGTCC TCAGTTACAG AGAGTTGCGA
241 GCTACCATGT GCTGGGAGGT GAACCCAGGT CCTCTGGAAG AGCCAACCGT GCTCCTGGCT
301 GTTGAACCAT CAATCCAGCT CCCATTTCCT ACTTTGTGCC TATGTGTAAC CGGGCATGCA
361 TACATTAAAA CCAGAT

```

C229

```

1  CCTCCGCTGA TGAACACTTC TAATAAAGTA GCCGATAGA AAATTGATAC CAAAACTCA
61  GTAGCCTTCC TAAATAGCCA GGACCTACCC ACTGAGAAAG AAATTGGGGA ACCATCTCAT
121 ATATTCCAGC CCCCAATAT CTAGAATAA ATATAACTGA GATGAGAGTG TTGTAGAGTG
181 AAAAGAAGGA AATTATAGAA GATACCAGAA GATGAAATGG CTTAACATGC CTATGAATTG
241 GTAGGGATAA TATTGTGAAC GGTGACTACT AAAGCAGAGC AATGACAAAT TTAAATGAGC
301 CCCATCAAAA TTATAACATG ATTCTTCCAC GCAAACCTAA AATTGCCTGC GGGGTGATGT
361 GGGGAGGCAA TATGGCCGAG TGGGGCGAGG CGGTCTGCTG TAGAATAGGG TGA

```

D25

```

1  GATAAGCTTG ATATCGAATT CCTGCAGCGG CTTCTAACTG TTTTCTCAGG CTCTGGATAA
61  ATCAGTAACC ATTACCCCAA GAGTTCATTG CTAATCGATC CCTGAGTTCT GTAAAGCAAA
121 TGCCATGTAG GTATATCTCC AGGTAACCTT AAAAAAAAGA GAGAGAGAGA GGGGTCTTTT
181 TTTTGTGATA ACTTGATTTA TGAGTCTTTT TTATGCAAGT CAACTCAAAG GACTGTCAAA
241 ATTGAAACAA AACAAAAGTC AGCAGTCAGA AAATCATGCT CATATGCGTA TCATATGCTG
301 TACTAGCGCG GGCTTAGGGC TAGCTACT

```

Figure 3b. The DNA sequences of dinucleosomes from apoptotic mouse thymocytes.

The prefix *C* denotes a fragment derived from control thymocyte; the prefix *D* indicates a fragment derived from cells treated for 4 hours with dexamethasone (0.1 μ M). Residues in bold are polypurine/polypyrimidine tracts ≥ 20 bp. (Sequencing to ~98% accuracy).→

D27

```

1  GCCCCACCC CACCAGACTC CAGCCCATTG AATATAGGTC AGCCATTGCT CATGTGAACC
61 CATTACCCCA ATTCTGCCCC TCCCTTTGCC AGTTGAACTC AAATGAGGGC CTTTCTAGTC
121 ACAAAGCTGC TATATTTGTA TTGTTTCCTT GGCTATGGGG TGA CTGAAAA GTTGAGTTGG
181 TGAAGTCTTT GTATATGAAC TTGCATAGTT CTCTCTCAAT AAATTCAGTC TCTAGCATAT
241 ATATATATAT ATATATATAT ATATATATAT ATATATATAT AATTTTCAAA CTCACAGAAA
301 AGGTGGGTTC TTGTTTACAT ACATCCTTTG ATAAAATGTC AGTTTGCCCA CATAGATCCA
361 CCCACATTCC CATCCCAGAA AGAACAGCAG GGGGATCCAC TAG

```

D210

```

1  CTCCACACAT AGTCAGTGTC TGTCTGTCTG TCTGTCTGCC TGTCTTTTCT CCCCCTCCCC
61 TTCCCCCTCT CCCTCTCTCA CTCTCCTCCC CCCACCCCCA TCTTTATTTA TTTTTC CAAT
121 CCTGGAGATG GAACCTGCCT AGGGTTTTGG GCCTGTCATG TTAGTATCCT GCTGCATGCT
181 TTATCTCCTG ACCCTTTTTT GAACTCCCA AACACTGTCT TAATGAGTTT CCCAGGCTGG
241 CTTTGAAATT TCAATCCTCC TGTCTCAGCT TCCTAAATAG CTGGGATTAC AAGGCTGTGC
301 TACCAAGACC CAGCTGAGTC TCCTCCTCAA TAAAGTCAAT GCAAAGTC

```

D211

```

1  ACCCAGAGCC AAAAAATGTC AAATGTGGAA TGGTCTCTCT TAATCATGAG GCCCAGCTCT
61 GAGTCCTTAG ATTTTACTAT GTAACCTGAA GTGGCCACAG AAACCAGGGT TTTAGAAAGG
121 GACTGCGGAT GGGGAGTTCT AGAAAGGGGA AAGGGGGAGA AAGCAATCAAT GGAGATATTA
181 AGTAGGGAGT AGGGAGGGCG ATACAGAAGG AGAGATAAAT AACACCAAAG GCACCTGTAA
241 AGGCCACGGC GAATTATTAT TTTATAAGTT TACTTAATAT ATACATCACT TGTATCATGG
301 GAGAGCCATA GGCAATCGAA CCCATACTCA AAGAGCAGGT CTCCGTGGGA GCCAGTGCTC
361 AAGTGAATCC AAGAGACCAG CAATTCCTTC TTCCCATGTA GCATAGGGTG TATTT

```

D213

```

1  ACTTAATAGT TACTTGGGAG TTCTGGAGAC AACAAATATT TTGATGTGTT TTTAAAGGGT
61 GGGTGGTGAT GGCACATGCT TTAATCTCAT CATCAGAGCA GGCAGGCAG ACTTGAGTTG
121 TATCAGCTGT CACAGAGTTA GTCAATAGCT AGGCTAAAAG AGAACTGTCT TGAAAACACA
181 CACACACACA GTTAGTCACG GCTGGTGAGA TGGCTCAGCA GTTAAGAGCA CTGACTGCTC
241 TTCCAGACAT CCTGAATTTA ATTCCCAGAA CCACATGGTA GCTTACAACC ATCTGTAATG
301 G

```

D214

```

1  ACAGTAGTGC CTACCACATC AGATTATTAC AACAGCAAAT ATCTACATTA GCACAGGGGA
61 TGGATGGCCT TCTGTAAGGA TTATTGTCCC TACAATCGTA CGTGGCAGGA ATTCTCAAGG
121 CTTGCAGAAT GCACCAGCAG AGAATAATGG GTTAGCCACC AGGTCCATCC CCTTCCAACA
181 CTAAGGGCTT CATTTCCAGC TACATGGAGG CAGGCAGCTA TAGCTCTCAG CATCCCAAGA
241 ATCCCTCTGG ACAGGTGTGT TGCTAGGGGT TACGGCCTGC ATATGGGGTC AAACCGGTGT
301 CCAAGCTCCC AGGTCTCTGG AAGCATCTTT TAAGAACCAC AATTACCATT CC

```

D215

```

1  GTATGAGAAC ACAACTCAAT TTGGAGGTCT CACACTTCCT GATTTCCAAT TTGATTTTGA
61 TTAGTTATAA TTGATTAATC AAAATTGTGC TACTGGACAA TCAATGGAAA AGAATTGGGC
121 TGAGAAAGAA AACTCCAAAT TTTTTAGTTA AATTGTGTTT GAAGAGATGT GTTGATAGGA
181 GATGGTTTAA TAAAAGTACA GTCTTTTCAA TGAATGATAT TGGGGGAAAT ATAAAATAAA
241 CAAATGAAAT AAATAAAGTG GGAACCTTTT CGGTCTCT

```

Figure 3b continued. The DNA sequences of dinucleosomes from apoptotic mouse thymocytes.

The prefix *D* indicates a fragment derived from cells treated for 4 hours with dexamethasone (0.1 μ M). Residues in bold are polypurine/ polypyrimidine tracts ≥ 20 bp, and the underlined region is a d(AT)₂₂ microsatellite. (Sequencing to ~98% accuracy).→

D219

```

1  AACCAC TAAGACTAG TACATATCTA TATTTAGCAA TTTAAATATA GTAATATAGA
61 ATATATATTT TTATTTCTAT TTAATTATGA ATCCTGTCAA ATGTCTTACA GGCTTGCCCA
121 CAGACCGATC TCTATGGAGG GATATTCTCA ATTGAAGCCC CCTCCTTTCA GATGACTTAA
181 TTTGTGCCAA GTTGACATAA AACAATCCGG CATATCTGGT AAGGTAGCTC AGAGGGTAAG
241 GGTGCTTGCT GTCAAGCCTG AATTTGGGTG TCTTTTAACC CACAAAGCGG GAAAGAATAA
301 AAACCAGATT TCTACAAAGT TAGGCTCTGA CCTCCACACA ATGAGCAGGG AGGCAGGGTT
361 GGACATATTC CCTCCATCCC CCCGGTAATT AATTAATGT

```

D221

```

1  TACGAGTGTC AGTCGATTAC CTACCTAGTG TCCCGAGGGT TACCTCCTCG ATCTCTTGCA
61 TGGGTTCCCTC GATTTCCCTA GAAGTTGGGA TATCCACCTT GTTGTAATAA CTTGATTGGT
121 CATGGGGGAC TCGAGAACTG AGATCGACGT ATACATAGTT TTCTACCGGA TCAGCCGGTA
181 GTGACCTTTT TCTCCGGGTA ACCTGTGCGT CTGAAACACA CGGGGCCATG TCCCCCTGCG
241 GTCCGGGTTT CCCCCCTCA CCCACCCATC CCCTCACCCC CACCCACCCA TTCCCCCTGA
301 AAACCATATC GTAACCTTTA CATTTACTCG ATTTATGGAT TATTTTTTAC CTTTTTTTTT
361 TTTTTTTTTT TTTCA

```

D224

```

1  TGTTGCTTG CTTGTTTACA ATCTATCCAC TGA CTCCCTT CCAGTCCTCC CTCCCACAAT
61 TTGTCACCCC ATTCTCTGG TCCCAGTCC CCTAGAGGAA TCTCCCCAC CCTGGGGCCT
121 CAAGTCTCTG GAGGACTATG AGCGTCTTCT TCCACTGAGG GACATACCAG GCAGTCTCTC
181 GCTGTATATG TGTTTGGGGC CTCAGACTAG CTTGTGTATG ATGCCTGGTT GCTAGATCAC
241 TCTCTGGGAG CTCCAAGGGG GTCCAGTGGC TTCTAGGATG ACAGAAGCAG TTGGTGGGGG
301 GTGTTAGGCT ATTCTTGAGA GGTCTTGCC CCAAGGCAGC CTTGTCAGCA CGAGCCTGGA
361 TCTTGTAAG AAGAAAGCAG GACTCAGTCT TTCTTAGGTA TT

```

D226

```

1  TGTTGAGGGC TCCGCGCTTA GAACCGATCC TGGTTGAAGA CATGTCATGG GGACAAACTG
61 TCTCCATGCT TCTCATTTTC TTTGGGTTGT CCCCTCAACG AGAGTCCCAG GAAGAGCTCA
121 GCCACCCGC TCCGGGGTGT TCTTCAAGTG GCTGTCCCTT GTGTGAGCTT CAGCCAACT
181 CGCAGGGAAT AAAAGACTTG TTTTTCAGGG TTCTTTTACA AGCTGCAGC TCCAAAGAGT
241 CCCATCCTTG AATCTTCCCC AGATTGAAAT GGTAAGAAAA TAACAGCTGG GGAGTAGTGT
301 TTAGAGACAG GCCTCTGTGA GGGAGGCAGG GACAGATTTG GTCCCTTGGA TAGGAGTTTA
361 GCATGCACTG AAGTGCAGAT AGAAAGAAGT CCCCCTCATA TGAGGACCCA GAGAATGGCA
421 GCCTCTGTAA ACC

```

D228

```

1  ACCTTGAAC CTCTGTAACC TGTCCGATAG GCTCTATAAC ACCCCTACCC CTGAGCCACA
61 CTACAGCCTC TGTCATACAG GCAACTGCAA TCTAATCATG AGGAAAACCT ACACGAACTC
121 CAGTTTGGGG GCAGGTACCT AACCAGGACT TCTGAGAAAT GTCAAGACCA TTGAAAAACA
181 AAGTCTCTCA CAGCCAAGAT GAATCAAAGG AGACATAGTA ACTAGATTTT AAATGGTGGT
241 TTGAACAAGG ATAGTCCCCA CAGATTCATG TGCACGAATG CTTGGTCCAT AGAGAGTGGC
301 ACTATTGGTA GGTATGGCCT TGTGGAGGA AGTGTGTTAT CATAGAGGTG GGTCTGAGAT
361 CTAATATATG CTCAAGCTAT GCCTAGT

```

D230

```

1  GACCCTTGTG GGTGTTGGGC AAGACTCTGC TGGCAAGGTA GCCCGGGGCT CGAGTCTCGA
61 GTCGAGCGGA AGGGCAATTT ATAATTTTTA AAGTCAATAC TAGAAGCATT ACTACCATAT
121 TACAAAGTCT GACTGTCGAT TTATACCTAT GAATGCATGA CAGTGCAAAT TTTAATGCTT
181 CATTAAGAA ACATAGTTTT AAATCTTATC TTTATGTCTA CCTATTAGTA TAATAATCAC
241 ATTAAATATT ATCTTAACTA GAAGTGGCCT CAGAGGTCTA CTTTTTGGAC TGCTTTATGC
301 AACATGTTGG GAAACACTCT AAACCTAAGC CACCAATTTA AAGCTGGCTT GCTATCAATG
361 TAATACAATT ATTATTTTTT TAATTTTTTT TACTAGGTAT TTTCTTCGCT TCATTTCCAA
421 TGCTATCCCA AAGT

```

Figure 3b. The DNA sequences of dinucleosomes from apoptotic mouse thymocytes.

The prefix *D* indicates a fragment derived from cells treated for 4 hours with dexamethasone (0.1 μ M). Residues in bold are polypurine/ polypyrimidine tracts ≥ 20 bp. (Sequencing to ~98% accuracy).

1	acttaatagt	tacttgggag	ttctgggagac	aacaaatatt	ttgatgtgtt	tttaaagggg
	acagagctga	atagattgtg	agtcaagagt	aacgaaaagg	tagctgtgct	tcagtctgtg
	gcataattta	ctcacattag	tcaagaacaa	aacattttaa	aaaataaaga	ggtagctgat

61	gggtggtgat	ggcacatgct	ttaatctcat	catcagagca	gggcaggcag	acttgagttg
	gaaatgtcca	cagtcccagc	acttagagac	agacactggg	cctacaaacc	ctcagccagc
	atgtaaatac	tgaaaacaca	ttcgggtgaa	agattcaaac	ataaaaagac	tacctgatat

121	tatcagctgt	cacagagtta	gtcaatagct	aggctaaaag	agaactgtct	tgaaaacaca
	cggggctaca	taacaagggc	catatgacaa	acaaatctgg	gaaatctcac	tacctttctt
	ataattatat	ttgtatgaaa	tgtccataga	ggtagaaaag	ggatgggaac	ctaattggtct

181GG	GCTGGAGAGA	TGGCTCAGTG	GTTAAGAGCA	CTGACTGCTC	
	cacacacaca	gtagtcaCG	GCTGGTGAGA	TGGCTCAGCA	GTTAAGAGCA	CTGACTGCTC
	aaagatagca	agattcagGG	GCTGGAGAGA	TGGCTCAGCA	GTTAAGAGCA	CTGGCTGCTC
gGT	GCTGGAGAGA	TGGCTCAGCA	GTTAAGAGTA	CTGACTGTTC	
	aaaaatagaa	aat...gaGA	GCTGGAGAGA	TGGCTCAGCA	GTTAAAAGCA	CTGACTGCTC
aaaa	tcaaccccAG	GCTGGAGAGA	TGGCTCAGCA	GTTAAGAGCA	CTGACTGTTC
	TTCCAAAGGT	CCTGAGTTCA	AATCCCAGCA	ACCACATGGT	GGCTCACAAC	CATCTGTAAT
241	TTCCAGACAT	CCTGAATTTA	ATTCCCAG.A	ACCACATGGT	AGCTTACAAC	CATCTGTAAT
	TTCCAGAGGT	CCTGAGTTCA	ATTCCCAGCA	ACCACATGGT	GGCTCACAAC	CATCTGTAAT
	TTCCAGAGGT	CCTGAGTTCA	ATTCCCAGCA	ACCACATGGT	GGCTCACAAC	CATCTGTAAT
	TTCCAGAGGA	CCTGAGTTCA	ATTCCCAGCA	ACCACATGGT	GGCTCACAAC	CATCTGTAAT
	TTCCAAAGGT	CCTGAGTTCA	ATTCCCAGCA	AGCACATGGT	GGCTCACAAC	CATCTGTAAC
	GAGATCTGAT	GCCCTCTTCT	GGTCTGTCTG	AAGACAGCTA	CAGTGTACTT	ATATATAATA
301	GG.....
	GGGATCTGAT	GAACATTTCT	GGTGTGTCTG	AAGACAGTGA	CAGTAAATAT	ATATTTAAAG
	GGGATCCGAT	GCCCTCTTCT	GGTGTGTGTG	AAGACAACAA	CAGTGTGCCC	AAATACATAA
	GGGATCTGAT	GCCCTCTTCT	GGTGTGTCCA	AAGACAGCGG	TGGTGTACTC	ACATACATAA
	AGGATCTAAT	GCCCTCTTCT	GGTGTGTCTG	AAGACCGCTA	CAGTGTACTC	ATATAAATAA
	AATAAATAAA	TCTTTA	B2 CONSENSUS			
	D213			
	GATACACACA	CACACA	RAT LYSOZYME GENE (Accession No. L12459)			
	AATAAATAAA	TCTTGA	MOUSE MAJOR HISTOCOMPATIBILITY ANTIGEN GENE(V01527)			
	AGTAAAAAAT	TCTTTA	RAT INTESTINAL FATTY ACID BINDING PROTEIN GENE (M18080)			
	AATAAATCTT	AAAAAA	MOUSE B2 REPEAT IN THE 3' FLANK OF PROTEIN 53 (P53) (M64597)			

Figure 3c. The similarity of 105 bp (bases 199-304) of dinucleosome D213 with the B2 repeat consensus sequence and B2 repeats from an arbitrary selection of other genes.

The bases in capitals represent the B2 repeat sequence, and the shaded regions are where there is absolute homology between D213 and all the sequences shown. (B2 consensus sequence taken from Rogers, 1985)

3.3. DISCUSSION

In this work dinucleosomal fragments generated during murine thymocyte apoptosis were selected at random, cloned and sequenced.

Whilst the size distribution of the dinucleosomes was on average in the region of 360-400 base pairs as one would expect, the shortest fragment was only 278 base pairs long. This length of DNA cannot encompass two nucleosomal cores with an accompanying 142-143 base pairs each (that is, the length of DNA that makes contact with the histone octamer). There are a few possible explanations for this: either it is a mononucleosome with an abnormally long linker, or a shearing artefact has been introduced during cloning, perhaps where a single stranded nick was already present. The fragment is only a fraction shorter than the length of two nucleosomal cores ($2 \times 142 = 284$), so another interpretation is that it is a dinucleosome but that it has been digested by an exonuclease either during apoptosis or during cloning. Alternatively, assuming the proposal of Peitsch et al. to be correct, two single stranded nicks could have occurred sufficiently close together within the nucleosomal core to introduce a double stranded break so that this unusually small fragment corresponds to one nucleosome plus a half (Peitsch et al., 1993b).

The fragments were found to be generally AT rich (55.93% AT as opposed to 44.07% GC), which is in line with the mouse genome in its entirety (58.90% AT versus 41.40% GC) (Table 3(i)). There were no clear distinctions between the base contents of the fragments from the dexamethasone treated cells and those from cells incubated alone, although from the number that were sequenced it was difficult to make a proper comparison. However it does not appear that the endonuclease is selecting its site of action upon the basis of the base composition of the chromatin.

A similar study to this (Luukkämäki et al., 1993), carried out on oligonucleosomal fragments derived from rat chloroleukaemia cells exposed to ultra violet radiation, concluded that DNA fragmentation during apoptosis is non-random, and that the fragments of DNA produced were enriched in both long and short interspersed repeat elements. Their conclusion derives from the observed enrichment in microsatellites and homopurine/ homopyrimidine domains, all of which have been associated with the transformation of DNA from the usual right-handed B conformation to an unusual

conformation such as the left-handed Z-DNA helix. The implication is that such DNA would have the potential to be more readily degraded due to its modified structure.

However, the only microsatellite that was detected in the study described in this chapter was a stretch of d(AT)₂₂, which is highly resistant to the formation of Z-DNA (Herbert and Rich, 1996). Although it is doubtful whether stretches of homopurine/homopyrimidine sequence will accommodate Z-DNA, the fact that one strand is heavier than the other may preclude DNA containing such a sequence from taking on the usual B form, making it more obtrusive. However, this in no way represents some form of recognition site for the enzyme. The enrichment in these sequence features found both in this work and in the previous study (Luokkamäki et al., 1993) may be as a result of these sequences being more susceptible to digestion *only* if they are present within a region of the genome which is already being digested. It may also be the case that these sequences occur with a greater incidence in the smaller oligonucleosomes than in longer segments of DNA. The failure to find any form of sequence motif that could potentially be recognised by an endonuclease suggests that the enzyme is influenced primarily by the spatial arrangement of the chromatin rather than by the sequence of the DNA. A certain amount of influence is exerted by DNA sequence upon nucleosome positioning, for example when DNA is bent into a circle, short runs of AT have the minor groove facing inwards whereas runs of GC have the minor groove facing outwards (Simpson, 1986). It is also important that sequences that need to be recognised for the binding of transcription factors or polymerases are accessible i.e. either in the linker region or facing away from the histone core.

When the sequences of the dinucleosomes were searched against the Entrez Sequences database the only significant match was provided by 105 base pairs at the 3' end of sequence D213 (Figure 3c), which formed part of a B2 repeat. B2 repeats are short interspersed repeats of around 180 base pairs found in rodents, and are analogous to the *Alu* repeats found in primates (reviewed by Rogers, 1985). There is no physiological function known for the B2 repeats, although they have been suggested to have roles in DNA replication and also RNA processing, as the 3' end contains d(AATAAA) sequences which could act as a polyadenylation signal. They are also thought to be more abundant in tumour cells, although the reason for this is not known. They frequently occur within introns, and all the sequences retrieved from the database shown in Figure

3c contain the B2 repeat either within an intron or within the DNA closely flanking a gene. The sequence does not contain an open reading frame, although it is homologous to 4.5 SI RNA, which is found in the nucleoplasm. In addition, mRNAs containing B2 repeats have been found within the cytoplasm, so they are apparently transcribed although they are not functional. The association of B2 sequences with transcribed DNA hints that fragment D213 could originate from transcriptionally active DNA. This would correlate with the work of Arends et al. who found that the smaller oligonucleosomes, which in comparison with longer oligonucleosomes are enriched in the high mobility group proteins 1 and 2, derive from transcriptionally active chromatin which would be more susceptible to endonuclease digestion because of its more diffuse structure (Arends et al., 1990).

In summary, there was no particular sequence bias detected in the dinucleosomes that were sequenced. The identification of a sequence that is potentially part of a gene (the B2 repeat) could imply that the DNA being degraded came from transcriptionally active DNA. Although there was a very slight enrichment in microsatellites and homopurine/homopyrimidine tracts, the evidence for apoptotic internucleosomal degradation being non-random on account of these sequences being present is insufficient.

CHAPTER 4

DIFFERING REQUIREMENTS FOR EXTRACELLULAR CALCIUM IN THE INDUCTION OF APOPTOSIS IN THYMOCYTES

4.1. INTRODUCTION

Ca^{2+} is a second messenger that regulates many diverse processes such as muscle contraction, fertilisation and the transmission of nervous signals. The deregulation of Ca^{2+} signalling mechanisms has been implicated in ischaemia, cardiac arrhythmias, hypertension, manic depression and tumourigenesis (reviewed by Berridge, 1994). The main store of rapidly releasable Ca^{2+} lies within the endoplasmic reticulum (ER), although Ca^{2+} is also stored in the nucleus and the mitochondria. Ca^{2+} is either pumped out of the cell or kept within these organelles by Ca^{2+} -ATPases, leaving the resting Ca^{2+} concentration in the cytosol in the region of 100 nM, compared with an extracellular Ca^{2+} concentration of around 1 mM (Clapham, 1995; McConkey and Orrenius, 1996).

The so-called capacitative hypothesis for the elevation of Ca^{2+} within the cell in response to an external stimulus was first proposed by James Putney (Putney, 1986; Putney, 1990). This theory suggested that the entry of Ca^{2+} into the cell from the exterior was somehow regulated by the degree to which the stores within the ER were filled, i.e. as the Ca^{2+} stores within the ER become empty, Ca^{2+} is prompted to enter the cell from the exterior. The initial means of elevating the intracellular free Ca^{2+} concentration ($[\text{Ca}^{2+}]_i$) in non-excitabile cells like thymocytes is via the generation of inositol (1,4,5) trisphosphate ($\text{Ins}(1,4,5)\text{P}_3$) (see Figure 4a). Initially, cross-linking of a cell surface receptor activates phospholipase c (PLC). There are two classes of cell surface receptors that are able to mobilise Ca^{2+} : either a receptor coupled to a G protein which activates $\text{PLC}\beta$, or a tyrosine kinase receptor which activates $\text{PLC}\gamma$. PLC then converts phosphatidyl inositol (4,5)-bisphosphate (PtdInsP_2) into $\text{Ins}(1,4,5)\text{P}_3$ and diacylglycerol, which modulates protein kinase c (reviewed by Clapham, 1995).

The elevation of $[\text{Ca}^{2+}]_i$ is biphasic. $\text{Ins}(1,4,5)\text{P}_3$ binds to its receptor in the ER, which triggers the initial release of Ca^{2+} into the cytosol and the accompanying depletion of the stores within the ER. This depletion of the stores causes the subsequent influx of Ca^{2+} from outside the cell by an as yet unknown mechanism, resulting in an approximately 10-fold increase in $[\text{Ca}^{2+}]_i$. The Ca^{2+} enters the cell via the putative calcium-release-activated calcium (CRAC) channel to generate the influx current I_{CRAC} . Following removal of the agonist, $\text{Ins}(1,4,5)\text{P}_3$ is rapidly degraded and the influx of extracellular Ca^{2+} ceases when the ER Ca^{2+} stores have been refilled, so that the rise in $[\text{Ca}^{2+}]_i$ is transient. The Ca^{2+} is

then retained within the ER by the microsomal Ca^{2+} -ATPase (reviewed by Clapham, 1995).

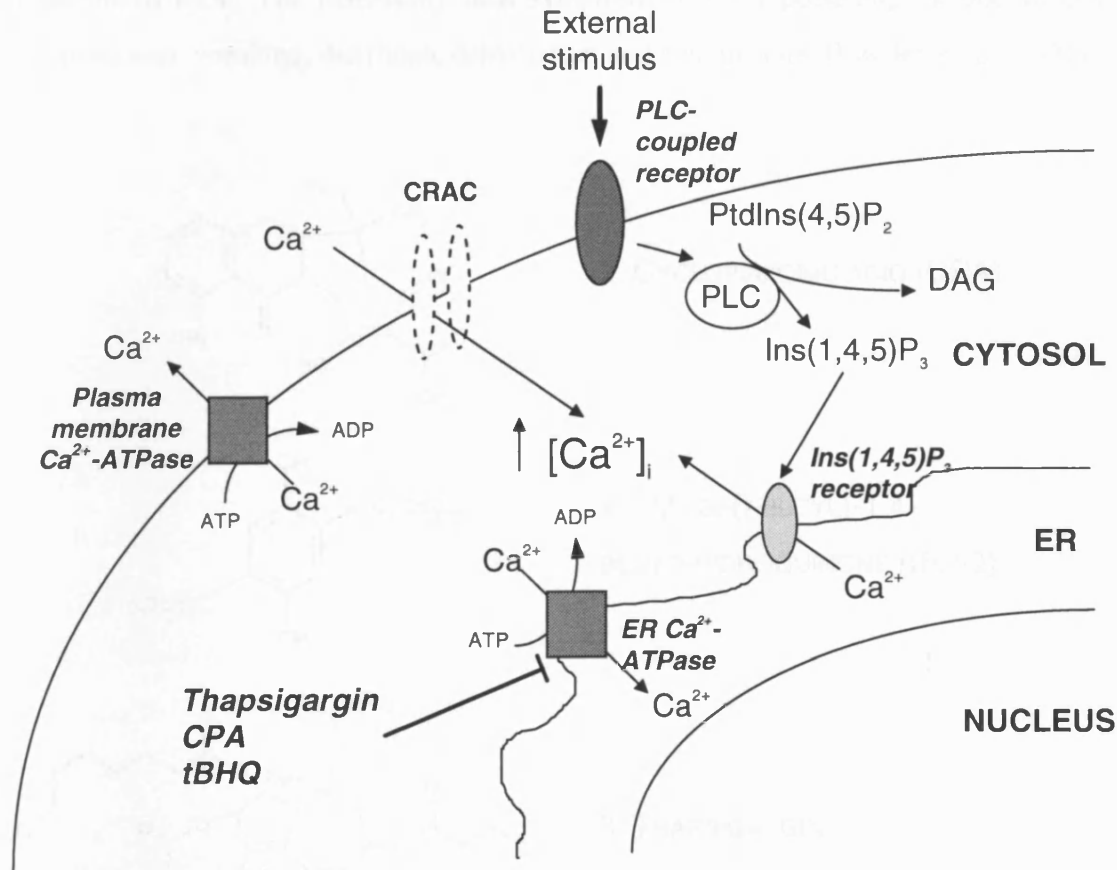


Figure 4a. An illustration of capacitative Ca^{2+} influx showing the point and mechanism of action of thapsigargin, CPA and tBHQ.

Binding of an external stimulus causes the activation of phospholipase c (PLC), which converts phosphatidyl inositol (4,5)-bisphosphate (PtdIns(4,5)P₂) to diacylglycerol (DAG) and inositol (1,4,5) trisphosphate (Ins(4,5)P₃). The binding of Ins(4,5)P₃ to its receptor in the ER membrane prompts the release of Ca^{2+} into the cytosol. The emptying of the Ca^{2+} stores in the ER causes the influx of extracellular Ca^{2+} (capacitative calcium entry) through the as yet unidentified calcium-release-activated calcium (CRAC) channel. The Ca^{2+} that has entered the cell is then sequestered by the Ca^{2+} -ATPase in the ER. Thapsigargin, CPA and tBHQ inhibit the Ca^{2+} -ATPase in the ER, preventing the re-compartmentalisation of Ca^{2+} which results in a permanent elevation in $[\text{Ca}^{2+}]_i$.

The work described in this chapter involves three compounds: thapsigargin, cyclopiazonic acid (CPA) and 2,5-di-(*t*-butyl)-1,4-benzohydroquinone (tBHQ) (Figure 4b). Thapsigargin is a tumour promoter derived from the plant *Thapsia garganica*, which has been known for centuries to cause skin irritation (Inesi and Sagara, 1992). Cyclopiazonic acid (CPA) is a mycotoxin produced by species of *Penicillium* and also by *Aspergillus flavus* and *Aspergillus oryzae*. These fungi cause food poisoning by growing

on foodstuffs, which allows them to secrete secondary metabolites like cyclopiazonic acid into the food. If these fungi are allowed to grow on grain fed to poultry, the ingested CPA accumulates in skeletal muscle, raising the possibility of human contact via contaminated meat. The potentially fatal symptoms of CPA poisoning include weight loss, weakness, vomiting, diarrhoea, dehydration and convulsions (Blunden et al., 1991).

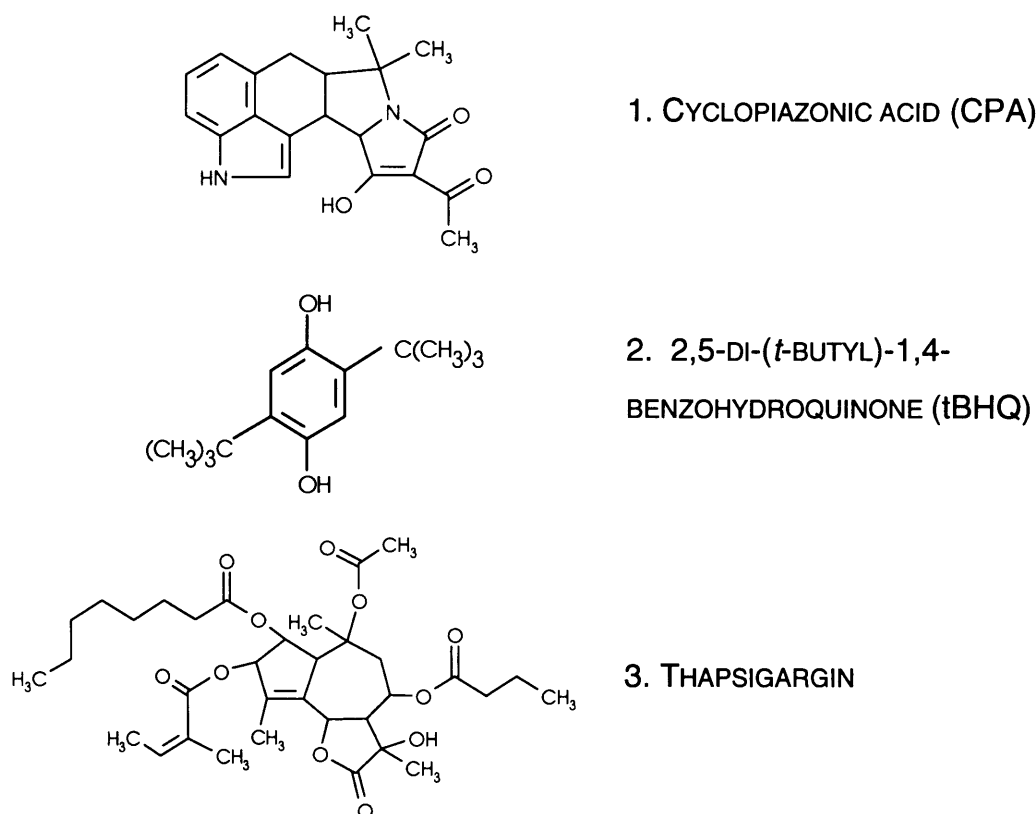


Figure 4b. The chemical structures of the three Ca^{2+} -ATPase inhibitors used in this study.

Despite these three agents having similar actions and effects, their chemical structures are markedly different.

These three agents all inhibit the Ca^{2+} -ATPase in the ER, but do not affect the plasma membrane Ca^{2+} -ATPase which maintains the Ca^{2+} gradient between the cytosol and the exterior (Thastrup et al., 1990; Gouy et al., 1990; Goeger et al., 1989; Seidler et al., 1990; Moore et al., 1987; Kass et al., 1989). Inhibition of the microsomal Ca^{2+} -ATPase deprives it of its ability to sequester Ca^{2+} , so the existing Ca^{2+} within the ER is released into the cytosol and the ER Ca^{2+} stores become empty. This causes an influx of extracellular Ca^{2+} which is unable to be re-sequestered by the ER, so the stores remain depleted and Ca^{2+} continues to enter the cell. Thus, these compounds result in the persistent elevation of $[\text{Ca}^{2+}]_i$ without the involvement of $\text{Ins}(1,4,5)\text{P}_3$. However, as the

Ca^{2+} -ATPase in the plasma membrane remains unaffected by these agents, a certain amount of Ca^{2+} is pumped back out of the cell, so that the $[\text{Ca}^{2+}]_i$ eventually reaches a plateau.

The other agents used in this chapter - the glucocorticoid dexamethasone, the topoisomerase II inhibitor etoposide, and staurosporine, a broad spectrum protein kinase inhibitor - are all able to induce apoptosis in thymocytes (Fearnhead et al. 1995a), but the extent of their effects upon Ca^{2+} signalling mechanisms is unknown, and it is unclear whether Ca^{2+} also plays a role in the induction of apoptosis by these compounds.

The work in this chapter initially focuses upon the participation of $[\text{Ca}^{2+}]_i$ elevation in the induction of apoptosis not only with respect to the Ca^{2+} -ATPase inhibitors thapsigargin, CPA and tBHQ but also dexamethasone, etoposide and staurosporine. The work continues by examining the relationship of proteolysis to the induction of apoptosis by the three Ca^{2+} -ATPase inhibitors. N α -tosyl-L-lysiny chloromethylketone (TLCK), an inhibitor of trypsin-like proteases, has been shown in thymocytes to inhibit both the morphological changes and degradation of DNA associated with apoptosis induced by dexamethasone, staurosporine, etoposide, thapsigargin and γ -irradiation (Fearnhead et al., 1995a). This indicates a requirement for proteolysis in thymocyte apoptosis, although the association of this step or steps with other signalling pathways is unclear. Thus, after initially verifying that CPA- and tBHQ-induced apoptosis were also able to be inhibited by TLCK, the relationship between the elevation of $[\text{Ca}^{2+}]_i$ and the proteolytic step mediated by TLCK is analysed.

4.2 RESULTS

4.2.1. The induction of apoptosis and $[Ca^{2+}]_i$ elevation by microsomal Ca^{2+} -ATPase inhibitors

Thapsigargin induced apoptosis in isolated rat thymocytes in agreement with previous reports (Jiang et al., 1994; Fearnhead et al., 1995a). Two more microsomal Ca^{2+} -ATPase inhibitors, CPA (Goeger et al., 1989; Seidler et al., 1990) and tBHQ (Moore et al., 1987; Kass et al., 1989), were also extremely effective inducers of apoptosis in thymocytes (Figure 4c). The three microsomal Ca^{2+} -ATPase inhibitors caused a concentration-dependent induction of apoptosis (Figure 4c).

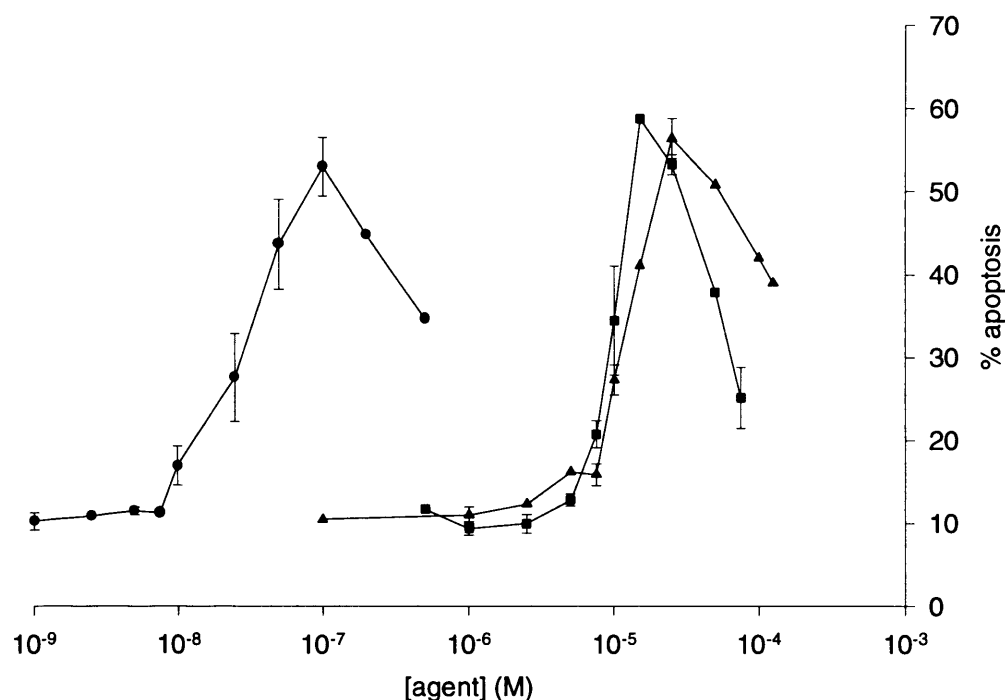


Figure 4c. The concentration-response curves of thapsigargin (—●—), CPA (—▲—) and tBHQ (—■—) with respect to apoptosis.

Thymocytes were incubated with the test agent and apoptosis was quantified by flow cytometry after 4 hours as described in section 2.1.3. Data is the mean \pm s.e.m., $n \geq 2$.

Thapsigargin was the most potent inducer with a $\log_{10} EC_{50}$ of -7.56 ± 0.10 (27.5 nM), whilst CPA and tBHQ were approximately 500-fold less potent having $\log_{10} EC_{50}$ values of -4.92 ± 0.03 (12.0 μ M), and -4.99 ± 0.04 (10.2 μ M) respectively. At the highest concentrations tested, all three microsomal Ca^{2+} -ATPase inhibitors showed a decreased

incidence of apoptosis in comparison with the maximum levels. This was not due to excess cytotoxicity, as the percentage of non-viable (propidium iodide including) cells seen was not substantially different to that seen with the concentrations inducing the maximum amount of apoptosis (data not shown).

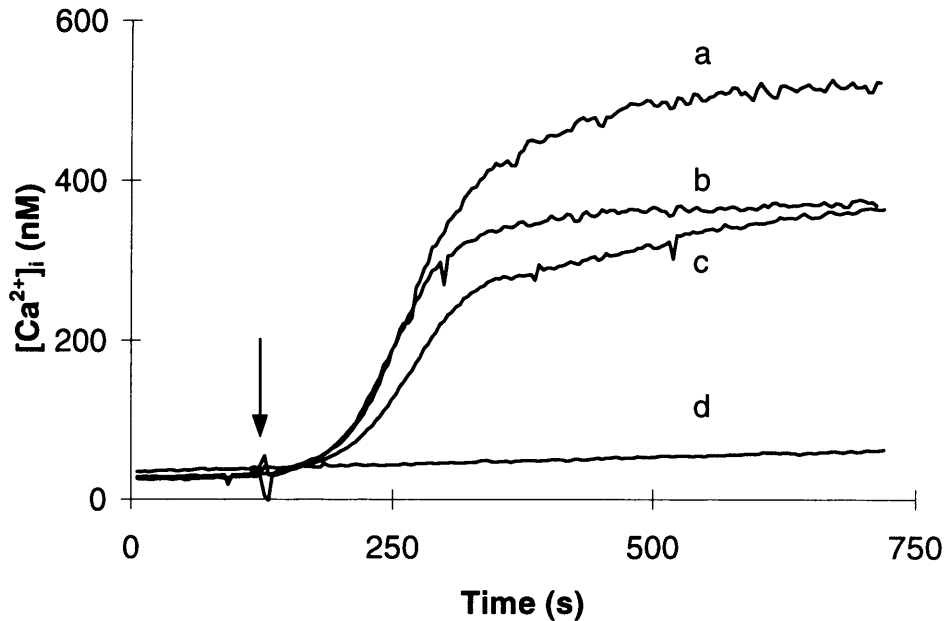


Figure 4d. The elevation in $[Ca^{2+}]_i$ in response to the three Ca^{2+} -ATPase inhibitors in comparison with the elevation in $[Ca^{2+}]_i$ caused by dexamethasone.

Thymocytes were loaded with fura-2 as described in section 2.3.2. At the time indicated by the arrow, either (a) thapsigargin (50 nM), (b) CPA (25 μ M), (c) tBHQ (25 μ M) or (d) dexamethasone (0.1 μ M) were added. Identical experiments were also conducted using etoposide (10 μ M) and staurosporine (1 μ M), but like dexamethasone they produced no measurable increase in $[Ca^{2+}]_i$ (data not shown). Traces are representative of three separate experiments.

In addition to the three Ca^{2+} -ATPase inhibitors, the effects of three other known apoptotic stimuli, dexamethasone, etoposide and staurosporine were investigated. To determine the immediate effects of each of the six agents upon $[Ca^{2+}]_i$, changes in $[Ca^{2+}]_i$ were monitored using the Ca^{2+} -responsive fluorescent dye fura-2 (section 2.3.1.). As expected, the three microsomal Ca^{2+} -ATPase inhibitors all induced a rapid and sustained increase in $[Ca^{2+}]_i$ (Figure 4d). In contrast dexamethasone (0.1 μ M), etoposide (10 μ M) and staurosporine (1 μ M) all induced apoptosis in agreement with previous reports (Wyllie 1980; Walker et al., 1991; Fearnhead et al., 1995a; Figures 4f-j) but did not cause any detectable rise in $[Ca^{2+}]_i$ over the time period monitored (10 min) (Figure 4d and data not shown).

4.2.2. The relationship between $[Ca^{2+}]_i$ increase and the initiation of apoptosis by thapsigargin

In preliminary experiments, low concentrations of thapsigargin (1-5 nM) were found to cause an increase in $[Ca^{2+}]_i$, but did not induce apoptosis above control levels. To further analyse the relationship between $[Ca^{2+}]_i$ increase and apoptosis for the microsomal Ca^{2+} -ATPase inhibitors, a concentration response for $[Ca^{2+}]_i$ elevation was constructed using thapsigargin (Figure 4e). The concentration response curve was steep, with $[Ca^{2+}]_i$ rising from a very low level at 5 nM to approaching maximum at 10 nM. The $\log_{10} EC_{50}$ for the $[Ca^{2+}]_i$ curve shown in Figure 4e was -8.07 ± 0.03 (8.5 nM) (Figure 4e), whilst for the induction of apoptosis the $\log_{10} EC_{50}$ was -7.56 ± 0.10 (27.5 nM) (Figure 4c). Thus, there is an indirect relationship between the increase in $[Ca^{2+}]_i$ and the levels of apoptosis induced by thapsigargin.

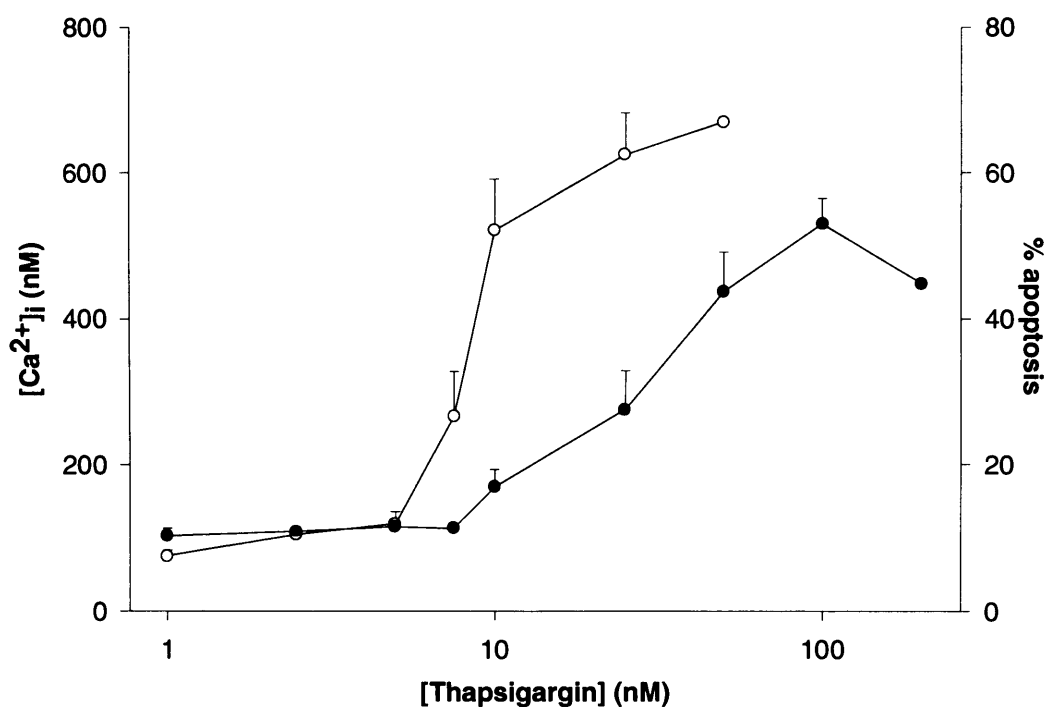


Figure 4e. A comparison of the concentration-response curves for thapsigargin-induced apoptosis and elevation of $[Ca^{2+}]_i$.

Thymocytes were incubated with thapsigargin for 4 hours and then apoptosis (filled circles) was quantified by flow cytometry. The elevation of $[Ca^{2+}]_i$ (open circles) was determined in thymocytes loaded with fura-2 between 380 and 580 seconds after the addition of thapsigargin (i.e. once a plateau had been reached). Data are mean \pm s.e.m.

4.2.3. EGTA inhibits apoptosis induced by the microsomal Ca^{2+} -ATPase inhibitors to a greater degree than other apoptotic stimuli

EGTA (2 mM) was used to lower extracellular free Ca^{2+} . In cells exposed to thapsigargin, CPA or tBHQ, EGTA reduced the levels of apoptosis to control levels (Figure 4f). EGTA also caused a significant inhibition ($p < 0.05$) of apoptosis in cells treated with either dexamethasone or etoposide, but the levels of apoptosis were not reduced to control levels as with the Ca^{2+} -ATPase inhibitors. EGTA had little effect when apoptosis was induced by staurosporine (Figure 4f).

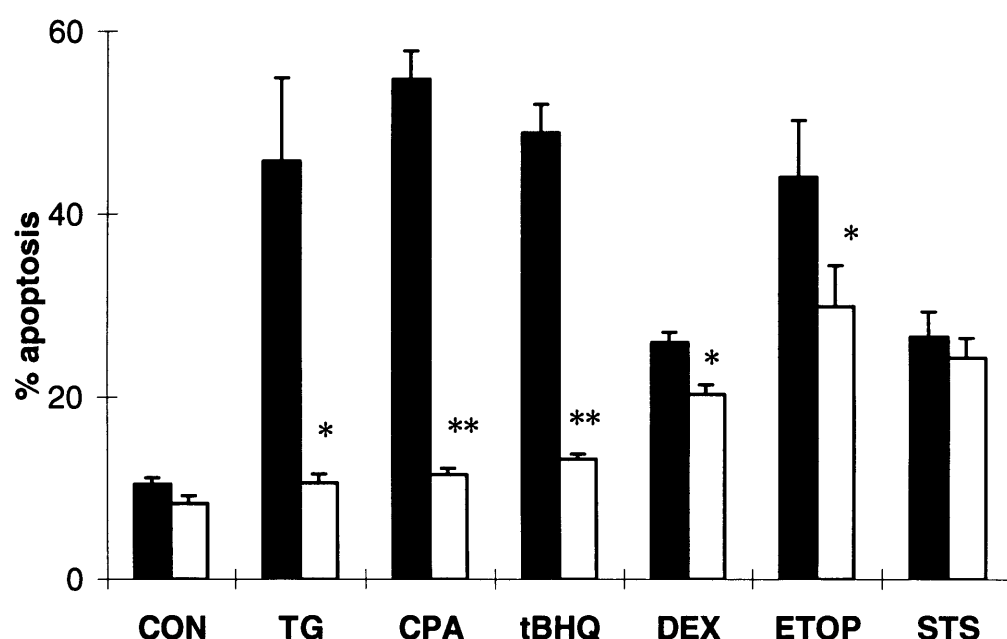


Figure 4f. The effect of removal of extracellular Ca^{2+} by buffering with EGTA on apoptosis.

Thymocytes were incubated either alone (con) or with thapsigargin (TG) (50 nM), CPA (25 μM), tBHQ (25 μM), dexamethasone (Dex) (0.1 μM), etoposide (ETOP) (10 μM) or staurosporine (STS) (1 μM) for 4 hours either in the absence (closed bar) or presence (open bar) of EGTA (2 mM). Data are mean \pm s.e.m., $n \geq 3$. For *, $p < 0.05$ and ** $p < 0.001$ by the Students t-test.

A characteristic of an apoptotic cell is the degradation of DNA into oligonucleosomes that are visualised as a ladder pattern following gel electrophoresis (section 3.1) (Wyllie, 1980). All six agents caused extensive DNA degradation into both oligonucleosomes (Figure 4g) and high molecular weight fragments (Figure 4h). A small amount of internucleosomal cleavage was seen in control cells consistent with the background levels of apoptosis seen in thymocytes (Figure 4g lane 1). In the presence of EGTA, laddering was reduced to control levels when the cells were incubated with the Ca^{2+} -ATPase

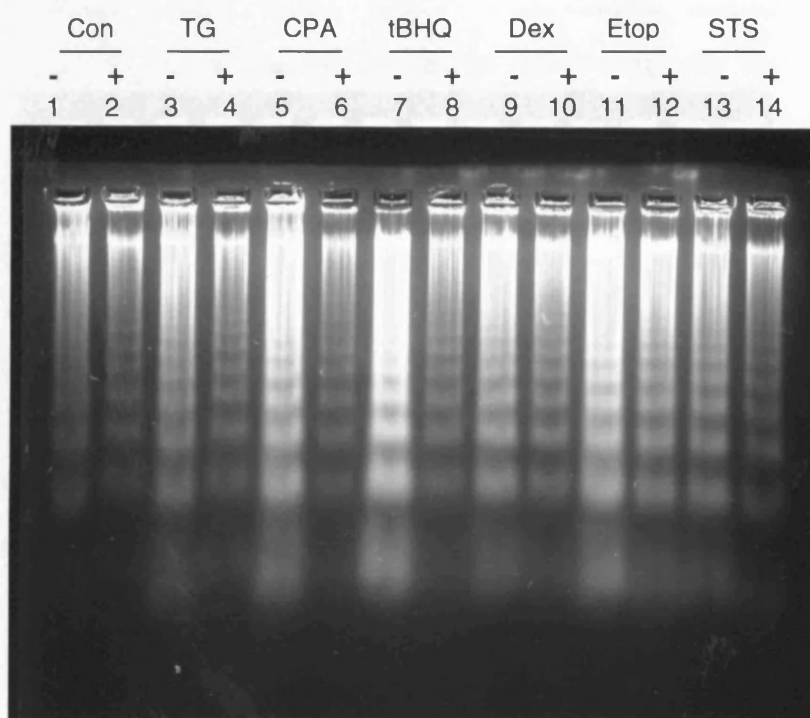


Figure 4g. *The effect of depleting extracellular Ca^{2+} on internucleosomal DNA degradation*

Thymocytes were incubated for 4 hours either under control conditions (lane 1-2) or in the presence of thapsigargin (TG) (50 nM) (lanes 3-4), CPA (25 μ M) (lanes 5-6), tBHQ (25 μ M) (lanes 7-8), dexamethasone (Dex) (0.1 μ M) (lanes 9-10), etoposide (Etop) (10 μ M) (lanes 11-12) or staurosporine (STS) (1 μ M) (lanes 13-14). The thymocytes were incubated either with the agent alone (-) or in the presence of EGTA (2 mM) (+). The gel is representative of at least 3 experiments.

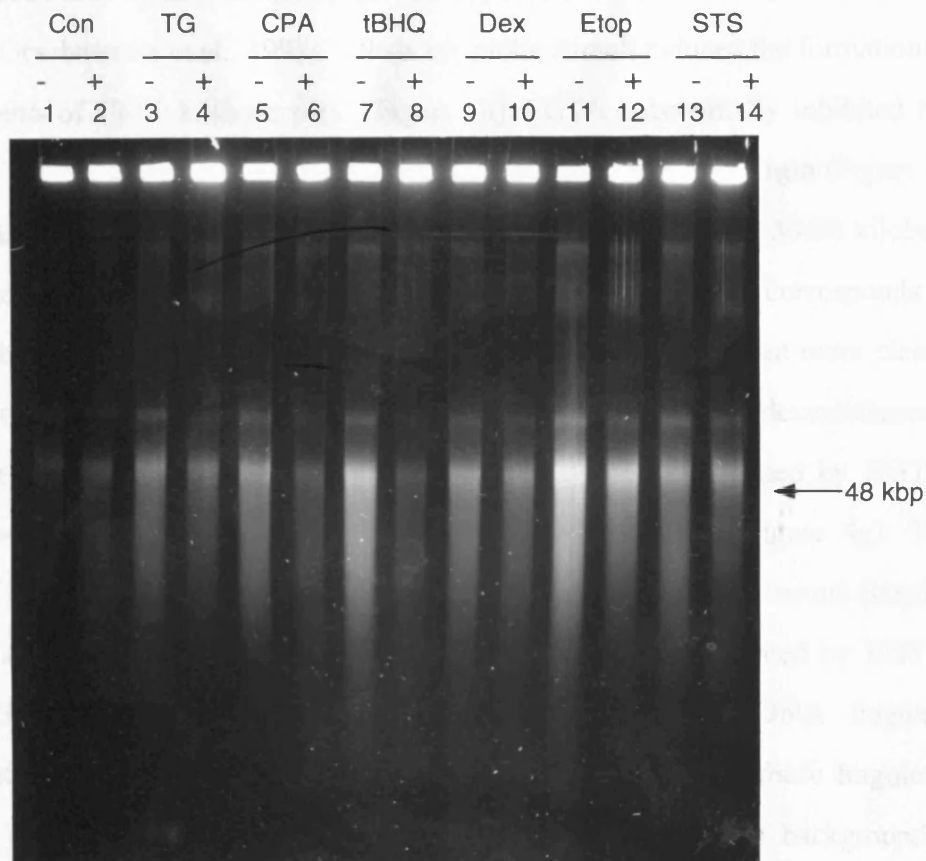


Figure 4h. The effect of depleting extracellular Ca^{2+} upon the formation of high molecular weight DNA fragments

Thymocytes were incubated for 4 hours either alone (lane 1-2) or in the presence of thapsigargin (TG) (50nM) (lanes 3-4), CPA (25 μM) (lanes 5-6), tBHQ (25 μM) (lanes 7-8), dexamethasone (Dex) (0.1 μM) (lanes 9-10), etoposide (Etop) (10 μM) (lanes 11-12) or staurosporine (STS) (1 μM) (lanes 13-14). The thymocytes were incubated either with the agent alone (-) or in the presence of EGTA (2 mM) (+). The gel is representative of at least 3 experiments.

inhibitors (Figure 4g lanes 4,6 and 8). Laddering induced by dexamethasone (lanes 9 and 10), etoposide (lanes 11 and 12) and staurosporine (lanes 13 and 14) was marginally reduced by EGTA, reflecting the flow cytometry data (Figure 4f).

Another indication of apoptosis is the formation of high molecular weight fragments of DNA that can be seen by field inversion gel electrophoresis (Walker et al., 1991; Brown et al., 1993; Oberhammer et al., 1993). All six apoptotic stimuli induced the formation of DNA fragments of 30-50 kilobase pairs (Figure 4h). EGTA substantially inhibited the formation of these fragments when cells were treated with either thapsigargin (Figure 4h lane 4), CPA (lane 6) or tBHQ (lane 8). Below the most intense band of 30-50 kilobase pairs a range of DNA fragments of decreasing size was visible, which corresponds to the smaller fragments formed during internucleosomal cleavage that are seen more clearly by conventional gel electrophoresis (Figure 4g). In cells treated with dexamethasone, etoposide or staurosporine, these smaller DNA fragments were diminished by EGTA, consistent with the slight inhibition of internucleosomal cleavage (Figure 4g). The formation of high molecular weight DNA fragments induced by dexamethasone (lanes 9 and 10) and staurosporine (lanes 13 and 14) were not substantially inhibited by EGTA, although EGTA appeared to be reducing high molecular weight DNA fragment formation induced by etoposide (lanes 11 and 12). The quantification of these fragments by scanning densitometry was attempted, but due to the high levels of background it was impossible to obtain meaningful data.

4.2.4. Econazole inhibits apoptosis induced by microsomal Ca^{2+} -ATPase inhibitors but not by other apoptotic stimuli

Econazole, an imidazole antimycotic, reduces the influx of extracellular Ca^{2+} in response to the depletion of intracellular stores in a number of cell types including rat thymocytes (Alvarez et al., 1991, Mason et al., 1993).

Econazole (10 μM) caused a partial but significant ($p < 0.05$) inhibition when apoptosis was induced by the three Ca^{2+} -ATPase inhibitors (Figure 4i). Apoptosis induced by dexamethasone, etoposide or staurosporine was not significantly affected. The extent to which the DNA was degraded into oligonucleosomes correlated with the flow cytometry

data: econazole reduced the levels of DNA fragmentation in thymocytes treated with thapsigargin, CPA or tBHQ, but not in cells exposed to dexamethasone, etoposide or staurosporine. Although econazole was selective in its inhibition of apoptosis, because the inhibition was only partial its mechanism of action was not further investigated.

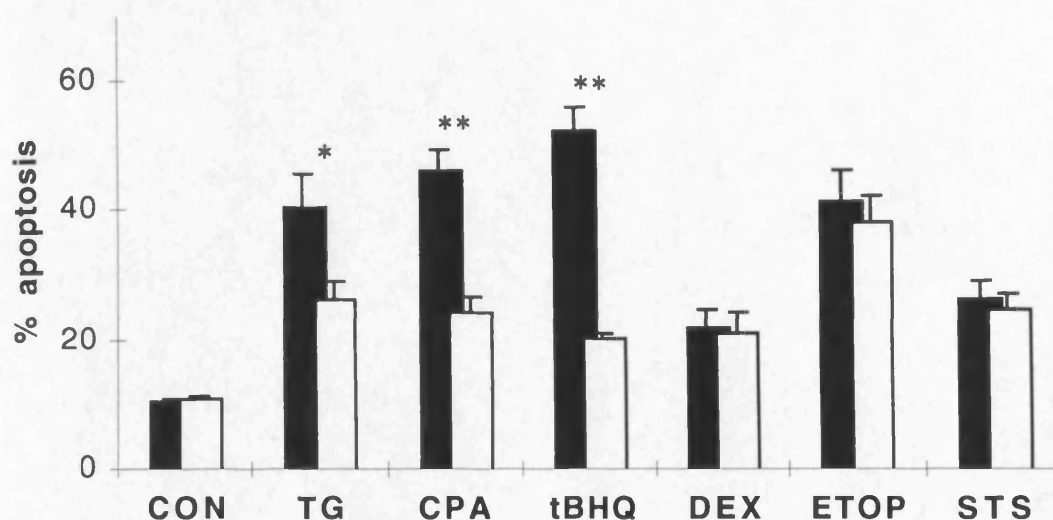


Figure 4i The effect of econazole upon apoptosis induced by a variety of different stimuli.

Thymocytes were incubated either alone (con) or with thapsigargin (TG) (50 nM), CPA (25 µM), tBHQ (25 µM), dexamethasone (DEX) (0.1 µM), etoposide (ETOP) (10 µM) or staurosporine (STS) (1 µM) for 4 hours either in the absence (closed bar) or presence (open bar) of econazole (10 µM). Data are mean \pm s.e.m., $n \geq 3$. For *, $p < 0.05$ and ** $p < 0.001$ by the Students t-test.

4.2.5. TLCK inhibits apoptosis by acting downstream of Ca^{2+} release

N α -tosyl-L-lysiny chloromethylketone (TLCK), which was originally synthesised as an inhibitor of trypsin-like proteases, has been shown to block thymocyte apoptosis induced by dexamethasone, etoposide, staurosporine and thapsigargin (Fearnhead et al., 1995a). To verify whether TLCK also inhibited apoptosis induced by CPA and tBHQ, thymocytes were preincubated for 1 hour in the presence or absence of TLCK (50 µM) and then further incubated for 4 hours with thapsigargin (50 nM), CPA (25 µM) or tBHQ (25 µM). TLCK significantly inhibited the induction of apoptosis in response to all three agents (Figure 4k). TLCK also inhibited DNA fragmentation consistent with the flow cytometry data and previous reports (Fearnhead et al., 1995a) (data not shown).

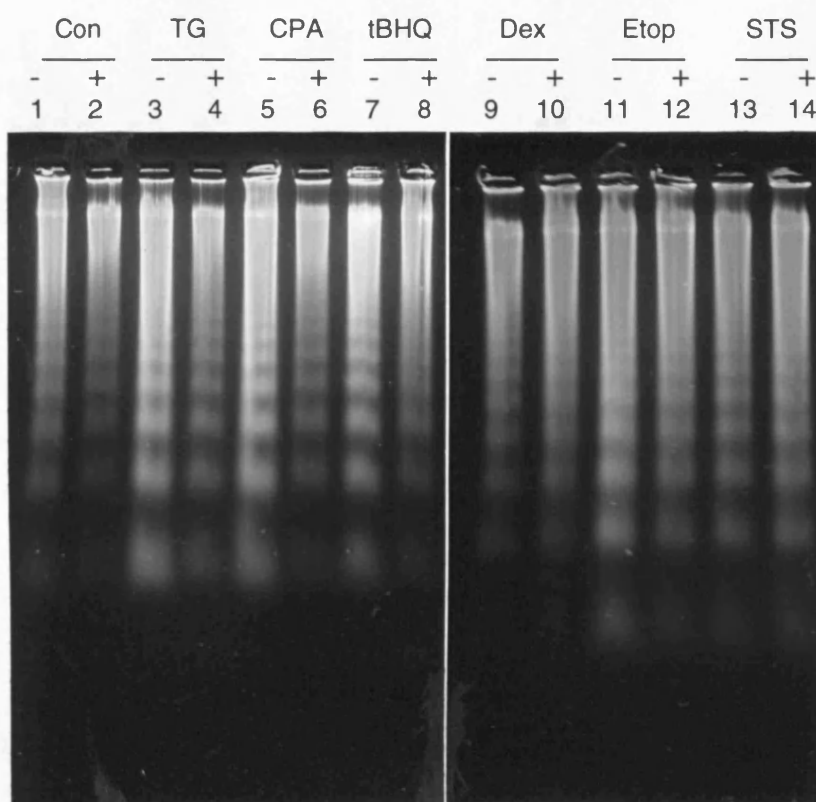


Figure 4j. The effect of inhibiting the uptake of extracellular Ca^{2+} upon internucleosomal DNA cleavage

Thymocytes were incubated for 1 hour either alone (-) or with econazole (10 μM) (+) and then for a further 4 hours either under control conditions (lanes 1 and 2) or in the presence of thapsigargin (TG) (lanes 3-4), CPA (lanes 5-6), tBHQ (lanes 7-8), dexamethasone (Dex) (lanes 9-10), etoposide (Etop) (lanes 11-12) or staurosporine (STS) (lanes 13-14). The gel is representative of three separate experiments.

Because TLCK is able to inhibit apoptosis caused by these agents which require an elevation of $[Ca^{2+}]_i$ to cause apoptosis, and it is unknown whether the effects of TLCK are restricted to the inhibition of trypsin-like proteases, the proposal that TLCK may be inhibiting apoptosis via the modulation of Ca^{2+} flux was investigated. Cells were incubated for 1 hour alone or with TLCK (50 μ M), loaded with fura 2, and the effects of the previously used concentrations of thapsigargin, CPA and tBHQ (Figure 4k) on $[Ca^{2+}]_i$ were investigated.

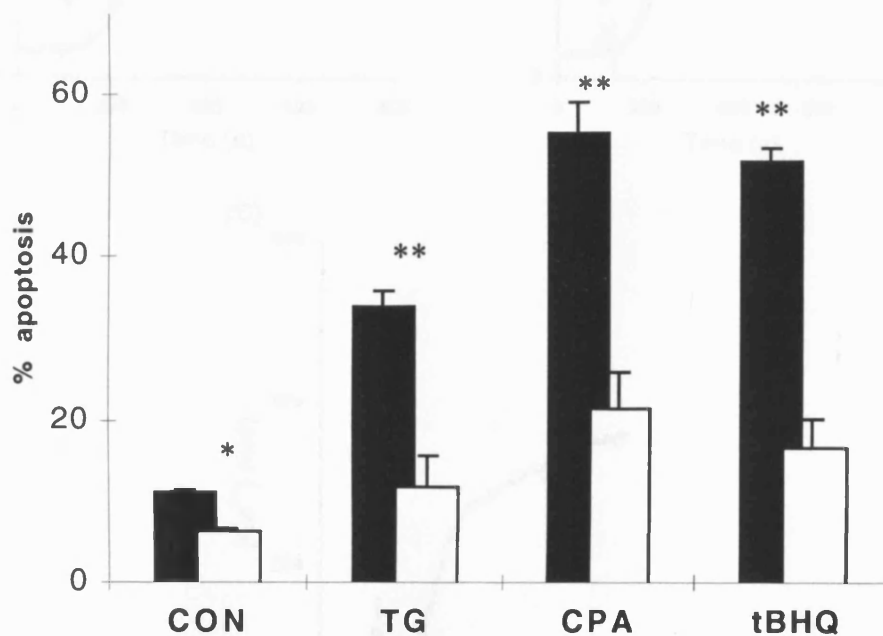


Figure 4k. *The inhibition by TLCK of apoptosis induced by the Ca^{2+} -ATPase inhibitors.*

Thymocytes were incubated for 1 hour either alone or in the presence of TLCK (50 μ M) and then incubated for a further 4 hours with either thapsigargin (TG) (50 nM), CPA (25 μ M) or tBHQ (25 μ M). Apoptosis was then quantified by flow cytometry. Data given is mean \pm s.e.m., $n \geq 3$. For *, $p < 0.05$ and ** $p < 0.001$ by the Students t-test.

Under these conditions TLCK was still able to inhibit apoptosis assessed by DNA fragmentation (data not shown). However, pre-incubation of the cells with TLCK had little effect on the levels of $[Ca^{2+}]_i$ elevation initiated by any of the three agents (Figure 4l). This confirms that TLCK acts to inhibit apoptosis downstream of an elevation in $[Ca^{2+}]_i$.

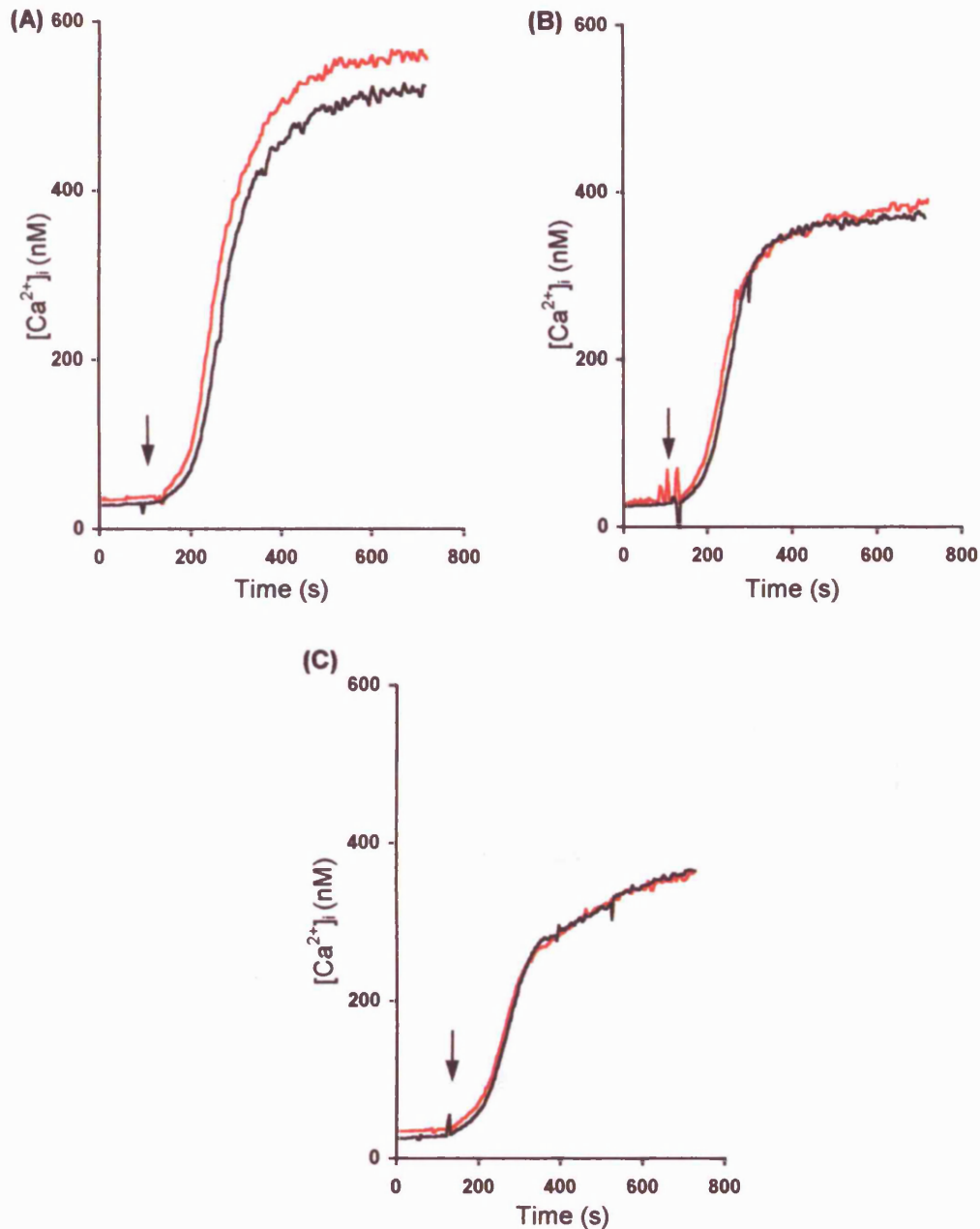


Figure 4I. TLCK does not inhibit the elevation of $[Ca^{2+}]_i$ in response to Ca^{2+} -ATPase inhibitors. Thymocytes were incubated in RPMI 1640 with 10% FCS for 1 hour either alone (black line) or in the presence of TLCK (50 μ M) (red line). The cells were then transferred to Krebs/ HEPES buffer and loaded with fura 2 as described in section 2.3.2. At the time indicated by the arrow, either (A) thapsigargin (50 nM), (B) CPA (25 μ M) or (C) tBHQ (25 μ M) were added. The data shown is representative of at least two different experiments.

4.3. DISCUSSION

Thapsigargin, cyclopiazonic acid and tBHQ, all of which are inhibitors of the microsomal Ca^{2+} pump (Figure 4a), are extremely effective inducers of apoptosis in isolated rat thymocytes (Figure 4c; Jiang et al., 1994). As can be seen from Figure 4c, thapsigargin, CPA and tBHQ all have very steep, characteristic concentration response curves. In addition, their concentration response curves are all biphasic, i.e. the levels of apoptosis decrease as the concentration of the agent increases. This cannot be explained merely as an increase in toxicity, as the level of dead cells at these concentrations are not substantially different to those observed with concentrations that induce the highest levels of apoptosis (data not shown).

This phenomenon could be attributable to two additional effects that the agents are having. Firstly, there exists the possibility that these agents are inhibiting their own mode of action to a certain extent. Mason et al. showed that that by treating isolated rat thymocytes either with thapsigargin at a concentration of 300 nM, or with CPA or tBHQ at 50 μM , the initial rapid rise in $[\text{Ca}^{2+}]_i$ is transient (Mason et al., 1991). Thus, at high concentrations these agents are capable of preventing the influx of extracellular Ca^{2+} , and hence act to inhibit apoptosis in a similar way to EGTA. A similar phenomenon has also been demonstrated using thapsigargin in human neutrophil granulocytes (Geiszt et al., 1995). As shown by the inhibitory effects of EGTA and econazole on the induction of apoptosis by these agents, a reduction in the influx of extracellular Ca^{2+} inhibits apoptosis.

Secondly, both thapsigargin and CPA have been shown to inhibit protein synthesis. It is well established that in the thymocyte model apoptosis is inhibited by the protein synthesis inhibitor cycloheximide (Cohen and Duke, 1984). In GH₃ pituitary cells, protein synthesis is inhibited by low levels of thapsigargin (2-3 nM), an effect which appears to be independent of Ca^{2+} release (Wong et al., 1993). CPA reduces protein synthesis by nearly a half in HeLa cells at 30 μM (Zaera et al., 1983). It is unknown whether tBHQ also behaves in a similar manner.

It was initially anticipated that the concentration response for $[\text{Ca}^{2+}]_i$ would correlate directly with the concentration response for apoptosis, i.e. a certain degree of $[\text{Ca}^{2+}]_i$

elevation would provide a corresponding level of apoptosis, and if the two plots were drawn on the same x -axis they would be able to be superimposed. However, a comparison of the two curves (Figure 4e) demonstrated that this was not the case, as a level of $[Ca^{2+}]_i$ approaching maximum is caused by a thapsigargin concentration that is considerably less than the concentration that gives the maximum apoptotic response. The two curves have comparable shapes, in that they make the transition from approximately minimum to nearly maximum within a fairly narrow concentration range, but the transition from a low level of $[Ca^{2+}]_i$ to a high level occurs at a lower concentration than the analogous transition with respect to apoptosis. For example, thapsigargin at 10 nM causes an elevation in $[Ca^{2+}]_i$ that is 67% of the maximum response, whereas the same concentration causes a level of apoptosis that is only 32% of the maximum apoptotic response. This is also borne out by comparing the EC_{50} value of thapsigargin with respect to $[Ca^{2+}]_i$ elevation (8.5 nM) and the EC_{50} value for apoptosis (27.5 nM).

Although concentration response curves for the effects of CPA and tBHQ upon $[Ca^{2+}]_i$ were not constructed, previous studies have shown that in rat thymocytes maximum levels of $[Ca^{2+}]_i$ were obtained using concentrations of 5-10 μ M (CPA) and approximately 10 μ M (tBHQ) (Mason et al., 1991). In agreement with the thapsigargin data, such concentrations of these agents do not yield a maximum apoptotic response (Figure 4c). One reason for these discrepancies between $[Ca^{2+}]_i$ levels and apoptosis could be the existence of an apoptosis threshold, whereby the $[Ca^{2+}]_i$ must reach a certain level before apoptosis is initiated. This threshold appears to be at a $[Ca^{2+}]_i$ of around 500-600 nM (Figure 4e; Mason et al., 1991). The reason for this may be that the components of a Ca^{2+} -dependent death pathway require the $[Ca^{2+}]_i$ to be of this magnitude for initiation. Also, there are substantial stores of Ca^{2+} in the mitochondria, although the mitochondrial Ca^{2+} transporters have a lower affinity for Ca^{2+} than the Ca^{2+} -ATPase in the ER, and mitochondria generally do not participate in Ca^{2+} signalling. However, mitochondrial damage has been reported in thymocytes induced into apoptosis by thapsigargin (Beaver and Waring, 1994) so it may be that when $[Ca^{2+}]_i$ reaches the threshold levels, disruption of the mitochondria may trigger apoptosis.

Whilst thapsigargin, CPA and tBHQ are all extremely effective at inducing apoptosis in isolated rat thymocytes, this is inhibitable either by the addition of the Ca^{2+} chelator

EGTA to the medium, or by blocking the capacitative Ca^{2+} influx mechanisms with econazole. Although econazole was not able to inhibit apoptosis as extensively as EGTA, the same inhibition of membrane changes (as detected by flow cytometry) and internucleosomal cleavage selective for the three Ca^{2+} -ATPase inhibitors is demonstrated. The inability of econazole to completely inhibit apoptosis may be as a result of other effects the compound is having. Whilst imidazole antimycotics like econazole are known as inhibitors of cytochrome P450, they have also been demonstrated to have other effects, for example in human platelets they suppress tyrosine phosphorylation and induce membrane depolarisation (Sargeant et al., 1994). In thymocytes, econazole has been demonstrated to have the opposing effects of both preventing the uptake of Ca^{2+} following the depletion of the internal stores by thapsigargin whilst simultaneously causing the release of Ca^{2+} from thapsigargin sensitive stores (Mason et al., 1993). Thus, econazole would never cause the levels of $[\text{Ca}^{2+}]_i$ to be sufficiently low to inhibit apoptosis as substantially as EGTA does, but it lowers $[\text{Ca}^{2+}]_i$ enough to have an effect.

Whichever means thapsigargin, CPA and tBHQ are using to kill the cell, they seem initially to use a distinct mechanism for inducing cell death to the pathway(s) used by dexamethasone, etoposide or staurosporine. A number of lines of evidence suggest this. The three agents all cause an instantaneous and prolonged elevation in $[\text{Ca}^{2+}]_i$, whereas dexamethasone, etoposide and staurosporine have no such effect (Figure 4d.). This is reflected in the selective abilities of EGTA and econazole to inhibit apoptosis induced by the six agents used in this work (Figures 4f-j). In addition, thapsigargin, CPA and tBHQ are all much more effective at inducing apoptosis in the space of 4 hours than dexamethasone, etoposide and staurosporine (Figures 4f and 4i). Apoptosis caused by the three Ca^{2+} -ATPase inhibitors may occur via a Ca^{2+} -dependent signalling mechanism, for example Ca^{2+} -dependent proteases, kinases or phosphatases, which eventually feed into a central death pathway used by all the agents in the study, which is inhibitable by TLCK. An elevation in $[\text{Ca}^{2+}]_i$ caused by thapsigargin has also been demonstrated to swell the mitochondria and decrease the cellular ATP content which again could stress the cell and cause apoptosis (Beaver and Waring, 1994; Waring and Beaver, 1996). As the deletion of autoreactive immature thymocytes via cross linking of the T cell receptor has been shown to cause an elevation in $[\text{Ca}^{2+}]_i$ (McConkey et al., 1989a), the microsomal Ca^{2+} -ATPase

inhibitors may be more effective at inducing apoptosis because they are using a 'preferred' endogenous death programme.

Furthermore, thymocytes isolated in the manner described in this chapter are a heterogeneous population, i.e. some are the highly immature CD4⁻CD8⁻ double negative cells, most are CD4⁺CD8⁺ double positive cells and a further subpopulation are the more mature CD4⁺ or CD8⁺ single positive cells. The T cell receptor (TcR) is present only on CD4⁺CD8⁺ double positive cells and single positive cells, and cross-linking of the TcR causes apoptosis via an elevation in $[Ca^{2+}]_i$ (McConkey et al., 1989a). Immature TcR⁻CD4⁻CD8⁻ double negative mouse thymocytes are resistant to apoptosis induced by the Ca²⁺ ionophore ionomycin, which acts to elevate $[Ca^{2+}]_i$, but in contrast the TcR⁺CD4⁺CD8⁺ double positive subpopulation are susceptible to ionomycin, whilst both populations are susceptible to dexamethasone (Andjelic et al., 1993). This acts to further demonstrate that there are distinct apoptotic pathways within the cell, and that a Ca²⁺-dependent pathway utilised by ionomycin, anti-CD3 and perhaps thapsigargin, CPA and tBHQ is only functional once the thymocytes have become CD4⁺CD8⁺ double positive cells. Despite this apparent restriction in the population of cells that are susceptible to apoptosis induced by agents that cause an elevation in $[Ca^{2+}]_i$, the majority of the cells used in this study are CD4⁺CD8⁺ (Cohen et al., 1993).

The published data implicating Ca²⁺ in apoptosis induced by dexamethasone and other synthetic glucocorticoids is somewhat inconsistent. It was initially suggested by McConkey et al. that methylprednisolone, which like dexamethasone is a synthetic glucocorticoid, induces an early and sustained increase in $[Ca^{2+}]_i$ in rat thymocytes, and that this and the accompanying apoptosis are inhibitable by EGTA (McConkey et al., 1989b). The intracellular Ca²⁺ chelator, bis-(*o*-aminophenoxy)-ethane-N,N,N',N'-tetraaceticacid/ tetra (acetoxymethyl) -ester (BAPTA-AM) prevents the formation of high molecular weight DNA fragments in thymocytes exposed to dexamethasone (Zhivotovsky et al., 1994), and the activation of the Ca²⁺-dependent protease calpain has been reported, also in thymocytes treated with dexamethasone (Squier et al., 1994), all of which would indicate the participation of Ca²⁺.

However, it has subsequently been illustrated that exposure of thymocytes to dexamethasone does not elicit any elevation in $[Ca^{2+}]_i$ (Iseki et al., 1993; Beaver and

Waring, 1994) and that extracellular Ca^{2+} is not required for dexamethasone induced DNA fragmentation (Waring and Sjaarda, 1995). This agrees with the data presented in Figure 4d. Another study (Ye et al., 1993) also fails to show substantial inhibition of DNA fragmentation in thymocytes treated with dexamethasone in the presence of EGTA. The results shown here with dexamethasone (Figures 4f-i) seem to be a compromise between the two arguments: a subpopulation of the cells are sensitive to inhibition by EGTA and would appear to require a sustained influx of extracellular Ca^{2+} to enter apoptosis, whereas the remainder are not.

Further evidence that an elevation in $[\text{Ca}^{2+}]_i$ is not a general means of inducing apoptosis in thymocytes is provided by the inability of the inhibitor of trypsin-like proteases TLCK to prevent an elevation in $[\text{Ca}^{2+}]_i$ in response to thapsigargin, CPA and tBHQ. TLCK inhibits apoptosis in thymocytes induced by all the stimuli used in this chapter (Fearnhead et al., 1995a; Figure 4k). This, when coupled with the fact that TLCK is incapable of inhibiting an increase in $[\text{Ca}^{2+}]_i$, places the target or targets for TLCK downstream of $[\text{Ca}^{2+}]_i$ elevation and onto a general apoptotic pathway which is used by all the agents. As $[\text{Ca}^{2+}]_i$ elevation is a means of elevating apoptosis which is not ubiquitous, it remains unaffected. The site or sites of action of TLCK are unknown, although its inhibition of a widespread effector of cell death is unlikely, as in the human monocytic cell line THP.1 it can act to enhance apoptosis (Zhu et al., 1995).

CHAPTER 5

THE PARTICIPATION AND INHIBITION OF ICE/CED-3 PROTEASES IN THE EXECUTION PHASE OF APOPTOSIS

5.1. INTRODUCTION

Peptide inhibitors have been used extensively to investigate the actions of the ICE/Ced-3 family proteases in apoptosis.

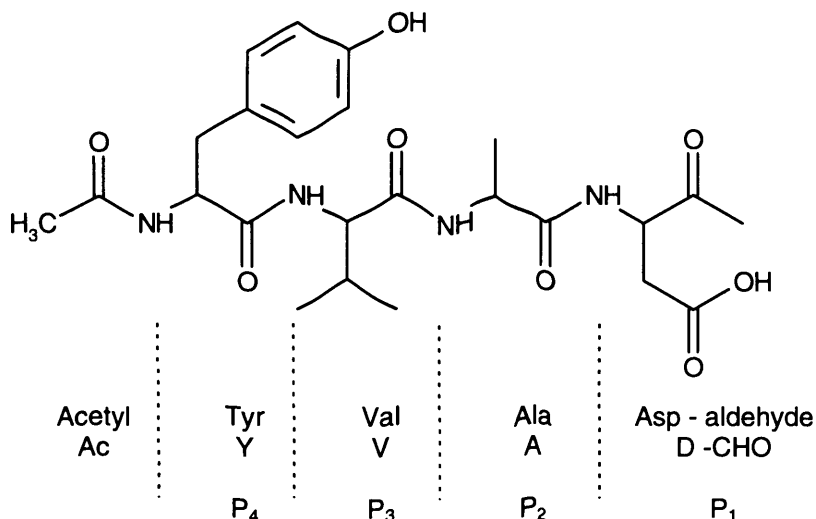


Figure 5a. The reversible ICE inhibitor, Acetyl-Tyr-Val-Ala-Asp-CHO (Ac-YVAD-CHO).

This inhibitor is based upon the cleavage site between Asp 116 and Ala 117 in proIL-1 β , except that the P₂ histidine in proIL-1 β has been substituted for an alanine to increase the effectiveness of the inhibitor (Thornberry et al., 1992)

The peptide sequences used in these inhibitors are based upon the recognition sequences present within the protein substrates. The first such inhibitor to be synthesised was Acetyl-Tyr-Val-Ala-Asp-aldehyde (Ac-YVAD-CHO) (Figure 5a) (Thornberry et al., 1992), which is based upon a sequence within proIL-1 β which is cleaved by ICE. The point at which ICE actually cleaves proIL-1 β has the sequence Tyr-Val-His-Asp, but it was found that changing the P₂ histidine to an alanine residue gave optimum ICE inhibition (Thornberry et al., 1992). This inhibitor has subsequently been used as a reversible inhibitor of ICE.

The inhibitor Acetyl-Asp-Glu-Val-Asp-aldehyde (Ac-DEVD-CHO) (Figure 5b) was initially used as an affinity tag to isolate the enzyme which was cleaving poly(ADP-ribose) polymerase (PARP) (Nicholson et al., 1995), as the tetrapeptide sequence used in this compound is the sequence at which PARP is cleaved during apoptosis (Figure 1g). Using this method, the enzyme CPP32 was isolated as being the protease responsible (Nicholson et al., 1995). However, despite the apparent success of using this approach to synthesise inhibitors of the ICE/Ced-3 family, only these two peptide sequences have been used in the study of apoptosis as the synthesis of these compounds is complex.

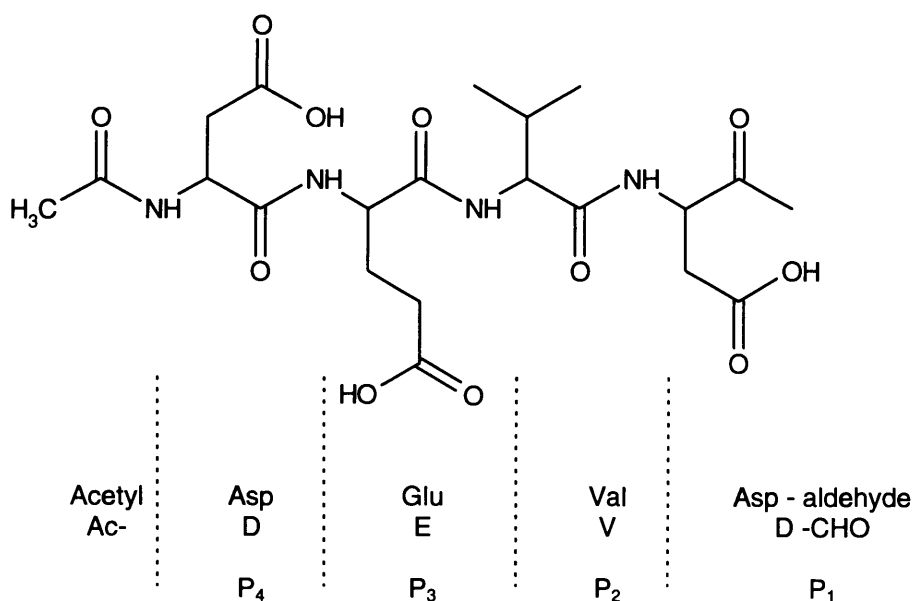


Figure 5b. The reversible inhibitor of CPP32, Acetyl-Asp-Glu-Val-Asp-aldehyde (Ac-DEVD-CHO). This inhibitor is based upon the amino acid sequence (Asp-Glu-Val-Asp 216/ Gly 217) within PARP which is cleaved during apoptosis (Nicholson et al., 1995)

The third principle inhibitor used in this work is benzyloxycarbonyl-Val-Ala-Asp-fluoromethylketone (Z-VAD.FMK) (Figure 5c), which is an irreversible, cell-permeable inhibitor of ICE (Chow et al., 1995). It is probably able to cross the plasma membrane due to the carboxyl group on the P₁ aspartate being in the form of an *O*-methyl ester, which is thought to be converted by intracellular esterases into the acid form in much the same way that fura-2 AM is converted to fura 2 (see section 2.3.1.).

Z-VAD.FMK is the peptide inhibitor which most consistently inhibits apoptosis in intact cells and the compound is being used increasingly in the study of apoptosis. Z-VAD.FMK has been shown to inhibit apoptosis in a diverse array of models of apoptosis. For example, it inhibits apoptosis caused by a range of chemical stimuli in both the human monocytic cell line THP.1 (Zhu et al., 1995) and in isolated rat thymocytes (Fearnhead et al., 1995b), in isolated rat hepatocytes exposed to staurosporine or transforming growth factor β_1 (Cain et al., 1996), in a B cell lymphoma cell line exposed to calcium ionophore or anti-IgM antibodies (An and Knox, 1996) and in a human fibroblast cell line exposed to staurosporine (Jacobson et al., 1996). It also inhibits *reaper*-mediated death in cells from *Drosophila* (Pronk et al., 1996), and it inhibits

interdigital cell death in the developing paws of embryonic mice (Jacobson et al., 1996).

The two aldehydes (Ac-YVAD-CHO and Ac-DEVD-CHO) both act as competitive, reversible inhibitors. They react with the thiol group on the active site cysteine, resulting in the oxidation of the substrate to the carboxylic acid. In contrast, Z-VAD.FMK reacts irreversibly with the thiol to form a thiomethylketone (reviewed by Thornberry and Molineaux, 1995).

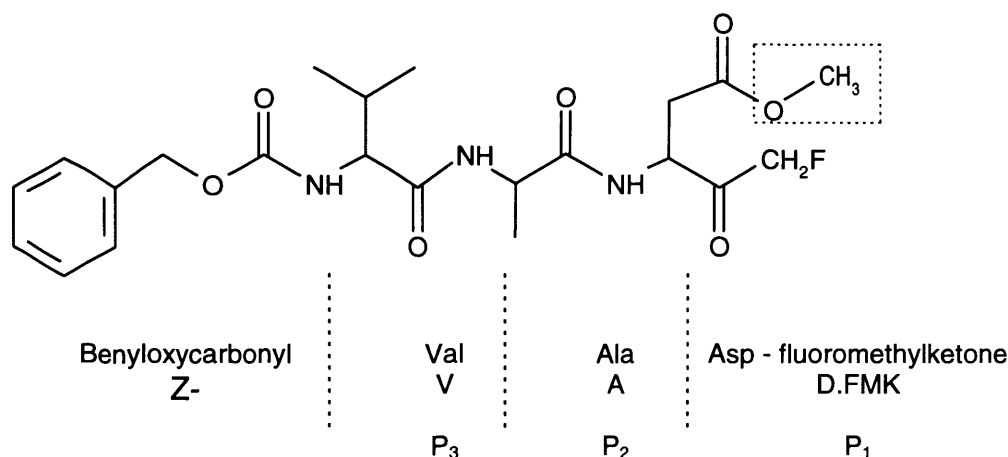


Figure 5c. Benzyloxycarbonyl-Val-Ala-Asp-fluoromethylketone (Z-VAD.FMK), an irreversible inhibitor of ICE-like proteases.

The P₁ aspartate residue is in the form of the O-methyl ester (shown within the dotted line) which reverts to a carboxyl group following the action of intracellular esterases.

The first part of the work in this chapter involves the human monocytic cell line THP.1 (see section 1.5.2.), and the effect of peptide inhibitors upon apoptosis in these cells both in intact cells and *in vitro*. The work is principally concerned with Z-VAD.FMK, and demonstrates that this inhibitor acts to block apoptosis by the hitherto unsuspected mechanism of preventing the proteolytic activation of CPP32.

The second part investigates ICE/Ced-3-like activity in Jurkat T lymphocytes induced to undergo apoptosis via the Fas-mediated signalling pathway (see section 1.3.5.). Initially, it was confirmed that as in THP.1 cells, Z-VAD.FMK inhibits apoptosis in these cells by preventing the activation of CPP32. The results conclude with an examination of the role of ICE in apoptosis in this system. ICE was initially implicated in the Fas signalling pathway because it is inhibited by Ac-Tyr-Val-Ala-Asp-chloromethylketone (YVAD.CMK) and Ac-YVAD-CHO, both of which were designed to inhibit ICE (Los et al., 1995; Enari et al., 1995), and by CrmA (Enari et al., 1995; Tewari and Dixit,

1995), a cowpox virus serpin which seems to be principally an inhibitor of ICE rather than other members of the ICE/Ced-3 family (Ray et al., 1992) (section 1.3.4.). Furthermore, the induction of apoptosis by Fas is enhanced by the overexpression of ICE, and inhibited by the expression of an antisense ICE construct (Los et al., 1995). In the work described in this chapter, no evidence for the participation of ICE in Fas-mediated apoptosis could be found.

5.2. RESULTS

5.2.1. Analysis of the cleavage *in vitro* of [35 S]PARP and [35 S]proIL-1 β by lysates derived from THP.1 cells

Initially, it was necessary to prepare a lysate which would be likely to possess the ability to cleave [35 S]PARP. THP.1 cells, a human monocytic tumour cell line, can be induced to undergo apoptosis by exposure to a variety of chemical stimuli, including thapsigargin, staurosporine, cycloheximide and etoposide (Zhu et al., 1995). This is enhanced by co-incubation with *N* α -tosyl-L-lysiny chloromethylketone (TLCK). The most effective inducer of apoptosis (63.6%) over a 4 hour time period was found to be a combination of cycloheximide (25 μ M) and TLCK (100 μ M) (Zhu et al., 1995). Thus, to obtain an effective lysate, THP.1 cells were incubated for 30 minutes, 1 hour, 2 hours, 3 hours and 4 hours and lysate prepared as described in section 2.4.2. In addition, lysate was prepared from untreated (control) cells.

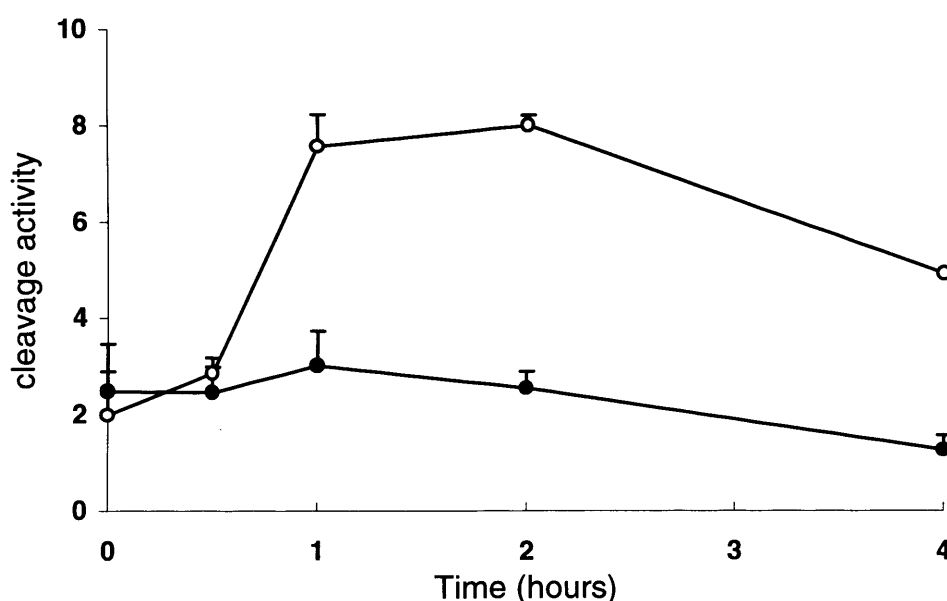


Figure 5d. Time course for the cleavage of [35 S]PARP and [35 S]proIL-1 β by lysate prepared from THP.1 cells exposed to cycloheximide and TLCK

THP.1 cells were incubated for the stated period of time (x-axis) with cycloheximide (25 μ M) and TLCK (100 μ M). Lysate was then prepared from these cells, and the ability of the lysates to cleave [35 S]PARP (open circles) or [35 S]proIL-1 β (closed circles) was assessed by SDS PAGE followed by quantification by scanning densitometry. The cleavage activity (y-axis) corresponds to the intensity of the 24 kDa band ([35 S]PARP) or the 17.5 kDa band ([35 S]proIL-1 β). Data represents the mean \pm s.e.m.

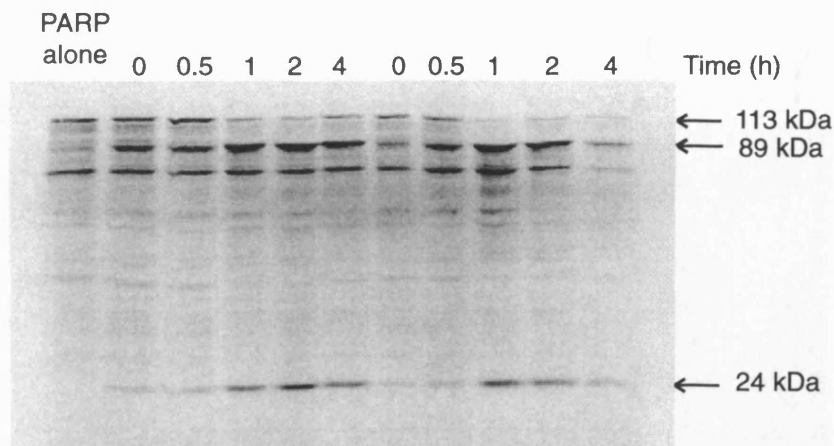
Whilst the control lysate had very little [35 S]PARP cleavage activity (Figure 5d), the

Figure 5d. continued

Time (h)	% apoptosis	% dead
0	1.5	0.1
0.5	2.3	0.3
1	3.2	0.4
2	10.8	0.6
4	52.4	2.6

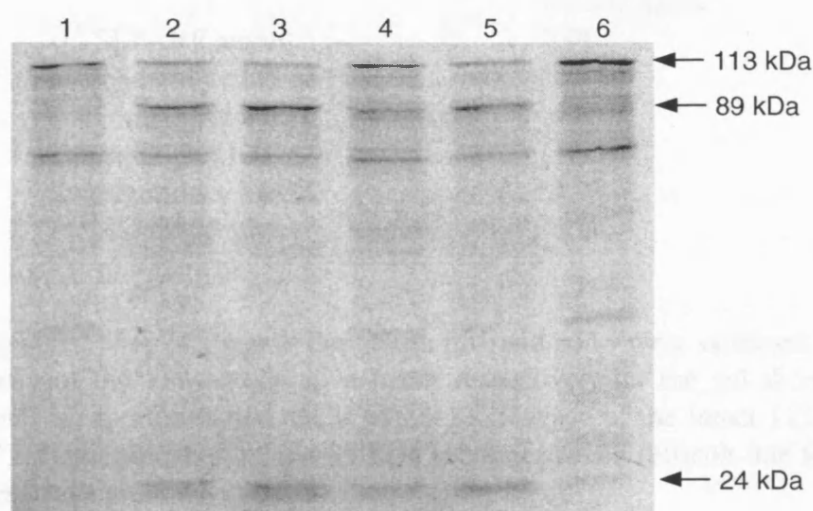
Percentages of apoptosis and necrosis measured in THP.1 cells.

THP.1 cells were exposed to cycloheximide (25 μ M) and TLCK (100 μ M) for the stated times and apoptosis and necrosis quantified by flow cytometry as described in Materials and Methods



Gel showing the extent of cleavage of [35 S]PARP by lysates prepared from THP.1 cells exposed to cycloheximide (25 μ M) and TLCK (100 μ M) for the time periods indicated.

(A)



(B)

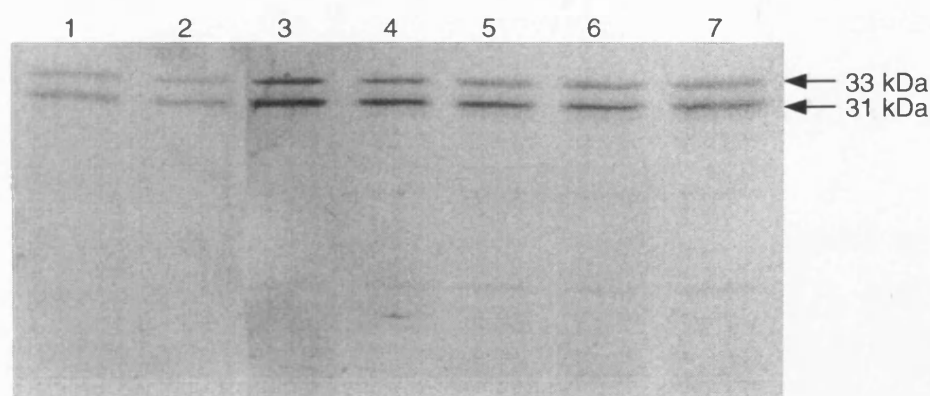


Figure 5e. Lysates from THP.1 cells exposed to a variety of stimuli cleave $[^{35}\text{S}]\text{PARP}$ but not $[^{35}\text{S}]\text{proIL-1}\beta$

(A) Lysates were prepared from THP.1 cells incubated for 1 hour either alone (lane 1), or with cycloheximide (25 μM) (lane 2), cycloheximide and TLCK (100 μM) (lane 3), thapsigargin (100 nM) (lane 4), thapsigargin and TLCK (lane 5), or etoposide (25 μM) (lane 6). The lysates (10 μg protein) were then incubated for 30 minutes at 37°C with $[^{35}\text{S}]\text{PARP}$. The active, apoptotic lysates were able to break down $[^{35}\text{S}]\text{PARP}$ from the intact 113 kDa from into 89 and 24 kDa fragments. (B) The same lysates were incubated under identical conditions with $[^{35}\text{S}]\text{proIL-1}\beta$. Lane 1, $[^{35}\text{S}]\text{proIL-1}\beta$ alone; lane 2, control lysate; lane 3, cycloheximide; lane 4, cycloheximide and TLCK; lane 5, thapsigargin; lane 6, thapsigargin and TLCK; lane 7, etoposide.

Figure 5e

		% conversion*
lane 1	([³⁵ S] PARP alone)	7.89
lane 2	cycloheximide (25 μ M)	27.86
lane 3	cycloheximide + TLCK (100 μ M)	44.85
lane 4	thapsigargin (100 nM)	11.95
lane 5	thapsigargin + TLCK	53.99
lane 6	etoposide (25 μ M)	11.69

* % conversion = $p_{24}/(p_{113}+p_{24})$, where the values p_{24} and p_{113} were obtained from scanning densitometry of the 113 and 24 kDa bands respectively on the gel shown in Figure 5e. This is only an approximation of the extent of cleavage of the intact 113 kDa band of [³⁵S]PARP, as quantification of the 89 kDa product proved difficult due to the presence of spurious bands around this band in some of the lanes.

lysates prepared from cells treated with cycloheximide and TLCK were all capable of cleaving [35 S]PARP to 89 and 24 kDa fragments. The lysate prepared following 30 minutes exposure to cycloheximide and TLCK had a mild ability to cleave [35 S]PARP, whereas by 1 or 2 hours the [35 S]PARP had been extensively degraded (Figure 5d). By the 4 hour time point, when intact cells would contain highly fragmented DNA and possess the ultrastructural changes associated with apoptosis (Zhu et al., 1995), the ability of the lysate prepared from these cells to cleave [35 S]PARP was decreasing (Figure 5d). In contrast, there was only slight cleavage of proIL-1 β , despite THP.1 cells containing high levels of ICE (Miller et al., 1993).

To verify that the ability of the cycloheximide/TLCK lysate to cleave [35 S]PARP was not unique to this particular stimulus, lysates were prepared from cells exposed for 1 hour to a number of chemical stimuli. All the stimuli used were able to cleave [35 S]PARP to 89 and 24 kDa fragments (Figure 5e), although in the case of etoposide the cleavage was only slight. The lysates possessed little ICE activity, which was assessed by the cleavage of proIL-1 β (Figure 5e).

5.2.2. Z-VAD.FMK inhibits PARP breakdown *in vivo* but not *in vitro*

Z-VAD.FMK is an extremely effective inhibitor of many facets of apoptosis induced by a number of chemical stimuli in intact THP.1 cells (Zhu et al., 1995). However, the effects of Ac-YVAD-CHO (Thornberry et al., 1992) and Ac-DEVD-CHO (Nicholson et al., 1995) upon apoptosis in intact cells was unknown at the time this work was undertaken.

THP.1 cells were incubated for 1 hour either alone or with Ac-DEVD-CHO, Ac-YVAD-CHO or Z-VAD.FMK (all 10 μ M), and then for 4 hours with cycloheximide and TLCK. Apoptosis was quantified by flow cytometry, DNA breakdown was analysed by FIGE and the status of PARP was determined by Western blotting. As shown previously (Zhu et al., 1995), Z-VAD.FMK was able to inhibit apoptosis extremely effectively (Figure 5f). However, both Ac-DEVD-CHO and Ac-YVAD-CHO had only a marginal effect (Figure 5f). Higher concentrations of the aldehyde inhibitors were not used as only limited quantities of these compounds were available.

To determine the effects of Ac-DEVD-CHO, Ac-YVAD-CHO and Z-VAD.FMK on PARP cleavage *in vitro*, [35 S]-labelled PARP was incubated with an active THP.1 lysate

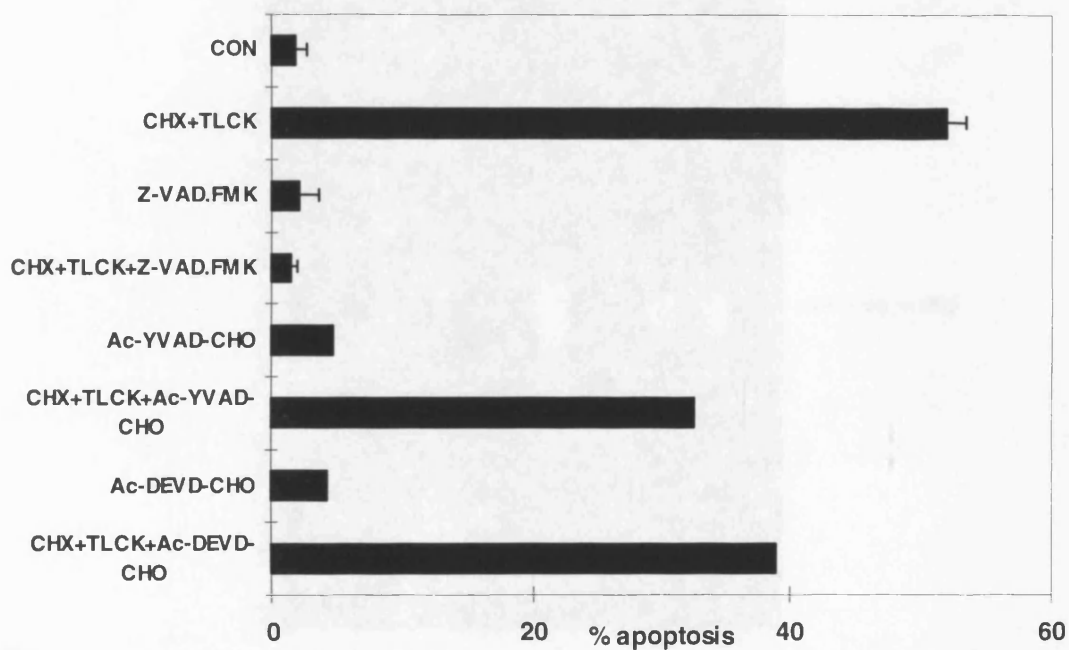
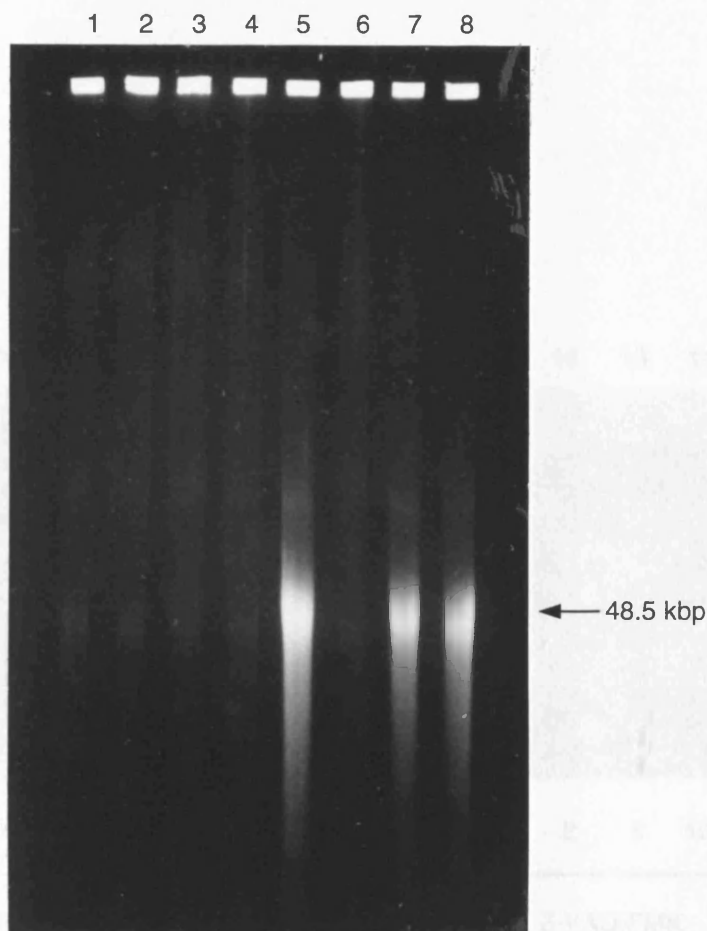


Figure 5f. *Ac-DEVD-CHO and Ac-YVAD-CHO partially inhibit and Z-VAD.FMK completely inhibits apoptosis in intact THP.1 cells.*

THP.1 cells ($2 \times 10^6/\text{ml}$) were incubated for 1 hour alone or in the presence of Ac-DEVD-CHO ($20 \mu\text{M}$), Ac-YVAD-CHO ($20 \mu\text{M}$) or Z-VAD.FMK ($10 \mu\text{M}$), then for a further 4 hours with cycloheximide (CHX) ($25 \mu\text{M}$) and TLCK ($100 \mu\text{M}$). (A) Apoptosis quantified by flowcytometry (see section 2.1.3). the value shown is the mean \pm s.e.m. of at least three determinations, except for the samples including Ac-YVAD-CHO or Ac-DEVD-CHO which were the mean of two (data provided by Huijun Zhu).

(B)



(C)

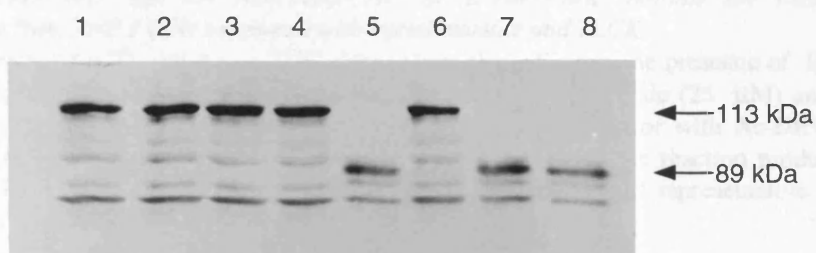


Figure 5f continued. *Ac-DEVD-CHO* and *Ac-YVAD-CHO* partially inhibit and *Z-VAD.FMK* completely inhibits apoptosis in whole *THP.1* cells.

THP.1 cells ($2 \times 10^6/\text{ml}$) were incubated for 1 hour alone or in the presence of *Ac-DEVD-CHO* (20 μM), *Ac-YVAD-CHO* (20 μM) or *Z-VAD.FMK* (10 μM), then for a further 4 hours in the presence of cycloheximide (CHX) (25 μM) and TLCK (100 μM). (B) Formation of high molecular weight DNA fragments by field inversion gel electrophoresis. Lane 1, control cells; lane 2, *Z-VAD.FMK*; lane 3, *Ac-YVAD-CHO*; lane 4, *Ac-DEVD-CHO*; lane 5, CHX and TLCK; lane 6, CHX, TLCK and *Z-VAD.FMK*; lane 7, CHX, TLCK and *Ac-DEVD-CHO*; lane 8, CHX, TLCK and *Ac-YVAD-CHO*. (C) Breakdown of PARP during apoptosis as revealed by the formation of the 89 kDa fragment, visualised by Western blotting. Lanes as in (B) (Data provided by Huijun Zhu.).

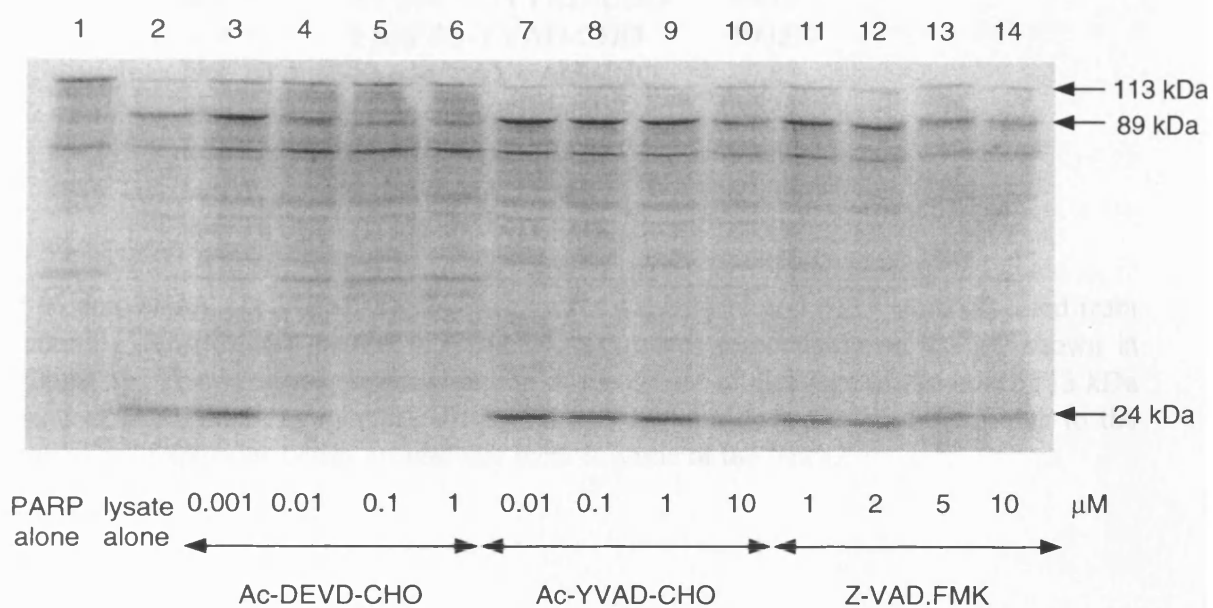


Figure 5g. *Ac-DEVD-CHO*, but not *Ac-YVAD-CHO* or *Z-VAD.FMK*, inhibits the cleavage of [^{35}S]PARP by lysate from THP.1 cells incubated with cycloheximide and TLCK

[^{35}S]PARP was incubated for 30 minutes at 37°C either alone (lane 1) or in the presence of lysate (10 μg protein) prepared from THP.1 cells incubated for 1 hour with cycloheximide (25 μM) and TLCK (100 μM). The lysate and [^{35}S]PARP were either incubated alone (lane 2) or with *Ac-DEVD-CHO* (lanes 3-6), *Ac-YVAD-CHO* (lanes 7-10) or *Z-VAD.FMK* (lanes 11-14). The reaction products were separated by SDS PAGE and visualised by autoradiography. This result is representative of three separate experiments.

Figure 5g.

		% conversion*
lane 1	[³⁵ S] PARP alone	0.00
lane 2	lysate alone	76.92
lane 3	0.001 μ M Ac-DEVD-CHO	81.76
lane 4	0.01 μ M Ac-DEVD-CHO	21.68
lane 5	0.1 μ M Ac-DEVD-CHO	0.00
lane 6	1 μ M Ac-DEVD-CHO	0.00
lane 7	0.01 μ M Ac-YVAD-CHO	97.76
lane 8	0.1 μ M Ac-YVAD-CHO	84.15
lane 9	1 μ M Ac-YVAD-CHO	100.00
lane 10	10 μ M Ac-YVAD-CHO	45.83
lane 11	1 μ M Z-VAD.FMK	74.51
lane 12	2 μ M Z-VAD.FMK	89.36
lane 13	5 μ M Z-VAD.FMK	69.28
lane 14	10 μ M Z-VAD.FMK	47.06

* % conversion = $p_{24}/(p_{113}+p_{24})$, where the values p_{24} and p_{113} were obtained from scanning densitometry of the 113 and 24 kDa bands respectively on the gel shown in Figure 5g. This is only an approximation of the extent of cleavage of the intact 113 kDa band of [³⁵S]PARP, as quantification of the 89 kDa product proved difficult due to the presence of spurious bands around this band in some of the lanes.

in the presence of varying concentrations of the inhibitors. As the lysate prepared from THP.1 cells exposed to cycloheximide and TLCK for 1 hour was very effective at cleaving [35 S]PARP, it was decided to use this as the standard 'active' lysate.

Following a 30 minute incubation with the active lysate alone, [35 S]PARP was extensively degraded to 89 kDa and 24 kDa fragments (Figure 5g lane 2). Ac-DEVD-CHO was able to completely inhibit the breakdown of [35 S]PARP at a concentration of 100 nM (Figure 5g lane 5). Conversely, Ac-YVAD-CHO was a poor inhibitor of the breakdown of [35 S]PARP, although the compound partially inhibited cleavage at a concentration of 10 μ M (Figure 5g lanes 7-10).

Surprisingly, Z-VAD.FMK did not entirely inhibit the cleavage of [35 S]PARP even at 10 μ M (Figure 5g lanes 11-14), a concentration which will inhibit both apoptosis and the breakdown of PARP in intact cells (Figure 5f). This result implies that when acting in intact THP.1 cells, Z-VAD.FMK does not inhibit PARP cleavage directly, as Ac-DEVD-CHO does, but acts at a point somewhere upstream on the proteolytic pathway. One manner in which it could be doing this is by inhibiting the proteolytic activation of the protease(s), which breaks down PARP.

It has been shown that it is possible to confer the ability to cleave [35 S]PARP onto an inactive lysate - in other words a lysate prepared from cells not exposed to an apoptotic stimulus - by heating it at 37°C for 1 hour in the presence of DTT (Nicholson et al., 1995). In doing this, it is presumed that the enzymes in the lysate are being taken through a similar procedure that occurs in the cell during the induction of apoptosis, including the conversion of the PARP-cleaving enzyme from its inactive proform into the active form. Thus, to obtain further evidence that Z-VAD.FMK is acting upstream of the cleavage of PARP, control lysates were incubated for 1 hour in either the absence or presence of Ac-DEVD-CHO, Ac-YVAD-CHO and Z-VAD.FMK. In some of the samples, the inhibitors were added after the lysates had been activated by the incubation (Figure 5h).

When the control lysate was incubated in the presence of Ac-DEVD-CHO (0.1 μ M), [35 S]PARP remained intact (Figure 5h lane 2), and again Ac-DEVD-CHO prevented the cleavage of PARP when it was added after the pre-incubation step (Figure 5h lane 9). However, it is impossible to discern whether Ac-DEVD-CHO was merely inhibiting directly the ability of the activated enzyme to cleave PARP, as it had done in Figure 5g,

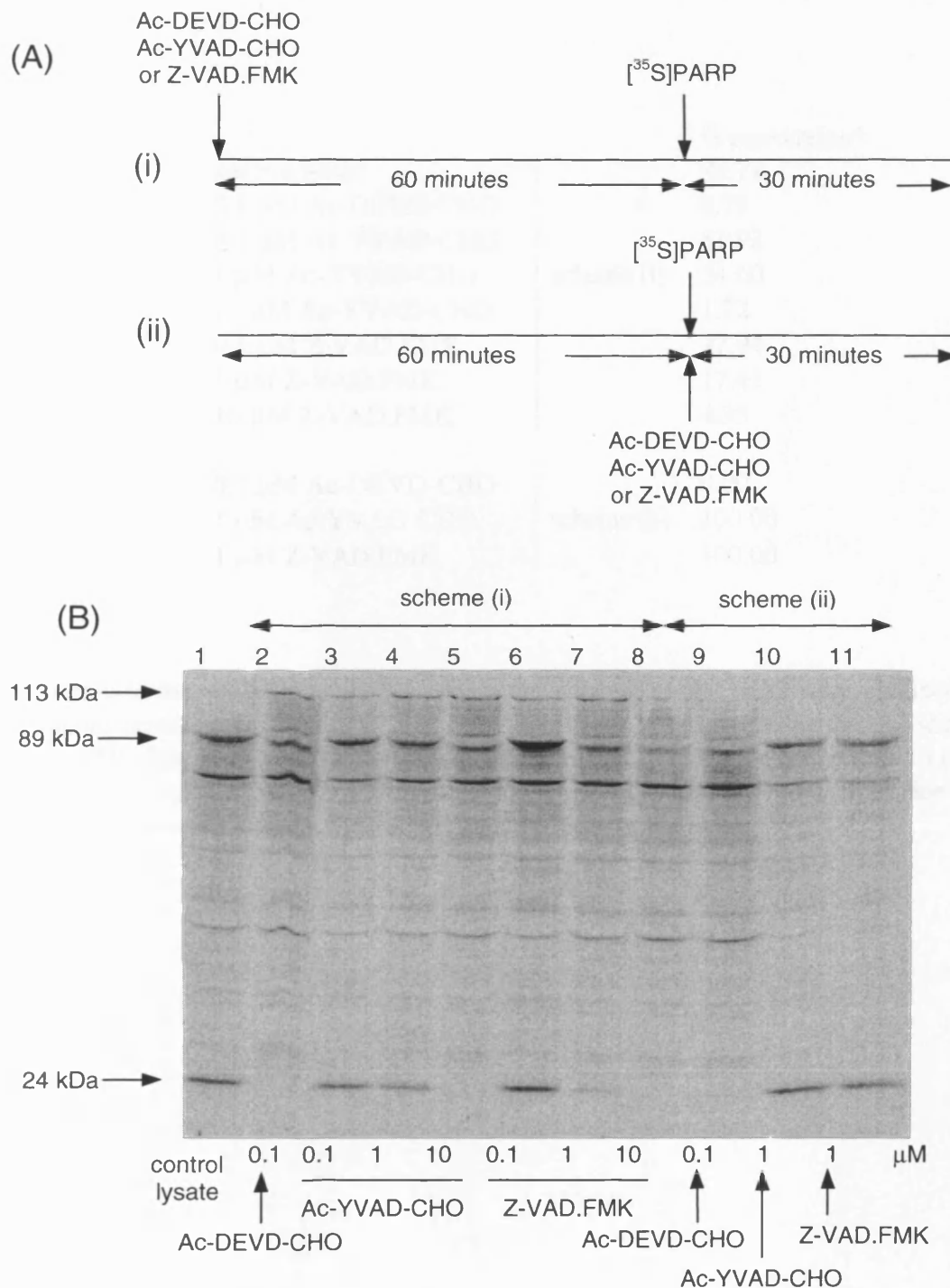


Figure 5h. Z-VAD.FMK inhibits activation of PARP protease activity in control cell lysates.

(A) Illustration of the design of this experiment. Lysate was prepared from control (unstimulated) THP.1 cells, and aliquots (30 μg) incubated at 37°C for 60 minutes either (i) with an inhibitor (lanes 2-8 on gel) or (ii) alone (lanes 1 and 9-11 on gel). $[^{35}\text{S}]\text{PARP}$ was then added to all the reactions. In the reactions shown in lanes 9-11 on the gel, inhibitor at the concentration indicated was also added at this point. All reactions were then incubated for a further 30 minutes at 37°C . (B) Lane 1, control lysate preincubated alone for 60 minutes; lane 2, lysate pre-incubated for 60 minutes with 100 nM Ac-DEVD-CHO; lanes 3-5, lysate preincubated with Ac-YVAD-CHO (100 nM-10 μM); lanes 6-8, lysate preincubated with Z-VAD.FMK (100 nM-10 μM); lane 9, lysate preincubated alone with $[^{35}\text{S}]\text{Ac-DEVD-CHO}$ (100 nM) added alongside $[^{35}\text{S}]\text{PARP}$; lane 10, as lane 9 using Ac-YVAD-CHO (1 μM); lane 11, as lane 9 using Z-VAD.FMK (1 μM). The breakdown of $[^{35}\text{S}]\text{PARP}$ was detected by SDS PAGE and autoradiography.

Figure 5h.

			% conversion*
lane 1	control lysate		99.71
lane 2	0.1 μ M Ac-DEVD-CHO		0.79
lane 3	0.1 μ M Ac-YVAD-CHO		81.92
lane 4	1 μ M Ac-YVAD-CHO	scheme (i)	54.60
lane 5	10 μ M Ac-YVAD-CHO		1.72
lane 6	0.1 μ M Z-VAD.FMK		77.94
lane 7	1 μ M Z-VAD.FMK		17.41
lane 8	10 μ M Z-VAD.FMK		4.35
lane 9	0.1 μ M Ac-DEVD-CHO		0.00
lane 10	1 μ M Ac-YVAD-CHO	scheme (ii)	100.00
lane 11	1 μ M Z-VAD.FMK		100.00

* % conversion = $p_{24}/(p_{113}+p_{24})$, where the values p_{24} and p_{113} were obtained from scanning densitometry of the 113 and 24 kDa bands respectively on the gel shown in Figure 5h. This is only an approximation of the extent of cleavage of the intact 113 kDa band of e [35 S]PARP, as quantification of the 89 kDa product proved difficult due to the presence of spurious bands around this band in some of the lanes.

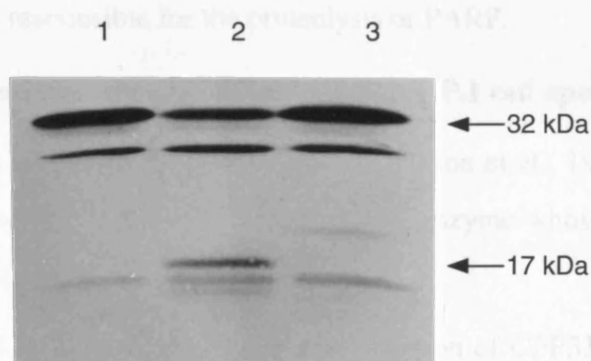


Figure 5i. Z-VAD.FMK inhibits the proteolytic activation of CPP32 in intact THP.1 cells.

THP.1 cells were incubated for 4 hours either alone (lane 1) or with cycloheximide (25 μ M) and TLCK (100 μ M) in the absence (lane 2) or presence (lane 3) of Z-VAD.FMK (10 μ M). The breakdown of CPP32 in the apoptotic cells (lane 2) to a 17 kDa fragment, which is inhibited by Z-VAD.FMK (lane 3), was detected by Western Blotting. (Blot by Dr. Marion MacFarlane).

or it was having additional effects upstream.

When the lysate was incubated in the presence of Ac-YVAD-CHO (10 μ M), the cleavage of [35 S]PARP was inhibited (Figure 5h lane 5), whereas Z-VAD.FMK was able to inhibit the activation of PARP cleavage activity when present at 1 μ M (Figure 5h lane 7). In contrast, when added following the pre-incubation step, Z-VAD.FMK at 1 μ M was incapable of inhibiting the cleavage of [35 S]PARP (Figure 5h lane 11). This contrast in the effects of Z-VAD.FMK provides further evidence that Z-VAD.FMK is inhibiting the activation of an enzyme responsible for the proteolysis of PARP.

5.2.3. Z-VAD.FMK inhibits the activation of CPP32 in THP.1 cell apoptosis

The ICE/Ced-3 homologue CPP32 can cleave PARP (Nicholson et al., 1995; Tewari et al., 1995). Therefore, this was an obvious candidate for an enzyme whose activation is being prevented by Z-VAD.FMK.

To verify that Z-VAD.FMK was acting to inhibit the activation of CPP32, a polyclonal antibody recognising both the p32 proform of the enzyme and the p17 subunit of the processed form (Figure 1f) was used to detect CPP32 in intact cells by Western blotting (Figure 5i). THP.1 cells were incubated for 4 hours either alone, or in the presence of cycloheximide and TLCK either with or without Z-VAD.FMK. In cells that had been incubated alone, CPP32 was predominantly in the intact, inactive 32 kDa form (Figure 5i lane 1), with a band also seen at approximately 29 kDa, which presumably correlates with the intact enzyme less the 3 kDa prodomain, and as such is probably inactive. This band is present in all three lanes and does not vary between lanes. In the cells that had been incubated with cycloheximide and TLCK alone, the 32 kDa proform of CPP32 had been cleaved at both the prodomain/p17 and p17/p12 junctions to yield the p17 subunit, i.e. the enzyme had been converted to its active form, although much of the CPP32 remained intact (Figure 5i lane 2). In contrast, cells that had been incubated with cycloheximide, TLCK and Z-VAD.FMK displayed predominantly intact CPP32 (Figure 5i lane 3), and no trace of the p17 subunit was apparent, although a faint band of approximately 20 kDa was visible in this lane. It is thought that this could be the p17 subunit with the 3 kDa prodomain still attached, but it is unknown whether this would be able to form an active enzyme in combination with a p12 subunit.

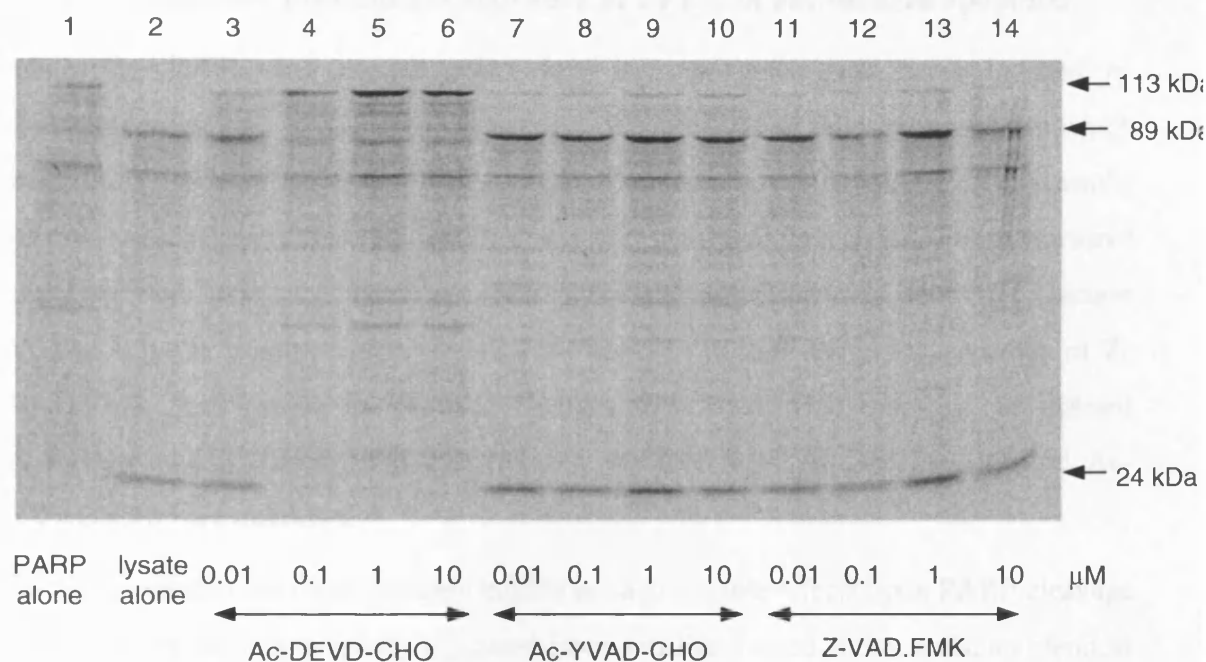


Figure 5j. *Ac-DEVD-CHO*, but not *Ac-YVAD-CHO* or *Z-VAD.FMK*, inhibits the proteolysis of [^{35}S]PARP by lysates prepared from Jurkat cells exposed to anti-Fas antibody

[^{35}S]PARP was incubated for 30 minutes at 37°C either alone (lane 1) or with lysate (10 μg protein) prepared from Jurkat cells incubated for 1 hour with anti-Fas antibody (lanes 2-14). The lysate was either used alone (lane 2) or with *Ac-DEVD-CHO* (lanes 3-6), *Ac-YVAD-CHO* (lanes 7-10) or *Z-VAD.FMK* (lanes 11-14). Samples were resolved by SDS PAGE and the [^{35}S]PARP breakdown products visualised by autoradiography. The gel is representative of three separate experiments.

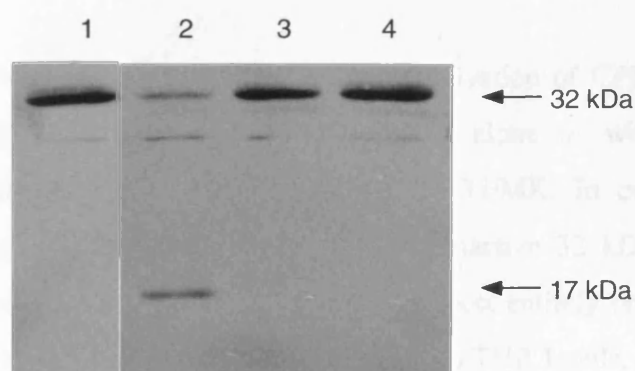


Figure 5k. *Z-VAD.FMK* inhibits the proteolytic activation of CPP32 during Fas-mediated apoptosis in Jurkat T lymphocytes.

Jurkat T lymphocytes were incubated for 1 hour with anti Fas antibody (100 ng/ml) either alone (lane 2) or in the presence of *Z-VAD.FMK* (10 μM) (lane 3). In addition, cells were incubated for 1 hour in the presence of *Z-VAD.FMK* alone (lane 4). The cleavage of CPP32 to a 17 kDa fragment upon Fas-induced apoptosis (lane 2) which is prevented by *Z-VAD.FMK* (lane 3) was detected by Western blotting. (Blot provided by Dr. Marion MacFarlane).

5.2.4. Z-VAD.FMK prevents the activation of CPP32 in Fas-induced apoptosis

Whilst the THP.1 cell model works very well, apoptosis was being induced by toxicological stimuli which, it could be argued, is a means of inducing apoptosis which would not routinely occur in living systems. Therefore in the remainder of this results section lysates derived from Jurkat T lymphocytes incubated with an anti-Fas monoclonal antibody were used, this being a physiological means of inducing apoptosis (section 1.3.5). A lysate prepared from Jurkat cells exposed to anti-Fas in the presence of Z-VAD.FMK was unable to produce changes associated with apoptosis in isolated thymocyte nuclei (Chow et al., 1995), but the effects of Ac-DEVD-CHO and Ac-YVAD-CHO are unknown.

To verify whether the three protease inhibitors had the same effects upon PARP cleavage *in vitro* when the active lysate originated from anti-Fas treated Jurkat cells, an identical experiment was undertaken to that described in section 5.2.2./Figure 5g. The anti-Fas lysate is able to degrade [³⁵S]PARP (Figure 5j lane 2), and once again Ac-DEVD-CHO is extremely effective at preventing the degradation of [³⁵S]PARP, completely abolishing its breakdown at 100 nM (Figure 5j lanes 3-6), whilst Ac-YVAD-CHO and Z-VAD.FMK are ineffective (Figure 5j lanes 7-14). This demonstrates that as in THP.1 cell apoptosis, the target of Z-VAD.FMK in Fas-induced apoptosis also lies upstream of PARP breakdown.

To confirm that Z-VAD.FMK also inhibits the proteolytic activation of CPP32 in cells exposed to anti-Fas, Jurkat T cells were incubated either alone or with anti-Fas monoclonal antibody, in the presence or absence of Z-VAD.FMK. In control cells (Figure 5k lanes 1 and 4) CPP32 is present in the intact, inactive 32 kDa form. In contrast, in cells exposed to anti-Fas for 1 hour, CPP32 is almost entirely broken down into the 17 kDa, active form (Figure 5k lane 2). Consistent with THP.1 cells, Jurkat cells exposed to anti-Fas in the presence of Z-VAD.FMK have intact CPP32 (Figure 5k lane 3). This demonstrates that CPP32 is activated in Fas-induced apoptosis, and that Z-VAD.FMK inhibits the activation of CPP32 induced by cross-linking of the Fas receptor.

5.2.5. Ac-DEVD-CHO, Ac-YVAD-CHO and Z-VAD.FMK all inhibit the cleavage of [³⁵S]proIL-1 β by purified recombinant ICE

To determine the effectiveness of the three inhibitors used in this study against purified

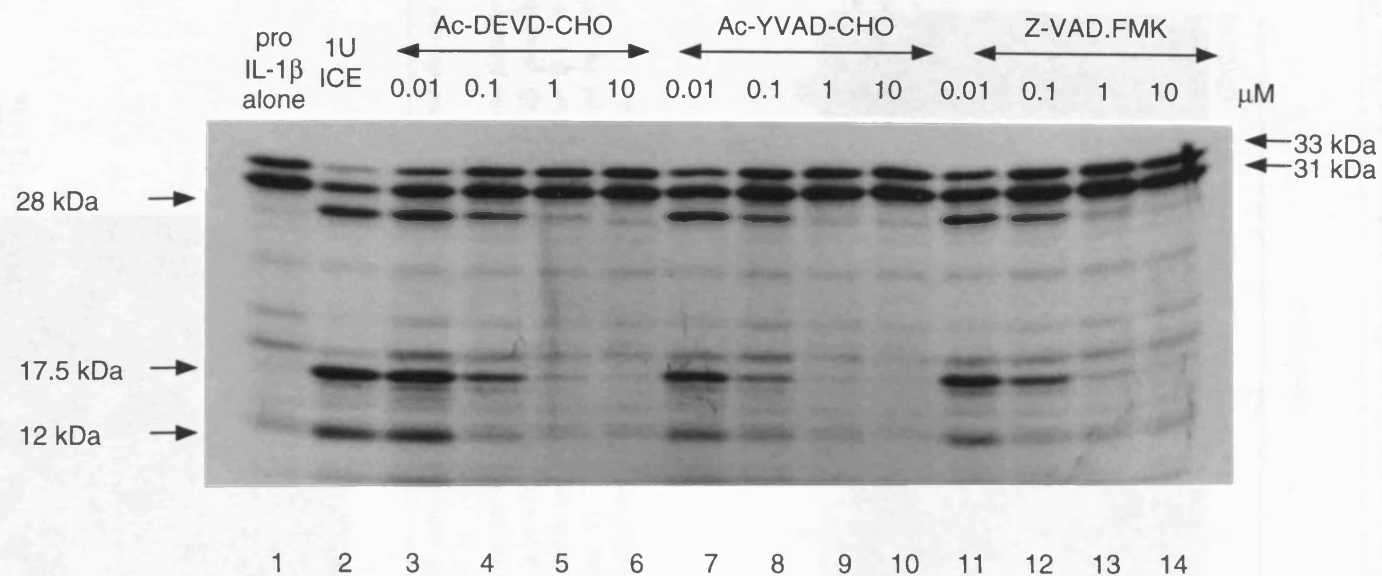


Figure 5I. *Ac-YVAD-CHO*, *Z-VAD.FMK* and *Ac-DEVD-CHO* all inhibit the cleavage of [35 S]*proIL-1 β* by purified recombinant ICE.

[35 S]*proIL-1 β* was incubated for 30 minutes at 37°C either alone (lane 1) or with 1 unit of purified recombinant ICE in the absence (lane 2) or presence of the inhibitors *Ac-DEVD-CHO* (lanes 3-6), *Ac-YVAD-CHO* (lanes 7-10) or *Z-VAD.FMK* (lanes 11-14). The breakdown products (28, 17.5 and 12 kDa) were then resolved by SDS PAGE and visualised by autoradiography. All the inhibitors were able to completely prevent [35 S]*proIL-1 β* cleavage at 1 μ M. The gel is typical of at least three separate experiments.

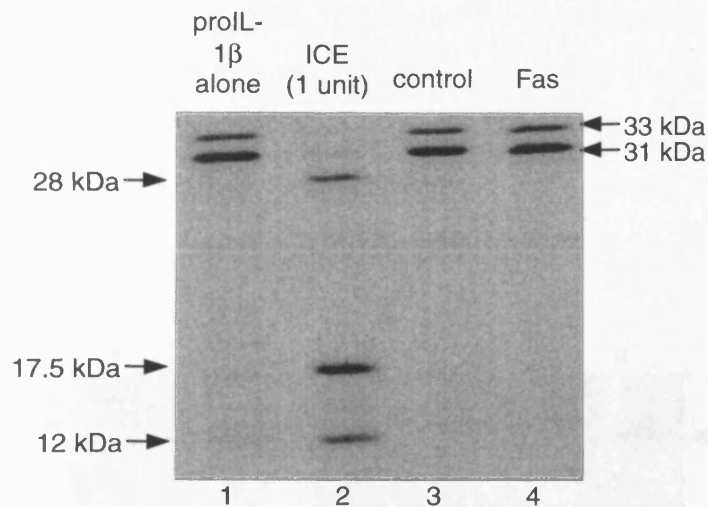


Figure 5m. Lysates from Jurkat cells exposed to anti-Fas antibody for 1 hour do not possess ICE activity

[³⁵S]proIL-1β was incubated for 30 minutes at 37°C either alone (lane 1) or in the presence of 1 unit of purified recombinant ICE (lane 2) as a positive control. In addition [³⁵S]proIL-1β was incubated with lysates prepared from Jurkat t lymphocytes incubated for 1 hour either alone (lane 3) or in the presence of anti-Fas antibody (100 ng/ml) (lane 4). The reaction products were resolved by SDS PAGE and visualised by autoradiography. The results are typical of at least three experiments.

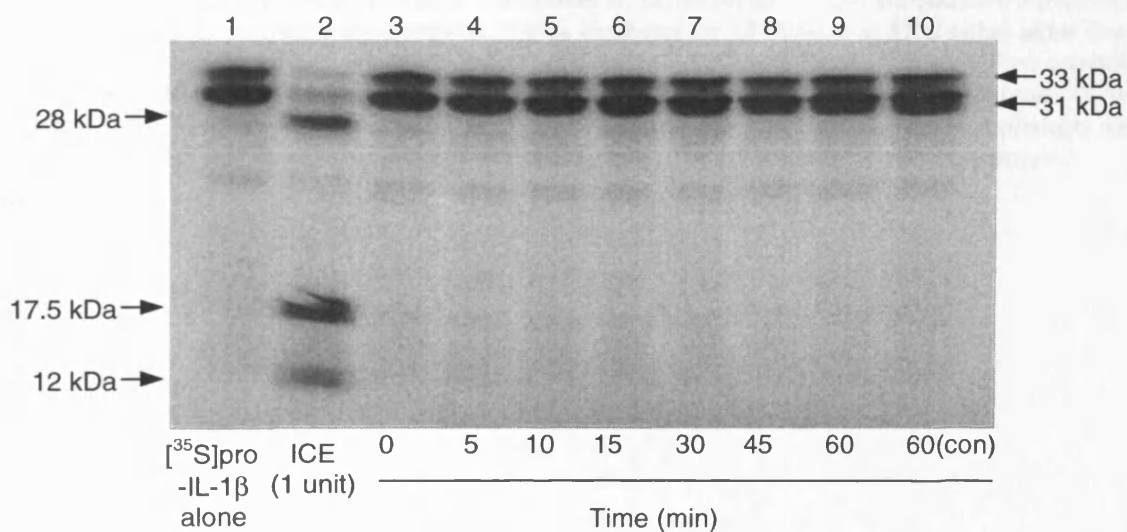


Figure 5n. Lysates from Jurkat T cells undergoing Fas-mediated apoptosis do not cleave [³⁵S]proIL-1β

[³⁵S]proIL-1β was incubated for 30 minutes at 37°C either alone (lane 1) or in the presence of lysate prepared from Jurkat cells incubated either alone (lanes 3 and 10) or with anti-Fas antibody (100 ng/ml) for the times stated (lanes 4-9). [³⁵S]proIL-1β was also incubated with one unit of purified recombinant ICE as a positive control (lane 2). The reaction products were resolved by SDS PAGE and visualised by autoradiography. The results are typical of at least three experiments.

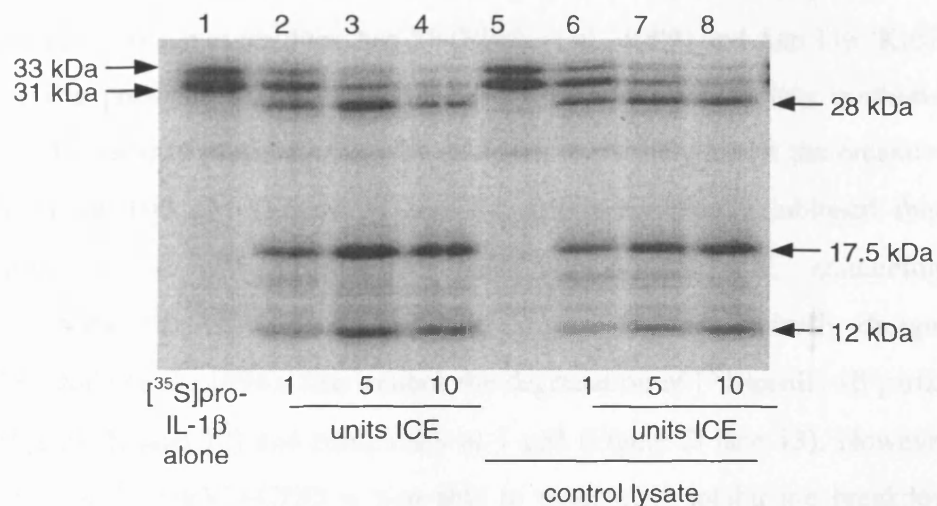


Figure 5o. An inhibitor of ICE activity is not present in lysates prepared from unstimulated Jurkat cells. 1, 5 or 10 units of purified recombinant ICE were incubated for 15 minutes at 37°C either alone (lanes 2-5) or with lysate from non-apoptotic Jurkat cells (lanes 6-8). These incubations were then combined with [³⁵S]proIL-1β and incubated for a further 30 minutes at 37°C. In addition, [³⁵S]proIL-1β was incubated for 30 minutes either alone (lane 1), or with lysate alone (lane 5). The reaction products were resolved by SDS PAGE and visualised by autoradiography. The gel is typical of two experiments.

ICE, [^{35}S]proIL-1 β was incubated with recombinant ICE (1 unit) for 30 minutes at 37°C in the presence or absence of either Ac-DEVD-CHO, Ac-YVAD-CHO or Z-VAD.FMK (Figure 5l). One unit of ICE is the amount required to generate 1 pmol of aminomethyl coumarin per minute at 25°C, using a saturating concentration of the fluorescent ICE substrate acetyl-Tyr-Val-Ala-Asp-aminomethylcoumarin (Thornberry, 1994).

When [^{35}S]proIL-1 β was incubated with ICE alone, the 31/33 kDa intact proIL-1 β was extensively degraded to 28 kDa, 17.5 kDa and 12 kDa fragments (Figure 5l lane 2), consistent with cleavage at residues Asp 27 (Black et al., 1989) and Asp 116 (Kostura et al., 1989). The presence of the inhibitor Ac-YVAD-CHO, which was synthesised to inhibit ICE (Thornberry et al., 1992), was sufficient to partially inhibit the breakdown of [^{35}S]proIL-1 β at 100 nM (Figure 5l lane 8), and it completely inhibited this at a concentration of 1 μM (Figure 5l lane 9). Z-VAD.FMK, containing the benzyloxycarbonyl-Val-Ala-Asp motif (Figure 5c) which was originally designed to inhibit ICE (Dolle et al., 1994), also inhibits the degradation of [^{35}S]proIL-1 β partially at 100 nM (Figure 5l lane 12) and completely at 1 μM (Figure 5l lane 13). However, the CPP32 inhibitor Ac-DEVD-CHO is also able to moderately inhibit the breakdown of [^{35}S]proIL-1 β at 100 nM (Figure 5l lane 4) and entirely abrogate its cleavage at 1 μM (Figure 5l lane 5). Thus, despite the fact that it was originally developed to inhibit the breakdown of PARP (Nicholson et al., 1995), Ac-DEVD-CHO also behaves as a reasonably good inhibitor of the action of ICE.

5.2.6. Fas-induced apoptosis in Jurkat T lymphocytes occurs without the participation of ICE

It has previously been demonstrated that the induction of apoptosis by anti-Fas antibody can be inhibited by the tetrapeptide inhibitors of ICE Ac-YVAD-CHO and YVAD.CMK (Enari et al., 1995; Los et al., 1995), the cowpox virus protein CrmA (Enari et al., 1995; Tewari and Dixit, 1995), which inhibits ICE (Ray et al., 1992) more so than family members such as CPP32 (Nicholson et al., 1995), and by ICE antisense DNA (Los et al., 1995). This evidence, coupled with the resistance of thymocytes from ICE knockout mice to apoptosis mediated by the Fas receptor (Kuida et al., 1995), would suggest that the action of ICE is involved in apoptosis caused by the ligation of the Fas receptor.

Initially, lysates were prepared from control cells and from cells that had been exposed to

anti-Fas antibody for 1 hour, and their ability to cleave [^{35}S]proIL-1 β was assessed (Figure 5m). ICE is the only known ICE/Ced-3 protease with the ability to cleave proIL-1 β . One unit of purified recombinant ICE was used as a positive control (Figure 5m lane 2), and this was able to degrade the [^{35}S]proIL-1 β into 28, 17.5 and 12 kDa fragments as seen in Figure 5l. Lysate prepared from control cells was unable to cleave [^{35}S]proIL-1 β , as was a lysate prepared from cells exposed to anti-Fas antibody for 1 hour (Figure 5m lanes 3 and 4). From previous studies, it is known that a lysate prepared from Jurkat cells exposed to anti-Fas for 1 hour is able to cause extensive degradation of DNA in isolated thymocyte nuclei which is indicative of apoptosis being well progressed (Chow et al., 1995). This would suggest that Jurkat cells undergoing Fas-mediated apoptosis do not possess ICE activity.

However, the transient activity of a protease like ICE prior to the activation of a protease with CPP32-like activity has been demonstrated in Fas-induced apoptosis by using fluorescent substrates containing either the Asp-Glu-Val-Asp site recognised by CPP32-like proteases or the Tyr-Val-Ala-Asp site recognised by ICE-like proteases, with the ICE-like activity peaking 10 minutes after the addition of anti-Fas (Enari et al, 1996). Thus, in the previous experiment it is possible that the failure to detect any ICE activity was because the lysate was prepared after a transient peak in ICE activity had passed. To study this, lysates prepared from Jurkat cells following incubation with anti-Fas antibody for increasing periods of time were assessed for their ability to cleave [^{35}S]proIL-1 β (Figure 5n).

Again 1 unit of purified recombinant ICE was used as a positive control to provide the characteristic breakdown products of proIL-1 β (Figure 5n lane 2). Control cells that had not been incubated with anti-Fas (Figure 5n lanes 3 and 10) were unable to degrade [^{35}S]proIL-1 β , as would be predicted. However, no ICE activity was seen in any of the lysates prepared from cells incubated with anti-Fas, even between the time points of 5 and 15 minutes (Figure 5n lanes 4-6) when the cleavage of the YVAD motif was seen in mouse W4 cells (Enari et al., 1996).

To test the possibility that there is some form of inhibitory factor present in the Jurkat lysate that could be preventing the action of ICE, an experiment was undertaken where recombinant ICE was incubated with unstimulated Jurkat lysate for 15 minutes, followed

by incubation with [^{35}S]proIL-1 β (Figure 5o). Thus, if there is a factor in the lysate which is inhibiting ICE, the cleavage of [^{35}S]proIL-1 β by the added recombinant ICE would also be inhibited. No difference was evident between the ability of recombinant ICE alone to cleave [^{35}S]proIL-1 β (Figure 5o lanes 2-4) and the ability of ICE that had been pre-incubated with Jurkat lysate to cleave [^{35}S]proIL-1 β (Figure 5o lanes 5-7). Thus, it seems that Jurkat lysate does not contain an inhibitory factor which could be preventing the action of ICE. The incapability of lysates prepared from Jurkat T cells to break down [^{35}S]proIL-1 β demonstrates that there is apparently no ICE activity in this system.

5.3. DISCUSSION

Prior to commencing the work described in this chapter, it had been established that the human leukaemic cell line THP.1 is able to undergo apoptosis in response to a variety of stimuli (Zhu et al, 1995). All of these stimuli are able to induce the breakdown of PARP, which is indicative of the activity of an ICE/Ced-3 like protease (Lazebnik et al., 1994). In agreement with what was happening in intact cells, it was found that lysates prepared from THP.1 cells exposed to an apoptotic stimulus were able to cause the breakdown of PARP labelled with [³⁵S]methionine *in vitro* (Figures 5d and 5e). In the case of cells exposed to cycloheximide and TLCK, a modest amount of cleavage could be seen at 30 minutes which had approached approximately maximum at 1-2 hours, and by 4 hours the ability of the lysate to degrade PARP was in decline. A population of intact THP.1 cells exposed to these agents only begin to display gross signs of apoptosis such as an increased uptake of Hoechst 33342 (see section 2.1.3.) at around 2 hours (MacFarlane et al., in press), whereas at the 4 hour time point most of the cells display an apoptotic phenotype (Zhu et al., 1995). Results obtained using the system described here suggest that proteolytic events like PARP degradation occur prior to the outward cellular changes associated with apoptosis. By the 4 hour time point many of the cells are fully apoptotic and the abatement in PARP degradation by this time may be a reflection of the proteolytic activity that is cleaving PARP having carried out its function and no longer being required (Figure 5d).

The ability of lysates from THP.1 cells exposed to a variety of chemical agents (Figure 5e) to degrade PARP confirms that this is a common phenomenon. The different extents to which the PARP is degraded by the lysates is reflected approximately in the degree of apoptosis in intact cells at 4 hours (Zhu et al., 1995), e.g. the most extensive apoptosis is seen with a combination of cycloheximide and TLCK, which in Figure 5e produces the most extensive [³⁵S]PARP breakdown. The marginal degradation of PARP by lysates prepared from cells exposed to etoposide may be as a result of this agent taking a longer period of time to initiate the implementation of apoptosis, possibly because it operates via a different signalling pathway to the other agents, e.g. via a p53 dependent mechanism.

Whilst the lysates prepared from THP.1 cells undergoing apoptosis were able to degrade

PARP, they were unable to substantially break down [^{35}S]proIL-1 β (Figures 5d and 5e), which would suggest that there is little ICE activity present. This is despite the fact that THP.1 cells possess high levels of ICE (Kronheim et al., 1992; Miller et al., 1993). However, only a small amount of ICE activity may be required to initiate an apoptotic protease cascade, which is unable to be detected by the technique employed. Although no positive evidence was found for the participation of ICE in THP.1 cell apoptosis, from the data presented in this chapter (Figures 5d and 5e) it is impossible to rule out its involvement absolutely.

In intact THP.1 cells, Z-VAD.FMK, an inhibitor of ICE/Ced-3-like proteases prevents the formation of any of the features of apoptosis examined, irrespective of the stimulus used to induce it (Figure 5f; Zhu et al., 1995). In contrast, when the ICE inhibitor Ac-YVAD-CHO (Thornberry et al., 1992) and the CPP32 inhibitor Ac-DEVD-CHO (Nicholson et al., 1995) were used in intact THP.1 cells their inhibitory effects were only slight at the concentration used (10 μM) (Figure 5f). The lack of inhibition of apoptosis in intact cells by Ac-DEVD-CHO and Ac-YVAD-CHO seen in this chapter may be because the hydrophilic nature of these compounds makes their entry into the cell difficult. Higher concentrations (e.g. 100-200 μM) of Ac-DEVD-CHO have been shown to abrogate apoptosis in intact cells (Nicholson et al., 1995; Schlegel et al., 1996; Enari et al., 1996). Despite this, apoptosis in motoneurons deprived of growth factor *in vitro* has been shown to be prevented by lower concentrations (around 1 μM) of Ac-YVAD-CHO (Milligan et al., 1995). The minimal effect of Ac-YVAD-CHO in THP.1 cells (Figure 5f) could either reflect a difference in uptake of the compound between different cell types, or the involvement of ICE or another protease that is also inhibited by Ac-YVAD-CHO in neuronal apoptosis but not in haematopoietic systems of apoptosis such as THP.1 cells. Z-VAD.FMK, on the other hand, is sufficiently hydrophobic to cross the plasma membrane in THP.1 cells at a concentration of 10 μM .

Although Ac-DEVD-CHO had little effect upon the degradation of PARP in intact cells, as mentioned above this is probably due to its poor cellular permeability. However, it was extremely effective at preventing the breakdown of [^{35}S]PARP *in vitro*, where hydrophilicity ceases to be a problem; 100 nM completely prevented the degradation of [^{35}S]PARP in both THP.1 and Jurkat cells (Figures 5g and 5j). This is in close agreement with Nicholson et al. who prevented the breakdown of [^{35}S]PARP by osteosarcoma cell

extracts with a similar concentration (10-100 nM) of the inhibitor (Nicholson et al., 1995). Ac-YVAD-CHO did not inhibit the breakdown of [35 S]PARP by either the THP.1 or Jurkat cell lysate, even at 10 μ M (Figures 5g and 5j). This again is in agreement with Nicholson et al., who found that Ac-YVAD-CHO had little effect upon PARP cleavage activity in an osteosarcoma cell lysate (Nicholson et al., 1995).

Z-VAD.FMK, however, was also unable to entirely inhibit the degradation of [35 S]PARP by lysates prepared from either THP.1 cells or Jurkat cells induced to undergo apoptosis even at a concentration of 10 μ M (Figures 5g and 5j). This is in complete contrast to its effect in intact cells, where it completely inhibits the breakdown of PARP in both THP.1 cells (Zhu et al, 1995; Figure 5f) and Jurkat T lymphocytes (S.C. Chow, personal communication). PARP is cleaved during apoptosis by an ICE/Ced-3 like protease activity (Lazebnik et al., 1994), and such proteases must be proteolytically cleaved themselves to enable them to be active. This result with the Z-VAD.FMK would suggest that when it is acting in intact cells to prevent PARP breakdown (Zhu et al., 1995 and Figure 5f), it is not doing so by a direct competitive inhibition of the protease responsible for this as is the case with Ac-DEVD-CHO, which mimics the cleavage site within PARP. Instead, it appears to be acting at a point upstream of the activation of the protease which cuts PARP, which has already been activated in cells exposed to cycloheximide and TLCK or anti-Fas by the time they are harvested for preparation of the lysate. This conclusion also explains the observation by Chow et al. that the addition of Z-VAD.FMK to a lysate prepared from Jurkat T lymphocytes undergoing Fas-mediated apoptosis is unable to prevent isolated nuclei from taking on apoptotic morphology (Chow et al., 1995). Another possible reason that Z-VAD.FMK is failing to inhibit PARP cleavage *in vitro* is that the *O*-methyl ester group on the P₁ aspartate in the compound (Figure 5c) is not being removed, i.e. the esterases that are presumed to be carrying out this process in the intact cell have in some way been inactivated during the preparation of the lysate, thus preventing an ICE/Ced-3 protease from recognising this crucial amino acid. However, the fact that Z-VAD.FMK is able to inhibit the actions of ICE in the absence of any lysate at all (Figure 5l) would suggest that this is not in fact the case.

In the paper by Nicholson et al. (Nicholson et al., 1995), the conversion of an inactive lysate prepared from non-apoptotic THP.1 cells into a lysate with the capability of

cleaving [^{35}S]PARP by incubating it at 37°C for 1 hour prior to the addition of [^{35}S]PARP was described. Thus, it was reasoned that if Z-VAD.FMK is acting to prevent the activation of the protease which is cleaving PARP, then it should also prevent the conversion of an inactive lysate into one with PARP cleavage activity. The fact that Z-VAD.FMK can inhibit at 1 μM when it is added prior to [^{35}S]PARP, but not afterwards (Figure 5h), indicates that it inhibits more effectively upstream of PARP cleavage. However, another interpretation of these results could be that the preincubation step means that the inhibitor is getting a greater chance to hit its target(s). The Western blots demonstrating that Z-VAD.FMK prevents the conversion of CPP32 from the inactive 32 kDa proform into the active form, as indicated by the appearance of the 17 kDa subunit (Figures 5i and 5k), is confirmation of the hypothesis put forward from the results obtained using the [^{35}S]PARP *in vitro* (Figures 5g and 5j).

Since this work was published (Slee et al., 1996), Z-VAD.FMK has been confirmed as preventing the proteolytic activation of CPP32 in a number of other cell systems including a Burkitt lymphoma B cell line (An and Knox, 1996), CHO cells and fibroblasts exposed to staurosporine (Jacobson et al., 1996) and again in Fas-stimulated Jurkat cells (Armstrong et al., 1996). Moreover, Z-VAD.FMK has been demonstrated to inhibit both the specific cleavage of CPP32 and the resulting extensive apoptosis in the liver of mice injected with anti-Fas antibody (Rodriguez et al., 1996).

CPP32 was the first ICE/Ced-3 homologue found to have the ability to cleave PARP (Nicholson et al., 1995; Tewari et al., 1995), and since this discovery it has been shown that Mch3 (Fernandes-Alnemri et al., 1995b; Duan et al., 1996a; Lippke et al., 1996) and possibly MACH/FLICE/Mch5 (Muzio et al., 1996; Boldin et al., 1996; Fernandes-Alnemri et al., 1996) and Mch6/ICE-LAP6 (Srinivasula et al., 1996; Duan et al., 1996b) can also cleave PARP. It is now known that Z-VAD.FMK can also prevent the proteolytic activation of Mch3 (MacFarlane et al., in press), but whether it has the same effect upon FLICE or Mch6 remains to be determined. In addition to preventing the activation of proteases that degrade PARP, Z-VAD.FMK also prevents the activation of the ICE/Ced-3 homologues Ich-1_L and Mch2 (MacFarlane et al., in press), neither of which are thought to have a major role in PARP breakdown.

The structure of Z-VAD.FMK would suggest that it is a poor direct inhibitor of CPP32,

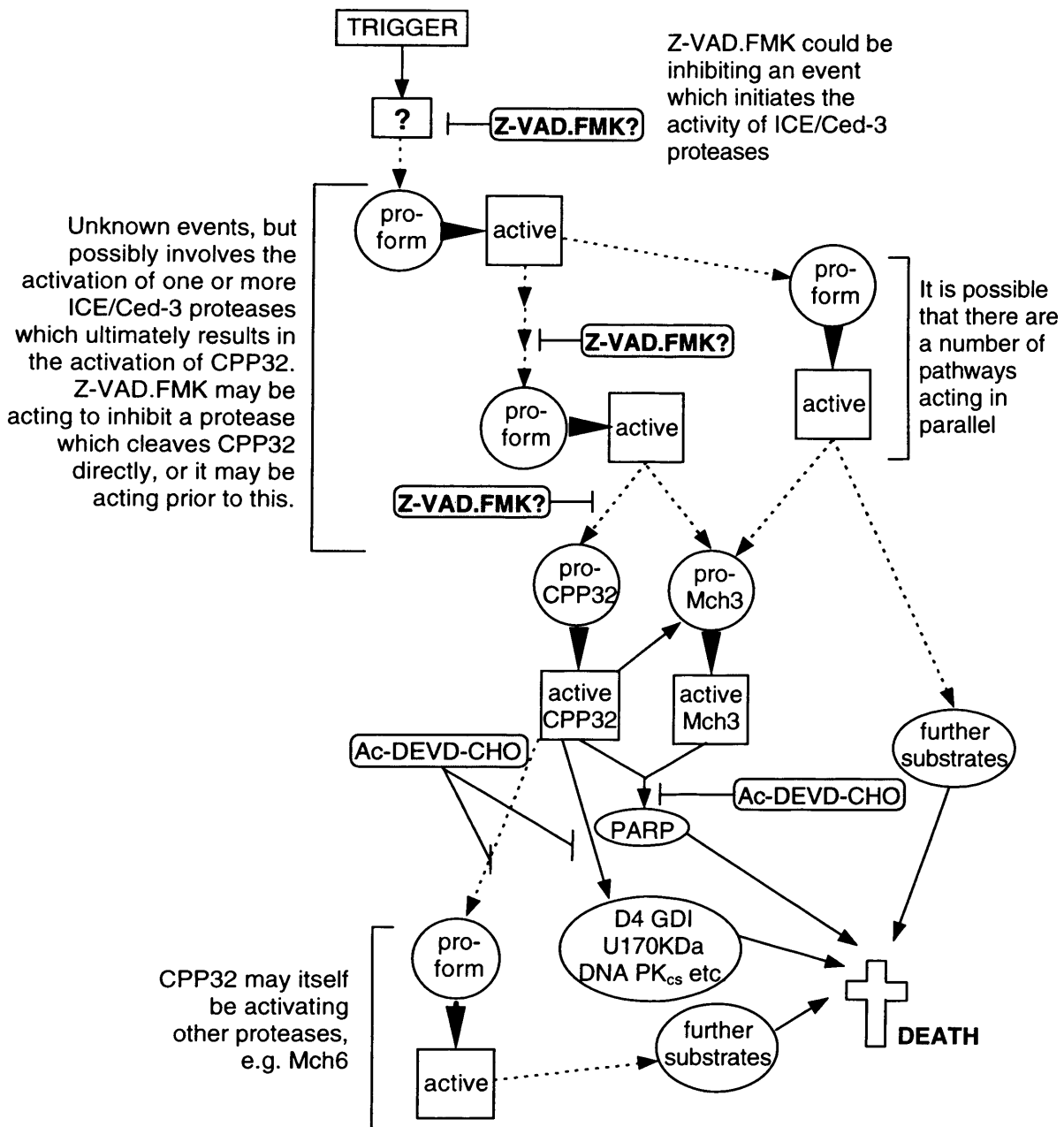


Figure 5p. A speculative scheme illustrating the potential mechanism(s) by which the ICE/Ced-3 family cause apoptosis.

An apoptotic trigger, e.g. cycloheximide and TLCK, induces an unknown event or events (question mark) which results in the release of an ICE/Ced-3-like proteolytic activity. This results, either directly or indirectly, in the activation of CPP32 and other proteases. Once activated, in addition to cleaving cellular proteins like PARP that ultimately result in the demise of the cell, CPP32 may continue to activate other ICE-like proteases such as Mch6. Z-VAD.FMK could be preventing the activation of CPP32 by acting at a target which is proximate to it, or at a point further upstream. Circles and squares represent inactive and active ICE/Ced-3 family members respectively. Solid arrows indicate established links, and arrows with a dotted line represent speculative links.

an enzyme which cleaves PARP. The elucidation of the three-dimensional structure of CPP32 has revealed that the S₄ pocket is narrow in order to closely surround the P₄ aspartate residue of the substrate Ac-DEVD-CHO (Rotonda et al., 1996). Although Z-VAD.FMK is a tripeptide and as such does not possess a P₄ amino acid, it does have a hydrophobic benzyl group at its N terminus (Figure 5c) which would be expected to preclude the inhibitor from forming a close interaction with CPP32. In contrast, the S₄ subsite in ICE is shallow and hydrophobic to encompass the P₄ tyrosine as found in the substrate Ac-YVAD-CHO (Walker et al., 1994a; Wilson et al., 1994). As can be seen from Figure 5l, Z-VAD.FMK does act as an effective inhibitor of ICE, presumably because the benzyloxycarbonyl (Z) group can be accommodated by the S₄ pocket in the enzyme. It is surprising, however, to find that Ac-DEVD-CHO can also inhibit the actions of ICE, despite the fact that the only shared residue between itself and Ac-YVAD-CHO, the preferred amino acid sequence for ICE cleavage, is the essential P₁ aspartate. As the S₄ pocket in ICE is less restricted than that of CPP32, it is quite possible that in spite of its hydrophobicity, the P₄ aspartate can still occupy the S₄ subsite sufficiently to enable Ac-DEVD-CHO to inhibit ICE activity. Conversely, Ac-YVAD-CHO makes an extremely poor inhibitor of CPP32 (Nicholson et al., 1995), presumably because its P₄ tyrosine cannot be accommodated by the narrow S₄ subsite of CPP32. Z-VAD.FMK has recently been demonstrated to possess the ability to inhibit CPP32 to a certain extent, although it disables ICE far more rapidly (Armstrong et al., 1996).

The fact that Z-VAD.FMK inhibits the proteolytic activation of CPP32 points to the potential existence of one or more ICE/Ced-3 homologues upstream of CPP32 that are required for the regulation of the activity of this enzyme, and which are target(s) of Z-VAD.FMK. However, the target or targets of Z-VAD.FMK remain unknown. Although ICE is believed to have the ability to proteolytically activate itself (Gu et al., 1995; Yamin et al., 1996), it is not understood whether CPP32 can also autoactivate - it can autoprocess when expressed in bacteria (Fernandes-Alnemri et al., 1995b) but this has never been demonstrated in eukaryotic cells. In the case of apoptosis being caused by ligation of the Fas receptor, which has been shown both here and previously (Chow et al., 1995) to be inhibited by Z-VAD.FMK, potential candidates for the proteolytic activity which is processing CPP32 are MACH/FLICE/Mch5 or Mch4, both of which are ICE homologues that are associated with the Fas receptor (Muzio et al., 1996; Boldin et

al., 1996; Fernandes-Alnemri et al., 1996). Although Z-VAD.FMK inhibits apoptosis caused by the overexpression of FLICE in the MCF-7 breast carcinoma cell line (Muzio et al., 1996), this inhibition is not necessarily a result of Z-VAD.FMK inhibiting FLICE directly. Mch4 has been demonstrated to cleave CPP32 *in vitro* (Fernandes-Alnemri et al., 1996), but again whether this enzyme can be inhibited by Z-VAD.FMK has yet to be determined. Although it has been suggested both that Mch2 (Fernandes-Alnemri et al., 1995a) is able to activate CPP32 (Liu et al., 1996a; Orth et al., 1996b) and vice versa (Srinivasula et al., 1996), the evidence that the activation of Mch2 is also prevented by Z-VAD.FMK (MacFarlane et al., in press) would suggest that Mch2 is not a major target for this inhibitor. Whilst Z-VAD.FMK may be inhibiting the protease directly responsible for the activation of CPP32, it could also be inhibiting a protease which lies further upstream, so that abolition of CPP32 activation is a result of one or more proteases between the Z-VAD.FMK target and CPP32 also being inactive (see Figure 5p). Given that Z-VAD.FMK is able to prevent the activation of a number of proteases in addition to CPP32 (MacFarlane et al., in press), this indicates that its target lies upstream of all four of the ICE/Ced-3 proteases that have been examined so far. Because of the proposed existence of a hierarchy amongst these four proteases (Fernandes-Alnemri et al., 1995b; Liu et al., 1996a; Orth et al., 1996b; Srinivasula et al., 1996), the immediate inhibition of one of these proteases may have the indirect effect of preventing the activation of the others.

It could be argued that because it is merely a tripeptide, Z-VAD.FMK is a less specific inhibitor than Ac-DEVD-CHO and Ac-YVAD-CHO, and it may be sufficiently non-specific for it to act as a general restraint on a wide range of ICE/Ced-3 proteases. However, the determination of the three dimensional structure of CPP32 (Rotonda et al., 1996) coupled with the fact that Z-VAD.FMK inhibits ICE over twenty times more readily than it inhibits CPP32 (Armstrong et al., 1996) would seem to contradict this argument. The nature of the inhibitory kinetics of Z-VAD.FMK towards other proteases is undetermined.

If the target(s) of Z-VAD.FMK lies upstream of CPP32, then given both the nature of its chemical structure and also the three dimensional structures of ICE and CPP32, it would be predicted that such a protease would be an ICE/Ced-3 family member that more closely resembles ICE than CPP32. Moreover, the 20 kDa fragment of CPP32 that can

be seen when apoptosis is inhibited by Z-VAD.FMK in THP.1 cells (Figure 5i) could have arisen as a result of the incomplete inhibition of the enzyme that is activating CPP32. A fragment of approximately 20 kDa would be produced if the intact 32 kDa proenzyme is cleaved only at the p17/p12 junction (see Figure 1f), the amino acid sequence at this point being Ile-Glu-Thr-Asp (Nicholson et al., 1995). The isoleucine residue in the P₄ position is hydrophobic, and from the three-dimensional structures of ICE (Walker et al., 1994a; Wilson et al., 1994) and CPP32 (Rotonda et al., 1996) one would perhaps predict that this position is being cut by an ICE-like protease rather than a CPP32-like protease.

Aside from these pieces of evidence, there are also indications in Fas-mediated systems of apoptosis that such a protease(s) exists upstream of a CPP32-like activity. Firstly, in Fas-mediated apoptosis in both mouse W4 cells (Enari et al., 1996) and in the livers of mice injected with anti-Fas antibody (Rodriguez et al., 1996), a transient peak of proteolytic activity towards a fluorescent substrate containing the YVAD motif recognised by ICE-like proteases has been recorded prior to the more sustained proteolysis of an analogous substrate for those proteases resembling CPP32. Secondly, Jurkat T cells expressing CrmA, a poxvirus protein that acts as a competitive ICE/Ced-3 protease inhibitor that is cleaved at the motif Leu-Val-Ala-Asp (Ray et al., 1992), were resistant to Fas-induced cell death, and also possessed intact CPP32, which indicates that CrmA is inhibiting a protease upstream of CPP32 (Chinnaiyan et al., 1996b). CrmA will inhibit CPP32 at high concentrations (Nicholson et al., 1995; Tewari et al., 1995), but it makes a far more effective inhibitor of ICE (Komiyama et al., 1994) which is unsurprising given that it possesses a hydrophobic leucine residue in its P₄ position. Again in Jurkat T cells undergoing Fas-mediated apoptosis, the proteolysis of fodrin from the intact 240 kDa form to a 150 kDa fragment occurs prior to the breakdown of PARP, U1-70 kDa snRNP and DNA-PK_{cs}, all three of which are substrates of CPP32-like proteases (Casciola-Rosen et al., 1996). This initial cleavage of fodrin is inhibitable by Z-VAD.FMK but not by Ac-DEVD-CHO (Greidinger et al., 1996). Also, the addition of recombinant ICE to unstimulated W4 cell extracts causes apoptotic morphology and DNA degradation in isolated mouse liver nuclei (Enari et al., 1996), and ICE has been shown to cleave CPP32 *in vitro* (Tewari et al., 1995).

However, in this chapter no evidence was found for the participation of ICE in the

induction of Fas-mediated apoptosis in Jurkat T cells as measured by the cleavage of [³⁵S]proIL-1 β (Figures 5m and 5n). No ICE protein has been found in Jurkat cells by Western blot detection (Miossec et al., 1996), although its mRNA is expressed (Wang et al., 1994). This would explain why [³⁵S]proIL-1 β remained intact during the induction of apoptosis (Figure 5m and 5n). Furthermore, purified recombinant ICE is unable to convert lysates prepared from unstimulated Jurkat cells into lysates that can cause characteristic apoptotic changes in isolated thymocyte nuclei, suggesting that not only does ICE not play a part in apoptosis in this model, but it is unable to artificially cause apoptotic events in these cells (S.C. Chow, personal communication).

The protease activity observed upstream of the actions of CPP32 described in the examples given above may be attributable to the actions of a protease associated with the Fas receptor such as MACH/FLICE/Mch5 or Mch4. The proteolytic actions of these enzymes have yet to be extensively characterised. Alternatively, there may be an ICE/Ced-3 family member whose structure resembles ICE, e.g. ICE_{rel}II/TX/Ich2 (Munday et al., 1995; Faucheu et al. 1995; Kamens et al., 1995), ICE_{rel}III/TY (Munday et al., 1995; Faucheu et al., 1996), or Ich3 (Wang et al., 1996a) (see Table 1) that may be responsible for the ICE/Ced-3 proteolytic activity observed prior to CPP32. Very little is currently known about the actions of these enzymes. It is also possible that enzymes such as these may be acting upstream of CPP32 in the THP.1 cell model, where apoptosis was being induced via chemical stimuli rather than by a Fas-mediated mechanism, and such an enzyme may be the target for Z-VAD.FMK.

ICE knockout mice are developmentally normal but lack the ability to produce mature IL-1 β (Kuida et al., 1995; Li et al., 1995). This demonstrates that the programmed cell death which must be occurring during the development of these animals can do so in the absence of ICE. This could indicate that ICE has no role in apoptosis at all, and its function is restricted to IL-1 β maturation, which is reflected in the inability to detect the actions of ICE in the Jurkat cell model. In contrast to the ICE null mice, CPP32 knockout mice are smaller than normal with serious brain abnormalities, and they die prematurely (Kuida et al., 1996). However, B lymphoblasts and embryonic fibroblasts derived from ICE knockout mice cannot undergo apoptosis induced by granzyme B (Shi et al., 1996), despite the fact that granzyme B is unable to cleave ICE (Darmon et al., 1994; Quan et al., 1996). There is also evidence to link ICE with apoptosis in mammary

epithelial cells caused by the loss of matrix attachment, as the expression of ICE mRNA is elevated upon the induction of apoptosis by either antibodies to β_1 integrin or by the overexpression of stromelysin-1, both of which prevent the cells from attaching to tissue culture plastic (Boudreau et al., 1995). This could indicate that ICE can participate in apoptosis in certain instances, but that its involvement is not as necessary as that of e.g. CPP32.

ICE is unusual amongst the ICE/Ced-3 family of proteases in that it is involved in a cellular process other than apoptosis, as it converts proIL-1 β into its mature pro-inflammatory form. IL-1 β could have a number of detrimental effects if released during apoptosis. As IL-1 β is known to be pro-inflammatory (Dinarello, 1996), the release of this cytokine during apoptosis would seem inappropriate because of the damaging effects of necrosis, which causes inflammation as a result of the release of immunogenic molecules from the ruptured cell. In addition, IL-1 β can have proliferative effects, and an ICE inhibitor has been demonstrated to prevent the release of mature IL-1 β by an acute myelogenous leukaemia cell line, and in doing so also prevent the proliferative effects of IL-1 β on these cells (Estrov and Talpaz, 1996). However, mature IL-1 β is released from HeLa cells exposed to perforin and granzyme B (Shi et al., 1996) and also by macrophages or freshly isolated monocytes co-incubated with cytotoxic T lymphocytes (Hogquist et al., 1991), cells that cause cell death via the actions of perforin and granzyme B, although this may be a secondary event arising as a result of the actions of other ICE/Ced-3 members during apoptosis.

To summarise, the protease inhibitor Z-VAD.FMK, which prevents the breakdown of PARP in intact cells, is unable to prevent *in vitro* the degradation of [35 S]-labelled PARP by lysates prepared from cells undergoing apoptosis either as a result of chemical stimuli or due to cross-linking of the Fas receptor. This result suggested that a target for Z-VAD.FMK lay prior to the activation of the PARP cleavage enzyme. As CPP32 is known to cleave PARP, analysis by Western blotting using an antibody raised to this enzyme confirmed that Z-VAD.FMK inhibits apoptosis by preventing the proteolytic activation of CPP32 in both THP.1 cells and Jurkat T lymphocytes. Further analysis of the degradation of [35 S]proIL-1 β by lysates prepared from Jurkat T cells demonstrated that the protease ICE does not participate in Fas-mediated apoptosis in Jurkat T cells.

CHAPTER 6

GENERAL DISCUSSION

6. GENERAL DISCUSSION

In this thesis, three aspects of apoptosis have been investigated - the degradation of DNA into nucleosomal fragments, the induction of apoptosis by the elevation of intracellular free Ca^{2+} ($[\text{Ca}^{2+}]_i$), and the execution of apoptosis by the action of the ICE/Ced-3 family of proteases. The relationship between these three seemingly distinct areas is illustrated in Figure 6a. Four agents that inhibit apoptosis have been used in this thesis: EGTA, econazole and TLCK which inhibit in thymocytes, and Z-VAD.FMK which has been used to inhibit apoptosis in THP.1 and Jurkat cells. The manner in which EGTA and econazole inhibit apoptosis is unlike the manner in which Z-VAD.FMK or TLCK inhibit apoptosis - EGTA and econazole inhibit by diminishing the levels of $[\text{Ca}^{2+}]_i$, and their effects are limited to only certain mechanisms of inducing apoptosis (see Figures 4f-j). By preventing a sustained elevation in $[\text{Ca}^{2+}]_i$, they are suppressing the as yet uncharacterised signalling mechanisms that somehow bring about the activation of the apoptotic execution machinery. In contrast, Z-VAD.FMK, and in thymocytes TLCK, inhibit at a stage in the implementation of apoptosis which appears to be common to all manners of inducing apoptosis examined so far, which means that these agents act further downstream of EGTA and econazole. One of the events which is involved in the ultimate decay of the cell is the breakdown of DNA, which is inhibited by Z-VAD.FMK (Fearnhead et al. 1996b; Zhu et al., 1995; Cain et al., 1996). A candidate enzyme for this in thymocytes is DNase I, which is inhibited by G-actin (Peitsch et al., 1993a). It has been proposed that actin is cleaved by an ICE/Ced-3-like activity during apoptosis, and this would allow the release of DNase I, enabling the cleavage of DNA (Kayalar et al., 1996).

The identity of the target(s) inhibited by TLCK in thymocyte apoptosis is undetermined. Although a protease is the likely target for this compound, it is impossible to dismiss the possibility that it may be acting in another manner entirely. It could be speculated that TLCK, originally synthesised as an inhibitor of trypsin, is inhibiting a member of the ICE/Ced-3 family, as the compound has been shown to prevent *in vitro* lamin breakdown in isolated nuclei (Lazebnik et al., 1995), which is caused by Mch2 (Takahashi et al., 1996; Orth et al., 1996a). However, TLCK does not inhibit CPP32 (Nicholson et al., 1995), and the concentration of TLCK required to prevent lamin breakdown *in vitro* is

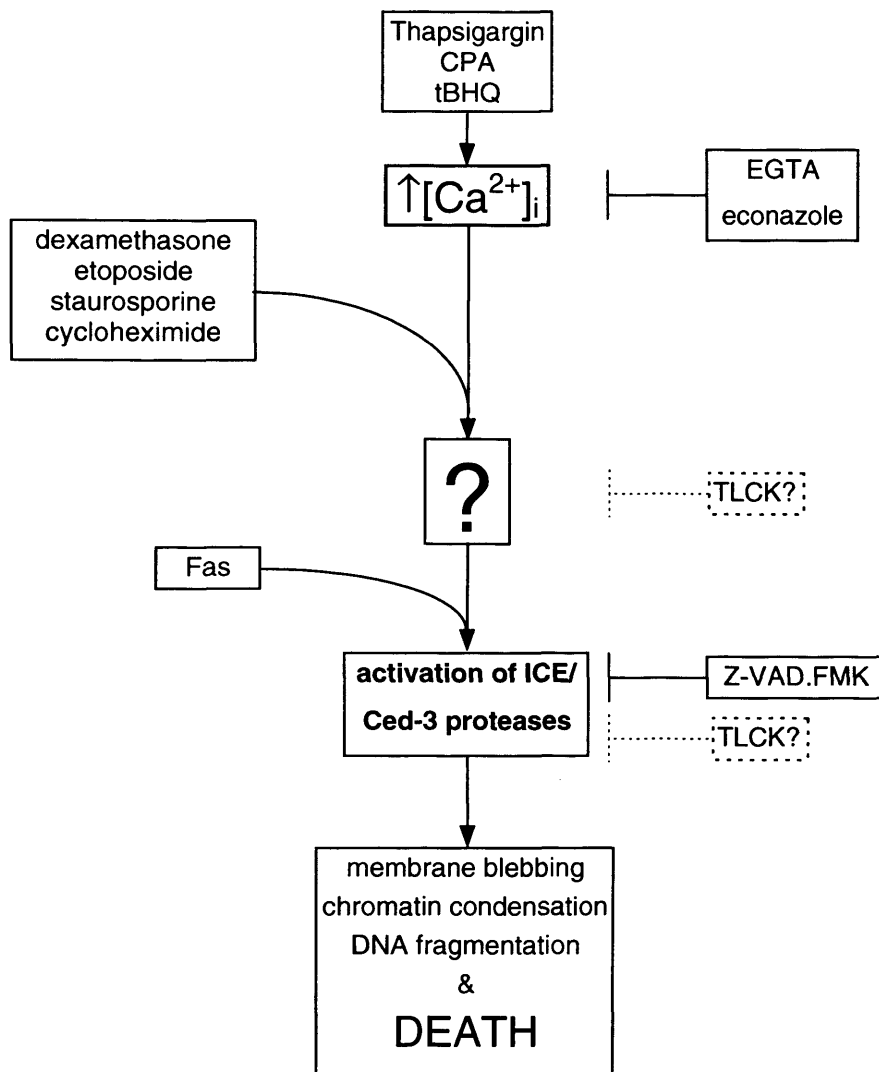


Figure 6a. *The relationships between the inducers and inhibitors of apoptosis used in this thesis.*

As EGTA and econazole only inhibit apoptosis induced by thapsigargin, CPA and tBHQ, they act at a point upstream of the protease inhibitors Z-VAD.FMK and TLCK, which inhibit all of the inducers used. (TLCK only inhibits in thymocytes and is therefore represented by a dashed line.) Whilst the mechanism by which the chemical inducers of apoptosis trigger the action of the ICE/Ced-3 proteases (represented by the question mark) is unknown, the ligation of the Fas receptor activates the ICE/Ced-3 protease MACH/FLICE/Mch5, whose actions go on to kill the cell. Although TLCK may be inhibiting some sort of ICE/Ced-3 activity in thymocytes, it is possible that it is inhibiting further upstream of this point.

twice that needed for the inhibition of apoptosis in intact thymocytes (Lazebnik et al., 1995; Fearnhead et al., 1995a). TLCK has been shown to prevent disruption of the mitochondrial transmembrane potential, an event which precedes the nuclear changes of apoptosis, in thymocytes treated with dexamethasone (Marchetti et al., 1996). However, the inhibitory effects of TLCK seen in thymocytes (Fearnhead et al. 1995a) are not common to all cell systems, as evidenced by the effect of the compound on THP.1 cells (Zhu et al, 1995; Chapter 5).

The aspects of apoptosis covered in the work reported in this thesis in many ways reflect the shifts in the field that have occurred during the three years in which this work was undertaken. When work on this thesis was started in the autumn of 1993, one of the principle subjects of research in the field was the mechanisms of DNA fragmentation, a phenomenon which is now recognised to be a part of the final stages of apoptosis and is used principally as a means of ascertaining whether or not a cell is apoptotic. However, around this time, a couple of papers were published in the journal *Cell* that have gone on to have widespread repercussions in the field of apoptosis, these papers being the studies by Robert Horvitz, Junying Yuan and colleagues describing the homology between the nematode cell death gene *ced-3* and the gene encoding the human protease interleukin-1 β converting enzyme (ICE) (Yuan et al., 1993), and the subsequent induction of apoptosis by the overexpression of ICE in fibroblasts (Miura et al., 1993). At this point ICE was unique: three years later it has become the archetype of a family with at least eleven mammalian members.

One of the principle reasons why there has been a dramatic growth in interest in the ICE/Ced-3 family of proteases (now referred to as Caspases (Alnemri et al., 1996)) is because they are a universal mechanism for effecting apoptotic cell death, and this is presumably why Z-VAD.FMK is so effective at inhibiting apoptosis and programmed cell death in cell models ranging from *Drosophila* to mammals (Pronk et al., 1996; Zhu et al., 1995; Fearnhead et al., 1995b; Jacobson et al., 1996). In contrast, the consequences of an elevation of $[Ca^{2+}]_i$ vary from one cell type to the next (see section 1.3.3). Furthermore, the enzyme(s) responsible for the breakdown of DNA appear to differ from one cell type to the next (see section 3.1.2).

It is probable that there are yet more ICE/Ced-3 family members awaiting discovery, as

well as more of their substrates, whose breakdown will further illustrate how a dying cell comes to exhibit the morphological and biochemical characteristics of apoptosis. Although our knowledge of the actions of these proteases has grown rapidly over the last couple of years, there is still much about them that remains unknown. For instance, little is known about the localisation within the cell of many of these enzymes. Whilst the proform of ICE is known to be cytosolic and then present on the plasma membrane once it has been activated (Singer et al., 1995; Miossec et al., 1996), and proMch3 is also thought to be cytosolic (Duan et al., 1996a), the whereabouts of the other proteases remains unknown. There has perhaps been an assumption that they are primarily cytosolic although there is little real data to support this, although the morphological changes associated with apoptosis such as membrane blebbing and cytoplasmic condensation have been shown to occur in enucleated cells (Jacobson et al., 1994; Schulze-Osthoff et al., 1994), so part of the cell death machinery must be non-nuclear. However, many of the substrates of the ICE/Ced-3 family - for example PARP, lamins, and the catalytic subunit of DNA-dependent protein kinase - are located in the nucleus so this would require at least some of the proteases to be present in the nucleus in their active form. Meanwhile, a second group of substrates are found on the periphery of the cell, e.g. fodrin, actin and Gas-2, so ICE/Ced-3-like proteolytic activity would also be required in this region of the cell. The determination of the location of these proteases has important implications with regard to which enzyme degrades which substrate, which in turn is important for the correct breakdown of the cell. It may also shed light upon both the regulation of these proteases and their inter-relationships.

Although the actions of ICE/Ced-3 family members in apoptosis are apparently ubiquitous, it is debatable whether there is a single common pathway of cell death, as the tissue distribution of these enzymes varies from protease to protease. Additional evidence to support a diversity of execution pathways has been provided by the generation of CPP32 knockout mice (Kuida et al., 1996). These mice possess no histological abnormalities in tissues such as the lung, kidney, liver and spleen, all of which express CPP32 in the wild type. Also, thymocytes isolated from the CPP32 null mice are as sensitive to Fas-mediated apoptosis and apoptotic stimuli like staurosporine and dexamethasone as the wild types, and apoptotic thymocytes from the CPP32 null mice still display the characteristic PARP breakdown products. This indicates that in a

number of tissues the absence of CPP32 can presumably be overcome by the action of another family member. However, these mice died at 1-3 weeks of age as a result of insufficient apoptosis in the brain, where Mch3, the ICE/Ced-3 homologue which most closely resembles CPP32, is not expressed (Fernandes-Alnemri et al., 1995b; Duan et al., 1996a; Lippke et al., 1996). This provides evidence that different combinations of ICE/Ced-3 homologues are present in different tissues, and that they cause apoptosis by different (although possibly analogous) cell type-dependent pathways.

The precise manner in which these proteases are triggered is still unresolved. The hypothesis that there is an amplification cascade where these proteases are arranged into some form of hierarchy has received support from *in vitro* studies which have placed certain proteases either upstream or downstream of others (Srinivasula et al., 1996; Orth et al. 1996b; Fernandes-Alnemri et al., 1996). However, the information has sometimes been contradictory (Srinivasula et al., 1996; Orth et al., 1996b), and it is difficult to know how realistic it is to compare what is occurring *in vitro* with what is taking place in the intact cell, especially as the intracellular location of the majority of these proteases is unknown. The work presented using Z-VAD.FMK in Chapter 5 provides evidence that there is a protease upstream of CPP32 responsible for the activation of this enzyme and which is inhibitable by Z-VAD.FMK. In addition, the discovery of the association of MACH/FLICE/Mch5 with the Fas and TNF α receptors (Boldin et al., 1996; Muzio et al., 1996; Fernandes-Alnemri et al., 1996) would suggest that this protease lies upstream of the other proteases that are activated during Fas-mediated apoptosis.

Although the discovery of MACH is an important one, the manner in which it is converted upon occupation of the Fas receptor from an inactive enzyme into an active protease remains uncertain. Furthermore, other than the killing of a target cell by cytotoxic T lymphocytes or Fas-mediated apoptosis, it is unknown how the ICE/Ced-3 family of proteases are activated in other methods of inducing apoptosis. If the cascade hypothesis is correct, then at the apex must be either an ICE/Ced-3 homologue with the ability to autoprocess, or another mechanism exists within the cell which can initiate this proteolysis independently of any ICE/Ced-3-like activity. Thus, there must be some form of restraint mechanism within the cell which can either suppress the activity of an autoactivated ICE/Ced-3 homologue, or prevent some other means of initiating ICE/Ced-3 protease activity from doing so until the correct signal is received.

One candidate for some form of suppressor is either Bcl-2 itself or a homologue such as Bcl-x_L. The overexpression of Bcl-2 and Bcl-x_L has been demonstrated to prevent the proteolytic activation of CPP32 and Mch3 (Boulakia et al., 1996; Chinnaiyan et al., 1996b; Monney et al., 1996; Jacobson et al., 1996), which places Bcl-2 and its homologues either upstream or at the point of activation of the ICE/Ced-3 homologues. This correlates with the relationship between the cell death genes in the nematode (Figure 1b), where the *ced-9* gene, which is homologous to Bcl-2 (Hengartner and Horvitz, 1994), prevents the actions of the pro-apoptotic death genes *ced-3* and *ced-4* (Hengartner et al., 1992).

It is unknown how Bcl-2 suppresses the activity of the proteases, and no evidence for a direct inter-relationship has been found. However, investigations using *in vitro* systems of apoptosis have suggested that there may be some form of regulation involving the mitochondria, where Bcl-2 is localised (Krajewski et al., 1993). A factor of around 50 kDa which possesses a proteolytic activity has been shown to be released from mitochondria, and whilst it is uncertain whether or not it is an ICE/Ced-3 protease, its activity is inhibited by Z-VAD.FMK, and its release is prevented by Bcl-2 overexpression (Susin et al., 1996). The release of this factor occurs concomitantly with a change in the mitochondrial transmembrane potential, which can be blocked in Fas-mediated apoptosis by the inhibitor of ICE/Ced-3 proteases YVAD.CMK (Castedo et al., 1996), and also by Z-VAD.FMK and TLCK in thymocytes treated with dexamethasone (Marchetti et al., 1996). Thus, it is uncertain whether these mitochondrial changes are initiating events or are a consequence of the activity of ICE/Ced-3 proteases. Another factor of 15 kDa which has been found to cause both the cleavage of CPP32 and apoptotic nuclear changes was identified as cytochrome c, which is usually localised between the inner and outer mitochondrial membranes (Liu et al., 1996b), although it is unknown if the release of this factor is modulated by Bcl-2.

However, Bcl-2-related mechanisms are unable to inhibit all forms of apoptosis. Fas-mediated cell death is not always blocked by Bcl-2 (Chinnaiyan et al., 1996b), probably because the ligation of the Fas receptor causes the immediate activation of MACH/FLICE/Mch5, and thus avoids a Bcl-2 control point. Likewise, the death of the target cell following cytotoxic T cell attack is poorly inhibited by Bcl-2 (Vaux et al., 1992) presumably since granzyme B is able to proteolytically activate a number of

ICE/Ced-3 proteases (Darmon et al., 1995; Martin et al., 1996; Quan et al., 1996; Gu et al., 1996; Wang et al., 1996a; Orth et al., 1996a). This would seem to place Bcl-2 and related proteins in the region represented by the question mark in Figure 6a.

Another mystery is whether there is a mammalian homologue of *ced-4*, one of the *C. elegans* genes that are required for programmed cell death in the nematode (Yuan and Horvitz, 1992). This gene apparently acts as an upstream positive regulator of *ced-3* (Yuan, 1996). It would seem strange if *ced-4* had no conserved mammalian counterpart whilst other genes that are involved in programmed cell death in the nematode such as *ced-3*, *ced-9* and *ces-2* all have mammalian homologues (Yuan et al., 1993; Hengartner and Horvitz, 1992; Metzstein et al., 1996). It is possible that a protein homologous to the *ced-4* gene product is responsible for the initiation of ICE/Ced-3-like activity in mammalian apoptosis.

The ultimate goal of research into apoptosis is to be able to find some way of using our knowledge of the phenomenon in the design of therapies for some of the conditions which apoptosis is known to influence (see section 1.4). One potential approach is the use of inhibitors of the ICE/Ced-3 family of proteases to prevent unwanted apoptosis. Z-VAD.FMK has been used successfully in mice to prevent the death by liver damage caused by the injection of anti-Fas antibodies, but to be completely effective the inhibitor had to be injected prior to the antibody and the dose had to be repeated at hourly intervals (Rodriguez et al., 1996). However, the mice that were protected with Z-VAD.FMK were still apparently healthy days or weeks later. Thus, although the cells exposed to anti-Fas had presumably made a decision to die, the fact that they were being prevented from committing suicide by the presence of Z-VAD.FMK did not apparently affect proper cellular function. It is unknown, however, whether Z-VAD.FMK has any tumour-promoting properties. The problems of tissue targeting will have to be addressed in the design of pharmaceuticals to moderate apoptosis, as, for example in designing an agent to prevent unwanted apoptosis as a therapy for a degenerative disease, it is vital that the drug does not put the patient at risk of tumour development.

In conclusion, the dependence upon an elevation of $[Ca^{2+}]_i$ of some, but not all, methods of inducing thymocyte apoptosis was demonstrated. EGTA and econazole, both agents that are able to reduce levels of $[Ca^{2+}]_i$, only inhibit apoptosis when induced in

thymocytes by agents like thapsigargin that act to inhibit the microsomal Ca^{2+} -ATPase. Whilst TLCK, an inhibitor of trypsin-like proteases, was able to block apoptosis in thymocytes induced by all the agents used, the same compound was unable to prevent the elevation of $[\text{Ca}^{2+}]_i$ induced by inhibitors of the microsomal Ca^{2+} -ATPase, thus placing the point of action of TLCK downstream of $[\text{Ca}^{2+}]_i$ elevation in the apoptotic pathway. It was also deduced that Z-VAD.FMK, an irreversible peptide inhibitor of the ICE/Ced-3 family of proteases (Thornberry and Molineaux, 1995), was unable to prevent the breakdown *in vitro* of PARP, a substrate of this protease family, despite its ability to prevent PARP cleavage in intact cells. This led to the discovery that Z-VAD.FMK inhibits apoptosis in both THP.1 cells and Jurkat T lymphocytes by preventing the proteolytic activation of the ICE/Ced-3 homologue CPP32. Also, the participation of ICE in Fas-mediated apoptosis was unable to be detected.

REFERENCES

- Allbritton, N.L., Verret, C.R., Wolley, R.C., and Eisen, H.N. (1988) Calcium ion concentrations and DNA fragmentation in target cell destruction by murine cloned cytotoxic T lymphocytes. *J. Exp. Med.* **167**, 514-527.
- Alnemri, E.S., Fernandes-Alnemri, T., and Litwack, G. (1995) Cloning and expression of four novel isoforms of human interleukin-1 β converting enzyme with different apoptotic activities. *J. Biol. Chem.* **270**, 4312-4317.
- Alnemri, E.S., Livingston, D.J., Nicholson, D.W., Salvesen, G., Thornberry, N.A., Wong, W.W., and Yuan, J. (1996) Human ICE/Ced-3 protease nomenclature. *Cell* **87**, 171
- Alvarez, J., Montero, M., and Garcia-Sancho, J. (1991) Cytochrome P-450 may link intracellular Ca²⁺ stores with plasma membrane Ca²⁺ influx. *Biochem. J.* **274**, 193-197.
- An, B. and Dou, Q.P. (1996) Cleavage of retinoblastoma protein during apoptosis: an interleukin 1 β converting enzyme-like protease as candidate. *Cancer Res.* **56**, 438-442.
- An, S. and Knox, K.A. (1996) Ligation of CD40 rescues Ramos-Burkitt lymphoma B cells from calcium ionophore and antigen receptor triggered apoptosis by inhibiting activation of the cysteine protease CPP32/Yama and cleavage of its substrate PARP. *FEBS Lett.* **386**, 115-122.
- Anand, R. and Southern, E.M. (1990) in: Gel electrophoresis of nucleic acids: a practical approach (Eds. Rickwood, D. and Hames, B.D.). *IRL Press, Oxford* 101-123.
- Andjelic, S., Jain, N., and Nikolic-Zugic, J. (1993) Immature thymocytes becomes sensitive to calcium-mediated apoptosis with the onset of CD8, CD4 and T cell receptor expression: A role for bcl-2? *J. Exp. Med.* **178**, 1745-1751.
- Arends, M.J., Morris, R.G., and Wyllie, A.H. (1990) Apoptosis - The role of the endonuclease. *Am. J. Path.* **136**, 593-608.
- Armstrong, R.C., Aja, T., Xiang, J., Gaur, S., Krebs, J.F., Hoang, K., Bai, X., Korsmeyer, S.J., Karanewsky, D.S., Fritz, L.C., and Tomaselli, K.J. (1996) Fas-induced activation of the cell death-related protease CPP32 is inhibited by Bcl-2 and by ICE family protease inhibitors. *J. Biol. Chem.* **271**, 16850-16855.

- Ayala, J.M., Yamin, T.-T., Egger, L.A., Chin, J., Kostura, M.J., and Miller, D.K. (1994) IL-1 β -converting enzyme is present in monocytic cells as an inactive 45k Da precursor. *J. Immunol.* **153**, 2592-2599.
- Barry, M.A. and Eastman, A. (1993) Identification of deoxyribonuclease II as an endonuclease involved in apoptosis. *Arch. Biochem. Biophys.* **300**, 440-450.
- Beaver, J.P. and Waring, P. (1994) Lack of correlation between early intracellular calcium ion rises and the onset of apoptosis in thymocytes. *Immunol. Cell Biol.* **72**, 489-499.
- Berridge, M.J. (1994) The biology and medicine of calcium signaling. *Mol. Cell. Endocr.* **98**, 119-124.
- Black, R.A., Kronheim, S.R., and Sleath, P.R. (1989) Activation of interleukin-1 β by a co-induced protease. *FEBS Lett.* **247**, 386-390.
- Boise, L.H., Gonzalez-Garcia, M., Postema, C.E., Ding, L., Lindsten, T., Turka, L.A., Mao, X., Nunez, G., and Thompson, C.B. (1993) *bcl-x*, a *bcl-2*-related gene that functions as a dominant regulator of apoptotic cell death. *Cell* **74**, 597-608.
- Boldin, M.P., Varfolomeev, E.E., Pancer, Z., Mett, I.L., Camonis, J.H., and Wallach, D. (1995) A novel protein that interacts with the death domain of Fas/APO-1 contains a sequence motif related to the death domain. *J. Biol. Chem.* **270**, 7795-7798.
- Boldin, M.P., Goncharev, T.M., Goltsev, Y.V., and Wallach, D. (1996) Involvement of MACH, a novel MORT-1/ FADD-interacting protease, in FAS/Apo-1 and TNF-receptor induced cell death. *Cell* **84**, 803-815.
- Boudreau, N., Sympton, C.J., Werb, Z., and Bissel, M.J. (1995) Suppression of ICE and apoptosis in mammary epithelial cells by extracellular matrix. *Science* **267**, 891-893.
- Boulakia, C.A., Chen, G., Ng, F.W.H., Teodoro, J.G., Branton, P.E., Nicholson, D.W., Poirier, G.G., and Shore, G.C. (1996) Bcl-2 and adenovirus E1B 19 kDa protein prevent E1A-induced processing of CPP32 and cleavage of poly(ADP-ribose) polymerase. *Oncogene* **12**, 529-535.

- Brancolini, C., Benedetti, M., and Schneider, C. (1995) Microfilament reorganisation during apoptosis: the role for Gas 2, a possible substrate for ICE-like proteases. *EMBO J.* **14**, 5179-5190.
- Brown, D.G., Sun, X.-M., and Cohen, G.M. (1993) Dexamethasone induced apoptosis involves cleavage of DNA to large fragments prior to internucleosomal fragmentation. *J. Biol. Chem.* **268**, 3037-3039.
- Browne, S.J., MacFarlane, M., Cohen, G.M., and Paraskeva, C. APC and Rb proteins are cleaved in apoptosis by a different ICE-like protease responsible for the cleavage of poly(ADP-ribose) polymerase. *Submitted*
- Buja, L.M., Eigenbrodt, M.L., and Eigenbrodt, E.H. (1993) Apoptosis and necrosis - basic types and mechanisms of cell death. *Arch. Path. Lab. Med.* **117**, 1208-1214.
- Bump, N.J., Hackett, M., Hugunin, M., Seshagiri S., Brady, K., Chen, P., Ferenz, C., Franklin, S., Ghayur, T., Li, P., Licari, P., Mankovich, J., Shi, L., Greenberg, A.H., Miller, L.K., and Wong, W.W. (1995) Inhibition of ICE family proteases by baculovirus antiapoptotic protein p35. *Science* **269**, 1885-1888.
- Cain, K., Inayat-Hussain, S.H., Wolfe, J.T., and Cohen, G.M. (1994) DNA fragmentation into 200-250 and/or 30-50 kilobasepair fragments in rat liver nuclei is stimulated by Mg^{2+} alone and Ca^{2+}/Mg^{2+} but not by Ca^{2+} alone. *FEBS Lett.* **349**, 385-391.
- Cain, K., Inayat-Hussain, S.H., Couet, C., and Cohen, G.M. (1996) A cleavage-site-directed inhibitor of interleukin-1- β -converting enzyme-like proteases inhibits apoptosis in primary cultures of rat hepatocytes. *Biochem. J.* **314**, 27-32.
- Casciola-Rosen L.A., Miller, D.K., Anhalt, G.J., and Rosen, A. (1994) Specific Cleavage of the 70-kDa Protein component of the U1 Small Nuclear Ribonucleoprotein is a Characteristic Biochemical feature of Apoptotic cell death. *J. Biol. Chem.* **269**, 30757-30760.
- Casciola-Rosen L.A., Anhalt, G.J., and Rosen, A. (1995) DNA-dependent Protein Kinase is one of a subset of autoantigens specifically cleaved early during apoptosis. *J. Exp. Med.* **182**, 1625-1634.

- Casciola-Rosen L.A., Nicholson, D.W., Chong, T., Rowan, K.R., Thornberry, N.A., Miller, D.K., and Rosen, A. (1996) Apopain/CPP32 cleaves proteins that are essential for cellular repair: a fundamental principle of apoptotic death. *J. Exp. Med.* **183**, 1957-1964.
- Castedo, M., Hirsch, T., Susin, S.A., Zamzami, N., Marchetti, P., Macho, A., and Kroemer, G. (1996) Sequential acquisition of mitochondrial and plasma membrane alterations during early lymphocyte apoptosis. *J. Immunol.* **157**, 512-521.
- Cerretti, D.P., Kozlosky, C.J., Mosley, B., Nelson, N., Van Ness, K., Greenstreet, T., March, C.J., Kronheim, S.R., Druck, T., Cannizzaro, L.A., Huebner, K., and Black, R.A. (1992) Molecular cloning of the Interleukin-1 β converting enzyme. *Science* **256**, 97-100.
- Chen, P., Nordstrom, W., Gish, B., and Abrams, J.M. (1996) *grim*, a novel cell death gene in *Drosophila*. *Genes & Dev.* **10**, 1773-1782.
- Chinnaiyan, A.M., O'Rourke, K., Tewari, M., and Dixit, V.M. (1995) FADD, a novel death domain-containing protein, interacts with the death domain of Fas and initiates apoptosis. *Cell* **81**, 505-512.
- Chinnaiyan, A.M., Tepper, C.G., Seldin, M.F., O'Rourke, K., Kischkel, F.C., Hellbardt, S., Krammer, P.H., Peter, M.E., and Dixit, V.M. (1996a) FADD/MORT1 is a common mediator of CD95 (Fas/APO-1) and Tumor Necrosis Factor Receptor-induced apoptosis. *J. Biol. Chem.* **271**, 4961-4965.
- Chinnaiyan, A.M., Orth, K., O'Rourke, K., Duan, H., Poirier, G.G., and Dixit, V.M. (1996b) Molecular ordering of the cell death pathway. *J. Biol. Chem.* **271**, 4573-4576.
- Chittenden, T., Harrington, E.A., O'Connor, R., Flemington, C., Lutz, R.J., Evan, G.I., and Guild, B.C. (1995) Induction of apoptosis by the Bcl-2 homologue Bak. *Nature* **374**, 733-736.
- Chow, S.C., Kass, G.E.N., McCabe, M.J.Jr., and Orrenius, S. (1992) Tributyltin increases cytosolic free Ca²⁺ concentration in thymocytes by mobilising intracellular Ca²⁺, activating a Ca²⁺ entry pathway and inhibiting Ca²⁺ efflux. *Arch. Biochem. Biophys.* **298**, 143-149.

- Chow, S.C., Weis, M., Kass, G.E.N., Holmström, T.H., Eriksson, J.E., and Orrenius, S. (1995) Involvement of multiple proteases during Fas-mediated apoptosis in T lymphocytes. *FEBS Lett.* **364**, 134-138.
- Clarke, A.R., Purdie, C.A., Harrison, D.J., Morris, R.G., Bird, C.C., Hooper, M.L., and Wyllie, A.H. (1993) Thymocyte apoptosis induced by p53-dependent and independent pathways. *Nature* **362**, 849-852.
- Cohen, G.M., Sun, X.-M., Snowden, R.T., Dinsdale, D., and Skilleter, D.N. (1992) Key morphological features of apoptosis may occur in the absence of internucleosomal DNA fragmentation. *Biochem. J.* **286**, 331-334.
- Cohen, G.M., Sun, X.-M., Snowden, R.T., Ormerod, M.G., and Dinsdale, D. (1993) Identification of a transitional preapoptotic population of thymocytes. *J. Immunol.* **151**, 566-574.
- Cohen, J.J. and Duke, R.C. (1984) Glucocorticoid activation of a calcium dependent endonuclease in thymocyte nuclei leads to cell death. *J. Immunol.* **132**, 38-42.
- Conroy, L.A., Jenkinson, E.J., Owen, J.J.T., and Michell, R.H. (1995) Phosphatidylinositol 4,5-bisphosphate hydrolysis accompanies T cell receptor-induced apoptosis of murine thymocytes within the thymus. *Eur. J. Immunol.* **25**, 1828-1835.
- Cryns, V.L., Bergeron, L., Zhu, H., Li, H., and Yuan, J. (1996) Specific cleavage of a-fodrin during Fas- and tumour necrosis factor-induced apoptosis is mediated by an interleukin-1 β -converting enzyme/Ced-3 protease distinct from the poly(ADP-ribose) polymerase protease. *J. Biol. Chem.* **271**, 31277-31282.
- Darmon, A.J., Ehrman, N., Caputo, A., Fujinaga, J., and Bleackley, R.C. (1994) The cytotoxic T cell proteinase granzyme B does not activate Interleukin-1 β converting enzyme. *J. Biol. Chem.* **269**, 32043-32046.
- Darmon, A.J., Nicholson, D.W., and Bleackley, R.C. (1995) Activation of the apoptotic protease CPP32 by cytotoxic T-cell-derived granzyme B. *Nature* **377**, 446-448.
- Debatin, K.-M. (1996) Disturbances of the CD95 (APO-1/Fas) system in disorders of lymphohaematopoietic cells. *Cell Death & Differ.* **3**, 185-189.

- Deng, G. and Podack, E.R. (1995) Deoxyribonuclease induction in apoptotic cytotoxic T lymphocytes. *FASEB J.* **9**, 665-669.
- Dinareello, C.A. (1996) Biologic basis for interleukin-1 in disease. *Blood* **87**, 2095-2147.
- Dolle, R.E., Hoyer, D., Prasad, C.V.C., Schmidt, S.J., Helaszek, C.T., Miller, R.E., and Ator, M.A. (1994) P₁ Aspartate-Based peptide a-((2,6-Dichlorobenzoyl)oxy) methyl ketones as potent time-dependent inhibitors of Interleukin-1 β -Converting Enzyme. *J. Med. Chem.* **37**, 563-564.
- Duan, H., Chinnaiyan, A.M., Hudson, P.L., Wing, J.P., He, W.-W., and Dixit, V.M. (1996a) ICE-LAP3, a novel mammalian homologue of the *Caenorhabditis elegans* cell death protein ced-3 is activated during Fas- and Tumour Necrosis Factor-induced apoptosis. *J. Biol. Chem.* **271**, 1621-1625.
- Duan, H., Orth, K., Chinnaiyan, A.M., Poirier, G.G., Froelich, C.J., He, W.-W., and Dixit, V.M. (1996b) ICE-LAP6, a novel member of the ICE/Ced-3 gene family, is activated by the cytotoxic T cell protease granzyme B. *J. Biol. Chem.* **271**, 16720-16724.
- Earnshaw, W.C. (1995) Apoptosis: lessons from *in vitro* systems. *Trends Cell Biol.* **5**, 217-220.
- Ellis, H.M. and Horvitz, H.R. (1986) Genetic control of programmed cell death in the nematode *C. elegans*. *Cell* **44**, 817-829.
- Ellis, R.E., Jacobson, D.M., and Horvitz, H.R. (1991) Genes required for the engulfment of cell corpses during programmed cell death in *Caenorhabditis elegans*. *Genetics* **129**, 79-94.
- Emoto, Y., Manome, Y., Meinhardt, G., Kisaki, H., Kharbanda, S., Robertson, M., Ghayur, T., Wong, W.W., Kamen, R., Weichselbaum, R., and Kufe, D. (1995) Proteolytic activation of protein kinase c δ by an ICE-like protease in apoptotic cells. *EMBO J.* **14**, 6148-6156.
- Enari, M., Hug, H., and Nagata, S. (1995) Involvement of an ICE-like protease in Fas-mediated apoptosis. *Nature* **375**, 78-81.

- Enari, M., Talanian, R.V., Wong, W.W., and Nagata, S. (1996) Sequential activation of ICE-like and CPP32-like proteases during Fas-mediated apoptosis. *Nature* **380**, 723-726.
- Estrov, E. and Talpaz, M. (1996) Role of interleukin-1 β converting enzyme (ICE) in leukaemia. *Cytokines and Molecular Therapy* **2**, 1-11.
- Fanidi, A., Harrington, E.A., and Evan, G.I. (1992) Cooperative interaction between c-myc and bcl-2 proto-oncogenes. *Nature* **359**, 554-556.
- Farrow, S., White, J.H.M., Martinou, I., Raven, T., Pun, K.-T., Grinham, C.J., Martinou, J.-C., and Brown, R. (1995) Cloning of a bcl-2 homologue by interaction with adenovirus E1B 19K. *Nature* **374**, 731-733.
- Faucheu, C., Diu, A., Chan, A.W.E., Blanchet, A.-M., Miossec, C., Herve, F., Collard-Dutilleul, V., Gu, Y., Aldape, R.A., Su, M.S.-S., Livingston, D.J., Hercend, T., and Lalanne, J.-L. (1995) A novel human protease similar to the interleukin-1 β converting enzyme induces apoptosis in transfected cells. *EMBO J.* **14**, 1914-1922.
- Faucheu, C., Blanchet, A.-M., Collard-Dutilleul, V., Lalanne, J.-L., and Diu-Hercend, A. (1996) Identification of a cysteine protease closely related to interleukin-1 β -converting enzyme. *Eur. J. Biochem.* **236**, 207-213.
- Fearnhead, H.O., Rivett, A.J., Dinsdale, D., and Cohen, G.M. (1995a) A pre-existing protease is a common effector of thymocyte apoptosis mediated by diverse stimuli. *FEBS Lett.* **357**, 242-246.
- Fearnhead, H.O., Dinsdale, D., and Cohen, G.M. (1995b) An interleukin 1- β converting enzyme-like protease is a common mediator of apoptosis in thymocytes. *FEBS Lett.* **375**, 283-288.
- Fernandes, R. and Cotter, T.G. (1993) Activation of a calcium magnesium independent endonuclease in human leukaemic cell apoptosis. *Anticancer Res.* **13**, 1253-1260.
- Fernandes-Alnemri, T., Litwack, G., and Alnemri, E.S. (1994) CPP32, a novel human apoptotic protein with homology to *Caenorhabditis elegans* cell death protein Ced-3 and mammalian interleukin 1- β converting enzyme. *J. Biol. Chem.* **269**, 30761-30764.
- Fernandes-Alnemri, T., Litwack, G., and Alnemri, E.S. (1995a) Mch-2, a new member of the apoptotic Ced3/ICE cysteine protease gene family. *Cancer Res.* **55**, 2737-2742.

- Fernandes-Alnemri, T., Takahashi, A., Armstrong, R., Krebs, J., Fritz, L., Tomaselli, K.J., Wang, L., Yu, Z., Croce, C.M., Salveson, G., Earnshaw, W.C., Litwack, G., and Alnemri, E.S. (1995b) Mch3, a novel human apoptotic cysteine protease highly related to CPP32. *Cancer Res.* **55**, 6045-6052.
- Fernandes-Alnemri, T., Armstrong, R.C., Krebs, J., Srinivasula, S.M., Wang, L., Bullrich, F., Fritz, L.C., Trapani, J.A., Tomaselli, K.J., Litwack, G., and Alnemri, E.S. (1996) *In vitro* activation of CPP32 and Mch3 by Mch4, a novel human apoptotic cysteine protease containing two FADD-like domains. *Proc. Natl. Acad. Sci.* **93**, 7464-7469.
- Gaido, M.L. and Cidlowski, J.A. (1991) Identification, purification and characterisation of a calcium-dependent endonuclease (NUC18) from an apoptotic rat thymocytes: NUC18 is not histone 2B. *J. Biol. Chem.* **266**, 18580-18585.
- Geiszt, M., Kalsi, K., Szeberenyi, J.B., and Ligeti, E. (1995) Thapsigargin inhibits Ca^{2+} entry into human neutrophil granulocytes. *Biochem. J.* **305**, 525-528.
- Getzenberg, R.H., Pienta, K.J., Ward, W.S., and Coffey, D.S. (1991) Nuclear structure and the three-dimensional organisation of DNA. *J. Cell. Biochem.* **47**, 289-299.
- Goeger, D.E. and Riley, R.T. (1989) Interaction of cyclopiazonic acid with rat skeletal muscle sarcoplasmic reticulum vesicles - effect on Ca^{2+} binding and Ca^{2+} permeability. *Biochem. Pharmacol.* **38**, 3995-4003.
- Goldberg, Y.P., Nicholson, D.W., Rasper, D.M., Kalchman, M.A., Koide, H.B., Graham, R.K., Bromm, M., Kazemi-Esfarjani, P., Thornberry, N.A., Vaillancourt, J.P., and Hayden, M.R. (1996) Cleavage of huntingtin by apopain, a proapoptotic cysteine protease, is modulated by the polyglutamine tract. *Nat. Genet.* **13**, 442-449.
- Golstein, P., Marguet, D., and Depraetere, V. (1995) Homology between reaper and the cell death domains of Fas and TNFR1. *Cell* **81** 185-186.
- Götz, C. and Montenarh, M. (1995) p53 and its implication in apoptosis. *Int. J. Oncol.* **6**, 1129-1135.
- Gouy, H., Cefai, D., Christensen, S.B., Debre, P., and Bismuth, G. (1990) Ca^{2+} influx in human T lymphocytes is induced independently of inositol phosphate production by

- mobilisation of intracellular Ca^{2+} stores. A study with the Ca^{2+} endoplasmic reticulum-ATPase inhibitor thapsigargin. *Eur. J. Immunol.* **20**, 2269-2275.
- Greenberg, A.H. (1996) Activation of apoptosis pathways by granzyme B. *Cell Death & Differ.* **3**, 269-274.
- Greidinger, E.L., Miller, D.K., Yamin, T.-T., Casciola-Rosen, L., and Rosen, A. (1996) Sequential activation of three distinct ICE-like activities in Fas-ligated Jurkat cells. *FEBS Lett.* **390**, 299-303.
- Grether, M.E., Abrams, J.M., Agapite, J., White, K., and Steller, H. (1995) The *head involution defective* gene of *Drosophila melanogaster* functions in programmed cell death. *Genes & Dev.* **9**, 1694-1708.
- Grynkiewicz, G., Poenie, M., and Tsien, R.Y. (1985) A new generation of Ca^{2+} indicators with greatly improved fluorescence properties. *J. Biol. Chem.* **260**, 3440-3450.
- Gu, Y., Wu, J., Faucheu, C., Lalanne, J.L., Diu, A., Livingston, D.J., and Su, M.S-S. (1995) Interleukin-1 β converting enzyme requires oligomerisation for activity of processed forms *in vivo*. *EMBO J.* **14**, 1923-1931.
- Gu, Y., Sarnecki, C., Fleming, M.A., Lippke, J.A., Bleackley, R.C., and Su, M.S-S. (1996) Processing and activation of CMH-1 by Granzyme B. *J. Biol. Chem.* **271**, 10816-10820.
- Hahne, M., Peitsch, M.C., Irmeler, M., Schroter, M., Lowin, B., Rousseau, M., Bron, C., Renno, T., French, L., and Tschopp, J. (1995) Characterisation of the non-functional Fas ligand of *gld* mice. *Int. Immunol.* **7**, 1381-1386.
- Hale, A.J., Smith, C.A., Sutherland, L.C., Stoneman, V.E.A., Longthorne, V.L., Culhane, A.C., and Williams, G.T. (1996) Apoptosis: molecular regulation of cell death. *Eur. J. Biochem.* **236**, 1-26.
- Harlow, E. and Lane, D.P. (1988) Antibodies: A Laboratory Manual *Cold Spring Harbor Press, Cold Spring Harbor, New York*

- Hasegawa, J., Kamada, S., Kamiike, W., Shimizu, S., Imazu, T., Matsuda, H., and Tsujimoto, Y. (1996) Involvement of CPP32/Yama(-like) proteases in Fas-mediated apoptosis. *Cancer Res.* **56**, 1713-1718.
- Hedgecock, E.M., Sulston, J.E., and Thomson, J.N. (1983) Mutations affecting programmed cell deaths in the nematode *Caenorhabditis elegans*. *Science* **220**, 1277-1279.
- Hengartner, M.O., Ellis, R.E., and Horvitz, H.R. (1992) *Caenorhabditis elegans* gene *ced-9* protects cells from programmed cell death. *Nature* **356**, 494-499.
- Hengartner, M.O. and Horvitz, H.R. (1994) *C. elegans* cell survival gene *ced-9* encodes a functional homologue of the mammalian proto-oncogene *bcl-2*. *Cell* **76**, 665-676.
- Hockenbery, D.M., Oltvai, Z.N., Yin, X.-M., Millman, C.L., and Korsmeyer, S.J. (1993) Bcl-2 functions in an antioxidant pathway to prevent apoptosis. *Cell* **75**, 241-251.
- Hogquist, K.A., Nett, M.A., Unanue, E.R., and Chaplin, D.D. (1991) Interleukin-1 is processed and released during apoptosis. *Proc. Natl. Acad. Sci.* **88**, 8485-8489.
- Hugunin, M., Quintal, L.J., Mankovich, J.A., and Ghayur, T. (1996) Protease activity of *in vitro* transcribed and translated *Caenorhabditis elegans* cell death gene (*ced-3*) product. *J. Biol. Chem.* **271**, 3517-3522.
- Inaba, T., Inukai, T., Yoshihara, T., Seyschab, H., Ashmun, R.A., Canman, C.E., Laken, S.J., Kastan, M.B., and Look, A.T. (1996) Reversal of apoptosis by the leukaemia-associate E2A-HLF chimaeric transcription factor. *Nature* **382**, 541-544.
- Iseki, R., Kudo, Y., and Iwata, M. (1993) Early mobilization of Ca^{2+} is not required for glucocorticoid induced apoptosis in thymocytes. *J. Immunol.* **151**, 5198-5207.
- Jacobson, M.D., Burne, J.F., and Raff, M.C. (1994) Programmed cell death and Bcl-2 protection in the absence of a nucleus. *EMBO J.* **13**, 1899-1910.
- Jacobson, M.D. and Raff, M.C. (1995) Programmed cell death and bcl-2 protection in very low oxygen. *Nature* **374**, 814-816.
- Jacobson, M.D., Weil, M., and Raff, M.C. (1996) Role of Ced-3/ICE-family proteases in staurosporine-induced programmed cell death. *J. Cell Biol.* **133**, 1041-1051.

- Jiang, S., Chow, S.C., Nicotera, P., and Orrenius, S. (1994) Intracellular Ca^{2+} signals activate apoptosis in thymocytes: studies using the Ca^{2+} -ATPase inhibitor thapsigargin. *Exp. Cell Res.* **212**, 84-92.
- Kamens, J., Paskind, M., Hugunin, M., Talanian, R.V., Allen, H., Banach, D., Bump, N., Hackett, M., Johnston, C.G., Li, P., Mankovich, J.A., Terranova, M., and Ghayur, T. (1995) Identification and Characterisation of ICH-2, a Novel member of the Interleukin- 1β converting enzyme family of cysteine proteases. *J. Biol. Chem.* **270**, 15250-15256.
- Kass, G.E.N., Duddy, S.K., Moore, G.A., and Orrenius, S. (1989) 2,5-Di-(*tert*-butyl)-1,4-benzohydroquinone rapidly elevates cytosolic Ca^{2+} concentration by mobilising the inositol 1,4,5-trisphosphate-sensitive Ca^{2+} pool. *J. Biol. Chem.* **264**, 15192-15198.
- Kaufmann, S.H. (1989) Induction of endonucleolytic DNA cleavage in human acute myelogenous leukaemia cells by etoposide, camptothecin and other cytotoxic anticancer drugs: a cautionary note. *Cancer Res.* **49**, 5870-5878.
- Kaufmann, S.H., Desnoyers, S., Ottaviano, Y., Davidson, N.E., and Poirier, G.G. (1993) Specific proteolytic cleavage of Poly(ADP-ribose) polymerase: an early marker of chemotherapy-induced apoptosis. *Cancer Res.* **53**, 3976-3985.
- Kayagaki, N., Kawasaki, A., Ebata, T., Ohmoto, H., Ikeda, S., Inoue, S., Yoshino, K., Okumura, K., and Yagita, H. (1995) Metalloproteinase-mediated release of human Fas ligand. *J. Exp. Med.* **182**, 1777-1783.
- Kayalar, C., Ord, T., Testa, M.P., Zhong, L.-T., and Bredesen, D.E. (1996) Cleavage of actin by interleukin- 1β converting enzyme to reverse DNase I inhibition. *Proc. Natl. Acad. Sci.* **93**, 2234-2238.
- Kerr, J.F.R., Wyllie, A.H., and Currie, A.R. (1972) Apoptosis: a basic biological phenomenon with wide-ranging implications in tissue kinetics. *Br. J. Cancer* **26**, 239-257.
- Khodarev, N.N. and Ashwell, J.D. (1996) An inducible lymphocyte nuclear $\text{Ca}^{2+}/\text{Mg}^{2+}$ -dependent endonuclease associated with apoptosis. *J. Immunol.* **156**, 922-931.

- Kiefer, M.C., Brauer, M.J., Powers, V.C., Wu, J.J., Umansky, S.R., Tomei, L.D., and Barr, P.J. (1995) Modulation of apoptosis by the widely distributed Bcl-2 homologue Bak. *Nature* **374**, 736-739.
- Kluck, R.M., McDougall, C.A., Harmon, B.V., and Halliday, J.W. (1994) Calcium chelators induce apoptosis - evidence that raised intracellular ionised calcium is not essential for apoptosis. *Biochim. Biophys. Acta*. **1223**, 247-254.
- Komiyama, T., Ray, C.A., Pickup, D.J., Howard, A.D., Thornberry, N.A., Peterson, E.P., and Salvesen, G. (1994) Inhibition of interleukin-1 beta converting enzyme by the cowpox virus serpin CrmA: an example of cross-class inhibition. *J. Biol. Chem.* **269**, 19331-19337.
- Kostura, M.J., Tocci, M.J., Limjuco, G., Chin, J., Cameron, P., Hillman, A.G., Chartrain, N.A., and Schmidt, J.A. (1989) Identification of a monocyte specific pre-interleukin-1 β convertase activity. *Proc. Natl. Acad. Sci.* **86**, 5227-5231.
- Krajewski, S., Tanaka, S., Takayama, S., Schibler, M.J., Fenton, W., and Reed, J.C. (1993) Investigations of the subcellular distribution of the Bcl-2 oncoprotein: residence in the nuclear envelope, endoplasmic reticulum and outer mitochondrial membranes. *Cancer Res.* **53**, 4701-4714.
- Kronheim, S.R., Mumma, A., Greendreet, T., Glackin, P.J., Van Ness, K., March, C.J., and Black, R.A. (1992) Purification of interleukin-1 β converting enzyme, the protease that cleaves the interleukin-1 β precursor. *Arch. Biochem. Biophys.* **296**, 698-703.
- Kuida, K., Lippke, J.A., Ku, G., Harding, M.W., Livingston, D.J., Su, M.S.-S., and Flavell, R.A. (1995) Altered cytokine export and apoptosis in mice deficient in interleukin 1- β converting enzyme. *Science* **267**, 2000-2003.
- Kuida, K., Zheng, T.S., Na, S., Kuan, C.-Y., Yang, D., Karasuyama, H., Rakic, P., and Flavell, R.A. (1996) Decreased apoptosis in the brain and premature lethality in CPP32 deficient mice. *Nature* **384**, 368-372.
- Kumar, S., Kinoshita, M., Noda, M., Copeland, N.G., and Jenkins, N.A. (1994) Induction of apoptosis by the mouse *Nedd2* gene, which encodes a protein similar to the

- product of the *Caenorhabditis elegans* cell death gene *ced-3* and the mammalian IL-1 β -converting enzyme. *Genes & Dev.* **8**, 1613-1626.
- LaGree, K.A., Lee, A.T., Stetten, G., and Strauss, P.R. (1988) The human Jurkat (FHCRC-11) cell line is heterogeneous in ploidy and cell size and releases detergent-soluble DNA. *Exp. Hematol.* **16**, 686-690.
- Lam, M., Dubyak, G., and Distelhorst, C.W. (1993) Effect of glucocorticosteroid treatment on intracellular calcium homeostasis in mouse lymphoma cells. *Mol. Endocr.* **7**, 686-693.
- Lam, M., Dubyak, G., Chen, L., Nunez, G., Miesfeld, R.L., and Distelhorst, C.W. (1994) Evidence that Bcl-2 represses apoptosis by regulating endoplasmic reticulum-associated Ca²⁺ fluxes. *Proc. Natl. Acad. Sci.* **91**, 6569-6573.
- Lampe, P.A., Cornbrooks, E.B., Juhasz, A., Johnson, E.M. Jr., and Franklin, J.L. (1995) Suppression of programmed neuronal death by a thapsigargin-induced Ca²⁺ influx. *J. Neurobiol.* **26**, 205-212.
- Latchman, D.S. (1990) Gene Regulation: A Eukaryotic Perspective *Unwin Hyman Press, London*.
- Lazebnik, Y.A., Cole, S., Cooke, C.A., Nelson, W.G., and Earnshaw, W.C. (1993) Nuclear events of apoptosis *in vitro* in cell-free mitotic extracts: a model system for analysis of the active phase of apoptosis. *J. Cell Biol.* **123**, 7-22.
- Lazebnik, Y.A., Kaufmann, S.H., Desnoyers, S., Poirier, G.G., and Earnshaw, W.C. (1994) Cleavage of poly(ADP-ribose) polymerase by a proteinase with properties like ICE. *Nature* **371**, 346-347.
- Lazebnik, Y.A., Takahashi, A., Moir, R.D., Goldman, R.D., Poirier, G.G., Kaufmann, S.H., and Earnshaw, W.C. (1995) Studies of the lamin protease reveal multiple parallel biochemical pathways during apoptotic execution. *Proc. Natl. Acad. Sci.* **92**, 9042-9046.
- Li, P., Allen, H., Banerjee, S., Franklin, S., Herzog, L., Johnston, C., McDowell, J., Paskind, M., Rodman, L., Salfeld, J., Towne, E., Tracey, D., Wardwell, S., Wei, F.-Y., Wong, W., Kamen, R., and Seshadri, T. (1995) Mice deficient in IL-1 β -converting

- enzyme are defective in production of mature IL-1 β and resistant to endotoxic shock. *Cell* **80**, 401-411.
- Lippke, J.A., Gu, Y., Sarnecki, C., Caron, P.R., and Su, M.S.-S. (1996) Identification and characterisation of CPP32/Mch2 Homologue 1, a Novel Cysteine Protease similar to CPP32. *J. Biol. Chem.* **271**, 1825-1828.
- Liu, X., Kim, C.N., Pohl, J., and Wang, X. (1996a) Purification and characterisation of an interleukin-1 β -converting enzyme family protease that activates cysteine protease P32 (CPP32). *J. Biol. Chem.* **271**, 13371-13376.
- Liu, X., Kim, C.N., Yang, J., Jemmerson, R., and Wang, X. (1996b) Induction of apoptotic program in cell-free extracts: requirement for dATP and cytochrome c. *Cell* **86**, 147-157.
- Los, M., Van de Craen, M., Penning, L.C., Schenk, H., Westendorp, M., Baeuerle, P.A., Droge, W., Krammer, P.H., Fiers, W., and Schulze-Osthoff, K. (1995) Requirement of an ICE/Ced-3 protease for Fas/ APO-1-mediated apoptosis. *Nature* **375**, 81-83.
- Lowe, S.W., Schmitt, E.M., Smith, S.W., Osborne, B.A., and Jacks, T. (1993) p53 is required for radiation induced apoptosis in mouse thymocytes. *Nature* **362**, 847-849.
- Luokkamäki, M., Servomaa, K., and Rytomaa, T. (1993) Onset of chromatin fragmentation in chloroma cell apoptosis is highly sensitive to UV and begins at non-B DNA conformation. *Int. J. Radiat. Biol.* **63**, 207-213.
- MacFarlane, M., Cain, K., Sun, X.-M., Alnemri, E.S., and Cohen, G.M. Processing of at least four ICE-like proteases occurs during the execution phase of apoptosis in human monocytic tumour cells. *J. Cell Biol.* In Press
- Marchetti, P., Castedo, M., Susin, S.A., Zamzami, N., Hirsch, T., Macho, A., Haeflner, A., Hirsch, F., Geuskens, M., and Kroemer, G. (1996) Mitochondrial permeability transition is a central coordinating event in apoptosis. *J. Exp. Med.* **184**, 1155-1160.
- Mariani, S., Matiba, B., Baumler, C., and Krammer, P.H. (1995) Regulation of cell surface APO-1/Fas (CD95) ligand expression by metalloproteases. *Eur. J. Immunol.* **25**, 2303-2307.

- Martin, S.J., O'Brien, G.A., Nishioka, W.K., McGahon, A.J., Mahboubi, A., Saido, T.C., and Green, D.R. (1995) Proteolysis of fodrin (non-erythroid spectrin) during apoptosis. *J. Biol. Chem.* **270**, 6425-6428.
- Martin, S.J., Amarante-Mendes, G.P., Shi, L., Chuang, T.-H., Casiano, C.A., O'Brien, G.A., Fitzgerald, P., Tan, E.M., Bokoch, G.M., Greenberg, A.H., and Green, D.R. (1996) The cytotoxic cell protease granzyme B initiates apoptosis in a cell-free system by proteolytic processing and activation of the ICE/Ced-3 family protease, CPP32, via a novel two-step mechanism. *EMBO J.* **15**, 2407-2416.
- Mashima, T., Naito, M., Fujita, N., Noguchi, K., and Tsuruo, T. (1995) Identification of actin as a substrate of ICE and an ICE-like protease and involvement of an ICE-like protease but not ICE in VP-16 induced U937 apoptosis. *Biochem. Biophys. Res. Comm.* **217**, 1185-1192.
- Mason, M.J., Garcia-Rodriguez, C., and Grinstein, S. (1991) Coupling between intracellular Ca^{2+} stores and the Ca^{2+} permeability of the plasma membrane. *J. Biol. Chem.* **266**, 20856-20862.
- Matsushima, K., Copeland, T.D., Onozaki, K., and Oppenheim, J.J. (1986) Purification and biochemical characteristics of two distinct human interleukins 1 from the myelomonocytic THP-1 cell line. *Biochemistry* **25**, 3424-3429.
- McConkey, D.J., Hartzell, P., Amador-Perez, J.F., Orrenius, S., and Jondal, M. (1989a) Calcium-dependent killing of immature thymocytes by stimulation via the CD3/T cell receptor complex. *J. Immunol.* **143**, 1801-1806.
- McConkey, D.J., Nicotera, P., Hartzell, P., Bellomo, G., Wyllie, A.H., and Orrenius, S. (1989b) Glucocorticoids activate a suicide process in thymocytes through an elevation of cytosolic Ca^{2+} concentration. *Arch. Biochem. Biophys.* **269**, 365-370.
- McConkey, D.J. (1996) Calcium-dependent, interleukin 1 β converting enzyme inhibitor-insensitive degradation of lamin B1 and DNA fragmentation in isolated thymocyte nuclei. *J. Biol. Chem.* **271**, 22398-22406.
- Metzstein, M.M., Hengartner, M.O., Tsung, N., Ellis, R.E., and Horvitz, H.R. (1996) Transcription regulator of programmed cell death encoded by *Caenorhabditis elegans* gene *ces-2*. *Nature* **382**, 545-547.

- Miller, D.K., Ayala, J.M., Egger, L.A., Raju, S.M., Yamin, T.-T., Ding, G.J.-F., Howard, A.D., Palyha, O.C., Rolando, A.M., Salley, J.P., Thornberry, N.A., Weidner, J.R., Williams, J.H., Chapman, K.T., Jackson, J., Kostura, M.J., Limjuco, G., Molineaux, S.M., Mumford, R.A., and Calaycay, J.R. (1993) Purification and characterization of active human interleukin-1 β -converting enzyme from THP-1 monocytic cells. *J. Biol. Chem.* **268**, 18062-18069.
- Milligan, C.E., Prevette, D., Yaginuma, H., Homma, S., Cardwell, C., Fritz, L.C., Tomaselli, K.J., Oppenheim, R.W., and Schwartz, L.M. (1995) Peptide inhibitors of the ICE protease family arrest programmed cell death of motoneurons *in vivo* and *in vitro*. *Neuron* **15**, 385-393.
- Miossec, C., Decoen, M.-C., Durand, L., Fassy, F., and Dju-Hercend, A. (1996) Use of monoclonal antibodies to study interleukin-1 β converting enzyme expression: only precursor forms are detected in interleukin-1 β -secreting cells. *Eur. J. Immunol.* **26**, 1032-1042.
- Miura, M., Zhu, H., Rotello, R., Hartweig, E.A., and Yuan, J. (1993) Induction of apoptosis in fibroblasts by IL-1 β -converting enzyme, a mammalian homologue of the *C. elegans* cell death gene *ced-3*. *Cell* **75**, 653-660.
- Miyashita, T. and Reed, J.C. (1992) Bcl-2 gene transfer increases relative resistance of S49.1 and WEHI7.2 lymphoid cells to cell death and DNA fragmentation induced by glucocorticoids and multiple chemotherapeutic drugs. *Cancer Res.* **52**, 5407-5411.
- Monney, L., Otter, I., Olivier, R., Ravn, U., Mirzasaleh, H., Fellay, I., Poirier, G.G., and Borner, C. (1996) Bcl-2 overexpression blocks activation of the death protease CPP32/Yama/apopain. *Biochem. Biophys. Res. Comm.* **221**, 340-345.
- Montague, J.W., Gaido, M.L., Frye, C., and Cidlowski, J.A. (1994) A calcium-dependent nuclease from apoptotic rat thymocytes is homologous with cyclophilin. *J. Biol. Chem.* **269**, 18877-18880.
- Moore, G.A., McConkey, D.J., Kass, G.E.N., O'Brien, P.J., and Orrenius, S. (1987) 2,5-Di(*tert*-butyl)-1,4-benzohydroquinone - a novel inhibitor of liver microsomal Ca²⁺ sequestration. *FEBS Lett.* **224**, 331-336.

- Motoyama, N., Wang, F., Roth, K.A., Sawa, K., Nakayama, K., Negishi, I., Senju, S., Zhang, Q., Fujii, S., and Loh, D. (1995) Massive cell death of immature haematopoietic cells and neurons in Bcl-x-deficient mice. *Science* **267**, 1506-1510.
- Muchmore, S.W., Sattler, M., Liang, H., Meadows, R.P., Harlan, J.E., Yoon, H.S., Nettesheim, D., Chang, B.S., Thompson, C.B., Wong, S.L., Ng, S.C., and Fesik, S.W. (1996) X-ray and NMR structure of human Bcl-x_L, an inhibitor of programmed cell death. *Nature* **381**, 335-341.
- Munday, N.A., Vaillancourt, J.P., Ali, A., Casano, F.J., Miller, D.K., Molineaux, S.M., Yamin, T.-T., Yu, V.L., and Nicholson, D.W. (1995) Molecular cloning and pro-apoptotic activity of ICE_{rel}II and ICE_{rel}III, members of the ICE/Ced-3 family of cysteine proteases. *J. Biol. Chem.* **270**, 15870-15876.
- Muzio, M., Chinnaiyan, A.M., Kischkel, F.C., O'Rourke, K., Shevchenko, A., Ni, J., Scaffidi, C., Bretz, J.D., Zhang, M., Gentz, R., Mann, M., Krammer, P.H., Peter, M., and Dixit, V.M. (1996) FLICE, a novel FADD homologous ICE/Ced-3-like protease, is recruited to the CD95 (Fas/Apo-1) death-inducing signalling complex. *Cell* **84**, 817-827.
- Na, S., Chuang, T.-H., Cunningham, A., Turi, T.G., Hanke, J.H., Bokoch, G.M., and Danley, D.E. (1996) D4-GDI, a substrate of CPP32, is proteolyzed during Fas-induced apoptosis. *J. Biol. Chem.* **271**, 11209-11213.
- Nagata, S. and Golstein, P. (1995) The Fas Death Factor. *Science* **267**, 1449-1455.
- Neamati, N., Fernandez, A., Wright, S., Kiefer, J., and McConkey, D.J. (1995) Degradation of lamin B1 precedes oligonucleosomal DNA fragmentation in apoptosis thymocytes and isolated thymocyte nuclei. *J. Immunol.* **154**, 3788-3795.
- Nicholson, D.W., Ali, A., Thornberry, N.A., Vaillancourt, J.P., Ding, C.K., Gallant, M., Gareau, Y., Griffin, P.R., Labelle, M., Lazebnik, Y.A., Munday, N.A., Raju, S.M., Smulson, M.E., Yamin, T.-T., Yu, V.L., and Miller, D.K. (1995) Identification and inhibition of the ICE/Ced-3 protease necessary for mammalian apoptosis. *Nature* **376**, 37-43.
- Nikonova, L.V., Beletsky, I.P., and Umansky, S.R. (1993) Properties of some nuclear nucleases of rat thymocytes and their changes in radiation-induced apoptosis. *Eur. J. Biochem.* **215**, 893-901.

- Oberhammer, F., Wilson, J.W., Dive, C., Morris, I.D., Hickman, J.A., Wakeling, A.E., Walker, P.R., and Sikorska, M. (1993) Apoptotic death in epithelial cells: cleavage of DNA to 300 and/or 50 kb fragments prior to or in the absence of internucleosomal fragmentation. *EMBO J.* **12**, 3679-3684.
- Oberhammer, F.A., Hochegger, K., Froschl, G., Tiefenbacher, R., and Pavelka, M. (1994) Chromatin condensation during apoptosis is accompanied by degradation of lamin A+B, without enhanced activation of cdc2 kinase. *J. Cell Biol.* **126**, 827-837.
- Oltvai, Z.N., Millman, C.L., and Korsmeyer, S.J. (1993) Bcl-2 heterodimerises *in vivo* with a conserved homologue, Bax, that accelerates programmed cell death. *Cell* **74**, 609-619.
- Ormerod, M.G., Sun, X.-M., Snowdon, R.T., Davies, R., Fearnhead, H., and Cohen, G.M. (1993) Increased membrane permeability of apoptotic thymocytes: a flow cytometric study. *Cytometry* **14**, 595-602.
- Orrenius, S. (1995) Apoptosis: molecular mechanisms and implications for human disease. *J. Intern. Med.* **237**, 529-536.
- Orth, K., Chinnaiyan, A.M., Garg, M., Froelich, C.J., and Dixit, V.M. (1996a) The Ced-3/ICE-like protease Mch2 is activated during apoptosis and cleaves the death substrate lamin A. *J. Biol. Chem.* **271**, 16443-16446X.
- Orth, K., O'Rourke, K., Salvesen, G.S., and Dixit, V.M. (1996b) Molecular ordering of apoptotic mammalian Ced-3/ICE-like proteases. *J. Biol. Chem.* **271**, 20977-20980.
- Peitsch, M.C., Polzar, B., Stephan, H., Crompton, T., MacDonald, H.R., Mannherz, H.G., and Tschopp, J. (1993a) Characterisation of the endogenous deoxyribonuclease involved in nuclear DNA degradation during apoptosis (programmed cell death). *EMBO J.* **12**, 371-377.
- Peitsch, M.C., Muller, C., and Tschopp, J. (1993b) DNA fragmentation during apoptosis is caused by frequent single-strand cuts. *Nucleic Acids Res.* **21**, 4206-4209.
- Peter, M.E., Kischkel, F.C., Hellbardt, S., Chinnaiyan, A.M., Krammer, P.H., and Dixit, V.M. (1996) CD95 (APO-1/Fas)-associated signalling proteins. *Cell Death & Differ.* **3**, 161-170.

- Pronk, G.J., Ramer, K., Amiri, P., and Williams, L.T. (1996) Requirement of an ICE-like protease for induction of apoptosis and ceramide generation by REAPER. *Science* **271**, 808-810.
- Putney, J.W.Jr. (1986) A model for receptor-regulated calcium entry. *Cell Calcium* **7**, 1-12.
- Putney, J.W.Jr. (1990) Capacitative calcium entry revisited. *Cell Calcium* **11**, 611-624.
- Quan, L.T., Tewari, M., O'Rourke, K., Dixit, V.M., Snipas, S.J., Poirier, G.G., Ray, C., Pickup, D.J., and Salvesen, G.S. (1996) Proteolytic activation of the cell death protease Yama/CPP32 by granzyme B. *Proc. Natl. Acad. Sci.* **93**, 1972-1976.
- Raff, M.C. (1992) Social controls on cell survival and cell death. *Nature* **356**, 397-400.
- Ray, C.A., Black, R.A., Kronheim, S.R., Greenstreet, T.A., Sleath, P.R., Salvesen, G.S., and Pickup, D.J. (1992) Viral inhibition of inflammation: cowpox virus encodes an inhibitor of the interleukin-1 β converting enzyme. *Cell* **69**, 597-604.
- Reed, J.C. (1995) Regulation of apoptosis by bcl-2 family proteins and its role in cancer and chemoresistance. *Curr. Op. Oncol.* **7**, 541-546.
- Rodriguez, I., Matsuura, K., Ody, C., Nagata, S., and Vassalli, P. (1996) Systematic injection of a tripeptide inhibits the intracellular activation of CPP32 -like proteases *in vivo* and fully protects mice against Fas-mediated fulminant liver destruction and death. *J. Exp. Med.* **184**, 2067-2072.
- Rodriguez-Tarduchy, G., Malde, P., Lopez-Rivas, A., and Collins, M.K.L. (1992) Inhibition of apoptosis by calcium ionophores in IL-3-dependent bone marrow cells is dependent upon production of IL-4. *J. Immunol.* **148**, 1416-1422.
- Rogers, J.H. (1985) The origin and evolution of retroposons. *Int. Rev. Cytol.* **93**, 187-279.
- Rosen, A. (1996) Huntingtin: a new marker along the road to cell death? *Nat. Genet.* **13**, 380-382.
- Rotonda, J., Nicholson, D.W., Fazil, K.M., Gallant, M., Gareau, Y., Labelle, M., Peterson, E.P., Rasper, D.M., Ruel, R., Vaillancourt, J.P., Thornberry, N.A., and

- Becker, J.W. (1996) The three dimensional structure of apopain/CPP32, a key mediator of apoptosis. *Nat. Struct. Biol.* **3**, 619-625.
- Roy, N., Mahadevan, M.S., McLean, M., Shutler, G., Yaraghi, Z., Farahani, R., Baird, S., Besner-Johnston, A., Lefebvre, C., Kang, X., Salih, M., Aubry, H., Tamai, K., Guan, X., Ioannou, P., Crawford, T.O., de Jong, P., Surh, L., Ikeda, J., Korneluk, R.G., and Mackenzie, A. (1995) The gene for neuronal apoptosis inhibitory protein is partially deleted in individuals with spinal muscular atrophy. *Cell* **80**, 167-178.
- Sambrook, J., Fritsch, E.F., and Maniatis, T. (1989) *Molecular Cloning: A Laboratory Manual Cold Spring Harbor Press, Cold Spring Harbor, New York*
- Sargeant, P., Farndale, R.W., and Sage, S.O. (1994) The imidazole antimycotics econazole and miconazole reduce agonist-evoked protein-tyrosine phosphorylation and evoke membrane depolarisation in human platelets: cautions for their use in studying Ca^{2+} signalling pathways. *Cell Calcium* **16**, 413-418.
- Schlegel, J., Peters, I., Orrenius, S., Miller, D.K., Thornberry, N.A., Yamin, T.-T., and Nicholson, D.W. (1996) CPP32/Apopain is a key interleukin 1 β converting enzyme-like protease involved in Fas-mediated apoptosis. *J. Biol. Chem.* **271**, 1841-1844.
- Schulze-Osthoff, K., Walczak, H., Droge, W., and Krammer, P.H. (1994) Cell nucleus and DNA fragmentation are not required for apoptosis. *J. Cell Biol.* **127**, 15-20.
- Schwartzman, R.A. and Cidlowski, J.A. (1993) Apoptosis: The biochemistry and molecular biology of programmed cell death. *Endocr. Rev.* **14**, 133-151.
- Seidler, N.W., Jona, I., Vegh, M., and Martonosi, A. (1989) Cyclopiazonic acid is a specific inhibitor of the Ca^{2+} -ATPase of sarcoplasmic reticulum. *J. Biol. Chem.* **264**, 17816-17823.
- Shi, L., Chen, G., MacDonald, G., Bergeron, L., Li, H., Miura, M., Rotello, R.J., Miller, D.K., Li, P., Seshadri, T., Yuan, J., and Greenberg, A.H. (1996) Activation of an interleukin 1 converting enzyme-dependent apoptosis pathway by granzyme B. *Proc. Natl. Acad. Sci.* **93**, 11002-11007.
- Singer, I.I., Scott, S., Chin, J., Bayne, E.K., Limjuco, G., Weidner, J., Miller, D.K., Chapman, K., and Kostura, M.J. (1995) The Interleukin 1- β converting enzyme (ICE) is

- localised on the external cell surface membranes and in the cytoplasmic ground substance of human monocytes by immuno-electron microscopy. *J. Exp. Med.* **182**, 1447-1459.
- Singer, M. and Berg, P. (1991) Genes and genomes. *University Science Books, Mill Valley, California*
- Sleath, P.R., Hendrickson, R.C., Kronheim, S.R., March, C.J., and Black, R.A. (1990) Substrate specificity of the protease that processes human interleukin-1 β . *J. Biol. Chem.* **265**, 14526-14528.
- Slee, E.A., Zhu, H., Chow, S.C., MacFarlane, M., Nicholson, D.W., and Cohen, G.M. (1996) Benzyloxycarbonyl-Val-Ala-Asp(OMe) fluoromethylketone (Z-VAD.FMK) inhibits apoptosis by blocking the processing of CPP32. *Biochem. J.* **315**, 21-24.
- Smith, C.A., Williams, G.T., Kingston, R., Jenkinson, E.J., and Owen, J.J.T. (1989) Antibodies to CD3/ T-cell receptor complex induce cell death by apoptosis in immature T cells in thymic cultures. *Nature* **337**, 181-184.
- Song, Q., Lees-Miller, S.P., Kumar, S., Zhang, N., Chan, D.W., Smith, G.C.M., Jackson, S.P., Alnemri, E.S., Litwack, G., Khanna, K.K., and Lavin, M.F. (1996) DNA-dependent protein kinase catalytic subunit: a target for an ICE-like protease in apoptosis. *EMBO J.* **15**, 3238-3246.
- Sorenson, C.M., Barry, M.A., and Eastman, A. (1990) Analysis of events associated with cell cycle arrest at G2 phase and cell death induced by cisplatin. *J. Natl. Cancer Inst.* **82**, 749-755.
- Squier, M.K.T., Miller, A.C.K., Malkinson, A.M., and Cohen, J.J. (1994) Calpain activation in apoptosis. *J. Cell Physiol.* **159**, 229-237.
- Srinivasula, S.M., Fernandes-Alnemri, T., Zangrilli, J., Robertson, N., Armstrong, R.C., Wang, L., Trapani, J.A., Tomaselli, K.J., Litwack, G., and Alnemri, E.S. (1996) The Ced-3/ interleukin 1 β converting enzyme-like homologue Mch6 and the lamin cleaving enzyme Mch2 α are substrates for the apoptotic mediator CPP32. *J. Biol. Chem.* **271**, 27099-27106.

- Story, M.D., Stephens, L.C., Tomasovic, S.P., and Meyn, R.E. (1992) A role for calcium in regulating apoptosis in rat thymocytes irradiated *in vitro*. *Int. J. Radiat. Biol.* **61**, 243-251.
- Suda, T., Takahashi, T., Golstein, P., and Nagata, S. (1993) Molecular cloning and expression of the Fas ligand, a novel member of the tumour necrosis factor family. *Cell* **75**, 1169-1178.
- Sun, D.Y., Jiang, S., Zheng, L.-M., Ojcius, D.M., and Young, J.D.-E. (1994) Separate metabolic pathways leading to DNA fragmentation and apoptotic chromatin condensation. *J. Exp. Med.* **179**, 559-568.
- Sun, X.-M. and Cohen, G.M. (1994) Mg^{2+} -dependent cleavage of DNA into kilobase pair fragments is responsible for the initial degradation of DNA in apoptosis. *J. Biol. Chem.* **269**, 14857-14860.
- Sun, X.-M., Snowdon, R.T., Skilleter, D.N., Dinsdale, D., Ormerod, M.G., and Cohen, G.M. (1992) A flow cytometric method for the separation and quantitation of normal and apoptotic thymocytes. *Analyt. Biochem.* **204**, 351-356.
- Susin, S.A., Zamzami, N., Castedo, M., Hirsch, T., Marchetti, P., Macho, A., Daugas, E., Geuskens, M., and Kroemer, G. (1996) Bcl-2 inhibits the mitochondrial release of an apoptogenic protease. *J. Exp. Med.* **184**, 1331-1341.
- Takahashi, T., Tanaka, M., Brannan, C.I., Jenkins, N.A., Copeland, M.G., Suda, T., and Nagata, S. (1994) Generalized lymphoproliferative disease in mice, caused by a point mutation in the Fas ligand. *Cell* **76**, 969-976.
- Takahashi, A., Alnemri, E.S., Lazebnik, Y.A., Fernandes-Alnemri, T., Litwack, G., Moir, R.D., Goldman, R.D., Poirier, G.G., Kaufmann, S.H., and Earnshaw, W.C. (1996) Cleavage of lamin A by Mch2 α but not CPP32: multiple interleukin 1 β -converting enzyme-related proteases with distinct substrate recognition properties are active in apoptosis. *Proc. Natl. Acad. Sci.* **93**, 8395-8400.
- Tewari, M. and Dixit, V.M. (1995) Fas-and tumour necrosis factor-induced apoptosis is inhibited by the poxvirus CrmA gene product. *J. Biol. Chem.* **270**, 3255-3260.
- Tewari, M., Quan, L.T., O'Rourke, K., Desnoyers, S., Zeng, Z., Beidler, D.R., Poirier, G.G., Salvesen, G.S., and Dixit, V.M. (1995) Yama/CPP32 β , a mammalian homologue

- of Ced-3, is a CrmA-inhibitable protease that cleaves the death substrate poly(ADP-Ribose) polymerase. *Cell* **81**, 801-809.
- Thastrup, O., Cullen, P.J., Drobak, B.K., Hanley, M.R., and Dawson, A.P. (1990) Thapsigargin, a tumor promoter, discharges intracellular Ca^{2+} stores by specific inhibition of the endoplasmic reticulum Ca^{2+} -ATPase. *Proc. Natl. Acad. Sci.* **87**, 2466-2470.
- Thompson, C.B. (1995) Apoptosis in the pathogenesis and treatment of disease. *Science* **267**, 1456-1462.
- Thornberry, N.A., Bull, H.G., Calaycay, J.R., Chapman, K.T., Howard, A.D., Kostura, M.J., Miller, D.K., Molineaux, S.M., Weidner, J.R., Aunins, J., Elliston, K.O., Ayala, J.M., Casano, F.J., Chin, J., Ding, G.J.-F., Egger, L.A., Gaffney, E.P., Limjuco, G., Palyha, O.C., Raju, S.M., Rolando, A.M., Salley, J.P., Yamin, T.-T., Lee, T.D., Shively, J.E., MacCoss, M., Mumford, R.A., Schmidt, J.A., and Tocci, M.J. (1992) A novel heterodimeric cysteine protease is required for interleukin-1 β processing in monocytes. *Nature* **356**, 768-774.
- Thornberry, N.A. (1994) Interleukin-1 β converting enzyme. *Methods Enzymol.* **244**, 615-631.
- Thornberry, N.A. and Molineaux, S.M. (1995) Interleukin 1- β converting enzyme: a novel cysteine protease required for IL-1 β production and implicated in programmed cell death. *Protein Sci.* **4**, 3-12.
- Tsuchiya, S., Yamabe, M., Yamaguchi, Y., Kobayashi, Y., Konno, T., and Tada, K. (1980) Establishment and characterisation of a human acute monocytic leukaemia cell line (THP-1). *Int. J. Cancer* **26**, 171-176.
- Ucker, D.S., Obermiller, P.S., Eckhart, W., Apgar, J.R., Berger, N.A., and Meyers, J. (1992) Genome digestion is a dispensable consequence of physiological cell death mediated by cytotoxic T lymphocytes. *Mol. Cell. Biol.* **12**, 3060-3069.
- Vaux, D.L., Aguila, H.L., and Weissman, I.L. (1992) Bcl-2 prevents death of factor-deprived cells but fails to prevent apoptosis in targets of cell mediated killing. *Int. Immunol.* **4**, 821-824.

- Veis, D.J., Sorenson, C.M., Shutter, J.R., and Korsmeyer, S.J. (1993) Bcl-2-deficient mice demonstrate fulminant lymphoid apoptosis, polycystic kidneys and hypopigmented hair. *Cell* **75**, 229-240.
- Walker, P.R., Smith, C., Youdale, T., Leblanc, J., Whitfield, J.F., and Sikorska, M. (1991) Topoisomerase II-reactive chemotherapeutic drugs induce apoptosis in thymocytes. *Cancer Res.* **51**, 1078-1085.
- Walker, N.P.C., Talanian, R.V., Brady, K.D., Dang, L.C., Bump, N.J., Ferenz, C.R., Franklin, S., Ghayur, T., Hackett, M.C., Hammill, L.D., Herzog, L., Hugunin, M., Houy, W., Mankovich, J.A., McGuiness, L., Orlewicz, E., Paskind, M., Pratt, C.A., Reis, P., Summani, A., Terranova, M., Welch, J.P., Xiong, L., Moller, A., Tracey, D.E., Kamen, R., and Wong, W.W. (1994a) Crystal structure of the cysteine protease interleukin-1 β -converting enzyme: a (p20/p10)₂ homodimer. *Cell* **78**, 343-352.
- Walker, P.R., Weaver, V.M., Lach, B., Leblanc, J., and Sikorska, M. (1994b) Endonuclease activities associated with high molecular weight and internucleosomal DNA fragmentation in apoptosis. *Exp. Cell Res.* **213**, 100-106.
- Wang, L., Miura, M., Bergeron, L., Zhu, H., and Yuan, J. (1994) *Ich-1*, an *Ice/Ced-3* related gene, encodes both positive and negative regulators of programmed cell death. *Cell* **78**, 739-750.
- Wang, X., Pai, J.-T., Wiedenfeld, E.A., Medina, J.C., Slaughter, C.A., Goldstein, J.L., and Brown, M.S. (1995) Purification of an interleukin-1 β converting enzyme-related cysteine protease that cleaves sterol regulatory element-binding proteins between the leucine zipper and transmembrane domains. *J. Biol. Chem.* **270**, 18044-18050.
- Wang, E. and Korsmeyer, S.J. (1996) Molecular thanatopsis: a discourse on the bcl-2 family and cell death. *Blood* **88**, 386-401.
- Wang, S., Miura, M., Jung, Y.-K., Zhu, H., Gagliardini, V., Shi, L., Greenberg, A.H., and Yuan, J. (1996a) Identification and characterisation of Ich-3, a member of the interleukin-1 β converting enzyme (ICE)/Ced-3 family and an upstream regulator of ICE. *J. Biol. Chem.* **271**, 20580-20587.

- Wang, X., Zelenski, N.G., Yang, J., Sakai, J., Brown, M.S., and Goldstein, J.L. (1996b) Cleavage of sterol regulatory element binding proteins (SREBPs) by CPP32 during apoptosis. *EMBO J.* **15**, 1012-1020.
- Waring, P. and Beaver, J. (1996) Cyclosporin A rescues thymocytes from apoptosis induced by very low concentrations of thapsigargin: effects on mitochondrial function. *Exp. Cell Res.* **227**, 264-276.
- Waring, P. and Sjaarda, A. (1994) Extracellular calcium is not required for gliotoxin or dexamethasone-induced DNA fragmentation: a reappraisal of the use of EGTA. *Int. J. Immunopharmacol.* **17**, 403-410.
- Watanabe-Fukunaga, R., Brannan, C.I., Copeland, N.G., Jenkins, N.A., and Nagata, S. (1992) Lymphoproliferation disorder in mice explained by defects in Fas antigen that mediates apoptosis. *Nature* **352**, 314-317.
- Weaver, V.M., Carson, C.E., Walker, P.R., Chaly, N., Lach, B., Raymond, Y., Brown, D.L., and Sikorska, M. (1996) Degradation of nuclear matrix and DNA cleavage in apoptotic thymocytes. *J. Cell Sci.* **109**, 45-56.
- Weis, M., Schlegel, J., Kass, G.E.N., Holmstrom, T.H., Peters, I., Eriksson, J., Orrenius, S., and Chow, S.C. (1995) Cellular events in Fas/APO-1 mediated apoptosis in Jurkat T lymphocytes. *Exp. Cell Res.* **219**, 699-708.
- White, K., Grether, M.E., Abrams, J.M., Young, L., Farrell, K., and Steller, H. (1994) Genetic control of programmed cell death in drosophila. *Science* **264**, 677-683.
- White, E. (1996) Life, death and the pursuit of apoptosis. *Genes & Dev.* **10**, 1-15.
- White, K., Tahaoglu, E., and Steller, H. (1996) Cell killing by the *Drosophila* gene reaper. *Science* **271**, 805-807.
- Whyte, M.K.B., Hardwick, S.J., Meagher, L.C., Savill, J.S., and Haslett, C. (1993) Transient elevations of cytoplasmic free calcium retard subsequent apoptosis in neutrophils *in vitro*. *J. Clin. Invest.* **92**, 446-455.
- Williams, G.T., Smith, C.A., McCarthy, N.J., and Grimes, E.A. (1992) Apoptosis: final control point in cell biology. *Trends Cell Biol.* **2**, 263-267.

- Williams, M.S. and Henkart, P.A. (1994) Apoptotic cell death induced by intracellular proteolysis. *J. Immunol.* **153**, 4247-4255.
- Wilson, K.P., Black, J.F., Thomson, J.A., Kim, E.E., Griffith, J.P., Navia, M.A., Murcko, M.A., Chambers, S.P., Aldape, R.A., Raybuck, S.A., and Livingston, D.J. (1994) Structure and mechanism of interleukin-1 β converting enzyme. *Nature* **370**, 270-275.
- Wong, W.L., Brostrom, M.A., Kuznetsov, G., Gmitter-Yellen, D., and Brostrom, C.O. (1993) Inhibition of protein synthesis and early protein processing by thapsigargin in cultured cells. *Biochem. J.* **289**, 71-79.
- Wyllie, A.H. (1980) Glucocorticoid-induced thymocyte apoptosis is associated with endogenous endonuclease activation. *Nature* **284**, 555-556.
- Xue, D. and Horvitz, H.R. (1995) Inhibition of the *Caenorhabditis elegans* cell-death protease Ced-3 by a Ced-3 cleavage site in baculovirus p35 protein. *Nature* **377**, 248-251.
- Xue, D., Shaham, S., and Horvitz, H.R. (1996) The *Caenorhabditis elegans* cell-death protein Ced-3 is a cysteine protease with substrate specificities similar to those of the human CPP32 protease. *Genes & Dev.* **10**, 1073-1083.
- Yamin, T.-T., Ayala, J.M., and Miller, D.K. (1996) Activation of the native 45 kDa precursor form of interleukin-1-converting enzyme. *J. Biol. Chem.* **271**, 13273-13282.
- Ye, X., Georgoff, I., Fleisher, S., Coffman, F.D., Cohen, S., and Fresa, K.L. (1993) The mechanism of epipodophyllotoxin-induced thymocyte apoptosis: possible role of a novel Ca²⁺ independent protein kinase. *Cell. Immunol.* **151**, 320-335.
- Yuan, J. and Horvitz, H.R. (1992) The *Caenorhabditis elegans* cell death gene *ced-4* encodes a novel protein and is expressed during the period of extensive programmed cell death. *Development* **116**, 309-320.
- Yuan, J., Shaham, S., Ledoux, S., Ellis, H.M., and Horvitz, H.R. (1993) The *C. elegans* cell death gene *ced-3* encodes a protein similar to mammalian interleukin 1- β converting enzyme. *Cell* **75**, 641-652.

- Yuan, J. (1996) Evolutionary conservation of a genetic pathway of programmed cell death. *J. Cell. Biochem.* **60**, 4-11.
- Zaera, E., Santamaria, F., Vazquez, D., and Jimenez, A. (1983) Inhibition of translation by the fungal toxin cyclopiazonic acid. *Curr. Microbiol.* **9**, 259-262.
- Zhang, C., Robertson, M.J., and Schlossman, S.F. (1995) A triplet of nuclease proteins (NP⁴²⁻⁵⁰) is activated in human Jurkat cells undergoing apoptosis. *Cell. Immunol.* **165**, 161-167.
- Zhivotovsky, B., Cedervall, B., Jiang, S., Nicotera, P., and Orrenius, S. (1994) Involvement of Ca²⁺ in the formation of high molecular weight DNA fragments in thymocyte apoptosis. *Biochem. Biophys. Res. Comm.* **202**, 120-127.
- Zhu, H., Fearnhead, H.O., and Cohen, G.M. (1995) An ICE-like protease is a common mediator of apoptosis induced by diverse stimuli in human monocytic THP.1 cells. *FEBS Lett.* **374**, 303-308.